WILLIAN BATISTA SILVA

THE MOLECULAR FUNCTIONS OF AUXIN SIGNALING IN TOMATO (Solanum lycopersicum L.)

Thesis presented to the Universidade Federal de Viçosa as part of the requirement of the Plant Physiology Graduate Program for the obtention of the degree of Doctor Scientiae.

VIÇOSA
MINAS GERAIS – BRAZIL
2018

Ficha catalográfica preparada pela Biblioteca Central da Universidade Federal de Viçosa - Câmpus Viçosa

T
S586m
2018

Silva, Willian Batista, 1987-
The molecular functions of auxin signaling in tomato (*Solanum lycopersicum* L.) / Willian Batista Silva. – Viçosa, MG, 2018.
ix, 162f. : il. (algumas color.) ; 29 cm.

Inclui apêndices.
Orientador: Wagner Luiz Araújo.
Tese (doutorado) - Universidade Federal de Viçosa.
Inclui bibliografia.

1. Plantas - Efeito da auxina. 2. Tomate - Fisiologia. 3. Tomate - Metabolismo. 4. Tomate - Maturação. 5. Mitocôndria. 6. Fotossíntese. 7. Fisiologia vegetal. I. Universidade Federal de Viçosa. Departamento de Biologia Vegetal. Programa de Pós-Graduação em Fisiologia Vegetal. II. Título.

CDD 22. ed. 571.2

WILLIAN BATISTA SILVA

THE MOLECULAR FUNCTIONS OF AUXIN SIGNALING IN TOMATO (*Solanum lycopersicum* L.)

Thesis presented to the Universidade Federal de Viçosa as part of the requirement of the Plant Physiology Graduate Program for the obtention of the degree of *Doctor Scientiae*.

APPROVED: March 2nd, 2018.

David Barbosa Medeiros

Dimas Mendes Ribeiro

Hans-Peter Braun

Agustín Zsögön

Wagner L. Araújo
(Adviser)

‘*Small things make big changes*’

ACKNOWLEDGMENTS

First of all, I would like to thank the Federal University of Viçosa (UFV), mainly to the Plant Physiology Graduate Program, for supporting and providing me all conditions required to develop my research. I am also grateful to the scholarship provided by CAPES (Coordination for the Improvement of Higher Level Personnel).

I want to say thank to my supervisor Prof. Wagner L. Araújo for his guidance and support. I am very grateful to him for trusting in my person and in my capacity. Everything between us started during the Brazilian Plant Physiology conference, where with patience he wisely guided me to the doctorate position at the department quoted above. I would like to say thank you very much for your friendship and always encouraging me to be a better person and scientist.

I also want to thank Prof. Dr. Hans-Peter Braun for his great support and for giving me the opportunity to spend one year in his lab at the Institut für Pflanzengenetik. Hannover - Germany, where I was able to deepen my knowledge in both plant metabolism and plant proteomic. In the same vein, I am also grateful to Dr. Tatjana Hildebrandt and Björn Heinemann, for their amazing support and help during the '*amino acids catabolism project'*, developed in Hannover with the financial support of the CAPES-DAAD (Deutscher Akademischer Austauschdienst).

I would like to thank Prof. Adriano Nunes-Nesi, Prof. Agustin Zsögön, Prof. Dimas Ribeiro, and Dr. David B Medeiros for their support, discussions and advices during the development of this project.

To all my colleagues from the "UCP group", former and current members, for the pleasant working atmosphere and for all the help provided in the lab. Special thanks go to David B. Medeiros, Franciele S. Oliveira, Acácio R. Salvador, Jorge Condori, Luiz Valente, Rebeca Omena and Auxiliadora Martins 'Dora', for their friendship and assistance within this work.

To people at the Institut für Pflanzengenetik, especially Tatjana Hildebrandt, Björn Heinemann, Leila Muslem, Saskia Brandt, Danielle Brito, Daniel Holl, Stefanie Liefold and Sara Fachinger. Special thanks to my Tunisian office colleagues and friends Ikram Belghith, Dr. Nèjia Farhat and Sarra Hichri. Given to the great contribution and friendship, I could not fail to mention the technical support received by Jens-Peter Barth, Marianne Langer, Dagmar Lewejohann, Christa Ruppelt, Michael Senkler and Edda Zieseniss.

I also express here my gratitude to all the professors, technicians, and colleagues at the Plant Physiology Graduate Program at the for the tremendous support offered to me.

Many thanks also for all other people who in some way had ever helped or supported me during my doctoral studies and whose names are not mentioned here.

Last, but by no means least, I sincerely would like to express my gratitude to my friends and family. My parents João Batista de Souza (in memory) and Maria Solange da Silva Souza as well as my siblings Leydiane F. da Silva Souza, and Wcleverson Batista Silva: even though we are still far away, we are connected by friendship and admiration. Finally, it is also highly important to me, to say thanks to Dom Edmar Peron and my dear partner Josino José Dellarmelina, once both have big contribution and importance in every step given in my life, were always supportive, believing in my capacity sometimes even more than I did**.**

BIOGRAPHY

Willian Batista Silva, son of João Batista de Souza (in memorian) and Maria Solange da Silva Souza, was born in Nova Xavantina, Mato Grosso state, Brazil, on November 8th, 1987. In 2007, he started the undergraduate course in Agronomy at the Mato Grosso State University (UNEMAT), Nova Xavantina, Mato Grosso state, Brazil and achieved the bachelor degree in June 2011. In March 2012, he started his Master course at the State University of Norte Fluminense Darcy Ribeiro (UENF), Campos dos Goytacazes, Rio de Janeiro, Brazil, achieving the Master degree in Crop Production in February 2014. In the same year, he started his doctoral studies at the Universidade Federal de Viçosa (UFV). From November 2016 to November 2017 he developed part of his research as a guest PhD student at the Leibniz Universität Hannover at Institut für Pflanzengenetik, Hannover, Germany, under the supervision of Prof. Dr. Hans-Peter Braun before finishing his doctoral studies in Plant Physiology at UFV under the supervision of Prof. Wagner L. Araújo.

CONTENTS

ABSTRACT

SILVA, Willian Batista, D.Sc., Universidade Federal de Viçosa, March, 2018. **The molecular functions of auxin signaling in tomato (Solanum lycopersicum L.).** Advisor: Wagner Luis Araújo.

The auxin is a phytohormone with intense participation in the growth and development process, as well as in crucial physiological processes to the plant establishment. Although its role in development control is already well established and has been extensively investigated, in our understanding, little or nothing is currently known about the impacts on the manipulation of the signaling levels of this hormone in the metabolic impact, as well as the link between auxin and photosynthetic and respiratory process both in leaves and fruit. In this vain, considering the metabolic importance in plant and the wide regulatory network of this system, in this thesis initially I present a review offering an important comparative complement of post-genomic strategies, such as the profile of the metabolites, providing information on the regulation of the metabolic network and thus allowing a more complete description of the cellular function of the plant. A comparative analysis was made by raising a question, if stable isotope mass spectrometry could replace radiolabelled approaches in metabolic studies? In addition, to better understand the functions of the modulation of auxin perception levels and how it conducts metabolic adjustments in different plant tissues, two experimental approaches were adopted for: (i) Characterize tomato plants with alterations in auxin signaling balance and their modulations in primary metabolism in tomato leaves and (ii) to analyze the role of auxin signaling in the ripening of tomato fruits. Briefly, the results indicate that auxin acts as an integrator of metabolism and adjustment and suggests that altered perceptions of this hormone affect the chloroplastic and mitochondrial metabolism in lighted leaves, suggesting a great participation of this phytohormone in the final productivity determination. Moreover, at the fruit level, auxin seems to control metabolic alterations very little, but controlling important steps in fruit maturation, controlling the metabolism of starch and sugars, providing new perspectives of integration between auxin and respiratory paths.

RESUMO

SILVA, Willian Batista, D.Sc., Universidade Federal de Viçosa, março de 2018. **As funções moleculares da sinalização da auxin em tomate (Solanum lycopersicum L.).** Orientador: Wagner Luis Araújo.

A auxina é um hormonio vegetal com intensa participação nos processos de crescimento e do desenvolvimento, bem como em processos fisiológicos cruciais para o estabelecimento das plantas. Embora o seu papel no controle do desvolvimento já é algo bem estabelcido e tem sido bastante investigado, em nosso conhecimento, pouco or nada atualmente é conhecido sobre os impactos na manipuação dos níveis da sinalização desse hormonio no impacto metabólico, bem como o link entre fotossintese e respiração em ambos frutos e folhas iluminadas. Nesse sentido, considerando a importâcia nos estudos metabólicos em plantas e a ampla rede regulatória desse sistema, nesta tese inicialmente, apresenta uma revisão oferecendo um complemento importante comparativo de estratégias pós-genômicas, como o perfil dos metabólitos, fornecendo informações sobre a regulação da rede metabólica e permitindo assim uma descrição mais completa da função celular da planta. Foi feito uma análise comparativa lançando uma pergunta se o uso de análises de espectrometrica de massa com isótopos estáveis substitur ferramentas de istótopos radioativos?. Adicionalmente, para compreender melhor as funções da modulação dos níveis de percepção da auxina e como ela conduz os ajustes metabólicos em diferentes tecidos vegetais, duas abordagens experimentais foram adotadas para: (i) caracterizar plantas de tomate com alterações no balanço de sinalização de auxina e suas modulações no mestabolism primario em folhas de tomate and (ii) analisar o papel da sinalização da auxina no amadurecimento dos frutos de tomate. Brevemente, os resultados indicam que a auxina atua como um integrador do crescimento e ajuste metabólico e sugere que alteradas percepções desse fitormonio afeta o metabolismo cloroplastidico e mitocondrial em folhas iluminadas, sugerindo uma grande participação desse homornio na determinação final da produtividade. Além do mais, a nível de fruto, a auxina parece controlar muito pouco as alterações metabolicas, porém controlando etapas importantes no amadurecimento dos frutos, controlando o metabolismo de amido e açucares, fornecendo novas perspecticas de integração entre auxina e vias respiratórias.

CHAPTER 1

General Introduction

1. General Introduction

Plants are sessile organisms and thus cannot escape from adverse environmental conditions that are a constant throughout their life cycle. However, plants also have the ability to adapt and acclimate to different environmental conditions, regulating both growth and development by extensive signaling pathways, exhibiting an unique developmental flexibility to ever-changing environmental conditions (Wolters and Jürgens, 2009; Vanstraelen and Benková, 2012). Plant growth and development are directly controlled by a group of small molecules with low molecular weight which are usually called phytohormones. They are produced in very low concentrations (e.g., <1mM and often <1uM) that are able to regulate a variety of cellular processes in plants, triggering and controlling physiological processes not only during plant growth and development but also in response to stresses (Salisbury and Ross, 1992; Davies, 2010; Novák et al., 2017). Moreover, phytohormones function as chemical messengers able to communicate plant cellular activities (Voß et al., 2014).

It is important to mention, however, that phytohormones do not act only in a linear way but their pathways are interconnected by a complex network of feedback loops and interactions that ultimately determine the final output of an individual phytohormones (Vanstraelen and Benková, 2012). This flexibility makes the regulation of phytohormones rather complicated to fully understand. Remarkably, the presence of an extensive network flexibility within phytohormone metabolism allow multiple transcriptional and post-transcriptional interactions at the level of metabolism, transport, signaling, and downstream responses to integrate internal and external stimuli that affect different development processes (Vanstraelen and Benková, 2012; Martins et al., 2018). From an evolutionary perspective, this suggest that the complexity of this entire system have been added from a pre-existing primary metabolic system in microalgae, increasing the complexity over time both in synthesis and signaling (Kenrick and Crane, 1997; Lu and Xu, 2015). In fact, microalgae and plants produce structurally identical phytohormones using relatively conserved biosynthetic pathways, which raises the question of whether the plant hormone pathway originated from hormone systems of microalgae (Spíchal, 2012), a them that was recently reviewed (Lu and Xu, 2015).

One possible explanation is that horizontal gene transfer from either bacteria or viruses to the ancestral plants could have also occurred, and this contributed to the genetic reservoir of phytohormones biosynthetic pathways in present-day land plants (Lu and Xu, 2015). For instance, the tryptophan-dependent IAA biosynthesis found in land plants is more likely to have been derived from horizontal gene transfer from bacteria (Yue et al. (2014). In fact, large gene families for synthesis and catabolism of phytohormones are observed in land plants, as well as the presence of multiple gene families encoding receptors and response regulators (Olszewski et al., 2002; Dharmasiri et al., 2005; Thines et al., 2007; Sauer et al., 2013). Notwithstanding, phytohormones signaling pathways are not highly conserved between land plants and eukaryotic microalgae (Lu and Xu, 2015). Together, such observations suggest that certain components of higher plant canonical phytohormone signaling systems emerged in microalgae, acquire more complexity with both the exploration of terrestrial environments and the development of more complex cellular systems, underlying the emergence of new genes (Pichersky and Gang, 2000; Lu and Xu, 2015).

Land plants use a wide variety of phytohormones including five well accepted classic hormones namely auxin, cytokinin, gibberellin (GA), abscisic acid (ABA) and ethylene. During the last decade evidence has accumulated to extend this concept to include also brassinosteroids (BRs), jasmonic acid, salicylic acid and strigolactones (Sánchez-Rodríguez et al., 2010; Wang and Irving, 2011; Pollock et al., 2012). Furthermore, attention has been recently given to another group of molecules with signaling function that belongs to different groups such as amino aliphatic (polyamines) and also biologically active peptides including the phytohormones peptides (PPT) such as phytosulfocin (PSK), CLAVATA3 (CLV3), Rapid Alkalization Factor (RALF), CLE family, S-locus cysteine rich proteins (SCP), Protein essential during penetration-1 (PEP1), plant natriuretic peptide (PNP) self-incompatibility factors (SCR/SP11), nodulation factor (ENOD40) and the florigen (FT) (Bahyrycz and Konopińska, 2007; Wheeler and Irving, 2010; Wang and Irving, 2011; Purwestri et al., 2017). Therefore, it seems reasonable to assume that novel players will be added to this list in the near future.

Three major growth-promoting phytohormones namely auxin, GAs and BRs are present in plants (Ross and Quittenden, 2016). Nevertheless, other hormones, as discussed below, can also promote growth in certain circumstances (Zaharah et al.,

2012). This thesis is largely focused on enhancing our current understanding on the role of auxin signaling in governing plant growth and impacting plant metabolism in general. This is mainly due to the fact that the auxin signaling pathway is a critical control point through which diverse environmental and hormonal factors are integrated into growth and developmental responses. Thus, in the following sections I briefly review the current knowledge regarding auxin metabolism, focusing mainly in auxin signaling pathways and further examine how auxin participate in the regulation of plant growth and fruit ripening by using available metabolite data. Given the pivotal role of metabolism in ultimately supporting both plant growth and development it is reasonable to assume that experiments which provide insights into metabolic flux coupled with its regulation would probably both improve our knowledge of biological systems and ultimately aid in the discovery of gene function in land plants. The thesis offers a review about the importance of different approaches to enhance knowledge of metabolic pathways, using stable and radiolabelled approaches in metabolic studies where, a question was raised about the capacity of substitution between techniques and that in the end, attempts are made to show that both approaches are indeed important and of complementary nature that probably could provide the best route towards a comprehensive understanding of plant cell metabolism. Furthermore, it is briefly discussed the conceptual basis of these approaches, as well as their historical application and limitations, finally providing an update on recent technical developments and additionally attempt to discuss the importance of more sensitive flux profiling methodologies using stable isotopes to enable us to pursue new avenues of research in order to increase our understanding of complex metabolic networks governing plant metabolism.

1.1. Auxin metabolism and implications for plant development

1.1.1. Auxin importance and story

Auxin plays important roles in virtually every aspect of plant growth and development (Davies, 2010). The concentration is variable not only throughout the plant body, but also within organs and during their different stages of development (Vanneste and Friml, 2009). This variable distribution is most likely due to the participation of several families of auxin-specific protein carriers, being the most

famous the PIN-FORMED (PIN) family of auxin efflux carriers which mediate cell-to-cell auxin transport (Zažímalová et al., 2010). The efficiency of auxin transport coupled with the dramatic phenotypes exhibit by certain mutants in Arabidopsis, has led to one widespread view that auxin signaling tends to overlook the important and complementary role of auxin metabolism (Kramer and Ackelsberg, 2015). Remarkably, during a plant life cycle, only few processes occur without the involvement of auxin (Quint and Gray, 2006). Thus, to date, it is virtually impossible to generate a mutant with total deficiency in auxin given the crucial importance of this hormone to plant viability.

Studies involving auxin dates back to Charles Darwin's time. Thus, a range of experiments on phototropism using plant growth substances were described in the book "The Power of Movement in Plants" (Darwin and Darwin, 1888). Briefly, these experiments verified the phototropism of grass coleoptiles (Phalaris canriensis) and allowed the authors to postulate the existence of a signal transported from the tip of the coleoptile to the bending regions lower down, characterizing the mobile signal functions (Davies, 2010; Enders and Strader, 2015). Subsequently, Fritz Went (1926), a graduate student from the Netherlands, was finally able to isolate the chemical by performing diffusion experiments using coleoptile tips into agar blocks. By replacing the tips of decapitated coleoptiles it culminated with (i) the stimulation of the growth of the decapitated coleoptiles and (ii) their bending when placed asymmetrically on these tips. Interestingly, this extremely simple experiment demonstrated the existence of a growth promoting chemical that was synthesized in the coleoptile tips and that moved basipetally, and further that when it is asymmetrically distributed resulted in a bending of the coleoptile away from the side with the higher concentration (Went, 1926; Went, 1937). It was the isolation of the first plant hormone originally named Wuchsstoff by Went (1927), that was later changed to auxin (from the Greek auxein, "to increase") by Kögl and a Haagen-Smit (1931).The compound was finally chemically identified as the simple compound indole acetic acid, universally known as IAA (Wildman, 1997). Afterwards, several independent and complementary investigations were able to fully characterize the precise manner in which this signal was able to move (Davies, 2010; Enders and Strader, 2015).

IAA is the most abundant hormone being of crucial physiological relevance in plants where it acts as regulator of growth by modulating cellular expansion, elongation

and proliferation, formation of floral organs, differentiation of vascular tissues, apical dominance, suppression of leaf abscission and several other processes (Ljung et al., 2002; Cheng et al., 2006). Furthermore, compelling evidence has implicated auxin in an infinity of physiological processes indicating that this molecule regulates the transcription of many genes(Woodward and Bartel, 2005).

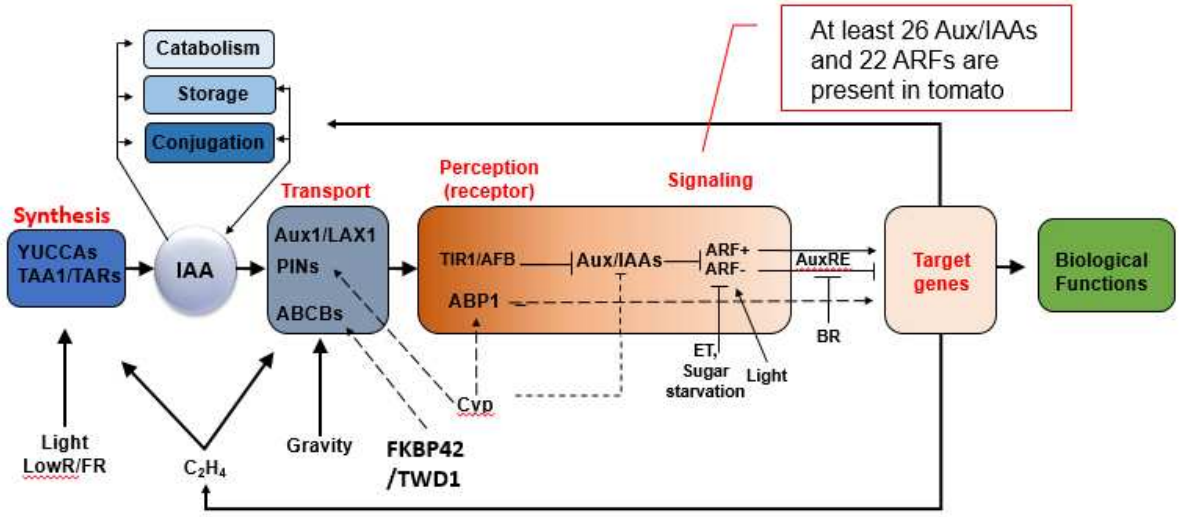

Fig. 1 – Auxin metabolism in higher plant. Auxin's effects depend upon its synthesis (blue box), transport (dark gray), perception (dark orange), signaling (light orange) and target gene responses following by biological functions (green box). Most of these functions are controlled by many genes with differing cell specificities. Auxin signaling in tomato are very complex once its step depend multi-interaction with at least 26 Aux/IAA and 22 ARFs (Figure adapted by Plant Cell, Introduction of Phytohormones, 2010 - (The Story of Auxin, 2010).

1.1.2. Auxin biosynthesis

Auxin are initially synthesized in shoot apices but also in leaf primordia, young leaves, root meristems, flowers, fruits and seeds (Azizi et al., 2015). The biosynthesis of auxin starts from tryptophan via the gene families ARABIDOPSIS1/TRYPTOPHAN AMINOTRANSFERASE RELATED (TAA1/TAR) and YUCCA (Cheng et al., 2006; Tivendale et al., 2014). The YUCCA (YUC) Flavin monooxygenase is encoded by 11 genes in Arabidopsis, which convert tryptophan to indole-3-pyruvic acid (IpyA) and then to indole-3-acetic acid in the so called Tryptophan-dependent auxin biosynthesis pathway (Zhao et al., 2001). It is important to mention that the TRYPTOPHAN AMINOTRANSFERASE OF ARABDOPSIS (TAA) family also leads to the conversion of tryptophan to IpyA (Yamada et al., 2009). Therefore, inactivation of TAA1 and its close homologs TAR1 and TAR2 leads to partial auxin deficiency and defects in

several developmental processes (Stepanova et al., 2008). Five different natural compounds are known as IAA precursor, including IPyA, Indol-3-acetaldoxime (IAOx), Indole-3-acetonitrile (IAN), indole-3-acetamide (IAM) and the indole-3- acetaldehyde (IAAld), which, apart from the IPyA pathway, is considered as the main IAA biosynthesis and is completely described already (Zhao, 2010; Zhao, 2012).

1.1.3. Auxin transport

Similarly to auxin biosynthesis, the Polar Auxin Transport (PAT) is essential for normal plant growth and development by providing directional and positional information that is essential for developmental processes such as vascular differentiation, apical dominance, organ development and tropic growth (Blakeslee et al., 2005). The polar transport of auxin from cell to cell is achieved through the coordinated process of efflux and influx transporters, encoded by PIN-FORMED (PIN) and P-GLYCOPROTEIN (PGP) (Cho et al., 2007; Petrášek and Friml, 2009; van Rongen, 2018) and AUXIN1/LIKE AUX1 (AUX/LAX) genes (Swarup and Péret, 2012; Harrison, 2017). Briefly, directional auxin transport is, on a cellular level, primarily controlled by an efflux carrier complex that is characterized by both the PIN family of proteins (Blakeslee et al., 2005; Křeček et al., 2009; Pattison and Catalá, 2012) and the ATP-binding cassette B (ABCB) family (Cho and Cho, 2013) (See in Fig. 1). Each member of the AUX1/LAX protein family (Swarup and Péret, 2012) is a functional auxin influx carrier and mediate auxin related developmental programs in different organs and tissues including the development of embryo (Wolters et al., 2011), root (Swarup et al., 2005; Swarup and Péret, 2012), flower (Swarup and Péret, 2012), lateral root (Casimiro et al., 2001; Jones et al., 2009), as well as gravitropism (Marchant et al., 1999) and maintenance of the cellular organization of embryonic roots (Ugartechea-Chirino et al., 2009).

1.1.4. Auxin signaling

Once auxin is synthesized (described above), which occurs at low concentrations, and it is further transported, auxin signal must reach different cells. To this end, signaling seems a crucial process promoting an amplifying effect of this hormone which is something already well understood in model species such as Arabidopsis and Solanum lycopersicum in the particular case of auxin. Changes in gene expression occur rapidly in response to exogenous auxin supply via an elegant signal transduction pathway, which has been reviewed elsewhere (Paponov et al., 2008; Salehin et al., 2015). According to Quint and Gray (2006), four gene-families member, namely as a SAURs [Small Auxin-Up RNAs], [Gretchen Hagen 3] GH3s, [Auxin/Indole Acetic acids] Aux/IAAs and Auxin Response Factor (ARF) genes are among the most thoroughly characterized, which are induced within minutes of auxin application (Fig.1 and Fig. 2).

Genetic and biochemical studies conducted in the last decades have revealed that distinct auxin acts as molecular glue bringing together F-box proteins (FBPs) of the TRANSPORT INHINITOR RESPONSE 1/AUXIN SIGNALING F-BOX (TIR1/AFB) family and members of the AUXIN/INDOLE ACETIC ACID (Aux/IAA) transcriptional repressor family (Tan et al., 2007; Leyser, 2017) (Fig.2). The F-box proteins are the substrate of SCF-type subunit ubiquitin protein ligase complex, named after three of their subunits, Skp1, Cullin and an F-box protein (SCF) (Fig.2) (Moon et al., 2004; Hua and Vierstra, 2011) (Fig.1). Briefly, the F-box itself is a motif at the amino terminal end of F-box protein, which interact with Skp1, interacting with Cullin and then with RING-H2 finger protein (RBX1) (Kamura et al., 1999; Zheng et al., 2002; Leyser, 2017) (Fig.2). In addition, this dimer transfers activated ubiquitin from an ubiquitin activing enzyme and conjugates it to target proteins named AUXIN/INDOLACETIC ACID (Aux/IAA) (Leyser, 2017). The complex SCF bring the target protein with carboxyl-terminal domain of F-box protein which TIR1/AFBs contain an auxin binding pocket (Tan et al., 2007). The auxin once bonded in this pocket stabilizes by docking of the Aux/IAA protein, mediated by a short protein motif in domain II. The AUX/IAA proteins are short-lived nuclear proteins that function as transcriptional regulators which act as a transcriptional repressors and do not interact directly with DNA but exert their regulatory activity through another group of proteins ARFs (Fig.2). At least 22 ARFs are present in tomato (Fig.1) (Ulmasov et al., 1997; Zouine et al., 2014; Leyser, 2017),

leading to the expression of downstream genes that perform the required and necessary responses (Ulmasov et al., 1995; Tan et al., 2007; Delker et al., 2008; Shabek and Zheng, 2014). Moreover, there are at least 26 AUX/IAA genes in the tomato genome (Audran-Delalande et al., 2012; Wu et al., 2012). Their half-lives time and the extent to which their half-lives reduce in response to applied auxin by interaction by domain II degron are highly conserved in different species (Dreher et al., 2006).

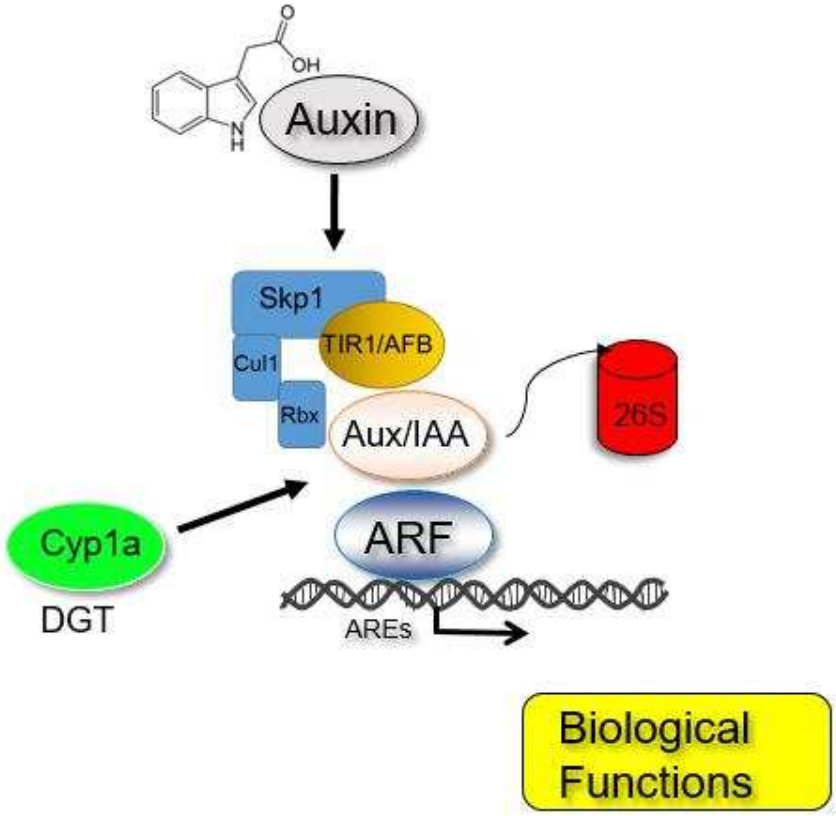

Fig. 2 – The main pathway for regulation of transcription by auxin. Auxin-inducible genes have auxin response elements (AREs) in their promoters, which are bound by dimers of the Auxin Response Factor (ARF – see in dark blue) protein family. Gene expression is prevented by recruitment of Aux/IAA (See in orange) transcriptional repressors to these promoters via their interaction with the ARFs. The Aux/IAAs recruit TOPLESS family (TPL) co-repressors which in turn recruit chromatin modifying enzymes (Not shown) that stabilize the repressed state. The auxin (gray) acts as a molecular glue bringing together Aux/IAAs and F-box proteins of the TIR1/AFB family (dark orange). These F-box proteins are part of an SCF-type E3 ubiquitin protein ligase complex that transfers activated ubiquitin (Ub) from an E1/E2 enzyme system. Polyubiquitination of the Aux/IAAs results in their degradation (See in Red). This releases repression at ARE-containing promoters and biological functions (yellow).

1.1.5. Auxin sensibility and response mediated by Aux/IAA family

A set of Aux/IAA mutants alleles have been described in a variety of species belonging to different clades of plants such as liverworts Marchantia polymorpha, the moss Physcomitella patens, the monocots Oriza sativa and Zea mays and the dicots plants as Arabidopsis thaliana, tomato and potato (Fig. 3). These mutants results in auxin related pleiotropic phenotypes, which can exhibit developmental and physiological defects likes altered root formation and gravitropism, altered apical dominance and problems in embryo and photomorphogenic development (Reed, 2001; Liscum and Reed, 2002; Zenser et al., 2003). Cloning and characterization of these mutations allows a better understanding of auxin perception pathways and functional molecular structure of Aux/IAA gene family. Several of Aux/IAA genes have compounds names that reflects the phenotypes of mutant for corresponding gene (Reed, 2001). In fact, 29 Aux/Iaa genes have already been identified in A. thaliana and most of them well characterized (Abel et al., 1995; Liscum and Reed, 2002; Overvoorde et al., 2005; Dreher et al., 2006), while M. polymorpha presents a unique Aux/IAA (Kato et al., 2015), P. patens only 3 (Prigge et al., 2010), while in rice and maize these number is going out of t 31 (Jain et al., 2006; Wang et al., 2010) and finally according with Gao et al. (2016) potato and Audran-Delalande et al. (2012) in tomato genome, both present 25 Aux/IAA well characterized.

The number of Aux/IAA identified in other species is increasing because the disponibility of new sequenced genomes data. From 17 analyzed genomes ranged from 3 (P. patens) to 63 Aux/IAA members (Glycine max) and according with Wu et al. (2017) five clades (A, B, C, D, E) have been predicted based in the presence of five different motifs (1, 2, 3, 4, and 5). Aux/IAA with all five motif presents in four domains are designed as “canonicals”. Moreover, Wu et al. (2017) also shown that genome size are no correlated with the number of Aux/IAA, and the functional lack of Aux/IAA in green algae and chlorophytes can be evidence that these protein may have suffered pressures selection for proper adaptation of plants to land environment. In good agreement with Kato et al. (2015) and Prigge et al. (2010), lowers plants have smaller families of Aux/IAA than superior plants, and these set are likely related to clade A. Clade A include canonicals Aux/IAA that could probably be traced back to the origin of the plant kingdom (Wu et al., 2017). Increased number and divergence of extra Aux/IAAs in land plants could have been the results of adaptation in responses to

changing environment and enhancing complexity of developmental patterns. The expansion observed in the Aux/IAA gene family members is coincident with whole-genome duplication events (WGD) during evolution and in consequence give rise to functional redundancy or neo-functionalization (Wu et al., 2017).

The Aux/IAA proteins are nuclear short-lived transcription factors that have shown a repressor function of auxin-regulated genes in an auxin dosage dependent manner (Ulmasov et al., 1997; Gray et al., 2001; Overvoorde et al., 2005; Leyser, 2017). As schematized in Figure 3, most of the AUX/IAA (Canonicals) share similar structures with four conserved domains DI (purple), DII (green), DIII (yellow) and DIV (cyan) (Wu et al., 2012; Wu et al., 2017). DI is N-terminal Repressor Domain (RD) that contains D/E-L-X-L-X-L or related EAR-like (ethylene-responsive element binding factor-associated amphiphilic repression) motifs (Fig.3, see in purple). The DI is N-terminal Repressor Domain (RD) that contains D/E-L-X-L-X-L or related EAR-like (ethylene-responsive element binding factor-associated amphiphilic repression) motifs (Tiwari et al., 2001; Tiwari et al., 2004; Guilfoyle, 2015), which is required to interact with TOPLESS (TPL) co-repressor and to coordinates recruitment of chromatin remodelers complex and stabilizes repression of ARFs (Szemenyei et al., 2008) probably by the histone deacetylases (HDACs) (Pierre-Jerome et al., 2013). Domain DII “Degradation Domain”, which is highly conserved in phylogenetic alignment, contains a core sequence motif compounds of hydrophobic amino acids Gly–Trp–Pro–Pro–Val (GWPPV/I) (Fig 3, see in blue letters), a target of the SCFTIR1/AFB complex. By its biochemical nature, degron motif is able to insert on hydrophobic auxin binding pocket of TIR1 (Tan et al., 2007; Jing et al., 2015). Degron sequence is mainly determinant of rapid auxin-triggered protein (Tiwari et al., 2001; Zenser et al., 2001; Dreher et al., 2006). Remarkable, both DI and DII domains are associated with Aux/IAA proteins stability.

Finally, the DIII (Fig. 3 see in yellow) and DIV (Fig.3 see in cyan) or calling later Phox and Bem1 (PBP) C-terminal domain are responsable for homodimerization of Aux/IAA and AUX-ARF heterodimerization (Reed, 2001; Tiwari et al., 2001; Liscum and Reed, 2002; Tiwari et al., 2004; Guilfoyle, 2015). Namely, PBP domain can facilitates the formation of ARF-ARF, ARF-Aux/IAA, and Aux/IAA-Aux/IAA homo- and hetero-oligomers through electrostatics interactions (Han et al., 2014; Korasick et al., 2014; Guilfoyle, 2015). Many members of Aux/IAA sets lack some of four domains and

it will be reflected in Aux/IAA properties. Moreover, Aux/IAAs has two nuclear localization signals (NLS) (Fig.3 see in orange) (Malik et al., 2009). One of them is bipartite and comprises a part I with conserved KR aminoacids doublet presents between DI and DII Domain. The second part is located in DII and comprises a more variable stretch rich in basics residues (K/R) represented with more general motif RxxRK. A second NLS SV40-ike type is present in Domain IV (Worley et al., 2000; Audran-Delalande et al., 2012; Wu et al., 2017). Recently, it was showed that the Lys of KR doublet of NLS signals can accelerate the rates of Aux/IAA degradation (Moss et al., 2015). Ubiquitination and proteasome degradation in the presence of high concentration of auxin mediates rapid turn-over of AUX/IAAs (Gray et al., 2001; Dharmasiri et al., 2005; Dharmasiri et al., 2005; Tan et al., 2007), allowing transcriptional activation by ARFs (Zouine et al., 2014).

The ARFs family are responsible for regulates auxin responsive genes by binding to the palindromic cis-regulatory TGTCTC or related auxin response elements (AuxREs) (Kim et al., 1997; Ulmasov et al., 1999; Hagen and Guilfoyle, 2002; Leyser, 2017). Typical ARFs contains three conserved domains (Zouine et al., 2014). The N-terminal DNA-binding domain (DBD) which is plant-specific B3-type protein domain able to binds AuxREs sequences. In the middle region (MR) ARFs can harbor a activation domain (AD) with basic Glu-rich (Q-rich) or repression domain (RD) with Ser-rich (S-rich) amino acid sequence (Tiwari et al., 2003; Guilfoyle and Hagen, 2007). The third domain is the C-terminal dimerization domain (CTD) or PB1 (homologous of PB1 of Aux/IAA) that facilities the interaction with Aux/IAA and self-dimerization mentioned above (Ulmasov et al., 1999; Tiwari et al., 2003; Korasick et al., 2014).

The auxin concentration is a controller of Aux/IAAs half-life once under low auxin concentrations Aux/IAA proteins directly bind and the heterodimerization with ARFs repress its activity (Ulmasov et al., 1995; Kim et al., 1997; Ulmasov et al., 1997; Ulmasov et al., 1999; Tiwari et al., 2001; Tiwari et al., 2003; Tiwari et al., 2004; Piya et al., 2014). For a normal auxin responses, Aux/IAA may be degraded (See in 1.1.4. Auxin signaling and Fig. 2) and therefore ARFs are released for regulate downstream auxin responsive genes (Weijers et al., 2005; Pierre-Jerome et al., 2013). Several and sequential studies performed in A. thaliana showed that “high auxin” levels can promotes responses, when sensing and serving of molecular glue among both F-Box TIR1 and Aux/IAA auxin co-receptors, and consequently triggering SCFTIR1/AFB E3

ubiquitin ligase complex pathway for Aux/IAA owns degradation (Gray et al., 2001; Zenser et al., 2001; Dharmasiri et al., 2005; Dharmasiri et al., 2005; Tan et al., 2007). Additionally, the auxin concentration and auxin responsive gene expression does not display a simple linear relation, and thus its depends on Aux/IAAs dynamics and certain molecular thresholds along auxin gradients whose auxin affinity is marked by differential interaction of ternary modules among components of complex SCFTIR1/AFB E3-AUX/IAA-ARF (Fukaki et al., 2005; Weijers et al., 2005; Uehara et al., 2008; Piya et al., 2014; Winkler et al., 2017). Thereby, dynamics-auxin responses first depend on issues of gene expression of Aux/IAA family. It has been shown in A. thaliana and Solanum lycopersicum a spatial-temporal map for all Aux/IAA family genes revealing tissue specificity and co-expression patterns (Reed, 2001; Overvoorde et al., 2005; Dreher et al., 2006; Paponov et al., 2008; Audran-Delalande et al., 2012; Pierre-Jerome et al., 2013) that includes times of induction, term of response and hormonal crosstalk (Abel et al., 1995; Zenser et al., 2003) and the regulatory negative-feedback loop of most Aux/IAAs in response to auxin (Tiwari et al., 2001; Tian et al., 2002).

Auxin response also depend of post-translational activity of Aux/IAA repressors (Dinesh et al., 2016). Additionally, the DII domain is essential for auxin-dependent degradation, contributing to substrate binding and turn-over rates of protein, which variates in the ranges of 10 to 80 min (Ramos et al., 2001; Dreher et al., 2006). Furthermore, AtIAA31 with degenerate DII without conserved Lys residues has a half-life of more than 20 hours, and the overexpression of the non-canonical AtIAA20, AtIAA30, and AtIAA31 results in aberrant phenotypes (Sato and Yamamoto, 2008; Salehin et al., 2015). Most of Dominant and Semi-Dominant mutants with “low-auxin” or auxin-resistance phenotypes are consequence of active repression of auxin responsive genes. As showed in Fig 3, more than one point mutation per gene has been described in chemical mutagenesis screening of mutants. Such mutation that target conserved G or Q in degron motif can results in more weakly affected phenotype (Tian and Reed, 1999; Uehara et al., 2008; Prigge et al., 2010) (Fig. 3 see in purple bar). The same behavior was observed in overexpressed Aux/IAA gene harboring natural change amino acid (D-G) (Song and Xu, 2013) (Fig. 3 see in dark green bar). Others gain-of-function mutants can exhibit hypersensitive responses in an organ dependent manner (Deng et al., 2012) (Fig. 3 see in khaki bars). On the other hand,

loss-of-function mutants of Aux/IAA genes can be due to diverse mutagenesis strategies as described in Fig 3 (round balls at right of degron alignment). Most of them have already been characterized and screened from gain-of-function genetics background affecting Domains I, III and IV (suppressors) and a few in DII (revertant). The loss-of-function can be result of knock-out mutation (Insertional mutagenesis, Site-directed mutagenesis, Physical mutagenesis, or Single nucleotide mutagenesis causing stop codon or loss of affinity); Knock-down mutation (RNA gene silencing); or by overexpressing mutated domains. Complementarily, the loss of repressor capacity of Aux/IAA normally results in released of ARFs and activation of auxin regulated genes. ARFs therefore acts downstream SFCTIR1/AFB E3 ubiquitin ligase complex and degron mutations.

Recent studies have shown that in lower plants such as liverworts M. polymorpha loss-of-function or knock-down mutants results in wild type likes phenotypes but with strong response when exposed to auxin (Flores-Sandoval et al., 2015) (Fig. 3 see in yellow bar). However, moss P. patens seems to have a different type of regulation. Site directed mutagenesis of three Aux/IAA proteins results in insensitive plants with severe phenotype and constitutive gene expression of auxin related gene (Fig.3 see in green bar). Revertant and suppressors of degron mutation restores partially auxin responses, developing subtle or wild-type like phenotype (Lavy et al., 2016) (Fig. 3 see in light -blue bar).

In Arabidopsis, the analysis of single, double and triple mutants for Aux/IAA genes failed to reveal strong visible phenotype and the same pattern was observed in rice loss-of-function single mutants, suggesting genetics redundancy and overlapping functions among members (Overvoorde et al., 2005; Jun et al., 2011; Salehin et al., 2015) (Fig. 3 see in orange bars). In Solanaceae (tomato and potato) knock-down mutants generated by RNA-silencing mutagenesis produce severe auxin related phenotypes mostly hypersensitive to auxin suggesting that less genomics redundancy (Wang et al., 2005; Chaabouni et al., 2009; Bassa et al., 2012; Deng et al., 2012; Salehin et al., 2015) (Fig. 3 see in violet bar)

Gain-of-function AUX/IAA mutants were characterized revealing that amino acid changes in the degron motif or adjacent residues can extend protein half-life (Fig. 3 see in red letters) precluding SFCTIR1-AFB degradation and enhancing their repressor activity. The residues consist of proline pairs and are likely responsible for

the auxin resistant phenotypes observed in the mutants. Proline pairs are likely essential for AUX/IAA degradation and appear to be present in all degron motif domains, but only few have been confirmed through either in silico modelling or biochemical and biophysical assays (Tan et al., 2007; Jing et al., 2015). It has recently been shown that the spatial conformation of AUX/IAAs conditions their interaction with TIR1 (Jing et al., 2015). Isomerization of the peptide bond at the proline pair is catalyzed by the peptidyl-prolyl cis/trans isomerase activity of cyclophilins (CYP) (Fig.1 alignment). The loss-of-function in Aux/IAA family displayed an enhanced response to auxin in an organ-dependent manner or restores responses in gain-of-function backgrounds with constitutive activation of related genes. Interestingly, these mutants are able to partially rescue cyclophilin mutation. There are several phenotypes associated with Aux/IAA genes loss-of-function including modifications in gravitropim/phototropism, leaf expansion, root formation, and apical dominance. However, the functional redundancy or regulatory feedback that allow compensation for the absence of Aux/IAA protein might be the reason why in many situations abrupt changes or phenotypes are not observed (Wang et al., 2005). Among the 26 Aux/IAAs found in the tomato genome, the Aux/IAA9, a member of the subfamily IV of Aux/IAA family, is a mediator of the initiation of fruit formation and leaf morphology that is commonly expressed in leaves and fruits (Bassa et al., 2012). The iaa9 mutants are characterized by enhanced auxin perception, since it acts as a repressor of the auxin signaling (Zhang et al., 2007). They are also characterized by changes in leaf anatomy and the production of parthenocarpic fruits (Wang et al., 2005). Remarkably, the subfamily IV, which includes Aux/IAA9, is clearly distinguishable from the others Aux/IAA subfamilies once it present larger amino acid sequences (typically >300 amino acids) while the others subfamilies have ~200 amino acids (Wu et al., 2012). This difference is due to the increase in the number of amino acids in both the N-terminal region of the protein (~40 a 60 amino acids) in the I domain and over 50 amino acids between the I and II domain.

Low sensitivity to auxin, on the other hand, has been associated to a single auxin 'resistant' gene named diageotropica (dgt), which encode a cyclophilin. Tomato plants with loss-of-function of cyclophilin are characterized by highly altered pleiotropic phenotypes such as: gravitational responses, absence of lateral root branches, reduced apical dominance, altered vascular development, hyponastic leaves,

increased anthocyanin and chlorophyll synthesis and reduced fruit size (Zobel, 1973, 1974; Balbi and Lomax, 2003; Carvalho et al., 2011; Ivanchenko et al., 2015), typical of mutants with Aux/IAA gain-of-function. Additionally, homozygous dgt seedlings exhibited reduced sensitivity to the auxin IAA as demonstrated by both the lack of auxin-induced elongation and the reduced ethylene-seedlings production (Jackson, 1979; Kelly and Bradford, 1986). According to Coenen et al. (2002) the dgt mutation also disrupted auxin inhibition of growth and H+ secretion in roots. Moreover, DGT negatively regulates PIN auxin efflux transporters by affecting their plasma membrane localization during lateral root formation (Ivanchenko et al., 2015). Taken together, these physiological results indicate that the dgt mutation is likely able to affect specific steps in the perception or even in auxin signaling in tomato plants (Nebenführ et al., 2000). Therefore, it seems reasonable to assume that dgt as an important tool for the investigation of not only the influences of the reduction of levels of auxin signaling but also the metabolic adjustment as well as molecular mechanisms underlying auxin-mediated processes.

The CYP proteins, members of the immunophilin superfamily that harbor highly conserved mobile peptides, are present in a variety of plant species including moss (Physcomitrella patens), rice and tomato (Lavy et al., 2012). Most of the knowledge concerning CYP function comes from the genetic and physiological characterization of mutants. Mutations in CYPs, such as DIAGEOTROPICA (dgt) in tomato, LATERAL ROOTLESS 2 (lrt2) in rice and dgt in P. patens culminates with pleiotropic auxin-resistant phenotypes. This phenotypes includes the lack of lateral root primordia outgrowth, altered shoot and root gravitropism, epinasty and vascular system defects, among others, that resemble those of DII domain mutations in aux/iaa mutants (Jing et al., 2015). It has been previously shown that cyp-aux/iaa double mutants display intermediate phenotypes in both P. patens Ppiaa1b/Ppdgt (Prigge et al., 2010; Lavy et al., 2012) and tomato entire (aux/iaa9)/dgt (Ivanchenko et al., 2015). Jing et al. (2015)Moreover, cis-trans isomerization of the P-P peptide bond have been suggested to regulate the correct folding of AUX/IAA proteins and allowing their degradation (Jing et al., 2015). These authors also demonstrated the physical LTR2-AUX/IAA interaction, cis-proline activity of CYP on the P-P pair of the degron motif and that mutations on the described motif impair degradation (Jing et al., 2015). Previous studies also shown that dgt plants can perceive auxin and alters auxin induction of subset of the Aux/IAA

genes in tomato (Nebenführ et al., 2000). Additionally, mutation of ENTIRE/IAA9, a member of the auxin-responsive Aux/IAA protein family of transcriptional repressors, partially restores the inability of dgt to initiate lateral root primordia but not the primordia outgrowth (Ivanchenko et al., 2015).

Despite significant research efforts evidence of the Cyclophilin A functions in plant remains rather fragmentary. This gene is commonly expressed in both shoots and roots and it is located in both nucleus and cytoplasm during root organogenesis whereas the protein DGT is a mobile signal (Oh et al., 2006; Ivanchenko et al., 2015). The connection between the cyclophilins A and developmental control via auxin signaling has been suggested by using dgt mutants once it affect the expression of Aux/IAA genes family in different levels, depending of the tissue, organ, or even the developmental stage (Nebenführ et al., 2000). Although the role of auxins in the control of development is already well established and much has been investigated about the role of different hormones affecting both plant growth and development, little or nothing is currently known concerning the impacts on the manipulation of auxin signaling and signal transduction on energy metabolism. Plant mitochondria play an essential and key role in the biosynthesis of adenosine triphosphate (ATP) through oxidative phosphorylation (Møller, 2001; Plaxton and Tran, 2011). Accordingly, the tricarboxylic acid (TCA) cycle in the mitochondria is fundamental in catalyzing the oxidation of acetyl-CoA into CO_2, simultaneously producing NADH, $FADH_2$, ATP and carbon skeletons which act as substrate for several other metabolic processes (Fernie et al., 2004; Araujo et al., 2012). These compounds are essential to support plant growth and are of pivotal importance in responses to different environmental conditions (Millar et al., 2011; Berkowitz et al., 2016; Mishra and Chan, 2016). Compelling evidence has recently demonstrated that plant hormones can regulate networks affecting mitochondrial metabolism (Berkowitz et al., 2016). Interestingly, it has previously been suggested that auxin regulates mitochondrial respiration to meet the increased energy demand for growing cells (Leonova et al., 1985). Although the role of auxin in controlling plant growth and development is well established, our understanding on the interaction between auxin and central metabolism remains limited. That said, early findings demonstrated that compounds that inhibit the TCA cycle and respiratory chain also inhibited auxin-induced growth (Thimann, 1977). However, the possible connections between auxin signaling and metabolic aspects of whole plant function

remains to be elucidated. To investigate how and to which extent auxin impact metabolic processes, here we used tomato mutants as a model system to elucidate the impact of auxin signaling in leaf primary metabolism. For this purpose, tomato mutants with either increased (entire) or reduced (diageotropica, dgt) auxin signaling, both in cv. Micro-Tom, were used.

Layout and aims of the chapters

This thesis is largely focused on the role of auxin signaling in different tissues and during fruit development. Thus, the main objectives of this work were: (i) to gain more insights into how and to which extent manipulation of auxin signaling might differently affect plant growth in general; (ii) to identify novel connections between auxin signaling and fruit ripening, from a metabolic viewpoint. To reach these goals several different but complementary experimental approaches were undertaken and therefore this thesis is organized as a compilation of four independent stand-alone chapters. In each chapter an introduction and discussion as well as details of the methods used are included. At the end of this thesis, one chapter entitled “Concluding Remarks” synthesizes the main findings of this work and a brief discussion about the challenges and perspectives in understanding auxin signaling function during plant development is additionally presented.

Chapter 2- Can stable isotope mass spectrometry replace radiolabelled approaches in metabolic studies?

The metabolic network is one of the best characterized networks within biological systems. Plant metabolic studies were relatively neglected for a couple of decades, but they have received tremendous attention in the last decade. Metabolic pathways and the key regulatory points thereof can be deduced using isotopically labelled substrates. In this chapter we offer an important complement to other post-genomic strategies such as metabolite profiling providing insights into the regulation of the metabolic network and thus allowing a more thorough description of plant cellular function.

Chapter 3 - Auxin signaling modulates tomato plant growth through changes in photosynthetic and mitochondrial metabolism

The role of auxin in growth and development has been extensively explored. Furthermore, the use of genetic and biochemical studies has allowed major advances in identifying the maintenance of their levels. Changes in the levels of this hormone, as well as its response to it are usually characterized by dramatic phenotypes and visible changes in growth. We show that mutations in auxin signaling compromise photosynthetic capacity and alter primary metabolism, modulating growth through significant alterations in the mitochondrial respiratory process. This study brings novel insights into the ability of auxin to control plant growth by adjusting leaf central metabolism and simultaneously impacting both photosynthetic and respiratory metabolism. Collectively, our findings suggest that alterations in auxin signaling have dramatic effects on primary metabolism, particularly on photosynthesis and respiratory process, which impact whole plant growth and function. Our results collectively indicate that auxin acts as an integrator of developmental and metabolic programs and suggests that the altered auxin signaling affects both mitochondrial and chloroplastidic metabolism in illuminated leaves.

Chapter 4 – The auxin-resistant diageotropica is an essential gene during tomato ripening

Fruit ripening is a highly complex process which is regulated by phytohormones. Auxin plays an important role during the initial stages of fruit establishment, once it participates in cell division and thus controlling the final fruit size. Although fruit ripening and its regulation have been extensively studied in fruits with different characters, the metabolic role auxin signaling play during this process remains unknown. To shed new light on the significance of auxin signaling in metabolic processes taking place during fruit ripening a range of parameters associated with fruit quality, pigment metabolism, and primary metabolite profiling were analyzed. Our results demonstrated that changes in ripening in auxin signaling mutants occur with relatively fewer changes in primary metabolism. Altogether, the uncovered data demonstrate the involvement of auxin signaling in controlling the mains steps from fruit set to ripening, by modifying

sugar content and starch metabolism. Our results also provide novel insights into the connections between auxin signaling and respiratory pathway.

Chapter 5 - Concluding remarks

Altogether, the results of this work clearly shown that auxin is involved on various processes of plant development. Moreover, our results indicate that this action is highly dependent on tissue, auxin concentration and/or developmental stage. Reductions in auxin signaling promoted a significant impact on growth and primary metabolism in leaves whilst it also impacted tomato fruit ripening with seemingly minor changes in comparison to leaf tissues. In this brief section I will discuss and integrate the results obtained in the previous chapters discussing potential regulatory modes governing this intricate metabolic network. Finally, possible avenues for future research on this topic are provided.

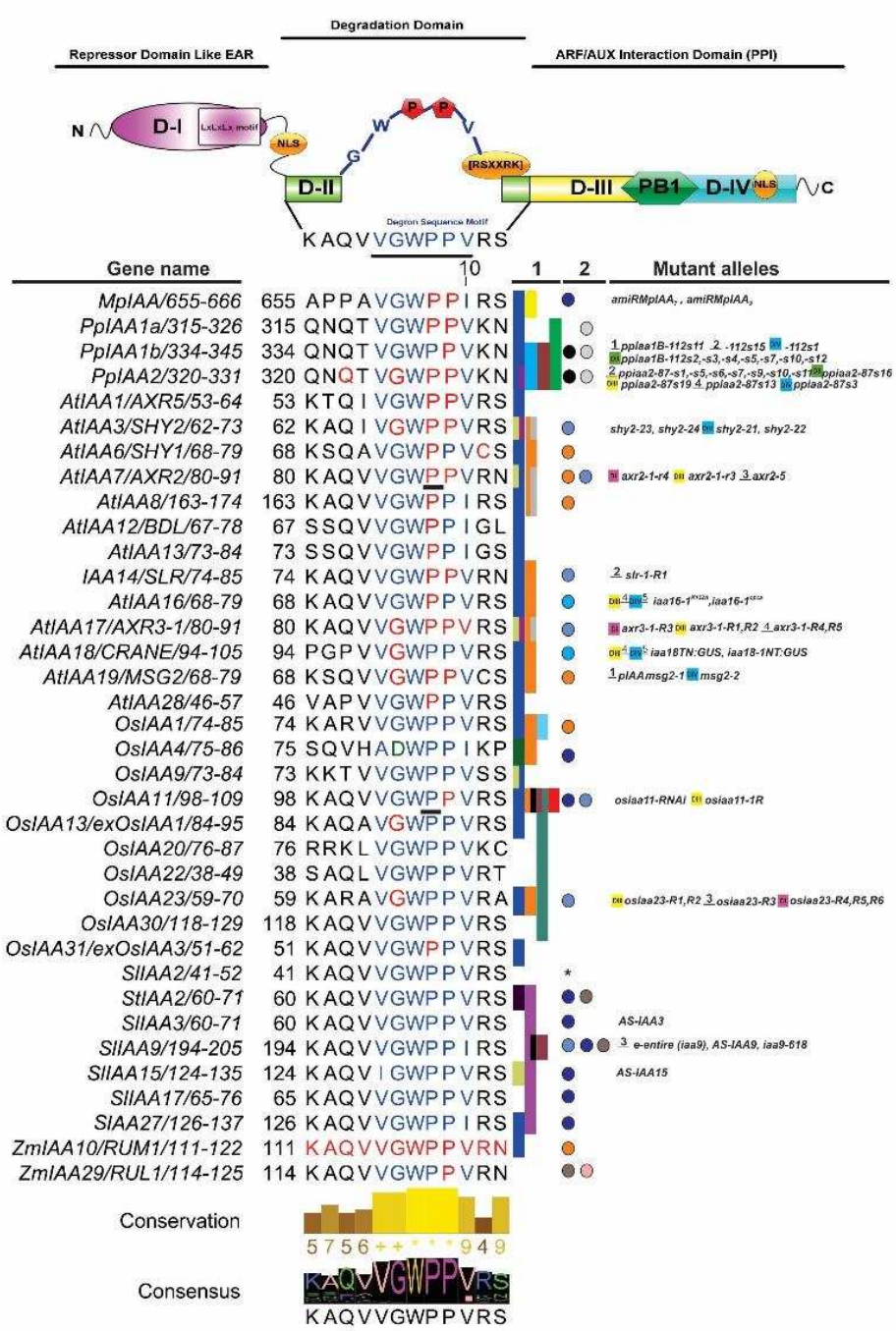

Fig. 3 - **Multiple Protein sequences alignment of Aux/IAA family in different species**. The amino acids sequencies aligment are showing the 4 domains presented in IAAs proteins: DI, Repressor domain like EAR (see in purple), DII, Degradation domain (see in light green) in detail the amino acid sequence higly conserved VGWPPV (In blue letters show amino acids beloinging to the dregon motif. Red letters shown amino acids changed in gain-of-function mutants. In black bold letters show cis-prolines confirmed by NMR estructural analysis or bioinformatics predictions. Fiinally the domain III and IV (DIII and DIV) showing in yelow and light blue respectively. Additionaly, the two NLS (see in organge circle-protein sequence). The multiple Protein sequences aligment was performed in Jalview plataform with T-Coffe program and corrected manually. The degron domain and the region of prolin (P)-prolin (P) (see in red letters) are presented for diferents species such as Marchantia polymorha, Physcomitrella patens, Arabidopsis thaliana, Oryza sativa, Solanum tuberosum, Solanum lycopersicum and Zea mays of different Aux/IAAs proteins. Iin additon, the conservation and consensus amino acids sequence are presentes below of protein aligment. Complementary, on the right side of the figure, is added according with the literature discription of gain and loss-of-fuction of Aux/IAAs and some auxin sensitivity and phenotipes of differents proteins in differents species (see number 1). In number 2, more information is gaved about CYP and the imporantance of onterection of P-P and their function as a peptidil-prolyl cis-trans isomerase of IAAs. In circle under differents colors are presented the mutantion kind.

Additional information

Material used in the alignment figure

The multiple Protein sequences aligment was performed in Jalview plataform (Waterhouse et al., 2009) with T-Coffe program and corrected manually. Proteins are listed bellow: BAS06558.1 MpIAA [Marchantia polymorha] (Flores-Sandoval et al., 2015; Kato et al., 2015); Q948Q2 PpIAA1a [Physcomitrella patens], Q948Q1 PpIAA1b [Physcomitrella patens], A9SFF9 PpIAA2 [Physcomitrella patens] (Prigge et al., 2010; Lavy et al., 2012); P49677 AtIAA1/AXR5 [Arabidopsis thaliana] (Park et al., 2002; Yang et al., 2004); Q38822 AtIAA3/SHY2 [Arabidopsis thaliana] (Kim et al., 1996; Reed et al., 1998; Soh et al., 1999; Tian and Reed, 1999; Tiwari et al., 2001; Tian et al., 2002; Tian et al., 2003; Goh et al., 2012); Q38824 AtIAA6/SHY1 [Arabidopsis thaliana] (Kim et al., 1996; Reed, 2001); Q38825 AtIAA7/AXR2 [Arabidopsis thaliana] (Timpte et al., 1992; Timpte et al., 1994; Colón-Carmona et al., 2000; Nagpal et al., 2000; Gray et al., 2001; Tiwari et al., 2001; Tan et al., 2007; Thommohaway et al., 2007); F4IKE9 AtIAA8 [Arabidopsis thaliana] (Tiwari et al., 2004; Overvoorde et al., 2005; Arase et al., 2012; Wang et al., 2013), Q38830 AtIAA12/BDL [Arabidopsis thaliana] (Hamann et al., 1999; Hamann et al., 2002; Weijers et al., 2005); A0A178VXT0 AtIAA13 [Arabidopsis thaliana] (Tiwari et al., 2004; Weijers et al., 2005); Q38832 IAA14/SLR [Arabidopsis thaliana] (Fukaki et al., 2002; Weijers et al., 2005); O24407 AtIAA16 [Arabidopsis thaliana] (Rinaldi et al., 2012; Korasick et al., 2014); P93830 AtIAA17/AXR3 [Arabidopsis thaliana] (Leyser et al., 1996; Rouse et al., 1998; Gray et al., 2001; Overvoorde et al., 2005; Pérez-Pérez et al., 2010); O24408 AtIAA18/CRANE [Arabidopsis thaliana] (Reed, 2001; Tiwari et al., 2004; Uehara et al., 2008); O24409 AtIAA19/MSG2 [Arabidopsis thaliana] (Tiwari et al., 2001; Tatematsu et al., 2004); Q9XFM0 AtIAA28 [Arabidopsis thaliana] (Rogg et al., 2001); Q5VRD1 OsIAA1 [Oryza sativa] (Song and Xu, 2013; Jing et al., 2015), A2ZRY8 OsIAA4 [Oryza sativa] (Song and Xu, 2013); Q6K846 OsIAA9 [Oryza sativa] (Luo et al., 2015); Q75GK0 OsIAA11 [Oryza sativa] (Zhu et al., 2012; Jing et al., 2015); Q10D34 OsIAA13/Ex OsIAA1 [Oryza sativa] (Thakur et al., 2001; Kitomi et al., 2012; Jing et al., 2015); Q5VRR0 OsIAA20 [Oryza sativa], Q69TU6 OsIAA22 [Oryza sativa], Q69VE0 OsIAA23 [Oryza sativa] (Jun et al., 2011; Jing et al., 2015), P0C132 OsIAA30 [Oryza sativa] (Jing et al.,

2015), P0C133 OsIAA31/ex OsIAA3 [Oryza sativa] (Nakamura et al., 2006; Sakamoto et al., 2013), A0MWP6 StIAA2 [Solanum tuberosum] (Kloosterman et al., 2006), G9HPV3 IAA2 [Solanum lycopersicum] (Audran-Delalande et al., 2012); G9HPV4 SlIAA3 [Solanum lycopersicum] (Chaabouni et al., 2009); K4BUC3 IAA9 [Solanum lycopersicum] and (Wang et al., 2005; Zhang et al., 2007; Mazzucato et al., 2015; Ueta et al., 2017) and this work, G9HPW3 SlIAA15 [Solanum lycopersicum] (Deng et al., 2012; Deng et al., 2012; Xu et al., 2015) ; G9HPW5 SlIAA17 [Solanum lycopersicum] (Su et al., 2015), G9HPX1 SlIAA27 [Solanum lycopersicum] (Bassa et al., 2012; Bassa et al., 2013); GRMZM2G037368 ZmIAA10/RUM1 [Zea mays] (Woll et al., 2005; von Behrens et al., 2011); GRMZM2G163848 ZmIAA29/RUL1 [Zea mays] (Zhang et al., 2015).

REFERENCE

Abel S, Nguyen MD, Theologis A (1995) ThePS-IAA4/5-like Family of Early Auxin-inducible mRNAs inArabidopsis thaliana. Journal of molecular biology **251:** 533-549

Arase F, Nishitani H, Egusa M, Nishimoto N, Sakurai S, Sakamoto N, Kaminaka H (2012) IAA8 involved in lateral root formation interacts with the TIR1 auxin receptor and ARF transcription factors in Arabidopsis. PLoS One **7:** e43414

Araujo WL, Nunes-Nesi A, Nikoloski Z, Sweetlove LJ, Fernie AR (2012) Metabolic control and regulation of the tricarboxylic acid cycle in photosynthetic and heterotrophic plant tissues. Plant, Cell & Environment **35:** 1-21

Audran-Delalande C, Bassa C, Mila I, Regad F, Zouine M, Bouzayen M (2012) Genome-wide identification, functional analysis and expression profiling of the Aux/IAA gene family in tomato. Plant and Cell Physiology **53:** 659-672

Azizi P, Rafii M, Maziah M, Abdullah S, Hanafi M, Latif M, Rashid A, Sahebi M (2015) Understanding the shoot apical meristem regulation: A study of the phytohormones, auxin and cytokinin, in rice. Mechanisms of development **135:** 1-15

Bahyrycz A, Konopińska D (2007) Plant signalling peptides: some recent developments. Journal of Peptide Science **13:** 787-797

Balbi V, Lomax TL (2003) Regulation of Early Tomato Fruit Development by theDiageotropica Gene. Plant Physiology **131:** 186-197

Bassa C, Etemadi M, Combier J-P, Bouzayen M, Audran-Delalande C (2013) Sl-IAA27 gene expression is induced during arbuscular mycorrhizal symbiosis in tomato and in Medicago truncatula. Plant Signaling & Behavior **8:** e25637

Bassa C, Mila I, Bouzayen M, Audran-Delalande C (2012) Phenotypes associated with down-regulation of Sl-IAA27 support functional diversity among Aux/IAA family members in tomato. Plant and cell physiology **53:** 1583-1595

Berkowitz O, De Clercq I, Van Breusegem F, Whelan J (2016) Interaction between hormonal and mitochondrial signalling during growth, development and in plant defence responses. Plant, cell & environment

Blakeslee JJ, Peer WA, Murphy AS (2005) Auxin transport. Current Opinion in Plant Biology **8:** 494-500

Carvalho RF, Campos ML, Pino LE, Crestana SL, Zsögön A, Lima JE, Benedito VA, Peres LE (2011) Convergence of developmental mutants into a single tomato model system:'Micro-Tom'as an effective toolkit for plant development research. Plant Methods **7:** 1-14

Casimiro I, Marchant A, Bhalerao RP, Beeckman T, Dhooge S, Swarup R, Graham N, Inzé D, Sandberg G, Casero PJ (2001) Auxin transport promotes Arabidopsis lateral root initiation. The Plant Cell Online **13:** 843-852

Chaabouni S, Jones B, Delalande C, Wang H, Li Z, Mila I, Frasse P, Latché A, Pech J-C, Bouzayen M (2009) Sl-IAA3, a tomato Aux/IAA at the crossroads of auxin and ethylene signalling involved in differential growth. Journal of Experimental Botany **60:** 1349-1362

Cheng Y, Dai X, Zhao Y (2006) Auxin biosynthesis by the YUCCA flavin monooxygenases controls the formation of floral organs and vascular tissues in Arabidopsis. Genes Dev **20:** 1790-1799

Cho M, Cho H (2013) The function of ABCB transporters in auxin transport. Plant Signaling & Behavior **8:** e22990

Cho M, Lee SH, Cho H-T (2007) P-Glycoprotein4 displays auxin efflux transporter–like action in Arabidopsis root hair cells and tobacco cells. The Plant Cell **19:** 3930-3943

Coenen C, Bierfreund N, Lüthen H, Neuhaus G (2002) Developmental regulation of H+-ATPase-dependent auxin responses in the diageotropica mutant of tomato (Lycopersicon esculentum). Physiologia Plantarum **114:** 461-471

Colón-Carmona A, Chen DL, Yeh K-C, Abel S (2000) Aux/IAA proteins are phosphorylated by phytochrome in vitro. Plant Physiology **124:** 1728-1738

Darwin C, Darwin FE (1888) The'Power of movement in plants.'--1880.

Davies PJ (2010) The Plant Hormones: Their Nature, Occurrence, and Functions. In PJ Davies, ed, Plant Hormones: Biosynthesis, Signal Transduction, Action! Springer Netherlands, Dordrecht, pp 1-15

Delker C, Raschke A, Quint M (2008) Auxin dynamics: the dazzling complexity of a small molecule's message. Planta **227:** 929-941

Deng W, Yan F, Liu M, Wang X, Li Z (2012) Down-regulation of SlIAA15 in tomato altered stem xylem development and production of volatile compounds in leaf exudates. Plant signaling & behavior **7:** 911-913

Deng W, Yang Y, Ren Z, Audran-Delalande C, Mila I, Wang X, Song H, Hu Y, Bouzayen M, Li Z (2012) The tomato SlIAA15 is involved in trichome formation and axillary shoot development. New Phytologist **194:** 379-390

Dharmasiri N, Dharmasiri S, Estelle M (2005) The F-box protein TIR1 is an auxin receptor. Nature **435:** 441-445

Dharmasiri N, Dharmasiri S, Weijers D, Lechner E, Yamada M, Hobbie L, Ehrismann JS, Jürgens G, Estelle M (2005) Plant development is regulated by a family of auxin receptor F box proteins. Developmental cell **9:** 109-119

Dinesh DC, Villalobos LIAC, Abel S (2016) Structural biology of nuclear auxin action. Trends in plant science **21:** 302-316

Dreher KA, Brown J, Saw RE, Callis J (2006) The Arabidopsis Aux/IAA protein family has diversified in degradation and auxin responsiveness. The Plant Cell **18:** 699-714

Enders TA, Strader LC (2015) Auxin activity: Past, present, and future. American journal of botany **102:** 180-196

Fernie AR, Trethewey RN, Krotzky AJ, Willmitzer L (2004) Metabolite profiling: from diagnostics to systems biology. Nature reviews molecular cell biology **5:** 763-769

Flores-Sandoval E, Eklund DM, Bowman JL (2015) A simple auxin transcriptional response system regulates multiple morphogenetic processes in the liverwort Marchantia polymorpha. PLoS genetics **11:** e1005207

Fukaki H, Okushima Y, Tasaka M (2005) Regulation of lateral root formation by auxin signaling in Arabidopsis. Plant biotechnology **22:** 393-399

Fukaki H, Tameda S, Masuda H, Tasaka M (2002) Lateral root formation is blocked by a gain-of-function mutation in the SOLITARY-ROOT/IAA14 gene of Arabidopsis. The Plant Journal **29:** 153-168

Gao J, Cao X, Shi S, Ma Y, Wang K, Liu S, Chen D, Chen Q, Ma H (2016) Genome-wide survey of Aux/IAA gene family members in potato (Solanum tuberosum): Identification, expression analysis, and evaluation of their roles in tuber development. Biochemical and biophysical research communications **471:** 320-327

Goh T, Kasahara H, Mimura T, Kamiya Y, Fukaki H (2012) Multiple AUX/IAA–ARF modules regulate lateral root formation: the role of Arabidopsis SHY2/IAA3-mediated auxin signalling. Phil. Trans. R. Soc. B **367:** 1461-1468

Gray WM, Kepinski S, Rouse D, Leyser O, Estelle M (2001) Auxin regulates SCFTIR1-dependent degradation of AUX/IAA proteins. Nature **414:** 271-276

Guilfoyle TJ (2015) The PB1 domain in auxin response factor and Aux/IAA proteins: a versatile protein interaction module in the auxin response. The Plant Cell **27:** 33-43

Guilfoyle TJ, Hagen G (2007) Auxin response factors. Current opinion in plant biology **10:** 453-460

Hagen G, Guilfoyle T (2002) Auxin-responsive gene expression: genes, promoters and regulatory factors. Plant molecular biology **49:** 373-385

Hamann T, Benkova E, Bäurle I, Kientz M, Jürgens G (2002) The Arabidopsis BODENLOS gene encodes an auxin response protein inhibiting MONOPTEROS-mediated embryo patterning. Genes & Development **16:** 1610-1615

Hamann T, Mayer U, Jurgens G (1999) The auxin-insensitive bodenlos mutation affects primary root formation and apical-basal patterning in the Arabidopsis embryo. Development **126:** 1387-1395

Han M, Park Y, Kim I, Kim E-H, Yu T-K, Rhee S, Suh J-Y (2014) Structural basis for the auxin-induced transcriptional regulation by Aux/IAA17. Proceedings of the National Academy of Sciences **111:** 18613-18618

Harrison CJ (2017) Auxin transport in the evolution of branching forms. New Phytologist **215:** 545-551

Hua Z, Vierstra RD (2011) The cullin-RING ubiquitin-protein ligases. Annual review of plant biology **62:** 299-334

Ivanchenko MG, Zhu J, Wang B, Medvecká E, Du Y, Azzarello E, Mancuso S, Megraw M, Filichkin S, Dubrovsky JG (2015) The cyclophilin A DIAGEOTROPICA gene affects auxin transport in both root and shoot to control lateral root formation. Development **142:** 712-721

Jackson MB (1979) Is the diageotropic tomato ethylene deficient? Physiologia Plantarum **46:** 347-351

Jain M, Kaur N, Garg R, Thakur JK, Tyagi AK, Khurana JP (2006) Structure and expression analysis of early auxin-responsive Aux/IAA gene family in rice (Oryza sativa). Functional & integrative genomics **6:** 47-59

Jing H, Yang X, Zhang J, Liu X, Zheng H, Dong G, Nian J, Feng J, Xia B, Qian Q (2015) Peptidyl-prolyl isomerization targets rice Aux/IAAs for proteasomal degradation during auxin signalling. Nature communications **6**

Jones AR, Kramer EM, Knox K, Swarup R, Bennett MJ, Lazarus CM, Leyser HO, Grierson CS (2009) Auxin transport through non-hair cells sustains root-hair development. Nature Cell Biology **11:** 78-84

Jun N, Gaohang W, Zhenxing Z, Huanhuan Z, Yunrong W, Ping W (2011) OsIAA23-mediated auxin signaling defines postembryonic maintenance of QC in rice. The Plant Journal **68:** 433-442

Kamura T, Conrad MN, Yan Q, Conaway RC, Conaway JW (1999) The Rbx1 subunit of SCF and VHL E3 ubiquitin ligase activates Rub1 modification of cullins Cdc53 and Cul2. Genes & development **13:** 2928-2933

Kato H, Ishizaki K, Kouno M, Shirakawa M, Bowman JL, Nishihama R, Kohchi T (2015) Auxin-mediated transcriptional system with a minimal set of components

is critical for morphogenesis through the life cycle in Marchantia polymorpha. PLoS genetics **11:** e1005084

Kelly MO, Bradford KJ (1986) Insensitivity of the diageotropica tomato mutant to auxin. Plant Physiology **82:** 713-717

Kenrick P, Crane PR (1997) The origin and early evolution of plants on land. Nature **389:** 33-39

Kim BC, Soh MS, Kang BJ, Furuya M, Nam HG (1996) Two dominant photomorphogenic mutations of Arabidopsis thaliana identified as suppressor mutations of hy2. The Plant Journal **9:** 441-456

Kim J, Harter K, Theologis A (1997) Protein–protein interactions among the Aux/IAA proteins. Proceedings of the National Academy of Sciences **94:** 11786-11791

Kitomi Y, Inahashi H, Takehisa H, Sato Y, Inukai Y (2012) OsIAA13-mediated auxin signaling is involved in lateral root initiation in rice. Plant science **190:** 116-122

Kloosterman B, Visser R, Bachem C (2006) Isolation and characterization of a novel potato Auxin/Indole-3-Acetic Acid family member (StIAA2) that is involved in petiole hyponasty and shoot morphogenesis. Plant Physiology and Biochemistry **44:** 766-775

Kögl F, a Haagen-Smit A (1931) Über die Chemie des Wuchsstoffs. Amsterdam Proceedings Section Science **34:** 1411-1416

Korasick DA, Westfall CS, Lee SG, Nanao MH, Dumas R, Hagen G, Guilfoyle TJ, Jez JM, Strader LC (2014) Molecular basis for AUXIN RESPONSE FACTOR protein interaction and the control of auxin response repression. Proceedings of the National Academy of Sciences **111:** 5427-5432

Kramer EM, Ackelsberg EM (2015) Auxin metabolism rates and implications for plant development. Frontiers in Plant Science **6:** 150

Křeček P, Skůpa P, Libus J, Naramoto S, Tejos R, Friml J, Zažímalová E (2009) The PIN-FORMED (PIN) protein family of auxin transporters. Genome Biology **10:** 249-249

Lavy M, Prigge MJ, Tigyi K, Estelle M (2012) The cyclophilin DIAGEOTROPICA has a conserved role in auxin signaling. Development **139:** 1115-1124

Leonova L, Gamburg K, Vojnikov V, Varakina N (1985) Promotion of respiration by auxin in the induction of cell division in suspension culture. Journal of plant growth regulation **4:** 169-176

Leyser H, Pickett FB, Dharmasiri S, Estelle M (1996) Mutations in the AXR3 gene of Arabidopsis result in altered auxin response including ectopic expression from the SAUR-AC1 promoter. The Plant Journal **10:** 403-413

Leyser O (2017) Auxin Signaling. Plant Physiology

Liscum E, Reed J (2002) Genetics of Aux/IAA and ARF action in plant growth and development. Plant molecular biology **49:** 387-400

Ljung K, Hull AK, Kowalczyk M, Marchant A, Celenza J, Cohen JD, Sandberg G (2002) Biosynthesis, conjugation, catabolism and homeostasis of indole-3-acetic acid in Arabidopsis thaliana. In Auxin Molecular Biology. Springer, pp 249-272

Lu Y, Xu J (2015) Phytohormones in microalgae: a new opportunity for microalgal biotechnology? Trends in Plant Science **20:** 273-282

Luo S, Li Q, Liu S, Pinas NM, Tian H, Wang S (2015) Constitutive Expression of OsIAA9 Affects Starch Granules Accumulation and Root Gravitropic Response in Arabidopsis. Frontiers in plant science **6**

Malik P, Zuleger N, Schirmer EC (2009) Transport of inner nuclear membrane proteins. In Nuclear Transport. Landes Bioscience, pp 133-145

Marchant A, Kargul J, May ST, Muller P, Delbarre A, Perrot-Rechenmann C, Bennett MJ (1999) AUX1 regulates root gravitropism in Arabidopsis by facilitating auxin uptake within root apical tissues. The EMBO Journal **18:** 2066-2073

Martins AO, Nunes-Nesi A, Araújo WL, Fernie AR (2018) To bring flowers or do a runner - GAs make the decision. Molecular Plant

Mazzucato A, Cellini F, Bouzayen M, Zouine M, Mila I, Minoia S, Petrozza A, Picarella ME, Ruiu F, Carriero F (2015) A TILLING allele of the tomato Aux/IAA9 gene offers new insights into fruit set mechanisms and perspectives for breeding seedless tomatoes. Molecular breeding **35:** 22

Millar AH, Whelan J, Soole KL, Day DA (2011) Organization and regulation of mitochondrial respiration in plants. Annual review of plant biology **62:** 79-104

Mishra P, Chan DC (2016) Metabolic regulation of mitochondrial dynamics. The Journal of cell biology **212:** 379-387

Møller IM (2001) Plant mitochondria and oxidative stress: electron transport, NADPH turnover, and metabolism of reactive oxygen species. Annual review of plant biology **52:** 561-591

Moon J, Parry G, Estelle M (2004) The ubiquitin-proteasome pathway and plant development. The Plant Cell **16:** 3181-3195

Moss BL, Mao H, Guseman JM, Hinds TR, Hellmuth A, Kovenock M, Noorassa A, Lanctot A, Villalobos LIAC, Zheng N (2015) Rate motifs tune auxin/indole-3-acetic acid degradation dynamics. Plant physiology **169:** 803-813

Nagpal P, Walker LM, Young JC, Sonawala A, Timpte C, Estelle M, Reed JW (2000) AXR2 encodes a member of the Aux/IAA protein family. Plant physiology **123:** 563-574

Nakamura A, Umemura I, Gomi K, Hasegawa Y, Kitano H, Sazuka T, Matsuoka M (2006) Production and characterization of auxin-insensitive rice by overexpression of a mutagenized rice IAA protein. The Plant Journal **46:** 297-306

Nebenführ A, White T, Lomax TL (2000) The diageotropica mutation alters auxin induction of a subset of the Aux/IAA gene family in tomato. Plant molecular biology **44:** 73-84

Novák O, Napier R, Ljung K (2017) Zooming In on Plant Hormone Analysis: Tissue- and Cell-Specific Approaches. Annual Review of Plant Biology **68:** 323-348

Oh K, Ivanchenko MG, White T, Lomax TL (2006) The diageotropica gene of tomato encodes a cyclophilin: a novel player in auxin signaling. Planta **224:** 133-144

Olszewski N, Sun T-p, Gubler F (2002) Gibberellin signaling biosynthesis, catabolism, and response pathways. The Plant Cell **14:** S61-S80

Overvoorde PJ, Okushima Y, Alonso JM, Chan A, Chang C, Ecker JR, Hughes B, Liu A, Onodera C, Quach H (2005) Functional genomic analysis of the AUXIN/INDOLE-3-ACETIC ACID gene family members in Arabidopsis thaliana. The Plant Cell **17:** 3282-3300

Paponov IA, Paponov M, Teale W, Menges M, Chakrabortee S, Murray JA, Palme K (2008) Comprehensive transcriptome analysis of auxin responses in Arabidopsis. Molecular Plant **1:** 321-337

Park JY, Kim HJ, Kim J (2002) Mutation in domain II of IAA1 confers diverse auxin-related phenotypes and represses auxin-activated expression of Aux/IAA genes in steroid regulator-inducible system. The Plant Journal **32:** 669-683

Pattison RJ, Catalá C (2012) Evaluating auxin distribution in tomato (Solanum lycopersicum) through an analysis of the PIN and AUX/LAX gene families. The Plant Journal **70:** 585-598

Pérez-Pérez JM, Candela H, Robles P, López-Torrejón G, Del Pozo JC, Micol JL (2010) A role for AUXIN RESISTANT3 in the coordination of leaf growth. Plant and cell physiology **51:** 1661-1673

Petrášek J, Friml J (2009) Auxin transport routes in plant development. Development **136:** 2675-2688

Pichersky E, Gang DR (2000) Genetics and biochemistry of secondary metabolites in plants: an evolutionary perspective. Trends in plant science **5:** 439-445

Pierre-Jerome E, Moss BL, Nemhauser JL (2013) Tuning the auxin transcriptional response. Journal of experimental botany **64:** 2557-2563

Piya S, Shrestha SK, Binder B, Stewart Jr CN, Hewezi T (2014) Protein-protein interaction and gene co-expression maps of ARFs and Aux/IAAs in Arabidopsis. Frontiers in plant science **5:** 744

Plaxton WC, Tran HT (2011) Metabolic adaptations of phosphate-starved plants. Plant Physiology **156:** 1006-1015

Pollock C, Koltai H, Kapulnik Y, Prandi C, Yarden R (2012) Strigolactones: a novel class of phytohormones that inhibit the growth and survival of breast cancer cells and breast cancer stem-like enriched mammosphere cells. Breast cancer research and treatment **134:** 1041-1055

Prigge MJ, Lavy M, Ashton NW, Estelle M (2010) Physcomitrella patens Auxin-Resistant Mutants Affect Conserved Elements of an Auxin-Signaling Pathway. Current Biology **20:** 1907-1912

Purwestri YA, Susanto FA, Tsuji H (2017) Hd3a Florigen Recruits Different Proteins to Reveal Its Function in Plant Growth and Development. In Plant Engineering. InTech

Quint M, Gray WM (2006) Auxin signaling. Current opinion in plant biology **9:** 448-453

Ramos JA, Zenser N, Leyser O, Callis J (2001) Rapid degradation of auxin/indoleacetic acid proteins requires conserved amino acids of domain II and is proteasome dependent. The Plant Cell **13:** 2349-2360

Reed JW (2001) Roles and activities of Aux/IAA proteins in Arabidopsis. Trends in plant science **6:** 420-425

Reed JW, Elumalai RP, Chory J (1998) Suppressors of an Arabidopsis thaliana phyB mutation identify genes that control light signaling and hypocotyl elongation. Genetics **148:** 1295-1310

Rinaldi MA, Liu J, Enders TA, Bartel B, Strader LC (2012) A gain-of-function mutation in IAA16 confers reduced responses to auxin and abscisic acid and impedes plant growth and fertility. Plant molecular biology **79:** 359-373

Rogg LE, Lasswell J, Bartel B (2001) A gain-of-function mutation in IAA28 suppresses lateral root development. The Plant Cell **13:** 465-480

Ross JJ, Quittenden LJ (2016) Interactions between Brassinosteroids and Gibberellins: Synthesis or Signaling? The Plant Cell **28:** 829-832

Rouse D, Mackay P, Stirnberg P, Estelle M, Leyser O (1998) Changes in auxin response from mutations in an AUX/IAA gene. Science **279:** 1371-1373

Sakamoto T, Morinaka Y, Inukai Y, Kitano H, Fujioka S (2013) Auxin signal transcription factor regulates expression of the brassinosteroid receptor gene in rice. The Plant Journal **73:** 676-688

Salehin M, Bagchi R, Estelle M (2015) SCFTIR1/AFB-based auxin perception: mechanism and role in plant growth and development. The Plant Cell **27:** 9-19

Salehin M, Bagchi R, Estelle M (2015) SCFTIR1/AFB-based auxin perception: mechanism and role in plant growth and development. The Plant Cell Online**:** tpc. 114.133744

Salisbury F, Ross C (1992) Plant Physiology. Belmont, CA: Wadsworth. In. Inc

Sánchez-Rodríguez C, Rubio-Somoza I, Sibout R, Persson S (2010) Phytohormones and the cell wall in Arabidopsis during seedling growth. Trends in plant science **15:** 291-301

Sato A, Yamamoto KT (2008) Overexpression of the non-canonical Aux/IAA genes causes auxin-related aberrant phenotypes in Arabidopsis. Physiologia plantarum **133:** 397-405

Sauer M, Robert S, Kleine-Vehn J (2013) Auxin: simply complicated. Journal of Experimental Botany **64:** 2565-2577

Shabek N, Zheng N (2014) Plant ubiquitin ligases as signaling hubs. Nature structural & molecular biology **21:** 293-296

Soh MS, Hong SH, Kim BC, Vizir I, Park DH, Choi G, Hong MY, Chung Y-Y, Furuya M, Nam HG (1999) Regulation of both light-and auxin-mediated development by theArabidopsis IAA3/SHY2 gene. Journal of Plant Biology **42:** 239

Song Y, Xu Z-F (2013) Ectopic overexpression of an auxin/indole-3-acetic acid (Aux/IAA) Gene OsIAA4 in rice induces morphological changes and reduces responsiveness to auxin. International journal of molecular sciences **14:** 13645-13656

Spíchal L (2012) Cytokinins–recent news and views of evolutionally old molecules. Functional Plant Biology **39:** 267-284

Stepanova AN, Robertson-Hoyt J, Yun J, Benavente LM, Xie D-Y, Doležal K, Schlereth A, Jürgens G, Alonso JM (2008) TAA1-mediated auxin biosynthesis is essential for hormone crosstalk and plant development. Cell **133:** 177-191

The Story of Auxin. (2010) The Plant Cell **22**

Su L, Audran C, Bouzayen M, Roustan J, Chervin C (2015) The Aux/IAA, Sl-IAA17 regulates quality parameters over tomato fruit development. Plant signaling & behavior **10:** e1071001

Swarup R, Kramer EM, Perry P, Knox K, Leyser HO, Haseloff J, Beemster GT, Bhalerao R, Bennett MJ (2005) Root gravitropism requires lateral root cap and epidermal cells for transport and response to a mobile auxin signal. Nature cell biology **7:** 1057-1065

Swarup R, Péret B (2012) AUX/LAX family of auxin influx carriers—an overview. Frontiers in Plant Science **3:** 225

Szemenyei H, Hannon M, Long JA (2008) TOPLESS mediates auxin-dependent transcriptional repression during Arabidopsis embryogenesis. Science **319:** 1384-1386

Tan X, Calderon-Villalobos LIA, Sharon M, Zheng C, Robinson CV, Estelle M, Zheng N (2007) Mechanism of auxin perception by the TIR1 ubiquitin ligase. Nature **446:** 640-645

Tatematsu K, Kumagai S, Muto H, Sato A, Watahiki MK, Harper RM, Liscum E, Yamamoto KT (2004) MASSUGU2 encodes Aux/IAA19, an auxin-regulated protein that functions together with the transcriptional activator NPH4/ARF7 to regulate differential growth responses of hypocotyl and formation of lateral roots in Arabidopsis thaliana. The Plant Cell **16:** 379-393

Thakur JK, Tyagi AK, Khurana JP (2001) OsIAA1, an Aux/IAA cDNA from rice, and changes in its expression as influenced by auxin and light. DNA research **8:** 193-203

Thimann KV (1977) Hormone action in the whole life of plants. Univ of Massachusetts Press

Thines B, Katsir L, Melotto M, Niu Y, Mandaokar A, Liu G, Nomura K, He SY, Howe GA (2007) JAZ repressor proteins are targets of the SCFCOI1 complex during jasmonate signalling. Nature **448:** 661-665

Thommohaway C, Kanlayanarat S, Uthairatanakij A, Jitareerat P (2007) Quality of fresh-cut guava (Psidium guajava L.) as affected by chitosan treatment. In International Conference on Quality Management of Fresh Cut Produce 746, pp 449-454

Tian Q, Nagpal P, Reed JW (2003) Regulation of Arabidopsis SHY2/IAA3 protein turnover. The Plant Journal **36:** 643-651

Tian Q, Reed JW (1999) Control of auxin-regulated root development by the Arabidopsis thaliana SHY2/IAA3 gene. Development **126:** 711-721

Tian Q, Uhlir NJ, Reed JW (2002) Arabidopsis SHY2/IAA3 inhibits auxin-regulated gene expression. The Plant Cell **14:** 301-319

Timpte C, Wilson AK, Estelle M (1994) The axr2-1 mutation of Arabidopsis thaliana is a gain-of-function mutation that disrupts an early step in auxin response. Genetics **138:** 1239-1249

Timpte CS, Wilson AK, Estelle M (1992) Effects of the axr2 mutation of Arabidopsis on cell shape in hypocotyl and inflorescence. Planta **188:** 271-278

Tivendale ND, Ross JJ, Cohen JD (2014) The shifting paradigms of auxin biosynthesis. Trends in plant science **19:** 44-51

Tiwari SB, Hagen G, Guilfoyle T (2003) The roles of auxin response factor domains in auxin-responsive transcription. The Plant Cell **15:** 533-543

Tiwari SB, Hagen G, Guilfoyle TJ (2004) Aux/IAA proteins contain a potent transcriptional repression domain. The Plant Cell **16:** 533-543

Tiwari SB, Wang X-J, Hagen G, Guilfoyle TJ (2001) AUX/IAA proteins are active repressors, and their stability and activity are modulated by auxin. The Plant Cell **13:** 2809-2822

Uehara T, Okushima Y, Mimura T, Tasaka M, Fukaki H (2008) Domain II mutations in CRANE/IAA18 suppress lateral root formation and affect shoot development in Arabidopsis thaliana. Plant and Cell Physiology **49:** 1025-1038

Ueta R, Abe C, Watanabe T, Sugano SS, Ishihara R, Ezura H, Osakabe Y, Osakabe K (2017) Rapid breeding of parthenocarpic tomato plants using CRISPR/Cas9. Scientific Reports **7**

Ugartechea-Chirino Y, Swarup R, Swarup K, Péret B, Whitworth M, Bennett M, Bougourd S (2009) The AUX1 LAX family of auxin influx carriers is required for the establishment of embryonic root cell organization in Arabidopsis thaliana. Annals of botany**:** mcp287

Ulmasov T, Hagen G, Guilfoyle TJ (1999) Dimerization and DNA binding of auxin response factors. The Plant Journal **19:** 309-319

Ulmasov T, Liu Z-B, Hagen G, Guilfoyle TJ (1995) Composite structure of auxin response elements. The Plant Cell Online **7:** 1611-1623

Ulmasov T, Murfett J, Hagen G, Guilfoyle TJ (1997) Aux/IAA proteins repress expression of reporter genes containing natural and highly active synthetic auxin response elements. The Plant Cell **9:** 1963-1971

van Rongen M (2018) The role of auxin transport in the control of shoot branching. University of Cambridge
Vanneste S, Friml J (2009) Auxin: a trigger for change in plant development. Cell **136:** 1005-1016
Vanstraelen M, Benková E (2012) Hormonal interactions in the regulation of plant development. Annual review of cell and developmental biology **28:** 463-487
von Behrens I, Komatsu M, Zhang Y, Berendzen KW, Niu X, Sakai H, Taramino G, Hochholdinger F (2011) Rootless with undetectable meristem 1 encodes a monocot-specific AUX/IAA protein that controls embryonic seminal and post-embryonic lateral root initiation in maize. The Plant Journal **66:** 341-353
Voß U, Bishopp A, Farcot E, Bennett MJ (2014) Modelling hormonal response and development. Trends in plant science **19:** 311-319
Wang H, Jones B, Li Z, Frasse P, Delalande C, Regad F, Chaabouni S, Latche A, Pech J-C, Bouzayen M (2005) The tomato Aux/IAA transcription factor IAA9 is involved in fruit development and leaf morphogenesis. The Plant Cell **17:** 2676-2692
Wang H, Jones B, Li Z, Frasse P, Delalande C, Regad F, Chaabouni S, Latche A, Pech J-C, Bouzayen M (2005) The tomato Aux/IAA transcription factor IAA9 is involved in fruit development and leaf morphogenesis. The Plant Cell Online **17:** 2676-2692
Wang J, Yan D-W, Yuan T-T, Gao X, Lu Y-T (2013) A gain-of-function mutation in IAA8 alters Arabidopsis floral organ development by change of jasmonic acid level. Plant molecular biology **82:** 71-83
Wang Y, Deng D, Bian Y, Lv Y, Xie Q (2010) Genome-wide analysis of primary auxin-responsive Aux/IAA gene family in maize (Zea mays. L.). Molecular biology reports **37:** 3991-4001
Wang YH, Irving HR (2011) Developing a model of plant hormone interactions. Plant Signaling & Behavior **6:** 494-500
Waterhouse AM, Procter JB, Martin DM, Clamp M, Barton GJ (2009) Jalview Version 2—a multiple sequence alignment editor and analysis workbench. Bioinformatics **25:** 1189-1191
Weijers D, Benkova E, Jäger KE, Schlereth A, Hamann T, Kientz M, Wilmoth JC, Reed JW, Jürgens G (2005) Developmental specificity of auxin response by pairs of ARF and Aux/IAA transcriptional regulators. The EMBO journal **24:** 1874-1885
Went FW (1926) On growth-accelerating substances in the coleoptile of Avena sativa. In Proc. Kon. Ned. Akad. Wet, Vol 30, p 1
Went FW (1927) Wuchsstoff und wachstum. De Bussy
Went FW (1937) Phytohormones.
Wheeler JI, Irving HR (2010) Evolutionary advantages of secreted peptide signalling molecules in plants. Functional Plant Biology **37:** 382-394
Wildman S (1997) The auxin-A, B enigma: scientific fraud or scientific ineptitude? Plant growth regulation **22:** 37-68
Winkler M, Niemeyer M, Hellmuth A, Janitza P, Christ G, Samodelov SL, Wilde V, Majovsky P, Trujillo M, Zurbriggen MD (2017) Variation in auxin sensing guides AUX/IAA transcriptional repressor ubiquitylation and destruction. Nature communications **8:** 15706
Woll K, Borsuk LA, Stransky H, Nettleton D, Schnable PS, Hochholdinger F (2005) Isolation, characterization, and pericycle-specific transcriptome analyses

of the novel maize lateral and seminal root initiation mutant rum1. Plant physiology **139:** 1255-1267

Wolters H, Anders N, Geldner N, Gavidia R, Jürgens G (2011) Coordination of apical and basal embryo development revealed by tissue-specific GNOM functions. Development **138:** 117-126

Wolters H, Jürgens G (2009) Survival of the flexible: hormonal growth control and adaptation in plant development. Nature Reviews Genetics **10:** 305-317

Woodward AW, Bartel B (2005) Auxin: regulation, action, and interaction. Ann Bot **95:** 707-735

Worley CK, Zenser N, Ramos J, Rouse D, Leyser O, Theologis A, Callis J (2000) Degradation of Aux/IAA proteins is essential for normal auxin signalling. The Plant Journal **21:** 553-562

Wu J, Peng Z, Liu S, He Y, Cheng L, Kong F, Wang J, Lu G (2012) Genome-wide analysis of Aux/IAA gene family in Solanaceae species using tomato as a model. Molecular Genetics and Genomics **287:** 295-311

Wu W, Liu Y, Wang Y, Li H, Liu J, Tan J, He J, Bai J, Ma H (2017) Evolution Analysis of the Aux/IAA Gene Family in Plants Shows Dual Origins and Variable Nuclear Localization Signals. International Journal of Molecular Sciences **18:** 2107

Xu T, Wang Y, Liu X, Gao S, Qi M, Li T (2015) Solanum lycopersicum IAA15 functions in the 2, 4-dichlorophenoxyacetic acid herbicide mechanism of action by mediating abscisic acid signalling. Journal of experimental botany **66:** 3977-3990

Yamada M, Greenham K, Prigge MJ, Jensen PJ, Estelle M (2009) The TRANSPORT INHIBITOR RESPONSE2 gene is required for auxin synthesis and diverse aspects of plant development. Plant physiology **151:** 168-179

Yang X, Lee S, So Jh, Dharmasiri S, Dharmasiri N, Ge L, Jensen C, Hangarter R, Hobbie L, Estelle M (2004) The IAA1 protein is encoded by AXR5 and is a substrate of SCFTIR1. The Plant Journal **40:** 772-782

Yue J, Hu X, Huang J (2014) Origin of plant auxin biosynthesis. Trends in plant science **19:** 764-770

Zaharah SS, Singh Z, Symons GM, Reid JB (2012) Role of Brassinosteroids, Ethylene, Abscisic Acid, and Indole-3-Acetic Acid in Mango Fruit Ripening. Journal of Plant Growth Regulation **31:** 363-372

Zažímalová E, Murphy AS, Yang H, Hoyerová K, Hošek P (2010) Auxin transporters—why so many? Cold Spring Harbor perspectives in biology **2:** a001552

Zenser N, Dreher KA, Edwards SR, Callis J (2003) Acceleration of Aux/IAA proteolysis is specific for auxin and independent of AXR1. The Plant Journal **35:** 285-294

Zenser N, Ellsmore A, Leasure C, Callis J (2001) Auxin modulates the degradation rate of Aux/IAA proteins. Proceedings of the National Academy of Sciences **98:** 11795-11800

Zhang J, Chen R, Xiao J, Qian C, Wang T, Li H, Ouyang B, Ye Z (2007) A single-base deletion mutation in SlIAA9 gene causes tomato (Solanum lycopersicum) entire mutant. Journal of plant research **120:** 671-678

Zhao Y (2010) Auxin biosynthesis and its role in plant development. Annu Rev Plant Biol **61:** 49-64

Zhao Y (2012) Auxin biosynthesis: a simple two-step pathway converts tryptophan to indole-3-acetic acid in plants. Molecular plant **5:** 334-338

Zhao Y, Christensen SK, Fankhauser C, Cashman JR, Cohen JD, Weigel D, Chory J (2001) A role for flavin monooxygenase-like enzymes in auxin biosynthesis. Science **291:** 306-309

Zheng N, Schulman BA, Song L, Miller JJ, Jeffrey PD, Wang P, Chu C, Koepp DM, Elledge SJ, Pagano M (2002) Structure of the Cul1–Rbx1–Skp1–F boxSkp2 SCF ubiquitin ligase complex. Nature **416:** 703-709

Zhu Z-X, Liu Y, Liu S-J, Mao C-Z, Wu Y-R, Wu P (2012) A Gain-of-Function Mutation in OsIAA11 Affects Lateral Root Development in Rice. Molecular Plant **5:** 154-161

Zobel R (1973) Some physiological characteristics of the ethylene-requiring tomato mutant diageotropica. Plant Physiology **52:** 385-389

Zobel R (1974) Control of morphogenesis in the ethylene-requiring tomato mutant, diageotropica. Canadian Journal of Botany **52:** 735-741

Zouine M, Fu Y, Chateigner-Boutin A-L, Mila I, Frasse P, Wang H, Audran C, Roustan J-P, Bouzayen M (2014) Characterization of the tomato ARF gene family uncovers a multi-levels post-transcriptional regulation including alternative splicing. PloS one **9:** e84203

CHAPTER 2

Can stable isotope mass spectrometry replace radiolabelled approaches in metabolic studies?

Chapter 2: Publications

Can stable isotope mass spectrometry replace radiolabelled approaches in metabolic studies?

Willian Batista Silva[a], Danilo M. Daloso[b], Alisdair R. Fernie[b], Adriano Nunes-Nesi[a], Wagner L. Araújo[a,*]

a Max Planck Partner Group at the Departamento de Biologia Vegetal, Universidade Federal de Viçosa, 36570-900, Viçosa-MG, Brazil

b Max-Planck-Institute of Molecular Plant Physiology Am Mühlenberg 1, 14476,Golm Potsdam, Germany

Type of authorship:	First author
Type of article:	Review article
Share of the work:	85%
Contribution to the publication:	Planned and performed the review, analyzed, prepared part of the figures and wrote parts of the paper
Journal:	Plant Science
5-year impact factor:	4.148
Date of publication:	13 of May 2016
Number of citations (google Scholar on March 21, 2018):	7
DOI:	10.1016/j.plantsci.2016.05.011
PubMed-ID:	27297990

Plant Science 249 (2016) 59–69

Contents lists available at ScienceDirect

Plant Science

journal homepage: www.elsevier.com/locate/plantsci

Review article

Can stable isotope mass spectrometry replace radiolabelled approaches in metabolic studies?

Willian Batista Silva[a], Danilo M. Daloso[b], Alisdair R. Fernie[b], Adriano Nunes-Nesi[a], Wagner L. Araújo[a,*]

[a] Max Planck Partner Group at the Departamento de Biologia Vegetal, Universidade Federal de Viçosa, 36570-900, Viçosa-MG, Brazil
[b] Max-Planck-Institute of Molecular Plant Physiology Am Mühlenberg 1, 14476,Golm Potsdam, Germany

ARTICLE INFO

Article history:
Received 24 November 2015
Received in revised form 21 April 2016
Accepted 13 May 2016
Available online 14 May 2016

Keywords:
Flux profiling
Isotopic labelling
Metabolic flux analysis
Plant systems biology
Primary metabolism

ABSTRACT

Metabolic pathways and the key regulatory points thereof can be deduced using isotopically labelled substrates. One prerequisite is the accurate measurement of the labeling pattern of targeted metabolites. The subsequent estimation of metabolic fluxes following incubation in radiolabelled substrates has been extensively used. Radiolabelling is a sensitive approach and allows determination of total label uptake since the total radiolabel content is easy to detect. However, the incubation of cells, tissues or the whole plant in a stable isotope enriched environment and the use of either mass spectrometry or nuclear magnetic resonance techniques to determine label incorporation within specific metabolites offers the possibility to readily obtain metabolic information with higher resolution. It additionally also offers an important complement to other post-genomic strategies such as metabolite profiling providing insights into the regulation of the metabolic network and thus allowing a more thorough description of plant cellular function. Thus, although safety concerns mean that stable isotope feeding is generally preferred, the techniques are in truth highly complementary and application of both approaches in tandem currently probably provides the best route towards a comprehensive understanding of plant cellular metabolism.
© 2016 Elsevier Ireland Ltd. All rights reserved.

Contents

1. Introduction

Metabolomics, the study of the metabolite complement of an organism or cell within a particular physiological condition, is a rapidly expanding research field with several applications ranging from broad phenotyping and diagnostic analysis to metabolic engineering and systems biology. Indeed, the metabolic network is one of the best characterized networks within biological systems. Plant metabolic studies were relatively neglected for a couple of decades, but they have received tremendous attention in the last decade [1], with significant developments in metabolite profiling considerably contributing to this renaissance. This is, at least in part, associated with such issues as the rising demand for bioenergy, concerns about crop yield stability particularly under the enhanced stress conditions anticipated with climate change, and bioprospecting for

* Corresponding author at: Departamento de Biologia Vegetal, Universidade Federal de Viçosa, Viçosa, 36570-900 Minas Gerais, Brazil.
E-mail addresses: williambatistadasilva@gmail.com (W. Batista Silva), daloso@mpimp-golm.mpg.de (D.M. Daloso), fernie@mpimp-golm.mpg.de (A.R. Fernie), nunesnesi@ufv.br (A. Nunes-Nesi), wlaraujo@ufv.br (W.L. Araújo).

http://dx.doi.org/10.1016/j.plantsci.2016.05.011
0168-9452/© 2016 Elsevier Ireland Ltd. All rights reserved.

active natural products with significant efficacy against human diseases. Metabolomics is a relatively young science but there is a vast history of biochemistry and analytical chemistry studies underpinning it. In fact, pioneering studies which established key metabolic pathways such as the tricarboxylic acid (TCA) cycle [2–5], as well as the glyoxylate [6] and the Calvin-Benson [7] cycles of plants were of pivotal importance in defining the structure of metabolic pathways. Thus, there is a vast body of descriptive and mechanistic data related to unravelling plant metabolic pathways and their regulation [8]. This fact notwithstanding, our ability to rationally engineer plant metabolism or to predict metabolic responses to stressful conditions as yet remains rather limited.

Given the pivotal role of metabolism in ultimately supporting both plant growth and development it is reasonable to assume that experiments which provide insights into metabolic flux coupled with its regulation would probably both improve our knowledge of biological systems and ultimately aid in the discovery of gene function in land plants. In this vein, a range of stable isotopic labeling experiments using for instance ^{13}C and ^{15}N-labelled precursors have been applied to investigate particular aspects of plant metabolism both in isolated organelles or cells [9], or in plant organs or whole plants [10–12]. Feeding experiments using stable isotopes (*e.g.*, ^{13}C and ^{15}N-labelled precursors) have been also extensively used to delineate metabolic pathways but may equally be used to investigate and quantify metabolic flux and thus enhancing our understanding of the structure and regulation of metabolic pathways [13]. Labeling experiments with ^{14}C-labelled substrates offer high sensitivity, and the fractionation of labelled metabolites and biomass components can readily indicate the fate of metabolized radiolabel [4]. Notably, the determination of radioisotope incorporation into biomass is not dependent of prior separation of metabolites *per se* and the presence of compounds which were not labeled does not impact the detection of radioactivity via scintillation counting or radiography [14].

In the past, radiolabelling was extensively used to discriminate metabolic intermediates belonging to a pathway and their respective order [15]. Thus, compounds that are more labelled are closest to the initial substrate, and the pathway can be defined according to the dilution of radiolabeling along the pathway. This is basically what allowed the differentiation of C3 and C4 modes of photosynthesis through the first labelled compound [16,17]. Notably, short term experiments with labelled compounds were used qualitatively both to determine the sequence of intermediates of specific metabolic pathways and to quantify unidirectional fluxes. Historically speaking, such measurements were carried using spectrophotometric or simple chromatographic separation. By simply comparing the cost of those methodologies, one can expect that it should be less expensive than methods offering both high accuracy and sensitivity for analysis of highly complex mixture of compounds that have been developed during the last decades.

Quantifying the $^{14}CO_2$ release by using different isotopomers of ^{14}C-glucose provided compelling evidence for the relative activity of different metabolic pathways [4]. For instance, by following the pattern of $^{14}CO_2$ evolution from various differentially labelled glucose supplied to plant tissues allowed the identification of alterations in metabolic flux involved in the oxidation of carbohydrates [18], as well as from the differential cycling through the oxidative pentose phosphate pathway (OPPP) or in pentan synthesis and TCA cycle [19,20]. This comparison is based on the ratios of $^{14}CO_2$ evolution from [1-^{14}C]-, [2-^{14}C]-, [3,4-^{14}C]-, and [6-^{14}C]glucose, that are typically used for understanding relative flux through different sections of the central pathways of carbohydrate oxidation [18,20,21]. In summary, by following the radioactivity distribution from different labelled substrates can be used as suitable method covering all major metabolic products (Fig. 1). Furthermore, it can be also applied as a sensitive method for determination of major flux in cells. Thus, although the utility of radiolabeling for the elucidation of metabolic pathways in plants has been extensively demonstrated in the past [22–24] it is still well suited to facilitate the elucidation of the metabolic behavior particularly following genetic or environmental perturbations.

Metabolomics studies are performed with the application of either nuclear magnetic resonance spectroscopy (NMR) or mass spectrometry (MS)-based methodologies. Briefly, NMR is quantitative and potentially non-destructive which offers the possibility to obtain real time metabolic concentrations in living cells. This fact apart, MS based platforms are more frequently used for metabolomics studies mostly due to its higher sensitivity and detection of larger number of metabolites (Fig. 1). In addition, isotope labeling offers advantages for both methods. The utilization of MS or NMR for detection of label incorporation allows the determination of isotopic enrichment (and in the case of NMR the exact isotope location) in individual metabolites (Fig. 1) without laborious chemical cleavage experiments such as those elegantly carried out previously following incubation with different ^{14}C labelled substrates [25–29]. Furthermore, analysis of the isotopomer abundance of labelled metabolites offer a perspective in understanding the way by which the fluxes are distributed within a particular plant metabolic network. Thus, in the context of systems biology, metabolic networks deduced by labeling techniques provide several opportunities for reconstruction and validation of both dynamic and stoichiometric models of metabolism. As alluded to above one inherent disadvantage of stable isotope labeling approaches is that the detection of metabolites is highly dependent upon analytical capabilities. Although there are different methods of metabolite analysis such as liquid and gas chromatography coupled with MS, capillary electrophoresis, and NMR, here we will concentrate our discussion on the general pros and cons of MS approaches in comparison to radiolabelled approaches that are currently used for analyzing metabolite fates in plants. Before doing so it is important to note that despite its low sensitivity NMR has two strong advantages as a tool for flux analysis. First, it can be used in a non-destructive manner and plant cell metabolism can thus be monitored *in vivo*. Secondly, it provides positional information as to where within a molecular isotope accumulates which is highly useful for flux estimation since it facilitates the estimation of reverse fluxes [30]. However, these features and general properties of NMR are the subject of several excellent recent reviews [30–32] so we chose to focus this article on MS approaches.

In this review, we discuss the conceptual basis of these approaches, as well as their historical application and limitations, finally providing an update on recent technical developments. Current methodological challenges that limit the dissection of plant metabolism and future perspectives are briefly discussed and particular emphasis is placed on the importance of developing novel methods. We additionally attempt to discuss the importance of more sensitive flux profiling methodologies using stable isotopes to enable us to pursue new avenues of research in order to increase our understanding of complex metabolic networks governing plant metabolism.

2. Natural abundance studies

Natural abundance studies use the small differences in isotopic ratios that are observed in nature and are usually expressed as the difference delta (δ) to samples in which no further tracer has been applied. The natural abundance of radioactive species is usually negligible but it can be considerable for stable isotopes (e.g. 1.1% for ^{13}C). The occurrence of isotope effects is mainly due to the preferential use of certain isotopes (e.g. ^{12}C compared to ^{13}C) in many biological (and chemical) processes, which is normally referred

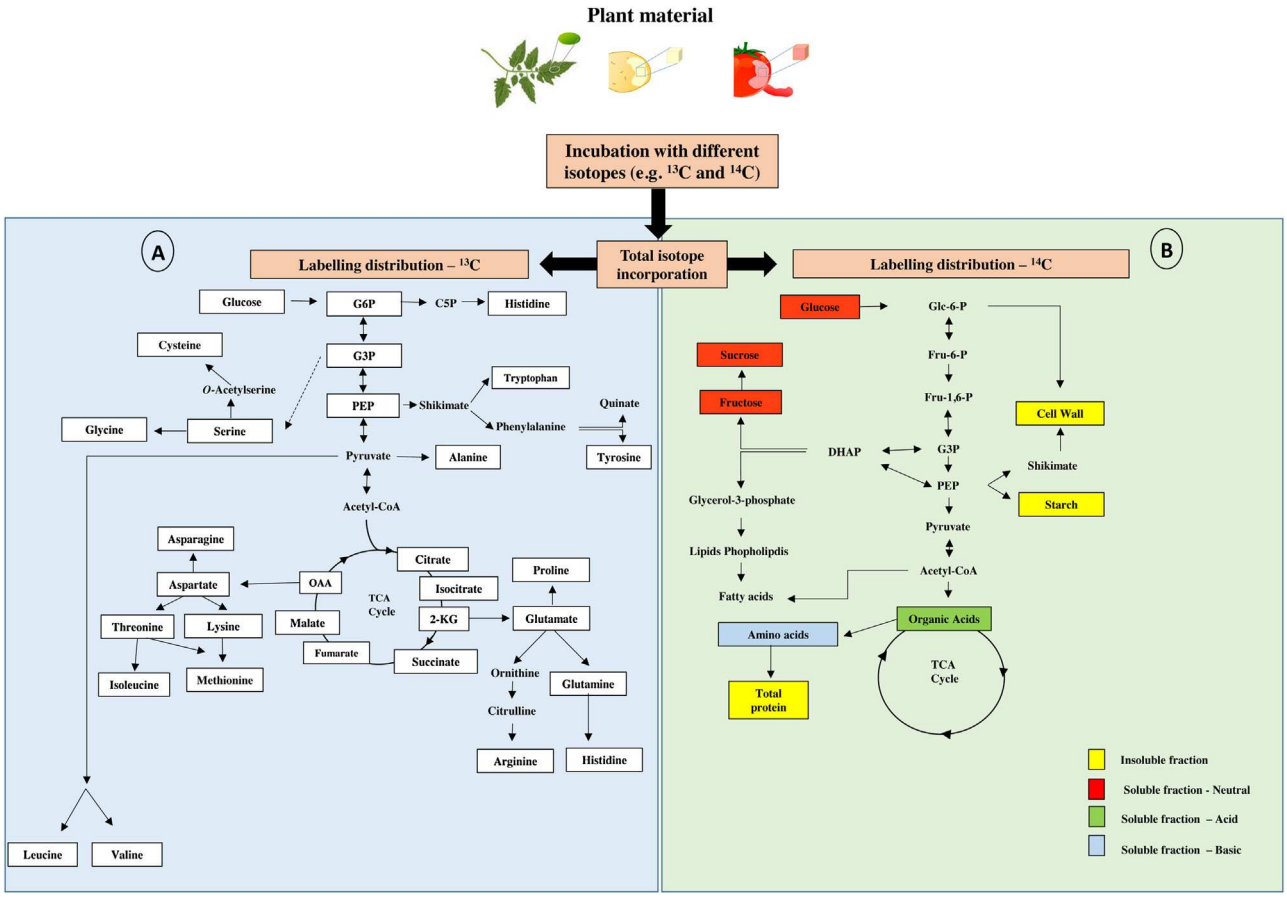

Fig. 1. Brief summary showing the different labelled compounds following feeding experiments. Different plant tissues and organs can be used for feeding experiments using, for instance, either ^{13}C or ^{14}C labelled substrates (e.g., glucose). After incubation and specific experimentation for each approach differential labelled compounds can be identified. (A) Feeding experiments using ^{13}C-labelled substrate can be used for identification of several metabolites involved in the central metabolism. The compounds normally identified are shown in white rectangle. Note that compounds involved with respiration and amino acid metabolism are normally found; (B) Distribution of some metabolites following ^{14}C-labelled precursor feeding with in accordance with the fractionation method. In yellow are shown the Metabolites identified in the insoluble fraction, in red the ones present in the neutral soluble fraction, in green those metabolites found in the acid soluble fraction, and in blue are the metabolites identify in soluble fraction basic.

to as isotopic discrimination meaning that heavy isotopes usually react slower. During the past decades it has been widely accepted that even minor fluctuations in natural abundance (e.g. ^{2}H, ^{13}C, ^{15}N, ^{18}O, and ^{35}S), which can be nowadays easily and with high precision measured, can offer critical and novel insights into the structure and function of ecosystem, providing immediate information with practical value for natural resource management [33,34].

Variations in the natural abundance of such isotopes normally occur not only because of differences in fixation pathways but also due to environmental and physiological conditions [35]. For instance, the naturally occurring variation in carbon isotope ratios ($\delta^{13}C$) between C3 and C4 plants is large enough to allow distinction between these groups of land plants and it has been also recently associated with mathematical modelling to identify metabolic aspects of C3-C4 intermediate species [36]. It is important to stress that not only photosynthesis but also day respiration fractionation seems to be important for δ, although its impact is rather complicated to be estimated due to the light inhibition of TCA cycle reactions and indeed mitochondrial metabolism in general [37]. Respiratory discrimination and its differences between autotrophic and heterotrophic plant organs has more than adequately been expertly reviewed elsewhere [38,39] and we will therefore not cover them in any detail here.

^{15}N natural abundance ($\delta^{15}N$) represents a powerful tool to investigate and understand nitrogen cycle over long time scales at both organism and ecosystem levels. As such, the nitrogen stable isotopic signature has been used to disentangle plant nitrogen sources [40]. Similarly, it can been also used to demonstrate that distinct metabolic reactions are certainly responsible for isotopic shifts between organic-N (amino acids) and absorbed inorganic nitrogen in leaf samples. Furthermore, $\delta^{15}N$ in amino acids is dependent on several factions including nitrate source, nitrate reduction as well as different metabolic reactions involved in photorespiration and amino acid biosynthesis [41]. Notably, $\delta^{15}N$ has been also suggested as an integrator of N cycling through ecosystems [42,43]. Similarly, the stable isotope ratio of both hydrogen and oxygen is highly variable in leaf water and can impact the isotope signature in several biological and atmospheric processes [33]. In this sense, analyses of ^{2}H and ^{18}O in both plant and soil water provided insights into changes in vegetation from a C4 grassland to a C3 woodland over a century of vegetation transition in North America [34]. As expertly recently revisited [33], the stable isotope composition of leaf water, which is extremely variable, has several useful applications based on the isotopic signals, and we will not discuss it further. To conclude, it is likely that studying stable isotopes at natural abundance and the dynamics of nutrient cycling can be used at both regional and global scales to enhance our knowledge concerning physiological, ecological and biogeochemical processes in different ecosystems.

Although our discussion focuses on the application of isotopically labelled substrates it is clear that abundances at natural levels are also an area of considerable current research. For instance,

the low abundance of biologically important isotopes, in particular ^{2}H, ^{13}C, and ^{15}N, requires the introduction of such isotopes into a system prior to any metabolic analysis. This is readily achieved by external supply of a labelled precursor and the possibility to analyze the redistribution behavior through the metabolism. An illustrative example of this possibility using ^{13}C-labeled precursors is presented in Fig. 1. This not only reduces the concentration threshold for the detection but also generates possibilities to explore metabolic pathways gaining information on the connection between precursors and their production following labelling. During the last few years we have witnessed remarkably progress in understanding the mechanisms that control natural isotopes signatures in whole plants and ecosystem. The current challenge lies in finding ways to interpret natural abundance of stable isotope data in terms of those processes in which they are intrinsically associated. Once this has been achieved, we assume that this approach will be harnessed for a wide range of practical applications [44]. Moreover, improving our understanding of the environmental and physiological mechanisms controlling whole-plant and foliar isotope composition will likely considerably advance our knowledge of plant acquisition and allocation of different nutrients. It is therefore not without precedence to suggest that stable isotope research should make use of the great potential of natural abundance measurements and its metabolic and ecologic connections, which may provide an easy, rapid and cost-effective means to understand different biological processes, and enabling scaling-up isotopic information to large spatial scales.

2.1. Comparison of selected isotopes: a short overview

Metabolic studies were initially supported by the use of isotopes, either as standards or as tracer molecules. The use of those molecules in metabolic studies were initially developed in pulsed stable isotope labeling experiments in animals [45]. Since this time, a broad range of stable isotope labeling experiments has been designed to investigate metabolic behavior in both plant and animal cells [46,47]. One point of pivotal importance that is usually overlooked in isotopic studies relies in the chemical purity which will clearly affect the results obtained. Radiolabelled compounds, by their nature, are unstable and thus it is often necessary to highly purify compounds that are only marginally labelled prior to measurement [48]. The rate of decomposition of some radioisotopes can be so rapid as to render purity checks mandatory when material is stored for longer periods. In the most extreme instances isotopes such as ^{11}C decay so rapidly as to completely preclude their storage [49] greatly complicating their experimental use. However, for others such as ^{14}C, the decay rate is extremely slow rendering them highly practical for experimental purposes. Given that several isotopes, mainly the stable ones, are also naturally present in organic compounds, the study of their metabolic behavior also requires a correction of the mass spectral output to account for the natural abundance of isotopes in the native metabolite [50]. Notably, in the case of MS analysis of non-volatile compounds it should be also performed for the presence of heavy isotopes in the chemicals used for derivatization [51], prior to any biological interpretation. The most common isotopes used nowadays are summarized in Table 1; ^{13}C is currently by far the most commonly employed isotope, due to the presence of carbon atoms in every bio-organic molecule and our relatively good understanding of carbon transfer reactions. The carbon isotope discrimination ($\delta^{13}C$) has been extensively used in plant studies providing significant insights in leaf physiological characteristics such as stomatal conductance and net photosynthesis that ultimately governs the concentration of CO_2 in the leaf intercellular air spaces and in the chloroplast [35]. Determination of $\delta^{13}C$ is of considerable importance in attempts to elucidate the genetic and environmental controls on plant water-use efficiency and can be very useful in further efforts to engineer better crops and manipulation of crop performance. The use of ^{13}C-labeled substrates has enabled the identification and elucidation of a range of metabolic pathways and is further summarized below.

Several applications of the main labeling strategies discussed here and used nowadays in plant metabolic studies are summarized in Table 2. It is important to note that the information presented in Table 2 should be interpreted with caution because the choice of the strategy is a rather complicated issue that is dependent on several issues, such as type of material under investigation, availability of equipment, and the biological question being addressed – all of which would clearly influence the final decision made by the researcher. Early studies with ^{14}C addressed several important biological questions mostly regarding the regulation of end-product synthesis such as starch and cell wall components [4–6]. Similarly, the proportion of radiolabeled substrate that is metabolized to soluble components may be also analyzed in attempt to understand carbon allocation and flux through different pathways. For instance, an *in vivo* strategy used two radioisotopes (^{3}H and ^{14}C) to unequivocally demonstrate that the oxidation of UDP-glucose appears more prominent than the oxidation of *myo*-inositol whereas the pathway involving the action of phosphomanose isomerase seems to be more active than that using GDP-glucose isomerase [52]. Although the mechanisms behind such intriguingly metabolic features are not at first glance clear it is probably associated with the most economic use of available resources. Similarly, one of the more unexpected discoveries by using positional labelled ^{14}C-glucose was the extensive duplication of glycolysis and the OPPP in the cytosol and plastid stroma, providing both energy and carbon skeletons for other metabolic pathways in these two compartments [53]. Early studies were also carried out with positionally radiolabeled glucoses to determine the flux through the OPPP [26] and the major pathways of central metabolism in maize root tips [20]. Further studies employing ^{14}C-glucose have ascertained the pivotal role of sucrose synthase in the regulation of carbohydrate partitioning and demonstrated a fascinating illustration of the flexibility of plant metabolism [54] (Table 2). It is, however, important to stress that the usage of specific radiolabeled substrates may not accurately identify the most predominant pathways under certain conditions. For instance, although precursors can be used when artificially supplied it might well be that they are neither present in high enough quantity *in vivo* nor effectively used due to sequestration or limited uptake [52]. Thus, labeling kinetics within the time-frame of such experiments should also be properly investigated. Collectively these studies have provided compelling evidence into relative rates of different metabolic pathways as well as mechanistic understanding of their regulation.

Hydrogen is a major element of living systems and two stable isotopes of hydrogen are naturally found namely protium ^{1}H, and deuterium ^{2}H, whereas one heavier and radioactive isotope tritium, ^{3}H is also found. Despite the highest detectability and absolute zero natural abundance the use of ^{3}H is extremely limited due to its radioactivity. This fact notwithstanding, tritium-labeled compounds often have high specific activities and can be introduced postsynthetically, for example, by the use of isotopic exchange reactions. This approach has been used in the investigation of the fate of gibberellins in seeds allowing the elucidation of fundamental steps in gibberellin metabolism [55]. In addition, tritium-labeled and ^{14}C-labeled compounds have been used to study the nucleotide biosynthetic and catabolic pathways in potato tubers showing the operation of a salvage pathway via quinolic acid [56], indicating practical applications for understanding specific metabolic aspects of land plants. Notably, the ubiquitous occurrence of hydrogen in every molecule and the facility for the formation of carbon–hydrogen bonds make the use of radioactive hydrogen isotopes highly attractive. At the same time, a natural

Table 1
Commonly used stable isotopes for metabolic studies. We summarize the mostly used compounds, some characteristics and reasons for their use and present few examples where they were used.

Isotope	Presence in plant cells	Key points	Application in plant biology	Reference
^{2}H	Universal	Low natural abundance; easily convertible	Water cycle components	[57,58]
^{13}C	Universal	stable incorporation	metabolic studies	[20,82,83,96]
^{15}N	Nucleic acids, proteins, and amino acids	Highly important in studying nitrogen metabolism	nitrogen metabolism	[70–72]
^{18}O	Universal	Carbon gain and leaf water relations	*in vivo* respiration; respiration/photosynthesis relationship	[66,67]

Table 2
Different applications of the main labelling strategies used currently in plant metabolic studies.

Heterotrophicvsautotrophic tissues	*Usefull substrate*	*Approach for label incorporation*	*Application*	*Observation*
Photosynthetic tissues in the light[*]				
	$^{14}CO_2$	Leaf discs are subjected to high $^{14}CO_2$ atmosphere	Determination of ^{14}C-enrichment in major pathways components (see Fig. 1 for details)	
	$^{13}CO_2$	Whole plants are transferred to growth chamber supplied with $^{13}CO_2$	Major method to analyze metabolic fluxes *in planta*. Can also be used to determine the rates of protein synthesis and degradation *in planta*.	The ^{13}C-enrichment will be diluted by ongoing carbon fixation of the natural $^{13}CO_2$ and thus must be corrected.
	^{13}C and ^{14}C-labelled compounds	Intact leaves, leaf discs or organelles are feed with buffered solutions enriched with the labelled substrate	Determination of the fate of C released from the labelled substrate. ^{13}C-labelled analysis offers better resolution of the metabolism compared to ^{14}C-labelled approaches.	The ^{13}C-enrichment can be corrected by using ^{12}C-substrate in parallel.
	^{13}C—$NaHCO_3^-$	Labelling previously isolated tissues or leaf discs	Useful to investigate the anaplerotic CO_2 fixation, for instance, the one mediated by PEPc in cells with C4 metabolism	
Photosynthetic tissues in the dark[**]				
	^{14}C-glucose	Leaf discs are feed with buffered solutions enriched with the labelled substrate	Important to analyze fluxes through glycolysis and respiratory metabolism in the dark.	Experiments can be performed by cutting off the carbohydrate supply and replace it by an exogenous supply of labelled substrate
	^{13}C-$NaHCO_3^-$	Feeding previouslly isolated tissue	Useful to investigate the anaplerotic CO_2 fixation mediated by PEPc in cells with CAM metabolism	The degradation of storage compounds can dilute the ^{13}C-enrichment observed in specific metabolites
	^{14}C-labelled substrates	Seedlings subjected solutions containing the radiolabelled compound	This approach has been used to investigate gluconeogenesis in Arabidopsis	
Non-photosynthetic tissues[***]				
	$^{15}NH4^+$, $^{15}NO_3^-$	$^{15}NH4^+$ and $^{15}NO_3^-$ added to cell suspension solution	Determination of the rates of protein synthesis and degradation.	
	$^{13}CO(^{15}NH_2)_2$	Plants grown under $^{13}CO(^{15}NH_2)_2$ enriched hydroponic solution	Investigation of the C and N incorporation using urea as source	
	$^{2}H_2O$	Seedlings grown on media with $^{2}H_2O$	Measure of protein turnover	Noteworthy, the use of $^{2}H_2O$ inhibit seed germination and seedling establishment
	^{35}S-methionine	Imbibition of seeds in ^{35}S-Met enriched solution	Analysis of protein synthesis and turnover in germinating seeds	
	^{14}C-labelled glucose	Labelling fruit and tuber discs	Important to analyze fluxes through glycolysis and respiratory metabolism as well as to assess the regulation of the substrates for end products such as starch and cell wall components	

[*] The ^{13}C-enrichment will be diluted by ongoing carbon fixation of the natural $^{13}CO_2$ and thus must be corrected. A possibility to correct the ^{13}C-enrichment is to use ^{12}C-substrate in parallel.
[**] The degradation of storage compounds can dilute the ^{13}C-enrichment observed in specific metabolites. Experiments can be performed by cutting off the carbohydrate supply and replace it by an exogenous supply of labelled substrate).
[***] Metabolism depends on provision of external substrate (e.g. sugars).

consequence to the contentment of forming the carbon–hydrogen bond is the ease with which that bond can also be cleaved. As it can be anticipated, if the molecule is labeled with ^{3}H at the cleavage site, the label might be lost, either through a chemical route (e.g., placing the label on an alpha or a ketone group) or through a biochemical means (e.g., metabolism). As such, in case of the site of

labeling for the ^{3}H label being critical, ^{3}H NMR presents itself as an invaluable tool allowing the confirmation of ^{3}H in the location expected. Despite these drawbacks, ^{3}H is an attractive option in support of metabolic pathway discovery efforts.

Studies employing deuterium (^{2}H) have been extensively used in both ecological [57] and in whole-tree water transport and water relocation contexts [58]. Furthermore, these studies have analyzed the differential enrichment of water molecules due to the limited evaporation and diffusion of the heavier forms in comparison to the lighter ones. This fact apart, ^{2}H in soil water displays a different profile as a result of evaporative enrichment making possible to investigate patterns of water acquisition following soil depth considering the absence of such fractionation during water uptake by plant roots. The usage of ^{2}H in metabolic studies is rather limited and as such it was only recently that by coupling $H/^{2}H$ isotope effects with elegant physiological and biochemical methods the prediction of a non-cyclic modular operation of the TCA cycle in the light was possible [59]. In this scenario, a functional mode formed by different enzymes of the TCA cycle including citrate synthase, mitochondrial NAD-dependent isocitrate dehydrogenase, cytosolic NADP-dependent isocitrate dehydrogenase, as well as 2-oxoglutarate dehydrogenase, is likely capable for the generation of (*i*) 2-oxoglutarate as precursor for amino acid biosynthesis during nitrate assimilation and (*ii*) fumarate from oxaloacetate within the illuminated leaf [59,60]. Taken together these studies provided evidence for the operation of the TCA cycle as complete cycle in photosynthetically active tissues during the night and that the flux distribution is modified to two weakly but connected branches during the day. Similarly, it was only recently shown that glycolate deprotonation to be of limited importance for glycolate oxidation whereas derivations obtained following kinetic isotope effects are in good agreement with a hydride transfer mechanism in plant glycolate oxidase catalysis [61]. In this interesting study the usage of deuterated glycolate in either natural or deuterated solvent was highly associated with isotope effects in the reaction performed by glycolate oxidase in both C3 and C4 plants and the importance of this exciting feature is expertly discussed in the context of the design of novel drugs and herbicides. Furthermore, ^{2}H has been used to evaluate the disequilibrium of the plastid phosphoglucomutase [62]. Thus, although the use of ^{2}H, which is universally present in organic molecules, is rather restricted due to its even lower natural abundance, ^{2}H has been used in labeling studies of different biosynthetic pathways and has the advantage of being either detected directly, by using ^{2}H NMR, or indirectly, using either ^{1}H or ^{13}C NMR [62]. However, it is not commonly used nowadays given that it readily interchanges with hydrogen from water, rendering the interpretation of the results somewhat difficult as well as by the fact that the use of $^{2}H_2O$ leads to reduced plant growth and development [63](Table 2). This fact apart, $^{2}H_2O$ labeling has been recently used to measure the replication and physiological status of the parasite *Leishmania mexicana* in murine inflammatory lesions [64] and this method might be well suited to plant studies as well by allowing the quantification of very low isotopic enrichments. This labeling strategy used is a highly promising method that might be, for instance, effectively used to measure growth dynamics and physiological aspects of other plant-microbe interactions *in situ*.

The three isotopes of oxygen ^{16}O, ^{17}O, and ^{18}O, are naturally present at abundances of 99.75, 0.04, and 0.21%, respectively [65]. Despite the widely recognized importance of ^{17}O in atmospheric chemistry research, our knowledge concerning the biological importance of this specific isotope remains rather limited to date. This fact apart, the oxygen isotope signature (or the $^{16}O/^{18}O$ composition) of plant material is of pivotal importance in physiological and ecological plant studies involved in the regulation of water loss in the search for improvements in water use efficiency and yield in crop species discussed in details in [66]. The precise mechanisms that contribute to changes in oxygen isotope signature remains elusive, but are mainly associated with plant water acquisition and movements, evaporative and diffusional effects during transpiration, and isotopic exchange involving organic molecules and plant water [66]. At an ecosystem scale, ^{18}O isotope discrimination is extensively used to understand partition of net carbon gain into photosynthetic and respiratory components. In this context, it is expected that this technique may be effectively used to address a wide range of questions associated with plant regulation of water loss and crop improvements, providing itself as a powerful tool for plant breeders. Furthermore, the ^{18}O isotope discrimination analysis by isotope ratio MS in plant organs enabled the measurement of the *in vivo* activity of the different pathways of mitochondrial electron transport chain [67]. Plant respiration can occurs through different metabolic pathways leading to production of energy, carbon skeletons, and alternatively only heat. The latter involves the plant unique alternative oxidase, which is embedded in the inner mitochondrial membrane and can oxidase oxygen in the presence of cyanide, an inhibitor of the cytochrome pathway. The activity of this alternative pathway, that circumvent the proton pumping protein complexes and therefore reduce the respiratory ATP production, can be determined based in the differential oxygen isotope fractionation between the cytochrome pathway and the alternative oxidase [67]. The ^{18}O isotope discrimination was also recently used to identify the plastidic glycolate/glycerate transporter which is a key component of photorespiration [68] and therefore further applications of this technique are highly feasible for a broad range of different fields in plant science. For instance, if one considers that variations in $\delta^{13}C$ are governed by fluctuations in stomatal conductance rates, a strong correlation between $\delta^{13}C$ and $\delta^{18}O$ would be expected and therefore concomitant analysis of $\delta^{13}C$ and $\delta^{18}O$ might offer powerful information about the physiological and environmental factors that control water-use efficiency.

Two stable isotope of N are present in the atmosphere, ^{14}N and ^{15}N, the first being present in a much higher abundance. The fundamental role of N for plant growth and development has been well described. N assimilation is a well-known pathway in which the involved enzymes have relatively low discrimination against ^{15}N incorporation [69].In this context, ^{15}N stable isotopes analyses are extensively used to investigate N metabolism and it has recently been applied to study metabolic changes following hypoxia in soybean roots [70] as well as resource allocation during growth in oak [71] and metabolic transitory changes in barley roots in response to phosphate limitation [72]. Furthermore, it is possible to monitor the incorporation of ^{15}N from amino acids into proteins and clearly distinguish natural abundance and enriched ion envelopes within the mass spectrum [73]. Thus, several studies using saturation or partial ^{15}N labeling in steady-state experiments in plants have been used as a means to perform quantitative proteomic characterization [73–76] such as measurement of protein synthesis and degradation, allowing a deeper understanding of metabolic aspects in land plants.

In plants, the use of stable isotope labeling by individual amino acids have been limited as a way to measure protein turnover because plants are autotrophic and actively able to synthesize all amino acids *de novo*. As alternative, $^{15}NO_3$ or $^{15}NH_4$ can be supplied to the medium of cell cultures [77,78], or to the rooting medium [79] and thus ^{15}N labeling kinetics of signature peptides of individual proteins can be further analyzed [73]. In addition, after ^{15}N labeling protein turnover measured by measuring kinetics of changes in ^{15}N incorporation into peptides from in-gel digestions of separated protein spots is a highly promising methodology [73] Alternatively ^{13}C, $^{2}H_2O$ and ^{18}O can be used in labeling experiments and *de novo* synthesis is tracked by the increase in the mass of the resulting proteins [63,80] (Table 2).

Notably, the use of ^{13}C and ^{15}N isotopes can be readily applied to investigate several pathways at the same time whereas the use of others isotopes (e.g. ^{2}H; ^{18}O; ^{14}C) are much better for single reaction monitoring. In addition, recent developments in proteomic analysis have enabled not only the identification but also the quantification of proteins helping to understand fundamental aspects of the regulation of plant cellular processes following both development and fluctuations in environmental conditions [79]. The simultaneous use of stable isotopes (^{13}C, ^{15}N, and ^{36}S) can be also used allowing the evaluation of different aspects of plant metabolism. Unlike carbon and nitrogen isotopes, however, stable isotopes of other elements (e.g. sulphur, selenium, phosphorus, boron, etc) are used infrequently, and their potential as tracers in biochemical and physiological studies are only beginning to be realized. Unravelling the metabolism of those less used elements in plants may lead to ways to increase fertilization efficiency as well as allowing a better understanding of metabolic pathways. Collectively, the data discussed above are suggestive that analysis using different isotopes may offer a robust means to investigate metabolic alterations following environmental stress or genetic impairments. We discuss some of the metabolic applications of the usage of both heavy and stable isotopes below.

3. Metabolic application of labeling approaches: current status

The use of isotopes of different chemical elements is a useful tool for plant physiologists, and are currently used to generate insights into how exactly the metabolism behaves in response to environmental conditions [44,81]. They provide insights into the isotopic composition of the plant material, which have great applications for instance in ecophysiology in analyzing plant water and nitrogen use efficiency [41]. Furthermore, isotopic labeling is powerful in determining metabolic fluxes, and its successful application has been reported for a range of species and tissues, including: *Escherichia coli* [82,83], the photoautotrophic cyanobacteria *Synechocystis* sp. [84], *Arabidopsis thaliana* [85] and rice [86], potato tubers [51,87] and tomato leaves [88] and fruits [89].

Despite the high use of ^{13}C it is important to note that feeding experiments with ^{14}C retain utility. Thus, a range of experiments within the last decades had provided information about the relative activities of the major pathways of carbohydrate oxidation in different species [89,90]. It has been also used to investigate post-translational redox activation of AGPase in potato tuber discs [91] and the key role of sucrose phosphate synthase in the regulation of sucrose and starch partition in response to water limitation [92] xxx. This approach was additionally recently used to demonstrate the occurrence of variations in carbon allocation throughout the diurnal cycle in both source and sink tissues [93] and that a higher proportion of carbohydrate oxidation is likely performed by the TCA cycle in poly ADP-ribose polymerase knockout mutants of *Arabidopsis* [94]. These approaches as well as relatively simple potentially provide rapid information concerning the metabolism of macromolecules such as starch, protein and cell wall and for this reason have recently been suggested to be an important complement to MS approaches for determining the temporal and spatial allocation of assimilated carbon during plant growth and following stress conditions. It is important to stress, however, that the incubation with ^{13}C- or ^{15}N-labelled substrates and the use of gas chromatography-time of flight-mass spectrometry (GC-TOF-MS) offers the possibility to determine higher resolution metabolic information (Table 3), additionally allowing the elucidation of metabolic pathways [95] and the key importance of metabolic reactions in the regulation of growth [71] or in response to stress [72]. Although this approach clearly requires considerable computational time it is far less laborious experimentally than current radiolabel fractionation procedures.

The metabolism of a ^{13}C-labelled substrate via different pathways produces distinct labeling patterns. The metabolic fate of [U-^{13}C]glucose was followed via a kinetic labeling approach in potato tuber discs with isotope labeling being followed by GC–MS (Fig. 1, Table 2). More recently, the fate of $^{13}CO_2$ supplied to illuminated tobacco and Arabidopsis rosettes were evaluated revealing patterns of carbon allocation and novel insights into photosynthetic fluxes [10,96]. Furthermore, whole plant metabolic flux analyses following $^{13}CO_2$ labeling have recently been established [10,86]. Moreover, this *in vivo* $^{13}CO_2$ labeling has been also used for investigation of protein turnover [80,97]. In addition, the metabolism of ^{13}C-pyruvate has been analyzed in isolated mitochondria from *Arabidopsis* plants with reduced manganese superoxide dismutase activity allowing the elucidation of the reasons associated with the decreased TCA cycle flux which is most likely caused by oxidative damage [98]. Furthermore, as a complement to the use of genetic approaches that provided compelling evidence of the alternative donation of electrons to the mitochondrial electron transport chain in plants, the usage of isotope tracer experimentation was able to elucidate the participation of the enzymes isovaleryl-CoA dehydrogenase and 2-hydroxyglutarate dehydrogenase during alternative respiration following carbon starvation [11]. By applying [U-^{13}C]lysine or [U-^{13}C]valine it was demonstrated that isovaleryl-CoA dehydrogenase is mainly associated with the degradation of the branched-chain amino acids, while 2-hydroxyglutarate dehydrogenase is involved exclusively in lysine degradation [11]. In the same vein, experiments with ^{13}C ring labelled phenylalanine, when coupled with analysis of phenylpropanoids, additionally provide important information concerning the nexus of primary and secondary metabolism [89,99,100]. Furthermore, isotope tracer experiments with ^{13}C-lactate and ^{13}C-glycolate supported a range of *in vitro* studies defining the function of glycolate oxidase-3 in roots of *A. thaliana* [101]. In addition, by using feeding experiments with ^{15}N-tyrosine it has been recently demonstrated that phenylalanine biosynthesis in petals of petunia occurs through an alternative pathway when the arogenate route is blocked [102]. The particular case studies discussed above, coupled with results from other published research, clearly indicated that the application of stable isotope labeling studies in plant science hold considerable promise as an indicator of metabolic status following different genetic or environmental conditions. It is important to mention that although the examples raised above go a long way to towards describing the structure of different pathways, our knowledge concerning their regulation remains rather fragmentary and more work is required to fully understand complex aspects of plant metabolism.

By using a combination of ^{13}C and ^{15}N labeling experiments, the metabolic behavior of soybean roots following hypoxia was recently elucidated providing compelling evidence for non-cyclic function of the TCA cycle mostly due to an inhibition at the level of the succinate dehydrogenase [70]. Interestingly, a combination of 13C- and 2H-labeled *L*-methionine experiments was capable of resolving the metabolic routes of aroma volatiles in melon fruit [103] whereas the use of 13C-phenylalanine demonstrated that amino acids catabolism into aroma volatiles take place through a transamination mechanism [104]. These examples coupled with others where the application of multiple (or simple) labeling experiments present excellent tools for pathway structure elucidation and for defining key points of metabolic regulation. Furthermore, they also present reasonable and comprehensive tools to access complex metabolic features in a detailed manner and to further explore possible mechanisms that are responsible for the patterns observed. It seems likely that the use of full labeling approaches with different isotopes will become even more frequently in the

Table 3
Overview of the measuring techniques applied in labelling studies and some of their characteristics.

Parameter	Stable isotopes mainly using ^{13}C-labelled precursors)	Radiolabelled approaches mainly using ^{14}C-labelled precursors	References
Equipment costs	Very high	High	
Price per sample	Low to medium	Low	
Time used in the lab during the sample preparation	Relatively rapid	Require much more time	[51]
Time for computational sample analysis	Require much more time	Relatively rapid	[51]
Metabolic resolution	Very high	Low	[51,114]
Possibility to analyze different metabolic pathways	Very high	High	[10,51,71]
Possibility to be applied to different tissues, organs or species	High	Limited in certain cases	[70,114]
Accuracy of measurement of isotope enrichment	Very high	Modest	[72]
Requirement of sample volume	Low	Very high	
Derivatization prior to measurement	Required*	Not required	[11,105]
Possibility of high throughput	High	Low	[10,51]

* Derivatization is not required for NMR measurements and it is not always required for MS

near future due to the widening access of metabolically minded biologists to mass spectrometry instrumentation.

4. Applications of stable and radioisotope labeling in plant metabolic studies

Labeling studies are directly dependent on administration of specific (radio)isotope labelled substrate to a tissue or organism and the capability to monitor the propagation of the tracer through the metabolic network. A pre requisite of this approach is that the structure of metabolic network should be known [105]. The application of labelled substrates in both prokaryote [82,106] and eukaryote cell cultures [107,108] is easily performed and widely accepted. However, its application to intact whole plants is complicated by several issues. Such issues are not only associated with the nature of the label to be introduced and its mode of introduction but also linked to the complexity of the plant cell metabolism (for example the intricate compartmentalization of the metabolic reactions) [109]. Thus, problems can arise by the external application of labelled compounds that may modify the entire metabolism, for instance when using high enough concentrations of tracer to allow enough enrichment in specific metabolic pools and thus great changes in metabolism may be observed. Thus, it is important to assure the uptake of the labelled substrate by the organism and that it is entirely integrated into the metabolism in a close manner to the pathway under investigation. Similarly, the use of cut or dissected plant material might lead to significant changes in their metabolism most likely due to wounding responses or even changes in oxygen availability [51] and the lack of photoassimilate export in certain tissues (Table 2). Furthermore, caution is clearly required even when working with whole plants to ensure maintenance of experimental conditions that are observed during the growth (e.g. soil and air water status, light intensity and quality, etc.; [105]). It seems reasonable to assume that only the usage of labelled CO_2, in concentrations near to those found in the environment, will avoid undesired side effects on metabolism. When considered together this clearly indicates that the choice of experimental approach should also, at least in part, be guided by the type of plant material under investigation.

A detailed comparison of these two labeling approaches is presented in Table 3. The techniques we refer to are GCMS and liquid scintillation counting for stable isotopes and radioisotopes, respectively. In brief, despite similar acquisition costs for equipment used in stable isotope (GCMS, for instance) or radioisotope (scintillation counter) analysis and similar low run costs per sample, there are a number of differences between these two approaches. First, it is important to mention that a higher metabolic resolution is usually obtained with stable isotopes. By contrast, radiolabelled approaches require a relatively long experimental time but much less computational time when compared to stable isotope studies. In addition, considering that both radioisotopes and stable isotopes may be purchased at approximately 100% labeling the signal to noise is assumedly far greater for radioisotopes. By stating that we assume that radioisotopes methods are relatively superior for quantifying the total amount of labelled material in situations where only a very small amount of molecules were labelled in a large pool of unlabeled molecules. Other parameters worthy of note are described in Table 3.

We should not forget that waste disposal for even non-radioactive chemical processes is nowadays an important issue and as such disposal of radioactive waste is an even greater challenge. At the same time, due to extremely expensive costs, the disposal of mixed waste such as flammable or highly toxic radioactive waste can be prohibitive, and in certain cases, very difficult to reach a vendor willing to deal with such disposal. Taken together, the mounting evidence discussed here indicates that before undertaking such approaches one should consider not only the possibility to answer specific biological questions but also the potential hazard to the experimenter involved as well as the radioactive waste to be produced and the availability of proper radioactive waste disposal.

It is important to highlight that although the possibility of high throughput analyses seems highly feasible for both approaches, it is in our opinion only currently available for stable isotopes. This is most likely due to difficulties in analyzing a huge number of radiolabelled samples, contamination problems on analyzing radiolabelled samples in mass spectrometry machines, and lastly by the long half-life of certain radioactive materials (e.g., ^{14}C). The last of which requires special caution during the experiments itself as well as during either the storage or disposal of the radioactive sample material. To recapitulate, the decision of which approach to be used is a rather complex feature that depends strongly on the specie being studied, the organization scale used in the study, as well as the biological question behind such study (Table 3). Furthermore, the combination of the two approaches described here promises to provide a comprehensive understanding of metabolic networks in biological systems, particularly in the green lineage.

Although not highlighted in Table 3, mathematical modelling approaches are an important tool to better understand and to predict responses of the entire metabolic network. Notably, these approaches have only been used for the analysis of a broad number of metabolic fluxes following stable isotope labeling experiments. Metabolic fluxes can be assumed to be a function of the velocity of reactions occurring *in vivo*. Accordingly, fluxes include not only the conversion rate of metabolic intermediates by enzymes but also the transport rate of metabolites between compartments [105,109]. In fact, metabolic fluxes are the final outcome of the interplay of gene and protein expression, enzyme kinetics, and metabolite concentrations. Quantitative prediction of the flow of metabolites can

be obtained with metabolic flux analysis (MFA), based on either flux balance analysis (FBA), which is obtained via stoichiometric constraints, or experimentally determined with ^{13}C-metabolic flux analysis (^{13}C-MFA), together with stoichiometric constraints [110]. Briefly, such methods were originally developed for microbial metabolic studies. However, during the last decades, they have extensively been adapted and used for plant metabolic analysis. It is not our intention to discuss such methods as they are the subject of several excellent recent reviews [109,110]. It is important to mention, however, that such approaches offer the possibility both to predict changes in the metabolic network under different environmental and/or genetic conditions and to provide a systemic overview of the whole plant metabolic network. Importantly, the challenges and opportunities for the practical application of those approaches are now being recognized and thus the development of novel methods are required for addressing new research questions in plant metabolic engineering and biotechnology.

Notably, the knowledge obtained by studying fluxes through metabolic networks is crucial for understanding plant cell function. Moreover, the analysis of fluxes are of pivotal importance for understanding and characterizing metabolic phenotypes in engineered lines, with several biotechnological applications, including measures of metabolic efficiency in both plant cells and tissues [111] as well as nutrient efficiency in crops [112]. It is important to mention that the use of the tools described here alongside other post-genomic techniques will likely allow the functional annotation of not only genes but also several novel metabolites. Furthermore, it seems reasonable to assume that development of next generation technologies including analytical and mathematical tools could provide additional parameters to a more comprehensive understanding of the metabolic networks. In this context, stable isotope approaches will most likely have a fundamental role in the development of this field when compared with radiolabelled approaches. Considering that all the necessary tools are accessible, including the widespread application of high resolution mass spectrometry based metabolomics, recent bioinformatics advances for automated isotopomer detection as well as the numerous stable isotope-labelled compounds that are now readily available, stable isotope labeling is expected to become common practice in metabolomics studies at the expense of reduced usage of radiolabelled isotopes in the near future. It is important to highlight that the cost of these labelled precursors may prohibit extensive studies, particularly for *in vivo* systems. From a practical viewpoint the researcher should also consider both the price and the availability of the labelled substrate to obtain meaningful results. Nevertheless, there are already available examples of ^{13}C-labelled metabolic profiling in whole plants [10,86] with clear practical applications allowing comprehensive analysis of several aspects of cellular metabolism.

5. Conclusions and perspectives

The importance of metabolic analysis coupled with analysis of flux is increasingly becoming an essential component of efforts to increase our understanding of the control and regulation of the metabolic networks. Studies involving both metabolic profiles and metabolic flux analysis are of high relevance particularly when used in conjunction with other post-genomic technologies and will additionally allow a better description of the metabolic network in several contexts. Likewise, the combination of both approaches (using stable and radiolabeled isotopes) discussed here, allowing the inclusion of the knowledge inferred from each other, will likely be highly informative in elucidating function of metabolic pathways in a network context. It seems also clear that the improvement of current techniques alongside the adaptation of large profiling technologies will enable us to pursue new avenue of research in order to increase our understanding of the complex network governing cellular metabolism. As analytical approaches become more advanced nowadays, the combined used of stable and radiolabeled isotopes should provide tools for many more important developments in plant science. We also posit that the coupling of modeling approaches and the feeding experiments discussed here can be highly pertinent to elucidate the underlying mechanisms of complex metabolic networks and pathways of intricate biological systems. One possibility is the usage of parallel labeling experiments [82,113] together with other approaches allowing measurements of compartment-specific fluxes to investigate the complexity underlying plant cell metabolism.

Finally, metabolic analysis such as those described here using isotopes are clearly providing novel insights into numerous biological questions. Thus, the time is ripe for scholars of different, but complementary fields, to join their efforts in developing new interdisciplinary approaches to further help elucidation of the many aspects of the regulation of the whole plant metabolism that still remains unclear. In closing, by coupling stable and radiolabeled approaches in plant science, we will definitely learn more about the role of metabolism in regulating important biological processes. Thus, we posit that stable labeling does not replace but rather function as a true complement of radiolabeled approaches which retain considerable utility particularly in the analysis of macromolecules. These studies have the potential to reveal new biotechnological opportunities, providing exciting opportunities for further investigations.

Acknowledgements

We apologize to all colleagues whose work has not been mentioned due to space limitations and thank anonymous reviewers for their valuable comments and suggestions. This work was supported by funding from the Max Planck Society (to ARF, ANN and WLA) and the National Council for Scientific and Technological Development (CNPq-Brazil, Grant 306355/2012-4 to A.N.N and Grant 483525/2012-0 to W.L.A.) and the FAPEMIG (Foundation for Research Assistance of the Minas Gerais State, Brazil, Grant APQ-01357-14 to W.L.A.). We also thank the scholarships granted by the Brazilian Federal Agency for Support and Evaluation of Graduate Education (CAPES-Brazil) to WBS and by CNPq to DMD. Research fellowships granted by CNPq-Brazil to ANN and WLA are also gratefully acknowledged.

References

[1] L.J. Sweetlove, A.R. Fernie, The spatial organization of metabolism within the plant cell, Annu. Rev. Plant Biol. 64 (2013) 723–746.
[2] H.A. Krebs, W.A. Johnson, Metabolism of ketonic acids in animal tissues, Biochem. J. 31 (1937) 645–660.
[3] H. Beevers, M. Gibbs, The direct oxidation pathway in plant respiration, Plant Physiol. 29 (1954) 322–324.
[4] T. ap Rees, H. Beevers, Pathways of glucose dissimilation in carrot slices, Plant Physiol. 35 (1960) 830–838.
[5] S.H. Lips, H. Beevers, Compartmentation of organic acids in corn roots I. Differential labeling of 2 malate pools, Plant Physiol. 41 (1966) 709–712.
[6] H.L. Kornberg, H. Beevers, A mechanism of conversion of fat to carbohydrate in castor beans, Nature 180 (1957) 35–36.
[7] M. Calvin, The path of carbon in photosynthesis, Angew. Chem. Int. Ed. Engl. 1 (1962) 65–75.
[8] L. Sweetlove, D. Fell, A. Fernie, Getting to grips with the plant metabolic network, Biochem. J 409 (2008) 27–41.
[9] D.M. Daloso, et al., Tobacco guard cells fix CO_2 by both RubisCO and PEPcase whilst sucrose acts as a substrate during light induced stomatal opening, Plant Cell Environ. 38 (2015) 2353–2371.
[10] M. Szecowka, et al., Metabolic fluxes in an illuminated *Arabidopsis rosette*, Plant Cell 25 (2013) 694–714.
[11] W.L. Araújo, et al., Identification of the 2-hydroxyglutarate and isovaleryl-CoA dehydrogenases as alternative electron donors linking lysine

catabolism to the electron transport chain of *Arabidopsis mitochondria*, Plant Cell 22 (2010) 1549–1563.
[12] E. Heinzle, F. Matsuda, H. Miyagawa, K. Wakasa, T. Nishioka, Estimation of metabolic fluxes, expression levels and metabolite dynamics of a secondary metabolic pathway in potato using label pulse-feeding experiments combined with kinetic network modelling and simulation, Plant J. 50 (2007) 176–187.
[13] C.Y.M. Cheung, R.G. Ratcliffe, L.J. Sweetlove, A method of accounting for enzyme costs in flux balance analysis reveals alternative pathways and metabolite stores in an illuminated *Arabidopsis* leaf, Plant Physiol. 169 (2015) 1671–1682.
[14] D.K. Allen, P.D. Bates, H. Tjellström, Tracking the metabolic pulse of plant lipid production with isotopic labeling and flux analyses: past, present and future, Prog. Lipid Res. 58 (2015) 97–120.
[15] M. Gibbs, O. Kandler, Asymmetric distribution of C^{14} in sugars formed during photosynthesis, Proc. Natl. Acad. Sci. U. S. A. 43 (1957) 446–451.
[16] H.P. Kortschak, C.E. Hartt, G.O. Burr, Carbon dioxide fixation in sugarcane leaves, Plant Physiol. 40 (1965) 209.
[17] M.D. Hatch, C.R. Slack, Photosynthesis by sugar-cane leaves: a new carboxylation reaction and the pathway of sugar formation, Biochem. J. 101 (1966) 103.
[18] A.P. Garlick, C. Moore, N.J. Kruger, Monitoring flux through the oxidative pentose phosphate pathway using [1-^{14}C] gluconate, Planta 216 (2002) 265–272.
[19] P.L. Keeling, J.R. Wood, R.H. Tyson, I.G. Bridges, Starch biosynthesis in developing wheat grain: evidence against the direct involvement of triose phosphates in the metabolic pathway, Plant Physiol. 87 (1988) 311–319.
[20] M. Dieuaide-Noubhani, G. Raffard, P. Canioni, A. Pradet, P. Raymond, Quantification of compartmented metabolic fluxes in maize root tips using isotope distribution from ^{13}C-or ^{14}C-labeled glucose, J. Biol. Chem. 270 (1995) 13147–13159.
[21] P.W. Harrison, N.J. Kruger, Validation of the design of feeding experiments involving [^{14}C] substrates used to monitor metabolic flux in higher plants, Phytochemistry 69 (2008) 2920–2927.
[22] L.M. Hill, A.M. Smith, Evidence that glucose 6-phosphate is imported as the substrate for starch synthesis by the plastids of developing pea embryos, Planta 185 (1991) 91–96.
[23] S.A. Coates, T. ap Rees, Metabolism of glucose monophosphates by leucoplasts and amyloplasts from soybean suspension cultures, Phytochemistry 35 (1994) 881–883.
[24] G.L. Wheeler, M.A. Jones, N. Smirnoff, The biosynthetic pathway of vitamin C in higher plants, Nature 393 (1998) 365–369.
[25] M. Fowler, T. Ap Rees, Carbohydrate oxidation during differentiation in roots of Pisum sativum, Biochim. Biophys. Acta (BBA)—Gen.Subj. 201 (1970) 33–44.
[26] M. Stitt, T. ap Rees, Pathways of carbohydrate oxidation in leaves of *Pisum sativum* and *Triticum aestivum*, Phytochemistry 17 (1978) 1251–1256.
[27] S.A. Hill, T. ap Rees, The effect of hypoxia on the control of carbohydrate metabolism in ripening bananas, Planta 197 (1995) 313–323.
[28] S.A. Hill, T. ap Rees, Fluxes of carbohydrate metabolism in ripening bananas, Planta 192 (1993) 52–60.
[29] T. ap Rees, J.H. Green, P.M. Wilson, Pyrophosphate: fructose 6-phosphate 1-phosphotransferase and glycolysis in non-photosynthetic tissues of higher plants, Biochem. J. 227 (1985) 299–304.
[30] S.K. Masakapalli, R.G. Ratcliffe, T.C. Williams, Quantification of ^{13}C enrichments and isotopomer abundances for metabolic flux analysis using ^{1}D NMR spectroscopy, in: M. Dieuaide-Noubhani, A.P. Alonso (Eds.), Plant Metabolic Flux Analysis, Springer-Humana Press, New York, 2014, pp. 73–86.
[31] H.K. Kim, Y.H. Choi, R. Verpoorte, NMR-based plant metabolomics: where do we stand where do we go? Trends Biotechnol. 29 (2011) 267–275.
[32] R.R. Forseth, F.C. Schroeder, NMR-spectroscopic analysis of mixtures: from structure to function, Curr. Opin. Chem. Biol. 15 (2011) 38–47.
[33] L.A. Cernusak, et al., Stable isotopes in leaf water of terrestrial plants, Plant Cell Environ. 39 (2015) 1087–1102.
[34] T.W. Boutton, S.R. Archer, A.J. Midwood, Stable isotopes in ecosystem science: structure, function and dynamics of a subtropical savanna, Rapid Commun. Mass Spectrom. 13 (1999) 1263–1277.
[35] G.D. Farquhar, J.R. Ehleringer, K.T. Hubick, Carbon isotope discrimination and photosynthesis, Annu. Rev. Plant Biol. 40 (1989) 503–537.
[36] H. Alonso-Cantabrana, S. von Caemmerer, Carbon isotope discrimination as a diagnostic tool for C4 photosynthesis in C3-C4 intermediate species, J. Exp. Bot. (2016), http://dx.doi.org/10.1093/jxb/erv1555.
[37] G. Tcherkez, G. Cornic, R. Bligny, E. Gout, J. Ghashghaie, In vivo respiratory metabolism of illuminated leaves, Plant Physiol. 138 (2005) 1596–1606.
[38] L.A. Cernusak, et al., Why are non-photosynthetic tissues generally 13C enriched compared with leaves in C3 plants? Review and synthesis of current hypotheses, Funct. Plant Biol. 36 (2009) 199–213.
[39] J. Ghashghaie, F.W. Badeck, Opposite carbon isotope discrimination during dark respiration in leaves versus roots—a review, New Phytol. 201 (2014) 751–769.
[40] V.M. Stahl, W. Beyschlag, C. Werner, Dynamic niche sharing in dry acidic grasslands – a ^{15}N-labeling experiment, Plant Soil 344 (2011) 389–400.
[41] G. Tcherkez, Natural ^{15}N/^{14}N isotope composition in C3 leaves: are enzymatic isotope effects informative for predicting the ^{15}N-abundance in key metabolites? Funct. Plant Biol. 38 (2011) 1–12.
[42] T. Kleinebecker, et al., Evidence from the real world: ^{15}N natural abundances reveal enhanced nitrogen use at high plant diversity in Central European grasslands, J. Ecol. 102 (2014) 456–465.
[43] D. Robinson, ^{15}N as an integrator of the nitrogen cycle, Trends Ecol. Evol. 16 (2001) 153–162.
[44] C.H. Blessing, R.A. Werner, R. Siegwolf, N. Buchmann, Allocation dynamics of recently fixed carbon in beech saplings in response to increased temperatures and drought, Tree Physiol. 35 (2015) 585–598.
[45] R. Schoenheimer, D. Rittenberg, The study of intermediary metabolism of animals with the aid of isotopes, Physiol. Rev. 20 (1940) 218–248.
[46] J. Vederas, The use of stable isotopes in biosynthetic studies, Nat. Prod. Rep. 4 (1987) 277–337.
[47] B. Schneider, Nuclear magnetic resonance spectroscopy in biosynthetic studies, Prog. Nucl. Magn. Reson. Spectrosc. 51 (2007) 155–198.
[48] C.S. Elmore, R.A. Bragg, Isotope chemistry; a useful tool in the drug discovery arsenal, Bioorg. Med. Chem. Lett. 25 (2015) 167–171.
[49] P.E.H. Minchin, M.R. Thorpe, Using the short-lived isotope ^{11}C in mechanistic studies of photosynthate transport, Funct. Plant Biol. 30 (2003) 831–841.
[50] A. Nanchen, T. Fuhrer, U. Sauer, Determination of metabolic flux ratios from ^{13}C-experiments and gas chromatography-mass spectrometry data, in: W. Weckwerth (Ed.), Metabolomics: Methods and Protocols, Humana Press, New York, 2007, pp. 177–197.
[51] U. Roessner-Tunali, et al., Kinetics of labelling of organic and amino acids in potato tubers by gas chromatography-mass spectrometry following incubation in ^{13}C labelled isotopes, Plant J. 39 (2004) 668–679.
[52] S.C. Sharples, S.C. Fry, Radioisotope ratios discriminate between competing pathways of cell wall polysaccharide and RNA biosynthesis in living plant cells, Plant J. 52 (2007) 252–262.
[53] T. ap Rees, Compartmentation of plant metabolism, in: A.B. Smith (Ed.), The Biochemistry of Plants, Academic Press, San Diego, 1987, pp. 1–25.
[54] A.P. Alonso, et al., A metabolic flux analysis to study the role of sucrose synthase in the regulation of the carbon partitioning in central metabolism in maize root tips, Metab. Eng. 9 (2007) 419–432.
[55] S.B. Rood, P.B. Kaufman, H. Abe, R.P. Pharis, Gibberellins and gravitropism in maize shoots: endogenous gibberellin-like substances and movement and metabolism of [^{3}H] gibberellin A20, Plant Physiol. 83 (1987) 645–651.
[56] R. Katahira, H. Ashihara, Profiles of the biosynthesis and metabolism of pyridine nucleotides in potatoes (*Solanum tuberosum* L.), Planta 231 (2009) 35–45.
[57] J.B. West, G.J. Bowen, T.E. Cerling, J.R. Ehleringer, Stable isotopes as one of nature's ecological recorders, Trends Ecol. Evol. 21 (2016) 408–414.
[58] F.C. Meinzer, et al., Dynamics of water transport and storage in conifers studied with deuterium and heat tracing techniques, Plant Cell Environ. 29 (2006) 105–114.
[59] G. Tcherkez, et al., In folio respiratory fluxomics revealed by ^{13}C isotopic labeling and H/D isotope effects highlight the noncyclic nature of the tricarboxylic acid cycle in illuminated leaves, Plant Physiol. 151 (2009) 620–630.
[60] L.J. Sweetlove, K.F. Beard, A. Nunes-Nesi, A.R. Fernie, R.G. Ratcliffe, Not just a circle: flux modes in the plant TCA cycle, Trends Plant Sci. 15 (2010) 462–470.
[61] Y. Dellero, et al., Experimental evidence for a hydride transfer mechanism in plant glycolate oxidase catalysis, J. Biol. Chem. 290 (2015) 1689–1698.
[62] J. Schleucher, P. Vanderveer, J.L. Markley, T.D. Sharkey, Intramolecular deuterium distributions reveal disequilibrium of chloroplast phosphoglucose isomerase, Plant Cell Environ. 22 (1999) 525–533.
[63] X.-Y. Yang, et al., Measuring the turnover rates of Arabidopsis proteins using deuterium oxide: an auxin signaling case study, Plant J. 63 (2010) 680–695.
[64] J. Kloehn, E.C. Saunders, S. O'Callaghan, M.J. Dagley, M.J. McConville, Characterization of metabolically quiescent Leishmania parasites in murine lesions using heavy water labeling, PLoS Pathog. 11 (2015) e1004683.
[65] V. Theodorou, K. Skobridis, D. Alivertis, I.P. Gerothanassis, Synthetic methodologies in organic chemistry involving incorporation of [^{17}O] and [^{18}O] isotopes, J. Label. Comp. Radiopharm. 57 (2014) 481–508.
[66] M.M. Barbour, Stable oxygen isotope composition of plant tissue: a review, Funct. Plant Biol. 34 (2007) 83–94.
[67] M. Ribas-Carbo, et al., Electron partitioning between the cytochrome and alternative pathways in plant mitochondria, Plant Physiol. 109 (1995) 829–837.
[68] T.R. Pick, et al., PLGG1 a plastidic glycolate glycerate transporter, is required for photorespiration and defines a unique class of metabolite transporters, Proc. Natl. Acad. Sci. U. S. A. 110 (2013) 3185–3190.
[69] R.D. Evans, Physiological mechanisms influencing plant nitrogen isotope composition, Trends Plant Sci. 6 (2001) 121–126.
[70] C. António, et al., Regulation of primary metabolism in response to low oxygen availability as revealed by carbon and nitrogen isotope redistribution, Plant Physiol. 170 (2016) 43–56.
[71] S. Herrmann, et al., Endogenous rhythmic growth in oak trees is regulated by internal clocks rather than resource availability, J. Exp. Bot. 66 (2015) 7113–7127.
[72] R. Alexova, C.J. Nelson, R.P. Jacoby, A.H. Millar, Exposure of barley plants to low Pi leads to rapid changes in root respiration that correlate with specific alterations in amino acid substrates, New Phytol. 206 (2015) 696–708.
[73] L. Li, C.J. Nelson, C. Solheim, J. Whelan, A.H. Millar, Determining degradation and synthesis rates of Arabidopsis proteins using the kinetics of progressive

^{15}N labeling of two-dimensional gel-separated protein spots, Mol. Cell. Proteom. 11 (2012) M111 (010025).
[74] E.L. Huttlin, A.D. Hegeman, A.C. Harms, M.R. Sussman, Comparison of full versus partial metabolic labeling for quantitative proteomics analysis in *Arabidopsis thaliana*, Mol. Cell. Proteom. 6 (2007) 860–881.
[75] R. Hebeler, et al., Study of early leaf senescence in *Arabidopsis thaliana* by quantitative proteomics using reciprocal ^{14}N/^{15}N labeling and difference gel electrophoresis, Mol. Cell. Proteom. 7 (2008) 108–120.
[76] A. Gruhler, W.X. Schulze, R. Matthiesen, M. Mann, O.N. Jensen, Stable isotope labeling of *Arabidopsis thaliana* cells and quantitative proteomics by mass spectrometry, Mol. Cell. Proteom. 4 (2005) 1697–1709.
[77] S.F. Martin, V.S. Munagapati, E. Salvo-Chirnside, L.E. Kerr, T. Le Bihan, Proteome turnover in the green alga *Ostreococcus tauri* by time course ^{15}N metabolic labeling mass spectrometry, J. Proteom. Res. 11 (2011) 476–486.
[78] G. Mastrobuoni, et al., Proteome dynamics and early salt stress response of the photosynthetic organism *Chlamydomonas reinhardtii*, BMC Genomics 13 (2012) 1.
[79] C.J. Nelson, R. Alexova, R.P. Jacoby, A.H. Millar, Proteins with high turnover rate in barley leaves estimated by proteome analysis combined with in planta isotope labeling, Plant Physiol. 166 (2014) 91–108.
[80] H. Ishihara, T. Obata, R. Sulpice, R.F. Alisdair, M. Stitt, Quantifying protein synthesis and degradation in *Arabidopsis* by dynamic $^{13}CO_2$ labeling and analysis of enrichment in individual amino acids in their free pools and in protein, Plant Physiol. 168 (2015) 74–93.
[81] M.M. Lehmann, et al., Malate as a key carbon source of leaf dark-respired CO_2 across different environmental conditions in potato plants, J. Exp. Bot. 66 (2015) 5769–5781.
[82] S.B. Crown, C.P. Long, M.R. Antoniewicz, Integrated ^{13}C-metabolic flux analysis of 14 parallel labeling experiments in *Escherichia coli*, Metab. Eng. 28 (2015) 151–158.
[83] S. Gopalakrishnan, C.D. Maranas, ^{13}C metabolic flux analysis at a genome-scale, Metab. Eng. 32 (2015) 12–22.
[84] T. Nakajima, et al., Integrated metabolic flux and omics analysis of *Synechocystis* sp. PCC 6803 under mixotrophic and photoheterotrophic conditions, Plant Cell Physiol. 55 (2014) 1605–1612.
[85] P. Lindén, O. Keech, H. Stenlund, P. Gardeström, T. Moritz, Reduced mitochondrial malate dehydrogenase activity has a strong effect on photorespiratory metabolism as revealed by ^{13}C labelling, J. Exp. Bot. (2016), http://dx.doi.org/10.1093/jxb/erw1030.
[86] F. Ma, L.J. Jazmin, J.D. Young, D.K. Allen, Isotopically nonstationary ^{13}C flux analysis of changes in *Arabidopsis thaliana* leaf metabolism due to high light acclimation, Proc. Natl. Acad. Sci. U. S. A. 111 (2014) 16967–16972.
[87] W.L. Araújo, A. Nunes-Nesi, S. Trenkamp, V.I. Bunik, A.R. Fernie, Inhibition of 2-oxoglutarate dehydrogenase in potato tuber suggests the enzyme is limiting for respiration and confirms its importance in nitrogen assimilation, Plant Physiol. 148 (2008) 1782–1796.
[88] W.L. Araújo, et al., Antisense inhibition of the iron-sulphur subunit of succinate dehydrogenase enhances photosynthesis and growth in tomato via an organic acid-mediated effect on stomatal aperture, Plant Cell 23 (2011) 600–627.
[89] Y. Zhang, et al., Multi-level engineering facilitates the production of phenylpropanoid compounds in tomato, Nat. Commun. 6 (2015) (Article number: 8635).
[90] S.N. Oliver, et al., Decreased expression of cytosolic pyruvate kinase in potato tubers leads to a decline in pyruvate resulting in an *in vivo* repression of the alternative oxidase, Plant Physiol. 148 (2008) 1640–1654.
[91] A. Tiessen, et al., Evidence that SNF1-related kinase and hexokinase are involved in separate sugar-signalling pathways modulating post-translational redox activation of ADP-glucose pyrophosphorylase in potato tubers, Plant J. 35 (2003) 490–500.
[92] P. Geigenberger, R. Reimholz, U. Deiting, U. Sonnewald, M. Stitt, Decreased expression of sucrose phosphate synthase strongly inhibits the water stress-induced synthesis of sucrose in growing potato tubers, Plant J. 19 (1999) 119–129.
[93] K. Kölling, M. Thalmann, A. Müller, C. Jenny, S.C. Zeeman, Carbon partitioning in *Arabidopsis thaliana* is a dynamic process controlled by the plants metabolic status and its circadian clock, Plant Cell Environ. 38 (2015) 1965–1979.
[94] P.A. Pham, et al., Analysis of knockout mutants reveals non-redundant functions of poly(ADP-ribose)polymerase isoforms in *Arabidopsis*, Plant Mol. Biol. 89 (2015) 319–338.
[95] E.R.A. Boex-Fontvieille, P.P.G. Gauthier, F. Gilard, M. Hodges, G.G.B. Tcherkez, A new anaplerotic respiratory pathway involving lysine biosynthesis in isocitrate dehydrogenase-deficient *Arabidopsis* mutants, New Phytol. 199 (2013) 673–682.
[96] T. Hasunuma, et al., Metabolic turnover analysis by a combination of in vivo ^{13}C-labelling from $^{13}CO_2$ and metabolic profiling with CE-MS/MS reveals rate-limiting steps of the C3 photosynthetic pathway in *Nicotiana tabacum* leaves, J. Exp. Bot. 61 (2010) 1041–1051.
[97] W.-P. Chen, et al., An automated growth enclosure for metabolic labeling of *Arabidopsis thaliana* with ^{13}C-carbon dioxide – an *in vivo* labeling system for proteomics and metabolomics research, Proteome Sci. 9 (2011) 1–14.
[98] M.J. Morgan, et al., Decrease in manganese superoxide dismutase leads to reduced root growth and affects tricarboxylic acid cycle flux and mitochondrial redox homeostasis, Plant Physiol. 147 (2008) 101–114.
[99] F. Matsuda, K. Morino, M. Miyashita, H. Miyagawa, Metabolic flux analysis of the phenylpropanoid pathway in wound-healing potato tuber tissue using stable isotope-labeled tracer and LC-MS spectroscopy, Plant Cell Physiol. 44 (2003) 510–517.
[100] V. Dal Cin, et al., Identification of genes in the phenylalanine metabolic pathway by ectopic expression of a MYB transcription factor in tomato fruit, Plant Cell 23 (2011) 2738–2753.
[101] M.K.M. Engqvist, et al., GLYCOLATE OXIDASE3 a Glycolate oxidase homolog of yeast l-lactate cytochrome c oxidoreductase, supports L-lactate oxidation in roots of *Arabidopsis*, Plant Physiol. 169 (2015) 1042–1061.
[102] H. Yoo, et al., An alternative pathway contributes to phenylalanine biosynthesis in plants via a cytosolic tyrosine:phenylpyruvate aminotransferase, Nat. Commun. 4 (2013) (Article number: 2833).
[103] I. Gonda, et al., Catabolism of *L*–methionine in the formation of sulfur and other volatiles in melon (*Cucumis melo* L.) fruit, Plant J. 74 (2013) 458–472.
[104] I. Gonda, et al., Branched-chain and aromatic amino acid catabolism into aroma volatiles in *Cucumis melo* L. fruit, J. Exp. Bot. 61 (2010) 1111–1123.
[105] R. Heise, et al., Flux profiling of photosynthetic carbon metabolism in intact plants, Nat. Protoc. 9 (2014) 1803–1824.
[106] K. Lenhart, et al., Evidence for methane production by saprotrophic fungi, Nat. Commun. 3 (2012) (Article number: 1046).
[107] S.K. Masakapalli, et al., Metabolic flux phenotype of tobacco hairy roots engineered for increased geraniol production, Phytochemistry 99 (2014) 73–85.
[108] M. Lehmann, et al., The metabolic response of *Arabidopsis* roots to oxidative stress is distinct from that of heterotrophic cells in culture and highlights a complex relationship between the levels of transcripts, metabolites, and flux, Mol. Plant 2 (2009) 390–406.
[109] N.J. Kruger, R.G. Ratcliffe, Fluxes through plant metabolic networks: measurements, predictions, insights and challenges, Biochem. J. 465 (2015) 27–38.
[110] B.H. Junker, Flux analysis in plant metabolic networks: increasing throughput and coverage, Curr. Opin. Biotechnol. 26 (2014) 183–188.
[111] X. Chen, Y. Shachar-Hill, Insights into metabolic efficiency from flux analysis, J. Exp. Bot. 63 (2012) 2343–2351.
[112] M. Simons, et al., Nitrogen-use efficiency in maize (*Zea mays* L.): from 'omics' studies to metabolic modelling, J. Exp. Bot. 65 (2014) 5657–5671.
[113] M.R. Antoniewicz, ^{13}C metabolic flux analysis: optimal design of isotopic labeling experiments, Curr. Opin. Biotechnol. 24 (2013) 1116–1121.
[114] W.L. Araújo, T. Tohge, A. Nunes-Nesi, T. Obata, A.R. Fernie, Analysis of kinetic labeling of amino acids and organic acids by GC–MS, in: M. Dieuaide-Noubhani, A.P. Alonso (Eds.), Plant Metabolic Flux Analysis, Springer-Humana Press, New York, 2014, pp. 107–119.

CHAPTER 3

Auxin signaling modulates tomato plant growth through changes in photosynthetic and mitochondrial metabolism

Chapter 3: Manuscript in preparation

Auxin signaling modulates tomato plant growth through changes in photosynthetic and mitochondrial metabolism

Willian Batista Silva[1,2], David B. Medeiros[1,2], Acácio Rodrigues-Salvador[1,2], Danilo M. Daloso[3],[§], Rebeca P. Omena-Garcia[1,2], Franciele Santos Oliveira[1,2], Lilian Ellen Pino[4], Lázaro Eustáquio Pereira Peres[4], Adriano Nunes-Nesi[1,2], Alisdair R. Fernie[3], Agustín Zsögön[1], Wagner L. Araújo[1,2*]

[1]Departamento de Biologia Vegetal, Universidade Federal de Viçosa, 36570-900, Viçosa, Minas Gerais, Brazil
[2]Max-Planck Partner Group at the Departamento de Biologia Vegetal, Universidade Federal de Viçosa, 36570-900, Viçosa, Minas Gerais, Brazil
[3]Central Metabolism Group, Max Planck Institute of Molecular Plant Physiology, 14476 Potsdam-Golm, Germany
[4]Departmento de Ciências Biológicas, Escola Superior de Agricultura Luiz de Queiroz, Universidade de São Paulo, Piracicaba 13418-900, Brazil

Type of authorship:	First author
Type of article:	Research article
Share of the work:	80%
Contribution to the publication:	planned and performed all experiments, analyzed data, prepared all figures and wrote parts of the paper
Journal:	Plant, Cell & Environment
5-year impact factor:	6.173
Situation:	Submitted, under review

Running title: Auxin signalling modulates growth in tomato

***Corresponding author:**
Wagner L. Araújo
Departamento de Biologia Vegetal,
Universidade Federal de Viçosa,
36570-900 Viçosa, Minas Gerais, Brazil
E-mail: wlaraujo@ufv.br
Tel: +55 31 3899.2169; Fax**:** +55 31 3899.2580

Footnotes:

§Present address: Departamento de Bioquímica e Biologia Molecular, Universidade Federal do Ceará, Fortaleza, Ceará, Brasil.

This work was supported by funding from the Max Planck Society (to W.L.A.), the Conselho Nacional de Desenvolvimento Científico e Tecnológico (CNPq-Brazil to W.L.A.), and the Fundação de Amparo à Pesquisa do Estado de Minas Gerais (FAPEMIG-Brazil, Grant APQ- 01078-15 and APQ-01357-14 to A.N.N and W.L.A.). We also thank the scholarships granted by the Brazilian Federal Agency for Support and Evaluation of Graduate Education (CAPES-Brazil) to WBS. DBM was supported by a CAPES post-doctoral grant. Research fellowships granted by CNPq-Brazil to ANN and WLA are also gratefully acknowledged.

Abstract

Auxin regulates a range of plant developmental and physiological processes, including embryogenesis, organogenesis, and shoot and root development. Recent studies have shown that plant hormones can also strongly regulate metabolic networks, which results in altered growth phenotypes. Here, we performed a detailed physiological and metabolic characterization of tomato mutants with either increased (entire) or reduced (diageotropica - dgt) auxin signaling. We show that reduced auxin perception n in dgt led to anatomical and physiological modifications including altered stomatal distribution along the leaf blade and reduced stomatal conductance, resulting in clear reductions in both photosynthesis and water loss in detached leaves. By contrast, plants with increased perception of auxin (entire) increased the photosynthetic capacity as deduced by higher V_{cmax} and J_{max}. Remarkably, our results demonstrate that dgt plants are characterized by impairments in the usage of starch that led to lower growth most likely associated with decreased respiration. Collectively, our findings support the link between auxin and photosynthetic rates and suggest that, despite the pleiotropic effects caused by the mutations, the alteration in auxin signaling seems to modulate primary metabolism, particularly photosynthetic and respiratory processes, impacting whole plant growth and function.

Summary statement:

Changes in the levels of auxin as well as its response to it are usually characterized by dramatic phenotypes and visible changes in growth. However, the connections between auxin signaling and primary metabolism in leaves remains unknown. We show that mutations in auxin signaling compromise photosynthetic capacity and alter primary metabolism, modulating growth through significant alterations in the mitochondrial respiratory process. Our findings suggest that alterations in auxin signaling have dramatic effects on primary metabolism, particularly on photosynthesis and respiration, which impact whole plant growth and function. Our results collectively indicate that auxin acts as an integrator of developmental and metabolic programs and suggests that the altered auxin signaling affects metabolism in illuminated leaves.

Key words: auxin; metabolic adjustment, mitochondria; photosynthesis; plant hormones; respiration; stomata

Introduction

Plant hormones are signals that relay information about internal and external conditions and thereby allow the maintenance of cell homeostasis. Auxin was first identified as a plant hormone on the basis of its ability to stimulate differential growth in response to different stimuli (Davis, 2005). Auxin distribution within plant tissues controls an impressive variety of developmental processes (Vanneste & Friml, 2009). Although there are numerous forms of auxin, the most abundant and physiologically relevant auxin is Indole-3-acetic acid (IAA) (Enders & Strader, 2015). Several processes are affected by IAA, among them, cell expansion, formation of floral organs, vascular tissue differentiation, apical dominance, side branching, and suppression of leaf abscission (Enders & Strader, 2015). Insights into auxin transport and signaling have allowed significant advances in elucidating its role in plant development (Mockaitis & Estelle, 2008). However, the molecular effectors by which this hormone exerts its effects and how auxin signaling affects primary metabolism remain largely unknown (Wang et al., 2005).

The auxin signaling pathway is mediated by a complex system of transcriptional regulators of the AUXIN/INDOLE ACETIC ACID (Aux/IAA) family (Delker, Raschke & Quint, 2008), controlling the interaction between auxin and its receptors including TRANSPORT INHIBITOR RESPONSE 1 (TIR1), which is a member of the AUXIN SIGNALING F-BOX PROTEIN (AFB) family (Leyser, 2017, Shabek & Zheng, 2014, Tan et al., 2007). Members of the Aux□IAA gene family have highly specific spatial and temporal expression patterns, thus contributing to the diversity of auxin responses in different plant, tissues, organs, and developmental stages (Audran-Delalande et al., 2012, Delker et al., 2008) For instance, down-regulation of the tomato (Solanum lycopersicum) Aux□IAA9 (SlIAA9, also known as ENTIRE), generates a constitutive

auxin response associated to specific phenotypes, such as leaf morphogenesis, in which the compound leaves of tomato are converted to simple leaves and the plants yield parthenocarpic fruits (Wang et al., 2005, Zhang et al., 2007). By contrast, the tomato diageotropica (dgt) mutant is characterized by reduced sensitivity to auxin caused by loss-of-function in a cyclophilin A protein, with peptidyl-prolyl trans-cis isomerase (PPIase) enzymatic activity (Oh et al., 2006). The dgt mutation leads to pleiotropic phenotypes, including impaired gravitropic response (Rice & Lomax, 2000), absence of lateral root branching (Muday et al., 1995), reduced polar auxin transport and apical dominance (Ivanchenko et al., 2015), and altered vascular development (Zobel, 1973). Furthermore, DGT is essential in determining final fruit size, through the control of cell division and cell expansion (Devoghalaere et al., 2012). In addition, the dgt mutation is also thought to disrupt a signaling cascade that includes the extracellular auxin binding protein 1 (ABP1) (Christian et al., 2003), a putative receptor for a non-canonical auxin signaling pathway. Interestingly, mutants of the ortholog of dgt have been discovered in the moss Physcomitrella patens (Lavy et al., 2012), and in rice (Oryza sativa) (Zheng et al., 2013). These mutants besides presenting similar phenotypes to that observed in tomato dgt plants additionally exhibit altered auxin sensitivity. Molecular and biochemical studies seeking to understand the role of cyclophilins in the auxin response were performed by studying the dgt ortholog from rice, LATERAL ROOTLESS 2 (LRT2) (Jing et al., 2015). In brief, the authors demonstrated that LRT2 can directly regulate the stability of Aux/IAA proteins, with OsIAA11, controlling the interaction between TIR1 and IAA and affecting the life span of Aux/IAA proteins as a mechanism regulating auxin signaling.

Plant mitochondria play an essential and key role in the biosynthesis of adenosine triphosphate (ATP) through oxidative phosphorylation (Hackett, 1959,

Plaxton & Tran, 2011). Accordingly, the tricarboxylic acid (TCA) cycle in the mitochondria is fundamental in catalyzing the oxidation of acetyl-CoA into CO2, simultaneously producing NADH, FADH2, ATP, and carbon skeletons which act as substrates for several metabolic processes (Araujo et al., 2012, Fernie et al., 2004). These compounds are essential to support plant growth and are of pivotal importance in responses to different environmental conditions (Berkowitz et al., 2016, Millar et al., 2011, Mishra & Chan, 2016). Recent compelling evidence has shown that plant hormones can regulate networks affecting mitochondrial metabolism (Berkowitz et al., 2016) and uncouple carbon and nitrogen metabolism (Ribeiro et al., 2012a, Ribeiro et al., 2012b). Interestingly, it has previously been suggested that auxin regulates mitochondrial respiration to meet the increased energy demand for growing cells (Leonova et al., 1985). Although the role of auxin in controlling plant growth and development is well established, our understanding on the interaction between auxin and central metabolism remains limited. However, early findings have demonstrated that compounds that inhibit the TCA cycle and respiratory chain also inhibited auxin-induced growth (Thimann, 1977). Furthermore, connections between mitochondrial function and auxin during plant growth and in response to stress have been observed (Berkowitz et al., 2016, Ivanova et al., 2014)

Although the importance of auxin for sugar metabolism and development has been established in tomato fruits (Chen et al., 2016, Li et al., 2017, Li et al., 2016, Sagar et al., 2013a, Sagar et al., 2013b) and Chinese pear (Pyrus ussuriensis) (Huang et al., 2014), the possible link between auxin signaling and metabolic aspects in leaves has not been investigated yet. Here, we used tomato mutants with either increased (entire) or reduced (diageotropica, dgt) auxin signaling. Our results demonstrated that dgt displayed a range of morphological and anatomical alterations as well as reduced

156 photosynthetic capacity. By contrast, the entire mutant was characterized by changes
157 in the levels of TCA cycle intermediates and nitrogen-related metabolites, indicating
158 that auxin can act as an integrator of developmental and metabolic programs in
159 illuminated tomato leaves.
160
161

Material and Methods

Plant material and growth conditions

Seeds of the tomato (Solanum lycopersicum cv Micro-Tom) wild-type (WT) and near isogenic lines (NILs) dgt and entire in the same genetic background (cv. Micro-Tom), obtained as described previously (Carvalho et al., 2011), were surface-sterilized with 5% sodium hypochlorite for 10 min, then washed with running distilled water and subsequently sowed in a tray with commercial substrate (Tropstrato HT©).

Seven days after germination (or following the appearance of the first true leaf), seedlings were transferred to 3.5 L pots containing the same commercial substrate supplemented with 5 g L^{-1} 4:14:8 NPK. Plants were grown in a greenhouse located in Viçosa (20°45′S, 42°15′W, 650 m above sea level), southeastern Brazil, with a minimum of 400 µmol photons m^{-2} s^{-1}. Plants were watered regularly and throughout the entire growth period were maintained under naturally fluctuating conditions of light intensity, temperature and relative air humidity. The mutated alleles were confirmed through Sanger DNA sequencing in an ABI Prism 3100 platform using primers specific for DGT (Solyc01g111170), 5'- GAGTCGCCGTTTTAGGCTTT-3' and 3'- GCAACACAACAACCAATTACG-5' and ENTIRE (Solyc04g076850), 5'- GTTGTCAAGTGTGTGACAGCC-3' and 3'- TGTCACTTACACATAGGGCCA-5'. The abundance of transcripts was confirmed by quantitative real time PCR (qRT-PCR), using specific primer pairs for DGT and ENTIRE: Forward 5'- GAGTCGCCGTTTTAGGCTTT-3', Reverse 5'-GCAACACAACAACCAATTACG-3' and Forward 5'- GTTGTCAAGTGTGTGACAGCC-3',Reverse 5'- TGTCACTTACACATAGGGCCA-3' respectively (for details see Supplemental Table S4).

187 **Growth analyses**

188 Growth parameters were determined in 4-weeks-old plants by measuring plant
189 height, stem diameter, number of leaves and specific leaf area (SLA). Leaf area was
190 measured using a scanner (Hewlett Packard Scanjet G2410, Palo Alto, California,
191 USA) and processing the resulting images on ImageJ (Schneider et al., 2012). SLA
192 was measured as described previously (Hunt et al., 2002). At the end of the
193 experiment, plants were harvested by cutting the shoot 1 cm above ground level, thus
194 separating shoots from roots. The roots, after water washing off soil contamination,
195 and shoots, were placed in labelled paper bags and brought to a forced air circulation
196 oven at 70 ℃ for five days, after which the dry weight of roots and shoots (stem,
197 petioles, and leaves) was determined in an electronic balance.

198

199 **Stomatal density, stomatal index, and leaf anatomy**

200 After 2h under sunlight, leaf impressions were taken from the abaxial and
201 adaxial surface of the third fully expanded leaf with dental resin imprints (Berger &
202 Altmann, 2000). After shaping the leaf surfaces, nail polish copies were made using a
203 colorless glaze (von Groll et al., 2002). The images were analyzed under a light
204 microscope (Olympus model AX70TRF; Olympus Optical, Tokyo, Japan) equipped
205 with a U-Photo System and digital camera (AxioCam HRc; Zeiss, Göttingen,
206 Germany). Stomatal density, stomatal index and stomatal pore aperture were
207 determined in at least 10 different fields of 0.10 mm^2 per leaf from at least seven
208 different plants.

209 For leaf anatomy analyses, sections of the terminal leaflet of the third fully
210 expanded leaf were hand cut from the widest part of the leaf using a razor blade and
211 stored in 100% methanol for epidermal analysis, or in formaldehyde – acetic acid (FAA)

in ethanol 70% (v/v) solution for 24h for transverse analysis (Feder & O'brien, 1968) and afterwards, embedded in resin (historesin), sectioned in (~5 µm, RM 2155 Automated Microtome, Leica. Sections were next mounted on a microscopy slide and stained with 1% (w/v) toluidine blue. Histological sections were observed under a light microscope (Olympus model AX70TRF; Olympus Optical, Tokyo, Japan) and images captured using a digital camera (AxioCam HRc; Zeiss, Göttingen, Germany). Images were analyzed using ImageJ (Schneider et al., 2012).

Water loss measurements

For water loss measurements, the weight of detached leaves, incubated with the abaxial side up under the same growth conditions described above, were determined over 4 h at the indicated time points. Water loss was calculated as a percentage of the initial fresh weight (Araújo et al., 2011).

Auxin sensitivity assays

In order to investigate root formation in response to auxin, an in vitro assay was performed using cotyledon explants taken from 8-day-old seedlings (after sowing) grown in culture medium. Five biological replicates composed by a Petri dish containing 20 explants were used for each treatment. The explants were kept for 10 days on Murashige-Skoog medium supplemented with vitamins B5 plus 30g/L of sucrose, 6g/L of agar and 0.4µM of NAA (α - naphthalene acetic acid - Sigma-Aldrich, St. Louis, MO, USA) at 25ºC 16-h day/8-h night (Murashige & Skoog, 1962). The auxin response curve using hypocotyl segments was performed using 10 day-old seedlings (after sowing) growing under greenhouse conditions. The explants were collected using a razor blade (~12cm) and placed in Petri dishes containing Kelly and Bradford

237 solution (Kelly and Bradford (1986) added with different IAA concentrations. After 24h,
238 hypocotyls were scanned at 300 dpi and the generated images were captured using a
239 digital camera (AxioCam HRc; Zeiss, Göttingen, Germany).
240
241 **Measurements of gas exchange and chlorophyll fluorescence**
242 Gas exchange parameters were determined simultaneously with chlorophyll a
243 (Chl a) fluorescence measurements as described in (Medeiros et al., 2016) using an
244 open-flow infrared gas exchange analyzer system (LI-6400XT; LI-COR Inc., Lincoln,
245 NE) equipped with an integrated fluorescence chamber (LI-6400-40; LI-COR Inc.).
246 Instantaneous gas exchanges were measured after 1 h illumination during the light
247 period under 1000 μmol m^{-2} s^{-1} at the leaf level (light saturation) of photosynthetically
248 active photon flux density (PPFD), determined by A/PPFD curves - net photosynthesis
249 (A_N) in response to PPFD curves (Supplemental Fig. S8 and Supplemental Table S1).
250 The reference CO_2 concentration was set at 400 μmol CO_2 mol^{-1} air. All measurements
251 were performed using the 2 cm^2 leaf chamber at 25℃, as well as a 0.5 stomatal ratio
252 (amphistomatic leaves), and leaf-to-air vapor pressure deficit was kept at 1.2 kPa,
253 while the amount of blue light was set to 10% PPFD to optimize stomatal aperture.
254 Briefly, the initial fluorescence emission (F_0) was by illuminating dark-adapted leaves
255 (1 h) with weak modulated measuring beams (0.03 μmol m^{-2} s^{-1}). A saturating white
256 light pulse (8000 μmol m^{-2} s^{-1}) was applied for 0.8 s to obtain the maximum
257 fluorescence (Laskowski et al., 2008), from which the variable-to-maximum Chl
258 fluorescence ratio, was then calculated: $F_v/F_m=[(F_m - F_0)/F_m)]$. In light-adapted leaves,
259 the steady-state fluorescence yield (Baggerman et al., 2005) was measured with the
260 application of a saturating white light pulse (8000 μmol m^{-2} s^{-1}) to achieve the light-
261 adapted maximum fluorescence (F_m'). A far-red illumination (2 μmol m^{-2} s^{-1}) was

applied after turn off the actinic light to measure the light-adapted initial fluorescence (F_{0}'). The capture efficiency of excitation energy by open photosystem II reaction centers ($F_{v'}/F_{m'}$) was estimated following (Logan et al., 2007) and the actual PSII8 photochemical efficiency (φPSII) was estimated as φPSII = $(F_{m'} – F_s)/F_{m'}$ (Genty et al., 1989).

According to Genty et al. (1989), Φ_{PSII} represents the number of electrons transferred per photon absorbed in the PSII, the electron transport rate (J_{flu}) was calculated as $J_{flu} = \Phi_{PSII}.\alpha.\beta.PPFD$, where α is leaf absorptance and reflects β the partitioning of absorbed quantum between and PSI and PSII. The product $\alpha\beta$ was determined according with previous studies of optical properties using a double integrated ball system ISP-REF (OceanOptics, Inc., Dunedin, Florida, EUA), measuring the reflectance (R) and transmittance (T) and then calculating the absorbtance (A), according with the followed equation: A= 1-(R+T). The β value was considered the standard fraction of quanta (0.5) and α was 0.85, where 0.425 is the product already shown in (Gilbert et al., 2012). Dark respiration (R_d) was measured after 2h in the dark period (at night), using the same gas exchange system described above and it was divided by two ($R_d/2$) to estimate the mitochondrial respiration rate in the light (R_L) (Niinemets et al., 2005, Niinemets et al., 2009) .

Photosynthetic light-response curves (A/PPFD) were determined using ambient CO_2 concentration (C_a) of 400 µmol CO_2 mol^{-1} and an initial PPFD of 1000 µmol photon m^{-2} s^{-1}. PPFD was next increased to 1200 µmol m^{-2} s^{-1}, 1400 µmol m^{-2} s^{-1} and thereafter decreased to 0 µmol m^{-2} s^{-1} (step changes to 1000, 800, 400, 200, 100, 50, 25, 10, and 0 µmol m^{-2} s^{-1}). Simultaneously, Chl a fluorescence parameters were obtained (Wong et al., 2012, Yin et al., 2009). The responses of A_N to C_i (A/C_i curves), were initiated at saturating light of 1000 µmol m^{-2} s^{-1} at 25ºC under ambient O_2 concentration (21%).

Measurements were taken at ambient CO_2 concentration (C_a) of 400 µmol mol^{-1} and once the steady state was reached, C_a was decreased stepwise to 50 µmol mol^{-1}. Upon completion of the measurements at low C_a, C_a was returned to 400 µmol mol^{-1} to restore the original A_N. Next, C_a was increased stepwise to 1600 µmol mol^{-1} in a total of 13 different C_a values (Long & Bernacchi, 2003). Following Rodeghiero et al. (2007), corrections were made for the leakage of CO_2 into and water vapor out of the leaf chamber of the LI-6400, and were applied to all gas exchange data. A/C_i and A_N/PPFD curves were obtained using the third leaf, totally expanded.

Determination of mesophyll conductance (g_m), maximum rate of carboxylation (V_{cmax}), maximum rate of carboxylation limited by electron transport (J_{max}) and photosynthetic limitations

The CO_2 concentration in the carboxylation sites (C_c) was calculated according to Harley et al. (1992) as:

$C_c = (\Gamma^* (J_{flu}+8 (A_N + R_L))/ (J_{flu} – 4(A_N + R_L))$.

where the conservative value of Γ* for tomato was taken from (Hermida-Carrera et al., 2016). The, g_m was estimated as the slope of the A_N vs C_i–C_c relationship as: $g_m=A_N/(C_i-C_c)$.

Thus, the g_m was estimated based on average over the points used in the relationship (C_i < 300 µmol mol^{-1}). Furthermore, the methods for estimating g_m include several assumptions as well as technical limitations, along with sources of error, which need to be considered to obtain reliable values (Pons et al., 2009). g_m was estimated according to the (Ethier & Livingston, 2004) method, which fits A_N/C_i curves with a nonrectangular hyperbola version of the Farquhar-von Caemmerer-Berry FvCB model,

based on the hypothesis that g_m reduces the curvature of the Rubisco-limited portion of an A_N/C_i curve.

From A_N/C_i and A_N/C_c curves, the maximum carboxylation velocity (V_{cmax}) and the maximum capacity for electron transport rate (J_{max}) were calculated by fitting the mechanistic model of CO_2 assimilation (Farquhar et al., 1980), using the C_i and C_c based on temperature of kinetic parameters of Rubisco (K_c and K_o) and V_{max}, J_{max}, and g_m were normalized to 25ºC using the temperature response and plug-in equations as previously described (Sharkey et al., 2007)

The photosynthetic limitations were estimated as described previously (Grassi & Magnani, 2005). Briefly, this method uses the values of A_N, g_s, g_m, V_{cmax}, Γ^*, C_c , K_m, and $K_m = K_c (1+ O/K_o)$ and permits the partitioning into the functional components of photosynthetic constraints related to stomatal (l_s), mesophyll (l_m), and biochemical (l_b) limitations:

$$l_s = \frac{(\frac{g_{tot}}{g_s}\frac{\partial A_N}{\partial C_c})}{(g_{tot} + \frac{\partial A_N}{\partial C_c})}$$

$$l_{\mathrm{m}} = \frac{\left(\frac{g_{tot}}{g_{\mathrm{m}}} x \frac{\partial A_N}{\partial C_c}\right)}{g_{tot} + (\frac{\partial A_N}{\partial C_c})}$$

$$l_b = \frac{g_{tot}}{(g_{tot} + \partial A_N/\partial C_c)}$$

g_{tot} is the total conductance to CO_2 from ambient air to chloroplasts: ($g_{tot} = 1/[(1/g_s)+(1/g_m)]$). The fraction $\partial A_N/\partial C_c$ was calculated as:

$$\frac{\partial A_N}{\partial C_c} = \frac{([V_{\mathrm{cmax}}(\Gamma^* + K_m)])}{(Cc + Km)^2}$$

Determination of metabolite levels

Leaf samples were harvested in different time points along of the light/dark cycle (0; 3; 6; 9; 12; 15; 18; 19; 21; and 24 h) , immediately frozen in liquid nitrogen and stored at -80ºC until further analysis. The extraction was performed by rapid grinding of tissue in liquid nitrogen and immediate addition of the appropriate extraction buffer. The levels of starch, sucrose, fructose and glucose in the leaf tissue were determined exactly as described previously (Fernie et al., 2001). Photosynthetic pigments were determined according to the methods by Porra et al. (1989). Malate and fumarate were determined according Nunes-Nesi et al. (2007). Proteins and amino acids were determined as described previously (Gibon et al., 2004). The metabolites profile was carried out in samples harvested at the middle of the day (Lisec et al., 2006). The extraction was performed using 1mL of methanol and shaking (800 rpm) at 70 ºC during 15 min, 60 µL of Ribitol (0.2mg mL^{-1}) was added as an internal standard. After that, the derivatization procedure was performed exactly as described in (Roessner et al., 2001). Peaks were manually annotated, and ion intensity was determined by the aid of TagFinder software (Luedemann et al., 2011), using a reference library from the Golm Metabolome Database (Kopka et al., 2004) and, following the recommended reporting format (Fernie et al., 2011).

Measurement of respiratory parameters based on $^{14}CO_2$ evolution

Estimation of the TCA cycle flux was calculated on the basis of $^{14}CO_2$ evolution (Nunes-Nesi et al., 2005). The experiment was carried out following incubation of

isolated leaf discs in 10 mM 2-(N-morpholine)-ethanesulphonic acid (MES)-KOH, pH 6.5, containing 0.3mM Glc and supplied with 0.62 KBq mL^{-1} of [1-^{14}C]- or [3,4-^{14}C] Glc under 150 µmol photons m^{-2} s^{-1} light. Evolved $^{14}CO_2$ was trapped in KOH and quantified by liquid scintillation counting. The fractionation of ^{14}C -Labeled material was performed exactly as detailed previously (Lytovchenko et al., 2002). The results were interpreted following recommendations of ap Rees and Beevers (1960).

Expression analysis by qRT-PCR

Quantitative real-time PCR (qRT-PCR) analysis was performed exactly as described by Zanor et al. (2009) with total RNA isolated from at least three biological replicates. The samples were harvested and snap frozen in liquid nitrogen. RNA extraction was performed using TRizol® reagent (Ambion, Life Technology) following the manufacturer's manual. Digestion with DNase I (Ambion; http://www.ambion.com/) was performed according to the manufacturer's instructions. The integrity of the RNA was checked on 1% (w/v) agarose gels, and the concentration was measured before and after DNase I digestion using a Nanodrop ND-1000 spectrophotometer (http://www.nanodrop.com/). DNA was synthesized from 1 µg of total RNA using SuperScript III reverse transcriptase (Invitrogen; http://www.invitrogen.com/) according to the manufacturer's instructions. The efficiency of cDNA synthesis was estimated by semi-quantitative PCR using two primer pairs amplifying 5' and 3' regions of the constitutive gene Actin (forward [5'-GGTCCCTCTATTGTCCACAG-3'] and reverse [5'-TGCATCTCTGGTCCAGTAGGA-3']. Gene expression values were normalized based on the Actin (Solyc03g078400.2.1) gene with the following primers, forward (5'-GGTCCCTCTATTGTCCACAG-3') and reverse (5'-TGCATCTCTGGTCCAGTAGGA-3'). The primers used for qRT-PCR were designed using the QuantiPrime software

384 (http:www.quantprime.de). Detailed primers information is described in the
385 Supplemental Table S4.
386
387 **Experimental Design and Statistical Analysis**
388 The data was obtained from the experiments using a completely randomized
389 design. The term significant is used here only when the change has been confirmed to
390 be significant ($P < 0.05$) by Student's t-test. All statistical analyses were performed
391 using the algorithm embedded into Microsoft Excel® (Microsoft, Seattle).
392

Results

Alterations in auxin signaling severely affect plant growth and water use efficiency

Here we investigated the physiological impacts of fluctuations on auxin signaling using previously characterized tomato mutants with either increased (entire, a mutation in the SlIAA9 gene) or reduced (diageotropica, dgt) auxin signaling. The mutants show a clearly distinct phenotype during vegetative growth (Fig. 1A and Table 1). In an attempt to show this differential perception of auxin, we initially confirmed that SlIAA9 and DGT expression were significantly reduced in entire and dgt mutant plants, respectively (Fig. 1B). Furthermore, the expression of DGT in the entire mutant and of SlIAA9 in the dgt mutant did not differ significantly compared to wild type (WT) control plants (Fig. 1B). We next evaluated the expression levels of the DGT and SlIAA9 genes in different tissues of WT plants. Our results showed that the basal expression of both genes is highly variable across the whole plant. Thus, whilst DGT is highly expressed in roots, young leaves, mature leaves, and open flowers, SlIAA9 is expressed in young leaves, mature leaves, flowers, and young fruits (Supplemental Fig. S1). Our results are in good agreement with both previously published results (Wang et al., 2009) and public RNA-Seq data in tomato cv. Micro-Tom plants (http://tomexpress.toulouse.inra.fr/select-data).

In order to confirm the alteration in the auxin perception in dgt and entire plants, we next investigated the auxin dose effect on both root formation and hypocotyl segment elongation (Supplemental Fig. S2). The entire mutant plants do not present a significant increase in auxin perception when compared to WT although it does respond differentially to exogenously applied auxin (Supplemental Fig. S2A, B). Interestingly, in WT plants the synthetic auxin, α-naphthalene acetic acid (NAA),

promoted root regeneration at concentrations above 0.1 µM, which is ten times higher than the critical concentration observed in entire (Supplemental Fig. S2). By contrast, dgt plants displayed reduced sensitivity to auxin (Supplemental Fig. S2). In response to exogenous auxin, dgt plants were characterized by reduced root production in explants (Supplemental Fig. S2 A, B) as well as failure of hypocotyls to elongate (Supplemental Fig. S2C).

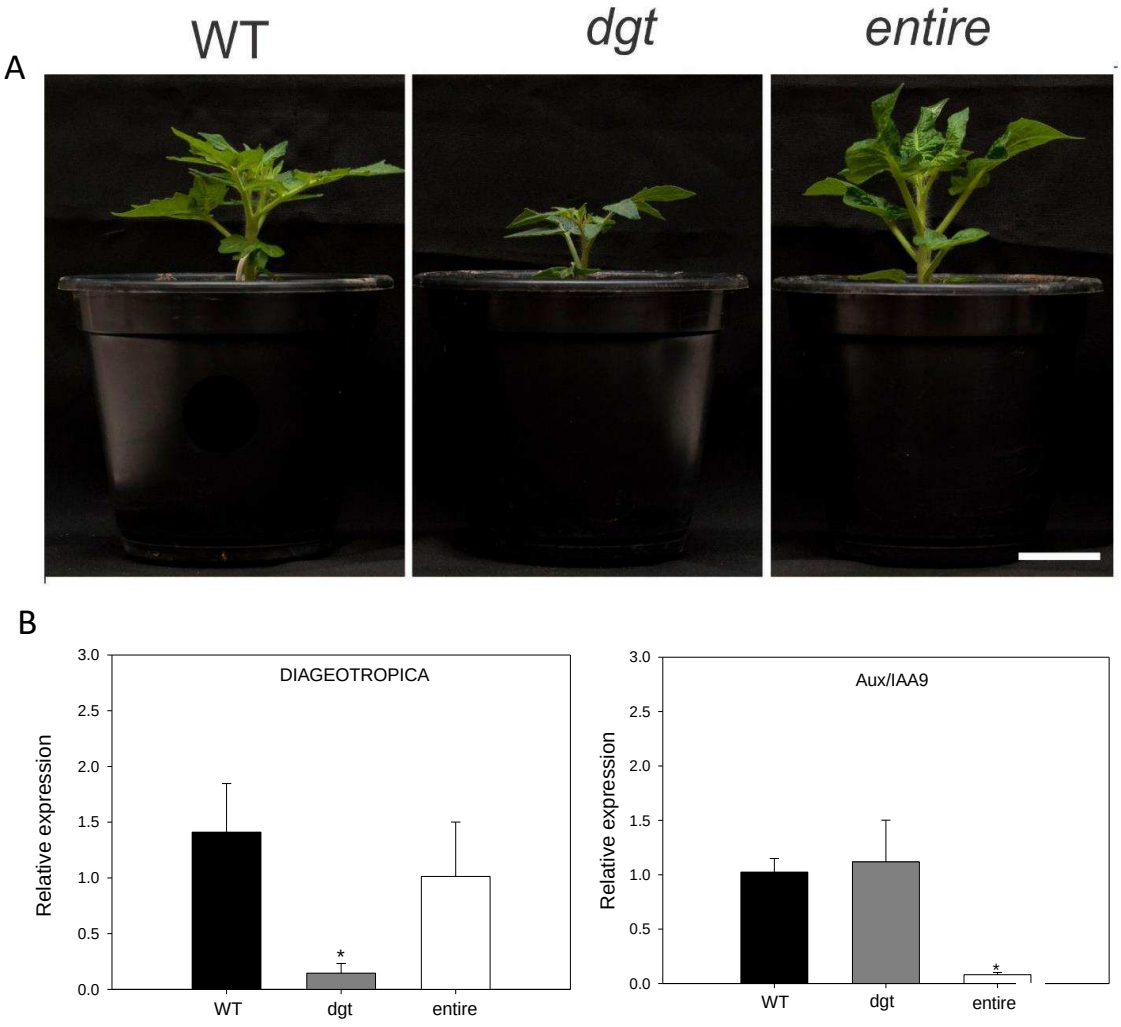

Fig.1 Phenotypic and molecular characterization of auxin signaling mutants. **A,** Representative images of 4-week-old plants with either increased (entire) or reduced (diageotropica, dgt) auxin signaling, compared to wild-type (WT, tomato cv. Micro-Tom) plants growing under optimal conditions. **B,** Relative transcript expression performed by quantitative Real Time PCR (qRT-PCR) showed significant reduction in the expression of mutant alleles, with no effect on the wild-type alleles. Data are normalized with respect to the average response calculated for the corresponding WT. WT, black bars; dgt, grey bars, entire, white bars. Data are means ± SE (n = 5). Asterisks (*) indicate that the values from auxin signaling mutants were determined by the Student's t-test to be significantly different ($P<0.05$) from the WT.

Table 1. Growth and morphology are altered in auxin signaling related mutants. Plants with either increased (entire) or reduced (diageotropica, dgt) auxin signaling were compared to wild-type (WT) plants growing under optimal conditions. Data are means ± SE (n=7) obtained in at least two independent assays; values set in bold indicate that the values from auxin signaling mutants were determined by the Student's t test to be significantly different (P≤0.05) from the WT (wild type).

Parameters*	WT	dgt	entire
Plant height (cm)	6.1 ± 0.2	**4.9 ± 0.2**	6.6 ± 0.4
Total leaf area (cm^2)	47.0 ± 3.7	**21.5 ± 1.9**	**43.8 ± 2.6**
SLA ($cm^2\ g^{-1}$)	177.6 ± 9.3	**254.2 ± 17.2**	**133.7 ± 1.5**
TDW (g)	0.29 ± 0.02	**0.13 ± 0.01**	**0.41 ± 0.02**
ASD (mm^{-2})	165.76 ± 10.2	**238.54 ± 9.7**	**91.07± 2.9**
AdSD (mm^{-2})	40.79 ± 2.89	**67.07 ± 2.1**	30.48 ± 2.2
ASI (%)	50.22 ± 2.39	**12.73 ± 0.5**	**47.55 ± 3.1**
Abaxial pore area (μm^2)	120.59 ± 0.87	**105.62 ± 5.6**	**194.95 ± 8.6**
Adaxial pore area (μm^2)	103.93 ± 2.52	**57.28 ± 2.0**	**134.33 ± 2.3**
Thickness (µm)	80.89 ± 8.45	**105.4 ± 14.8**	**48.98 ± 9.6**
RWC (%)	82.61 ± 1.38	80.97±0.58	85.53 ± 1.2

*SLA= Specific leaf area, TDW= Total dry weight, RWC= Relative water content, ASD= abaxial stomatal density, ASI= abaxial stomatal index.

435

436 In an attempt to show the effect of changes in auxin signaling, we decided to
437 analyze whole plant traits of both mutants. The entire plants were characterized by
438 increased number of leaves and total dry weight, but thinner leaves with reduced
439 specific leaf area (SLA) and stomatal density (Table 1 and Supplemental Fig. S3).
440 Although such leaf phenotypes could potentially affect water relations, relative water
441 content was invariant between WT and mutant plants (Table 1). Moreover, dgt plants
442 also exhibited higher SLA, increased stomatal density, stomatal index, reduced
443 stomatal pore diameters and leaf blade (Supplemental Fig. S3 and S4). These

morphological alterations culminated with changes in water use as demonstrated by enhanced water loss in detached leaves of entire, while in dgt water loss was decreased in comparison to WT plants (Supplemental Fig. S5).

Alterations in auxin signaling affect photosynthetic capacity

Given the alterations observed in morphology and growth, we next performed a full characterization of the photosynthetic capacity of dgt and entire mutants. In close agreement with the stomatal density and stomatal index changes (Table 1), a significant reduction of net photosynthesis (A_N), stomatal conductance (g_s), and transpiration (E) rates (12.5%, 28.5%, and 32.1% lower that WT values, respectively) was observed in dgt plants (Table 2). By contrast, significant increases in A_N, g_s, and E (10.42%, 21%, and 12.5% of that of WT, respectively) were observed in entire plants (Table 2). The dgt mutant further displays higher intrinsic water use efficiency (WUEi) than WT plants, whereas no difference in WUEi was found for entire (Table 2). On the other hand, no significant differences in R_d were observed in dgt plants but a two-fold increase was observed in entire plants (Table 2). Despite these changes, no significant changes in photorespiration (P_R), maximum PSII photochemical efficiency (F_v/F_m), actual PSII photochemical efficiency (F_v'/F_m') and the electron transport rate (J_{flu}) were found among the genotypes (Table 2). Photosynthetic light response curves revealed that mutants have altered A_N at high photosynthetic photon flux density (PPFD). The light-saturated A_N (A_{PPFD}), light saturation (I_s) and light compensation (I_c) points as well as light use efficiency ($1/\Phi$) were significantly higher in entire plants whereas only I_s was reduced in dgt plants (Supplemental Table S1 and Supplemental Fig. S6).

The response of A_N to leaf internal CO_2 concentration (A_N/C_i curves; Figure 2A) was also obtained and subsequently converted into responses of A_N to chloroplastidic

469 CO_2 concentration (A_N/C_c curves; Figure 2B). Essentially, both A_N/C_i and A_N/C_c curves
470 were similar regardless of genotype (Fig. 2). Under ambient CO_2 concentration (400
471 µmol mol^{-1}), C_i and C_c estimations were lower in dgt and higher in entire plants
472 compared to the WT (Table 3). We next estimated mesophyll conductance to CO_2 (g_m)
473 which showed similar values between genotypes (Table 3). Considering that g_m, as
474 well as day respiratory capacity (R_L), change dynamically under different
475 environmental conditions, we performed a sensitivity curve response of g_m under
476 different R_L (Supplemental Fig. S7). This analysis was performed considering different
477 percentages of R_L (100, 75, 50, 25 and 0%) and following the expected changes in g_m
478 (Supplemental Fig. S7). Our results showed no significant changes in g_m despite
479 alterations in R_L even when 100% of R_L was considered in relation to R_d (1.51; 1.37
480 and 2.70 µmol CO_2 m^{-2} s^{-1} in WT, dgt and entire, respectively). In addition, the
481 maximum carboxylation velocity (V_{cmax_cc}) and maximum capacity for electron transport
482 rate (J_{max_cc}) was similar between dgt and WT plants. On the other hand, increasing
483 auxin signaling led to higher V_{cmax_cc} and J_{max_cc} without impacting either J_{max_Ci}:V_{cmax_Ci}
484 or J_{max_Cc} :V_{cmax} (table 3). Moreover, the similarities in the J_{max}:V_{cmax} ratios suggest that
485 although differences in A_N were observed, an adequate functional balance between
486 carboxylation and electron transport rates probably occurred despite changes in auxin

signaling.

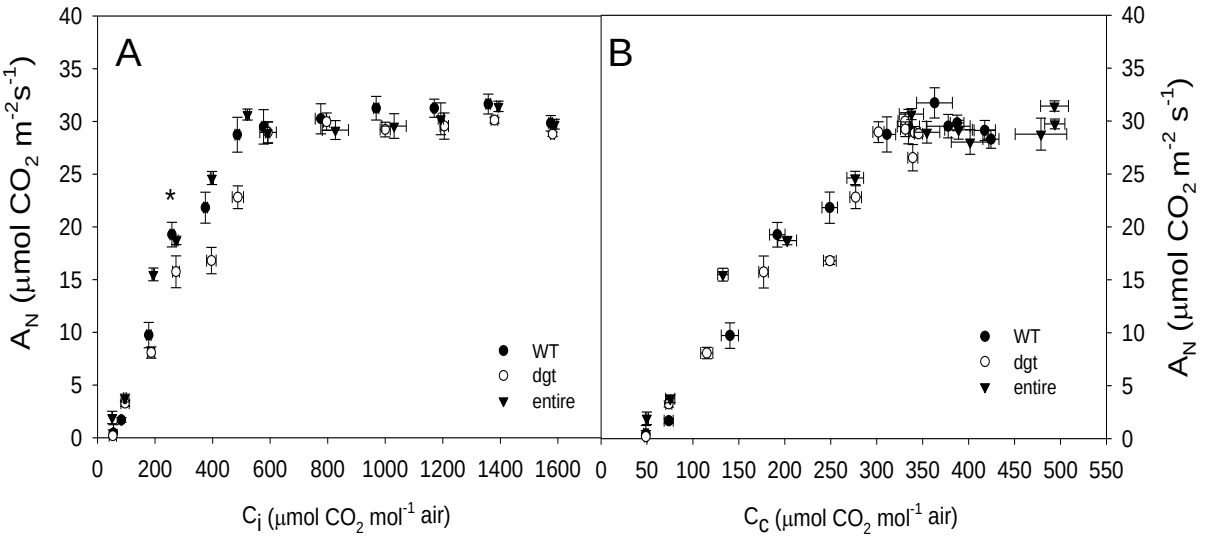

Fig 2. Net photosynthesis (AN) curves in response to sub-stomatal (Ci) or chloroplastic (Cc) CO2 concentration in auxin signaling mutants (dgt and entire). A, AN/Ci curve, and B, AN/Cc. Plants with either increased (entire) or reduced (diageotropica, dgt) auxin signaling were compared to wild-type (WT) plants growing under optimal conditions. WT, black circles; dgt, open circles; entire, black triangles. Data are means ± SE (n=7) obtained using the 3th fully expanded leaf from the apex of 4-week-old plants (vegetative stage). Asterisks (*) indicate that the values from auxin signaling mutants from this point and above were determined by the Student's t-test to be significantly different ($P<0.05$) from the WT.

The overall photosynthetic limitations were next partitioned into their functional components namely stomatal (l_s), mesophyll (l_m), and biochemical (l_b) limitations (Table 3). The photosynthetic rates were mainly constrained by l_b of around 50% in WT whereas l_s accounted for, on average, 28% and 24% and l_m contributed 22% and 26% in WT and entire plants, respectively. Remarkably, l_b was reduced to about 40% and followed by increased l_s to around 38% whereas l_m contributed 22% in dgt plants. These analyses demonstrated that auxin signaling-related mutants are affected mainly in l_s, in agreement with morphological alterations, particularly in dgt plants. This suggests a direct link between Diageotropica and photosynthetic capacity through morphological alterations. These results support the findings that variations in A, as described in Table 2 and 3, should be primarily associated with stomatal conductance.

509 Auxin signaling seems to be an important molecule to investigate their participation in

510 maximum photosynthetic rate in plants, consequently improving the productivity.

511

Table 2. Gas exchange and chlorophyll a fluorescence parameters are affected in auxin signaling related mutants. Data was obtained in four-week-old plants with either increased (entire) or reduced (diageotropica, dgt) auxin signaling were compared to wild-type (WT) plants growing under optimal conditions. Values are presented as means ± SE (n=7). Values set in bold indicate that the values from auxin signaling mutants were determined by the Student's t test to be significantly different (P≤0.05) from the WT.

Parameters*	WT	dgt	entire
A_N (µmol CO_2 m^{-2} s^{-1})	19.17 ± 0.62	**16.78 ± 0.30**	**21.18 ± 0.71**
g_s (mol H_2O m^{-2} s^{-1})	0.28 ± 0.01	**0.20 ± 0.008**	**0.34 ± 0.018**
E (mmol H_2O m^{-2} s^{-1})	3.68 ± 0.26	**2.50 ± 0.22**	**4.64 ± 0.28**
WUE_i (A/g_s)	69.32 ± 3.80	**83.01 ± 4.04**	61.89 ± 1.93
R_d (µmol CO_2 m^{-2} s^{-1})	1.43 ± 0.05	1.25 ± 0.11	**2.94 ± 0.14**
P_R (µmol CO_2 m^{-2} s^{-1})	3.69 ± 0.18	3.79 ± 0.29	3.66 ± 0.21
F_V/F_m	0.84 ± 0.001	0.84 ± 0.001	0.83 ± 0.001
F_V'/F_m'	0.59 ± 0.01	0.59 ± 0.011	0.61 ± 0.012
J_{flu} (µmol m^{-2} s^{-1})	170.75±3.71	161.54 ± 8.24	160.63±4.92

* A_N : Net photosynthesis rate; g_s : stomatal conductance; E: transpiration rate, WUE_i: intrinsic water-use efficiency; R_d : dark respiration; P_R : photorespiration rate; F_v/F_m : maximum PSII photochemical efficiency; F_v'/F_m'; actual PSII photochemical efficiency; J_{flu} : electron transport rate estimated by chlorophyll fluorescence parameters.

512

513

Table 3. Photosynthetic characterization of auxin signaling mutants. Data was obtained in four-week-old plants with either increased (entire) or reduced (diageotropica, dgt) auxin signaling and were compared to wild-type (WT) plants growing under optimal conditions. Values are presented as means ± SE (n=7). Values in bold indicate that the values from auxin signaling mutants were determined by the Student's t test to be significantly different (P≤0.05) from its corresponding WT.

Parameters*	WT	dgt	entire
C_i (µmol CO_2 mol^{-1})	276.32 ± 25.71	**208.82 ± 19.78**	**333.31 ± 17.49**
C_c (µmol CO_2 mol^{-1})	163.88 ± 9.75	**117.05 ± 7.97**	147.89 ± 8.90
g_m_Harley (mol CO_2 m^{-2} s^{-1} bar)	0.215 ± 0.012	0.232 ± 0.024	0.211 ± 0.015
g_m_Ethier (mol CO_2 m^{-2} s^{-1} bar)	0.234 ± 0.034	0.244 ± 0.056	0.224 ± 0.034
V_{cmax_Ci} (µmol m^{-2} s^{-1})	66.92 ± 3.69	64.41 ± 3.16	68.69 ± 2.60
V_{cmax_Cc} (µmol m^{-2} s^{-1})	107.81 ± 2.70	110.56 ± 9.25	**121.95 ± 1.48**
J_{max_Ci} (µmol m^{-2} s^{-1})	112.85 ± 7.79	112.68 ± 6.88	106.17 ± 7.21
J_{max_Cc} (µmol m^{-2} s^{-1})	134.40 ± 3.48	141.35 ± 7.62	**148.88 ± 1.97**
J_{max_Ci} :V_{cmax_Ci}	1.69 ± 0.12	1.99 ± 0.19	1.72 ± 0.02
J_{max_Cc} : V_{cmax_Cc}	1.02 ± 0.25	1.31 ± 0.07	1.22 ± 0.020
Stomatal limitation (l_s)	0.281 ± 0.015	**0.381 ± 0.018**	**0.241 ± 0.007**
Mesophyll limitation (l_m)	0.229 ± 0.011	0.224 ± 0.018	0.258 ± 0.004
Biochemical limitation (l_b)	0.493 ± 0.022	**0.395 ± 0.012**	0.501 ± 0.061

* C_i : sub-stomatal CO_2 concentration; C_c : Chloroplastic CO_2 concentration; gm: mesophyll conductance to CO_2 estimated according to the Harley; V_{cmax}_C_i or C_c: maximum carboxylation capacity based or Ci or Cc ; J_{max}_C_i or C_c: maximum capacity for electron transport rate based on C_i or Cc.

Auxin signaling modulates the levels of sugars and organic acids in tomato leaves

To further explore the consequences of changes in the auxin signaling mutants we conducted a detailed metabolic analysis in leaves. To this end, we first measured

528 the levels of starch, soluble sugars (glucose, fructose, and sucrose), amino acids, and
529 the organic acids, malate and fumarate during a diel cycle. Briefly, this analysis
530 revealed that dgt were characterized by a significant accumulation in the levels of
531 glucose (Fig. 3A), fructose (Fig. 3B), sucrose (Fig. 3C), and fumarate (Fig. 3D) during
532 the light period, but with no changes in malate (Fig. 3E) and starch (Fig. 3F). Overall,
533 plants with higher auxin sensitivity did not show significant changes in carbohydrate
534 and organic acid levels during the diurnal cycle in comparison with WT plants.
535 Interestingly, during the night, the usage of these accumulated metabolites in dgt
536 plants is not increased so that at the end of dark period higher levels were observed
537 (Fig. 3). Notably, starch metabolism seems to be highly affected in dgt plants,
538 particularly during the night (Fig. 3F). There were no significant changes in total protein
539 and amino acids, in either leaves or roots; however, nitrate concentration was greatly
540 reduced in leaves of dgt plants (Supplemental Fig. S8). Nevertheless, the dgt mutant
541 exhibited increased levels of photo-protective pigments such as carotenoids content
542 (Supplemental Fig. S9 E-B).

543 We further extended this metabolic study to measure the levels of the
544 intermediates of the primary plant metabolism by using an established gas
545 chromatography-mass spectrometry (GC-MS) protocol for metabolic profiling (Lisec
546 et al., 2006). This analysis revealed that among the 50 successfully annotated
547 compounds related to primary metabolism most of them displayed altered levels (Fig.
548 4). Namely, considerable changes in the levels of a wide range of amino acids, organic
549 acids, and sugars in the entire mutant were observed (Fig.4; the full dataset is
550 additionally provided as Supplemental Table S3). Specifically, entire plants were
551 characterized by increases in the levels of eight amino acids, namely β-alanine,
552 arginine, asparagine, glutamine, lysine, methionine, ornithine, and serine (Fig. 4 and

553 Supplemental Table S3). Similarly, in dgt mutant plants, ten of the individual amino
554 acids were significantly increased, namely arginine, asparagine, aspartate, glutamate,
555 glutamine, glycine, histidine, phenylalanine, proline, and tryptophan (Fig. 4 and
556 Supplemental Table S3). Interestingly, some organic acids detected had contrasting
557 behavior between the dgt and entire mutants including citrate, 2-oxoglutarate,
558 succinate, fumarate, and malate, whichwere all increased in dgt plants but decreased
559 in entire plants.

560 Notably, ascorbate was increased only in the dgt mutant. A similar trend is also
561 observed for sugar content in which dgt plants display significantly increases in
562 ribulose, glucose, fructose, and sucrose whereas maltose, ribose and ribulose were
563 reduced in entire plants (Supplemental Table S3). On assaying the levels of pyridine
564 dinucleotides we only observed higher levels of NADH and increased NADH/NAD^+
565 ratio in dgt mutant compared to WT plants (Supplemental Table S2).

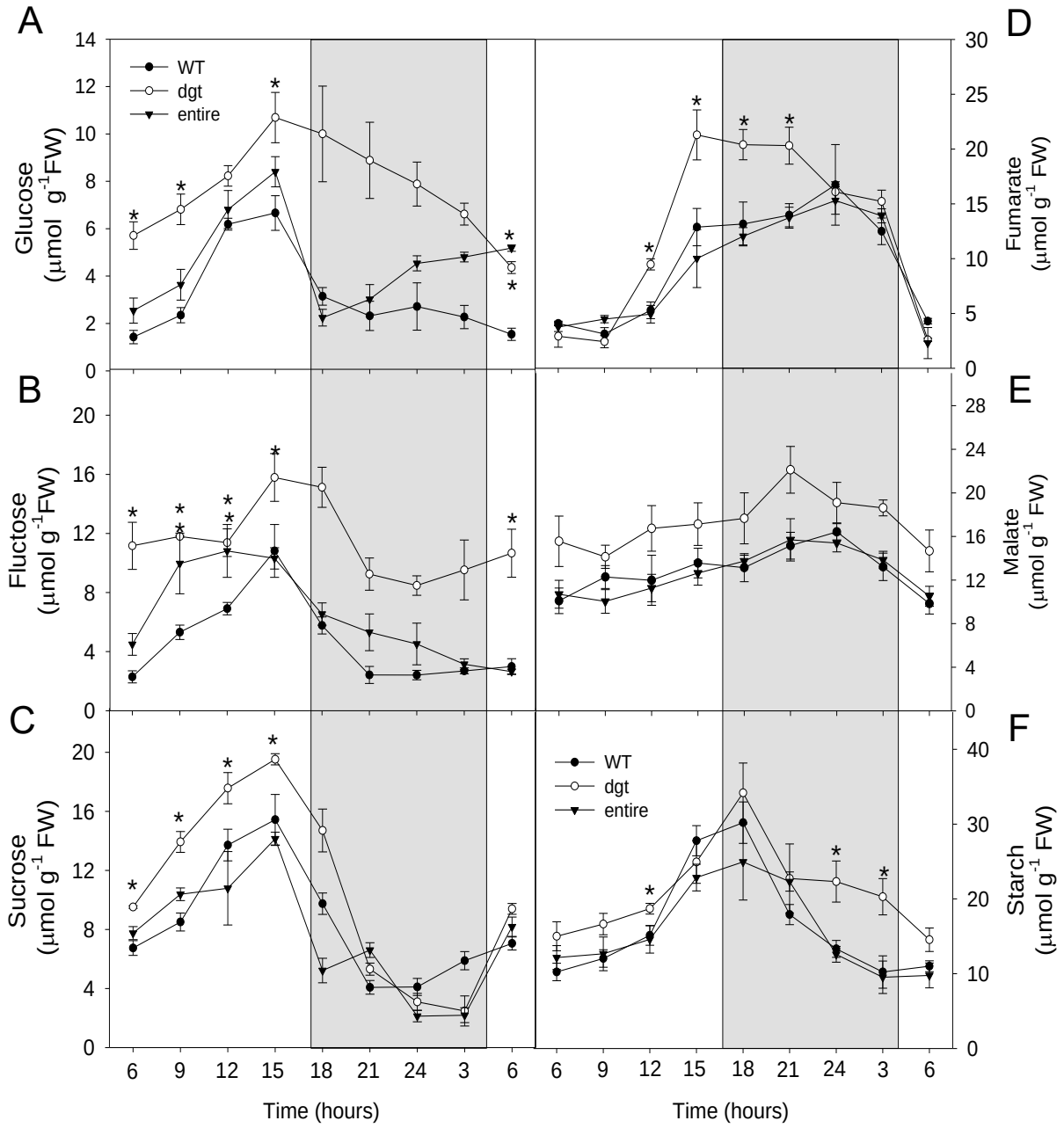

Fig 3. Leaf metabolite levels are altered in auxin signaling mutants during the diurnal cycle. Diurnal changes in key metabolite content in leaves of tomato plants with either increased (entire) or reduced (diageotropica, dgt) auxin signaling were compared to wild-type (WT) plants growing under optimal conditions. **A,** Glucose; **B**, Fructose; **C**, Sucrose; **D**, Fumarate; **E**, Malate and **F**, Starch levels were measured along a diurnal cycle. Samples were taken from the third fully expanded leaf from the apex of four-week-old plants (vegetative stage) harvested every three hours along the diurnal cycle. WT, black circle; dgt, open circle and entire, black triangles. Data are means ± SE (n=6). Asterisks (*) indicate that the values from auxin signaling mutants were determined by the Student's t-test to be significantly different ($P<0.05$) from the WT. Grey bar indicate the dark period; white bars indicate the light period. FW: Fresh weight.

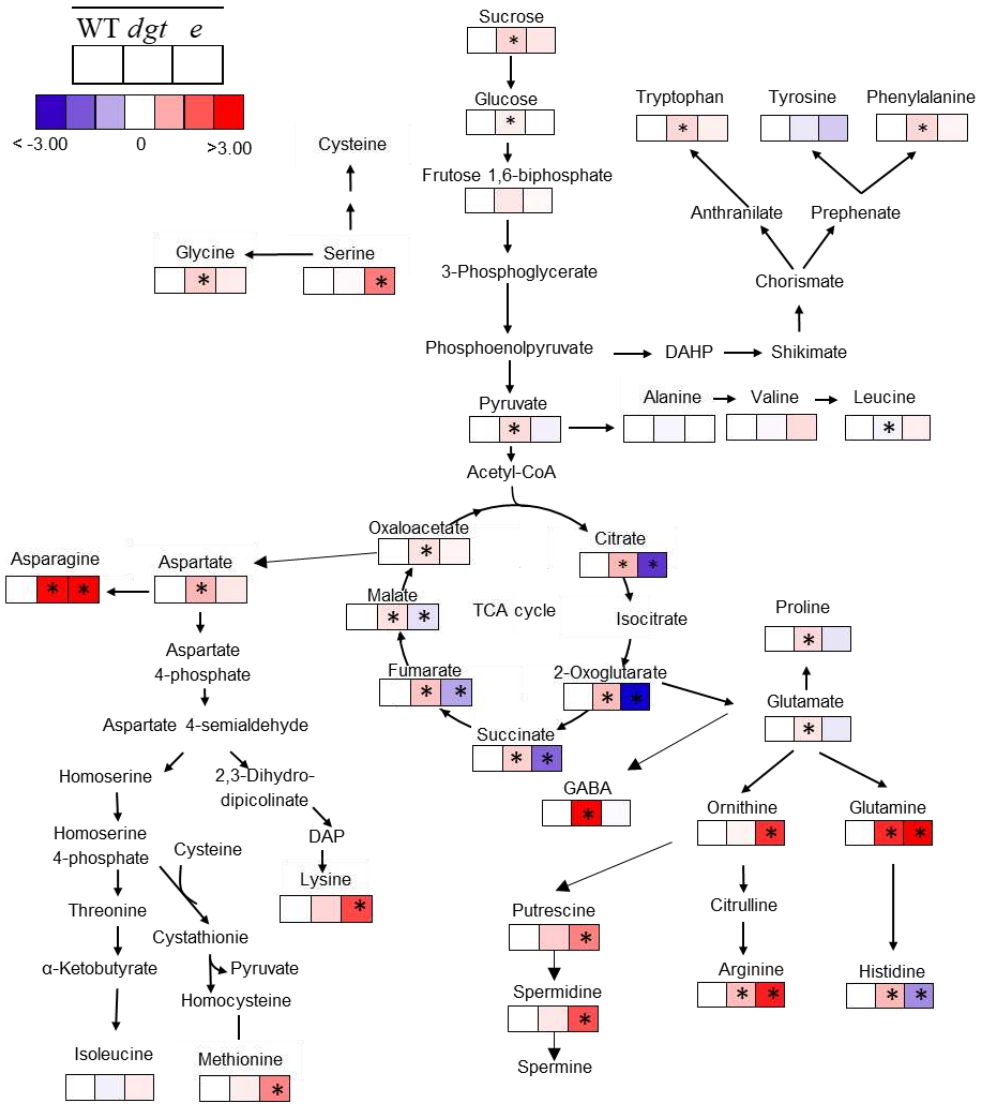

Fig. 4. Auxin signaling affects the relative metabolite content in tomato leaves. Changes in the relative metabolite content of tomato plants with either increased (entire) or reduced (diageotropica, dgt) auxin signaling were compared to wild-type (WT) plants growing under optimal conditions. Amino acids, organic acids, sugars and sugar alcohols were determined by GC-MS as described in "Materials and Methods". The full data sets from these metabolic profiling studies are additionally available in Supplemental Table 3. Data are normalized with respect to the average response calculated for the corresponding WT (to allow statistical assessment, individual plants from this set were normalized in the same way). Box in orange color indicate amino acids pathways. Different colors represent levels of metabolite fold change where red is increasing and blue is decreasing. Data were normalized with respect to mean response calculated from wild-type. Values are presented as means ± SE (n=6). Asterisks (*) indicate that the values from auxin signaling mutants were determined by the Student's t-test to be significantly different (P<0.05) from the WT.

Auxin signaling affects the flux through the TCA cycle

Given the changes in sugar and organic acid contents described above we next decided to assess the rate of respiration under normal growth conditions by performing

two complementary approaches. We directly evaluated the rate of light respiration in the mutants (dgt and entire) by measuring the $^{14}CO_2$ evolution following incubation of leaf discs with positionally-labelled ^{14}C-glucose (^{14}C-Glc) to assess the relative rate of flux through the TCA cycle and the metabolic flux analysis using ^{14}C-labed. This information is of pivotal significance given that metabolic pathways and the key regulatory point thereof can be deduced using isotopically labeled substrates (Batista Silva et al., 2016). For this purpose, we recorded the evolution of $^{14}CO_2$ following incubation of leaf discs supplied with [1-^{14}C]-Glc and [3,4-^{14}C]-Glc over a period of 6h. During this time, we collected the $^{14}CO_2$ evolved at hourly intervals. CO_2 can be released from the C1 position by the action of enzymes that are not associated with mitochondrial respiration, however, this does not happen for CO_2 released from the C3/C4 position (ap Rees & Beevers, 1960, Nunes-Nesi et al., 2007). Thus, the ratio of CO_2 evolution from C3,4 to C1 position of Glc provides a strong indication of the TCA cycle regarding other carbohydrate oxidation process. When the relative $^{14}CO_2$ release of the mutants and WT is compared for the various fed substrates, an interesting pattern emerges with a significant reduction occurring in the entire mutant following 3h of incubation with [1-^{14}C]-Glc (Fig.5-A). Thus, when supplied with [3,4-^{14}C]-Glc the $^{14}CO_2$ release was significantly increased in the entire mutant from 5h onward (Fig. 5B). Similarly, the C3,4/C1 ratio was increased in the entire mutant (Fig 5C). Thus, revealing that there is a higher proportion of carbohydrate oxidation by TCA cycle in illuminated leaves of entire plants, which is in close agreement with the results of our metabolic profiling. In addition, dark respiration was measured revealing approximately 90% higher rates of CO_2 evolution in entire plants (Fig 5D).

We next assessed the redistribution of radiolabel by incubating excised leaf discs from 4-week-old plants of dgt, entire and WT in [U-^{14}C-Glu] for period of 3h (Table

4). Interestingly, the dgt mutant exhibited and increased total radiolabel uptake and an increased incorporation in organic acids, sugar phosphate, amino acids, starch, and cell wall (Table 4). Thus, our data reveal a lower relative proportion of carbohydrate oxidation is performed by the TCA cycle in the plants with reduced perception to auxin (dgt plants). This result is in close agreement with the observation of reduced Rd in these plants. By contrast, entire mutant plants displayed an accelerated rate of oxidation of carbohydrates coupled with increases in respiratory rate under light conditions as well as increased dark respiration (Figure 5D and Table 4).

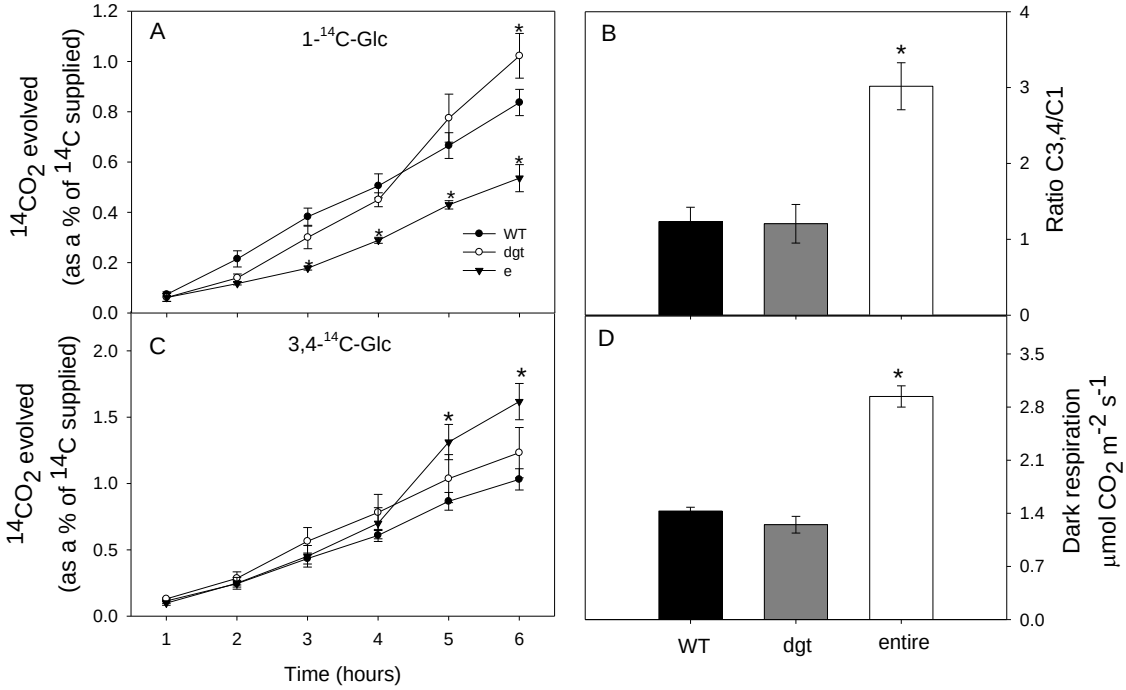

Fig 5. Respiratory parameters are affected in leaf samples of auxin signaling mutants. Changes in respiration of tomato plants with either increased (entire) or reduced (diageotropica, dgt) auxin signaling were compared to wild-type (WT) plants growing under optimal conditions. Evolution of 14CO2 from isolated leaf discs in the light. The leaf discs were taken from 4-week-old plants and were incubated in 10mM MES-KOH solution, pH 6.5, 0.3mM glucose supplemented with 0.62kBq mL-1 of (A) [1-14C]-Glc or (B) [3.4-14C] at an irradiance of 100 µmol m-1 s-1. The CO2 liberated was captured at hourly intervals in a KOH trap and the amount of radiolabel released was subsequently quantified by liquid scintillation counting. C, Ratio of carbon dioxide evolution from C3,4 to C1 position. D, Dark respiration measurements performed in 4-week-old plants. WT, black bars; dgt, grey bars, entire, white bars. Values are presented as means ± SE (n=4). Asterisks (*) indicate that the values from auxin signaling mutants were determined by the Student's t-test to be significantly different ($P<0.05$) from the WT.

Table 4. Respiratory carbon distribution is affected in leaf samples of auxin signaling mutants. Changes in respiratory carbon redistribution of radiolabel carbon after incubation in [U^{14}C]-glucose of tomato plants with either increased (entire) or reduced (diageotropica, dgt) auxin signaling were compared to wild-type (WT) plants growing under optimal conditions. Values are presented as means ± SE (n=4). Values in bold indicate that the values from auxin signaling mutants were determined by the Student's t test to be significantly different ($P \leq 0.05$) from its corresponding WT.

Parameter*	WT	dgt	entire
Label incorporated (Bq g-1 FW)			
Total uptake	111.52 ± 16.48	**195.54 ± 24.34**	117.02 ± 5.43
Organic acids + Hexose-P	22.97 ± 4.57	**49.90 ± 7.56**	**35.99 ± 1.50**
Amino acids	3.13 ± 0.42	**6.42 ± 0.56**	4.66 ± 0.68
Soluble sugars	61.61 ± 13.04	94.74 ± 10.24	47.62 ± 3.09
Starch	17.75 ± 2.31	**26.71 ± 4.01**	17.03 ± 1.22
Protein	0.66 ± 0.02	1.19 ± 0.17	0.92 ± 0.09
Cell wall	8.70 ± 0.25	**16.50 ± 2.83**	**10.77 ± 0.50**
Starch/Sucrose	0.24±0.03	0.27 ± 0.26	**0.35± 0.015**
Redistribution of radiolabel (as percentage of total assimilated)			
Organic acids + Hexose-P	21.19 ± 4.37	26.65 ± 1.08	**34.73 ± 1.27**
Amino acids	2.99 ± 0.35	3.53 ± 0.51	3.56 ± 0.18
Soluble sugars	55.40 ± 4.73	46.21 ± 0.79	**39.66 ± 0.66**
Starch	13.05 ± 0.46	14.20 ± 0.53	13.32 ± 0.65
Protein	0.63 ± 0.06	0.67 ± 0.09	0.74 ± 0.11
Cell wall	6.81 ± 0.96	8.66 ± 0.21	7.97 ± 0.29

*Leaf discs were cut from six separate plants of each genotype at the end of the night and illuminated at 150 µmol photons m^{-2} s^{-1} of PAR in Erlenmeyer flasks containing 0.62kBq mL^{-1} of unlabeled [U-14C-Glu]. After 3h the leaf discs were extracted and fractionated. FW, fresh weight.

Expression analysis of AUXIN RESPONSE FACTORS (ARF) and AUXIN/INDOLE-3-ACETIC ACID INDUCIBLE (Aux/IAA) genes

Auxin is considered a potent regulator of several aspects of plant function and this response is dependent on several genes that are highly expressed in response to

its application (Quint & Gray, 2006). Among the most thoroughly characterized genes are SAURs [Small Auxin-Up RNAs], GH3s Gretchen Hagen 3] and Aux/IAAs [Auxin/INDOLE ACETIC ACID INDUCED] gene families which are induced within minutes of auxin application (Hedden & Thomas, 2008). These genes products, as well as the Auxin Response Factors (ARFs), likely confer specificity of the auxin response through selection of target genes such as other transcription factors and effector genes (Li et al. 2016). We therefore investigated the expression levels of genes involved in auxin signaling including IAA1, IAA2, IAA3, ENTIRE/IAA9, IAA19, IAA29, ARF8, ARF10, DGT, and GH3 (Fig. 6). Transcript analysis revealed that ARF (ARF8 and ARF10) as well as IAA19 and IAA29 expression are upregulated in dgt mutant (Fig. 6). In entire mutant, the levels of IAA1, IAA2, IAA3, IAA19, IAA29, and GH3 were upregulated. Our results suggest that the DGT gene regulates the expression of members of the ARFs and Aux/IAAs families, while SlIAA9 (ENTIRE) can regulate genes of its own family (AUX/IAAs), as well as member of the GH3 family (Fig. 6).

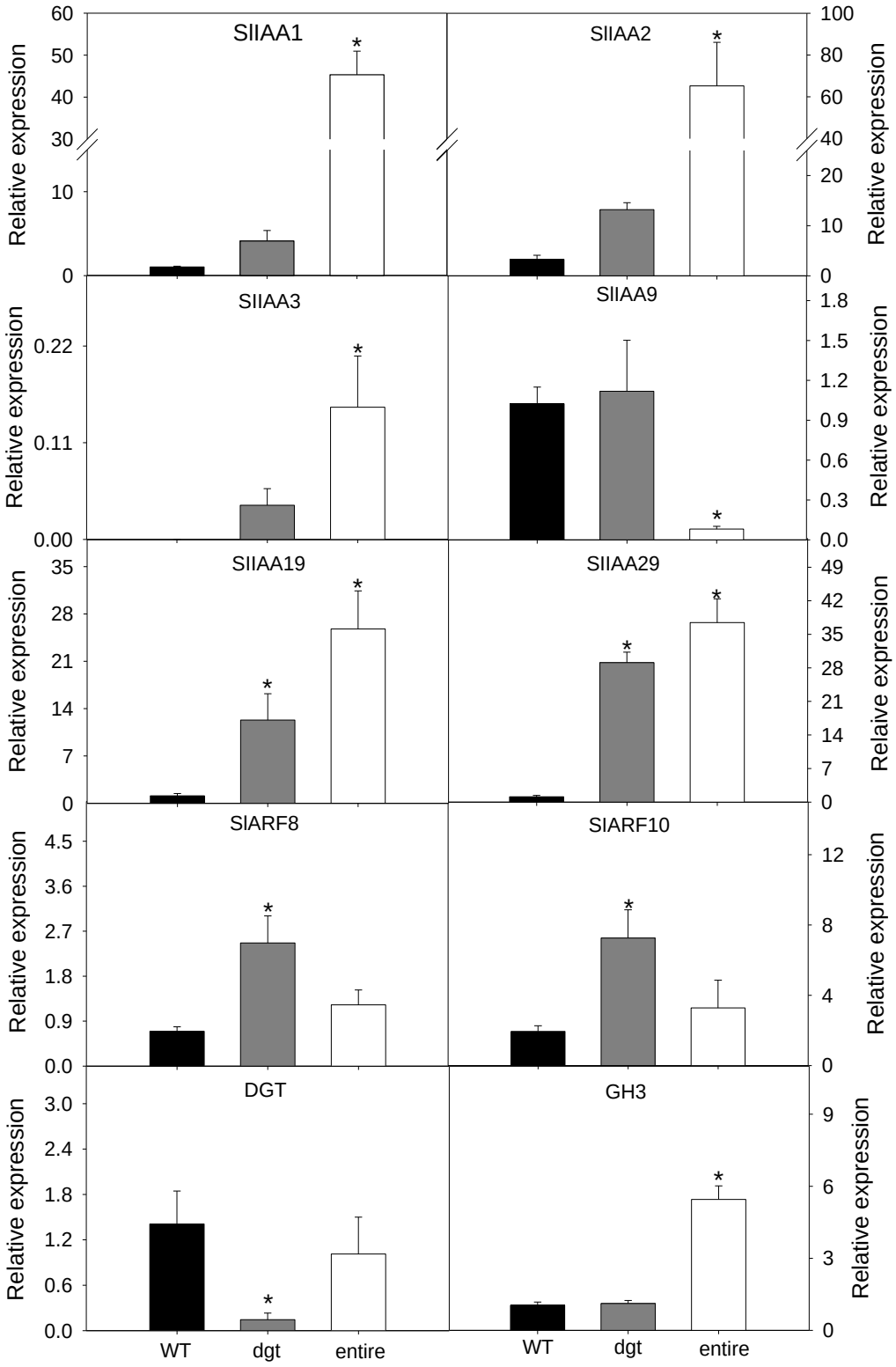

Fig 6. Relative transcript accumulation of members of SlIAA and SlARF family genes is affected in auxin signaling mutants. Relative expression levels of genes involved in auxin signaling (SlIAA and SlARF family genes) and homeostasis (GH3) are altered in tomato plants with either increased (entire) or reduced (diageotropica, dgt) auxin signaling when compared to wild-type (WT) plants growing under optimal conditions. The y-axis values represent the relative expression levels calculated using the $2^{-\Delta\Delta CT}$ method. Expression levels were normalized using actin and ubiquitin3 as reference. Values are presented as means ± SE (n=4) of independent biological replicates. Asterisks (*) indicate that the values from auxin signaling mutants were determined by the Student's t-test to be significantly different ($P<0.05$) from the WT.

Discussion

Auxin signaling impacts photosynthetic capacity and metabolism

Auxin acts as a general coordinator of plant growth and development mainly by relaying information over both long and short ranges (Leyser, 2017). The major mechanism by which auxin affects cellular responses is via changes in transcription, and thus several genes change their expression profile rapidly in response to auxin (Paponov et al., 2008). In addition, auxin is able to promote division in cell culture suspensions, which is accompanied by increased respiration (Leonova et al., 1985). It has been suggested that stimulation of cell axpansion is usually accompanied by the promotion of respiration (Bonner & Bandurski, 1952). Indeed, auxin can modulate plant growth by impacting innumerous processes such as photosynthesis and respiration (Bhardwaj et al., 2015, Ivanova et al., 2014). However, the link between auxin signaling and carbon metabolism in autotrophic tissues remain poorly understood. Combining physiological and biochemical approaches, we provide evidence that auxin signaling plays an important role in growth modulation associated with carbon metabolism. Two contrasting mutants exhibiting either reduced (dgt) or increased (entire) auxin signaling were used to provide evidence for a crucial role of this hormone on the regulation of photosynthesis and indeed primary metabolism in general within the illuminated leaf. We demonstrated that several anatomical parameters were strongly affected, culminating in significant changes in photosynthetic and respiratory capacity (Table 1; Supplemental Fig. S5-S6). Our results provide evidence that alterations in auxin signaling tightly controls plant morphology (Silva et al, 2018 in the press???), culminating in altered photosynthesis and linking with TCA cycle activity (Table 2 and Table 3). Reduced auxin signaling observed in dgt plants decreases the stomatal pore area but increase stomatal density in both sides of the leaf surface, resulting in higher

709 water use efficiency (Table 1, Supplemental Fig. S5). In fact, auxin regulates stomatal
710 patterning and development, basically by changes in its levels during stomatal
711 development (Le et al., 2014a, Le et al., 2014b). Stomatal apertures are the major
712 gateway for the movement of CO_2 from the atmosphere into the mesophyll of leaves,
713 controlling the movement of gases which also results in water vapor loss. Accordingly,
714 dgt showed reduced water loss (Supplemental Fig. S3) which can also be explained
715 by increases in the size of the leaf blade and reductions in total leaf area (Table 1 and
716 Fig. S5). Interestingly, even with increasing SLA and thickness of the leaf blade,
717 changes in g_m in comparison with WT were not observed in dgt plants.

718 Our results also revealed that increased auxin signaling in entire plants is
719 associated with enhanced photosynthetic capacity under ambient CO_2 concentration
720 as well as elevated transpiratory rates (E) which are most likely a consequence of
721 higher stomatal conductance (g_s) and increased V_{cmax} and J_{max} on a C_c basis. Although
722 these results correlate with improved plant biomass under optimal growth conditions,
723 it should be kept in mind that under low water availability the lower WUE_i presented by
724 entire plants represents a highly undesirable trait (Xu & Zhou, 2008). Considering the
725 importance of auxin in leaf venation patterning and xylem development in
726 angiosperms, as well stomatal cell morphology, this hormone may play an instrumental
727 role in the ecological success of angiosperms plants (Zhao, 2010). The link between
728 auxin biosynthesis and maximum photosynthetic rate through leaf venation has been
729 recently demonstrated, providing strong support to the theory that an increase in leaf
730 vein density, coupled with their efficient placement, can drive increases in leaf
731 photosynthetic capacity (McAdam et al., 2017). Identification of the precise mechanism
732 regulating this key anatomical feature and the exact nature of auxin in the regulation

733 of photosynthetic capacity remain important open questions that should be further
734 addressed.
735
736 **Respiratory metabolism is affected by changes in auxin signaling**
737 Our results further demonstrate that enhanced auxin signaling observed in
738 entire leads to increases not only in growth (Fig. 1), but also in respiratory and
739 photosynthetic rates (Table 2). By using complementary approaches, we further
740 confirmed that entire plants had increased respiration rates both in the dark and during
741 the day (Fig. 5), providing evidence that increased auxin signaling present in entire
742 plants stimulate respiration. In agreement with this observation, it has been suggested
743 that auxin may increase respiration rate indirectly through increased supply of
744 adenosine diphosphate (ADP) by promoting a rapid utilization of ATP in the expanding
745 cells (French & Beevers, 1953). We further observed that dgt plants seem to use less
746 transitory starch during the night leading to significant accumulation of different
747 respiratory substrates (e.g. sugars and organic acids), resulting in lower growth during
748 the vegetative stage (Fig. 3-4). The relationship between high respiratory rate and
749 rapid growth could be explained, at least partially, by the importance of the TCA cycle
750 activity in the regulation of the photosynthesis in illuminated leaves (Nunes-Nesi et al.,
751 2011, Nunes-Nesi et al., 2008). Nevertheless, the metabolic and molecular cues
752 underlying such connections remain contentious and therefore further work is still
753 required to establish how exactly auxin signaling is able to impact both photosynthesis
754 and respiration.
755 There is a growing body of evidence showing that premature or incomplete
756 exhaustion of starch results in lower rates of plant growth and that this balance requires
757 appropriate changes in the rates of starch synthesis and degradation (Smith & Stitt,

2007, Stitt & Zeeman, 2012). Even small disturbances in leaf starch turnover affect metabolism and growth. As such, incomplete exhaustion of starch during the night (Fig. 3) leading to an inefficient usage of carbon pool coupled with reduced respiration rates (Table 2) in dgt plants might explain, at least partially, the reduced growth observed (Fig. 1). On the other hand, the precise pattern of consumption of starch during the night in entire plants (Fig. 3) coupled with enhanced respiration rates (Table 2) is likely associated with the higher biomass observed in this genotype. It should also be mentioned that the profile of both organic acids and amino acids was strongly affected in entire plants. The majority of organic acids including citrate, isocitrate, 2-oxoglutarate, succinate and fumarate were decreased in entire plants, while BCAAs were reduced only in the dgt mutant, with few variations on TCA cycle intermediates, suggesting that dgt mutant are using BCAAs more efficiently as alternative respiratory substrates. Accordingly, carbon skeletons from amino acids can be converted to precursors or intermediates of the TCA cycle to support mitochondrial metabolism and ATP biosynthesis, whereas oxidation of certain amino acids (e.g. leucine, isoleucine, valine, lysine, and proline) can directly provide electrons into the mitochondrial electron transport chain (Araújo et al., 2010, Hildebrandt et al., 2015, Schertl et al., 2014). As such, the elevated dark and light respiration (Fig. 5 and Table 2) coupled with changes in the evolution of radiolabeled CO_2 observed in entire plants provide further support to our hypothesis that the TCA cycle is working faster in the auxin signaling enhanced entire mutant.

Effect of the diageotropica mutation on auxin response factors

Given the strong auxin-associated phenotypes, we investigated the effect of down-regulation of the SlIAA9 (entire) and DGT on the expression of auxin responsive

genes. The downregulation of SlIAA9, resulted in alteration of several genes members of the same family such as IAA2, IAA3, IAA19 and IAA29 as well as GH3 gene, which is related to auxin homeostasis. Notably, Aux/IAA genes are spatially and temporally expressed in a pattern which contributes to the specificity of auxin responses in different plant tissues, and are also rapidly induced by auxin, displaying different induction kinetics (Paponov et al., 2008, Park et al., 2002). Accordingly, the mutation in SlIAA9 seems to alter the expression pattern of other genes from the same family, once the endogenous levels of auxin are differentially perceived, selectively controlling the expression of SlIAA3 (Wang et al., 2009). In tomato, the down-regulation of SlIAA3 resulted in several alterations in auxin-related phenotypes during vegetative growth, such as apical dominance, and apical hook curvature. Moreover, this down-regulation also increases the expression of SlIAA9 and SlIAA29, as well as ARF2 and ARF8, which may contribute to the reduced auxin-responsiveness in IAA3 mutant plants (Chaabouni et al., 2009). When the tomato SlIAA9 was down-regulated, impacts on fruit growth and leaf morphology were observed, associated with the selective control of the expression of SlIAA3 (Chaabouni et al., 2009). This not only reveals different roles for the Aux/IAA members, but also emphasizes the high level of complexity permitted by the large number of Aux/IAA genes (Wang et al., 2005, Wang et al., 2009). Our findings strongly support the hypothesis that different members of the Aux/IAA family are involved in distinct developmental processes.

The mutation in DIAGEOTROPICA appears to be able not only to modulate the expression of the genes of the Aux/IAA family as shown before by Nebenführ et al. (2000), but also to affect the expression of members of the ARFs family (ARF8 and ARF10) (Fig. 6). In agreement with this, the diageotropica seems to alter auxin induction of a subset of Aux/IAA genes that act as transcriptional repressors by

808 complexing with Auxin-response element-binding proteins called ARFs (Nebenführ et
809 al., 2000). Collectively, these results confirm that dgt participates in auxin signal
810 transduction and suggest that a specific step in early auxin signaling is likely affect by
811 the DGT gene (Kepinski & Leyser, 2002). It is important to mention that similar
812 expression levels for individual SlIAA genes were observed in dgt plants with the
813 exception of IAA19 and IAA29 (Fig. 6) and this is in agreement with previous results
814 (Nebenführ et al. (2000). Recently, it has been proposed that a functional cyclophilin
815 A, a cis/trans peptidyl-prolyl isomerase, which is missing in dgt, effects post-
816 translational modifications in Aux/IAA proteins allowing their proteasomal degradation,
817 therefore leading to an activation of auxin signaling (Jing et al., 2015). Our results also
818 suggest that the functional lack of dgt can also regulate SlARFs genes increasing the
819 expression of SlARF8 and SlARF10, which are both expressed in leaves (Zouine et
820 al., 2014). The ARF gene family specifically controls auxin-dependent biological
821 responses (Zouine et al., 2014). Interestingly, both genes are involved in similar
822 processes during plant growth and development. As such, it is already known that
823 ARF8 appears to stimulate parthenocarpic fruit formation (Goetz et al., 2007), and
824 compelling evidence suggest that SlARF8 is a candidate regulator of tomato fruit set
825 (Ariizumi et al., 2013). Furthermore, ARF10 is also associated with blade outgrowth
826 and early fruit development in tomato (Hendelman et al., 2012). The expression profile
827 observed here suggests that the functional product of DGT seems to be not only an
828 important feature involved in leaf metabolism (Fig. 4), but is also able to modulate
829 important genes associated with fruit set and yield (Fig. 6).

830 In summary, our study brings novel insights into the ability of auxin signaling
831 genes to control plant growth by adjusting leaf development and central metabolism,
832 simultaneously impacting both photosynthetic and respiratory metabolism. To our

knowledge, this is the first attempt to explain how changes in auxin signaling are associated with impacts on primary metabolism. Taken together, our findings indicated that auxin signaling is a regulatory control point of not only developmental but also metabolic processes including mitochondrial and chloroplastidic metabolism in autotrophic tissues. Remarkably, changes in auxin signaling are likely to impact not only carbon assimilation and growth but also how plants rely on organic acids and amino acid metabolism to support respiratory processes coupled to changes in starch metabolism. Collectively, the results presented here demonstrated that changes in auxin signaling are of crucial significance in the regulation of both anatomical and physiological aspects that are seemingly important to mediate plant growth and function and are also of likely agronomic significance. Our observations clearly have implications to the understanding of auxin signaling and its connections to primary metabolism highlighting the potential of manipulation of auxin signaling for agronomic purposes. However, further experimentation focusing at the level of guard cell development and function in response to changes in auxin signaling will be required to fully define the precise mechanism by which energy metabolism and hormone-mediated control of growth are associated, as well as the significance of this connection in response to sub-optimal environmental conditions.

Acknowledgments

Discussions with Prof. Dimas M. Ribeiro, Prof. Fábio M. DaMatta, and Prof. Samuel V.C. Martins (all from Universidade Federal de Viçosa, Brazil) were highly valuable in the development of this work.

858 **Supplemental Data**

859 The following supplemental materials are available:

860 **Supplemental Fig. S1.** Relative expression pattern in different tissues of wild-type
861 (WT) plants cv. Micro-Tom of the genes DIAGEOTROPICA (DGT) and ENTIRE/
862 SIAux/IAA9 (IAA9).

863 **Supplemental Fig. S2.** Sensitivity to exogenous auxin is altered in auxin signaling
864 mutants.

865 **Supplemental Fig. S3.** Stomatal parameters are altered in auxin signaling mutants.

866 **Supplemental Fig. S4.** Leaf morphoanatomical parameters are altered in auxin
867 signaling mutants.

868 **Supplemental Fig. S5.** Fresh weight loss from detached leaves is affected in auxin
869 signaling mutants.

870 **Supplemental Fig. S6.** Net photosynthesis (A_N) curves in response to changes in
871 photosynthetically active photon flux density (PPFD) in auxin signaling mutants.

872 **Supplemental Fig. S7.** Sensitivity analysis of g_m under leaf respiration rate in the light
873 in auxin signaling mutants.

874 **Supplemental Fig. S8.** Metabolite levels are differentially altered in root and shoots of
875 auxin signaling mutants.

876 **Supplemental Fig. S9.** Auxin signaling impact on leaf pigment content.

877 **Supplemental Table S1:** Photosynthetic parameters from light-response curves are
878 affected in auxin signaling mutants.

879 **Supplemental Table S2.** Pyridine nucleotide levels and ratios are affected in response
880 to changes in auxin signaling.

881 **Supplemental Table S3:** Relative metabolite content in auxin signaling mutants.

882 **Supplemental Table S4.** Primers utilized for the qRT-PCR reactions.

REFERENCES

ap Rees T. & Beevers H. (1960) Pathways of Glucose Dissimilation in Carrot Slices. Plant Physiology, **35**, 830-838.

Araújo W.L., Ishizaki K., Nunes-Nesi A., Larson T.R., Tohge T., Krahnert I., Witt S., Obata T., Schauer N. & Graham I.A. (2010) Identification of the 2-hydroxyglutarate and isovaleryl-CoA dehydrogenases as alternative electron donors linking lysine catabolism to the electron transport chain of Arabidopsis mitochondria. The Plant Cell, **22**, 1549-1563.

Araújo W.L., Nunes-Nesi A., Osorio S., Usadel B., Fuentes D., Nagy R., Balbo I., Lehmann M., Studart-Witkowski C. & Tohge T. (2011) Antisense inhibition of the iron-sulphur subunit of succinate dehydrogenase enhances photosynthesis and growth in tomato via an organic acid–mediated effect on stomatal aperture. The Plant Cell, **23**, 600-627.

Ariizumi T., Shinozaki Y. & Ezura H. (2013) Genes that influence yield in tomato. Breeding Science, **63**, 3-13.

Baggerman G., Vierstraete E., De Loof A. & Schoofs L. (2005) Gel-based versus gel-free proteomics: a review. Combinatorial chemistry & high throughput screening, **8**, 669-677.

Batista Silva W., Daloso D.M., Fernie A.R., Nunes-Nesi A. & Araújo W.L. (2016) Can stable isotope mass spectrometry replace radiolabelled approaches in metabolic studies? Plant Science, **249**, 59-69.

Berger D. & Altmann T. (2000) A subtilisin-like serine protease involved in the regulation of stomatal density and distribution in Arabidopsis thaliana. Genes & development, **14**, 1119-1131.

Bhardwaj R., Kaur R., Bali S., Kaur P., Sirhindi G., K Thukral A., Ohri P. & P Vig A. (2015) Role of various hormones in photosynthetic responses of green plants under environmental stresses. Current Protein and Peptide Science, **16**, 435-449.

Bonner J. & Bandurski R.S. (1952) Studies of the physiology, pharmacology, and biochemistry of the auxins. Annual Review of Plant Physiology, **3**, 59-86.

Carvalho R.F., Campos M.L., Pino L.E., Crestana S.L., Zsögön A., Lima J.E., Benedito V.A. & Peres L.E. (2011) Convergence of developmental mutants into a single tomato model system:'Micro-Tom'as an effective toolkit for plant development research. Plant Methods, **7**, 18.

Chaabouni S., Jones B., Delalande C., Wang H., Li Z., Mila I., Frasse P., Latché A., Pech J.-C. & Bouzayen M. (2009) Sl-IAA3, a tomato Aux/IAA at the crossroads of auxin and ethylene signalling involved in differential growth. Journal of Experimental Botany, **60**, 1349-1362.

Ethier G. & Livingston N. (2004) On the need to incorporate sensitivity to CO2 transfer conductance into the Farquhar–von Caemmerer–Berry leaf photosynthesis model. Plant, Cell & Environment, **27**, 137-153.

Farquhar G.v., von Caemmerer S.v. & Berry J. (1980) A biochemical model of photosynthetic CO2 assimilation in leaves of C3 species. Planta, **149**, 78-90.

Feder N. & O'brien T. (1968) Plant microtechnique: some principles and new methods. American journal of Botany, 123-142.

Fernie A.R., Aharoni A., Willmitzer L., Stitt M., Tohge T., Kopka J., Carroll A.J., Saito K., Fraser P.D. & DeLuca V. (2011) Recommendations for reporting metabolite data. The Plant Cell, **23**, 2477-2482.

Fernie A.R., Roscher A., Ratcliffe R.G. & Kruger N.J. (2001) Fructose 2, 6-bisphosphate activates pyrophosphate: fructose-6-phosphate 1-phosphotransferase and increases triose phosphate to hexose phosphate cycling in heterotrophic cells. Planta, **212**, 250-263.

French R.C. & Beevers H. (1953) Respiratory and growth responses induced by growth regulators and allied compounds. American Journal of Botany, 660-666.

Genty B., Briantais J.-M. & Baker N.R. (1989) The relationship between the quantum yield of photosynthetic electron transport and quenching of chlorophyll fluorescence. Biochimica et Biophysica Acta (BBA)-General Subjects, **990**, 87-92.

Gibon Y., Bläsing O.E., Palacios-Rojas N., Pankovic D., Hendriks J.H., Fisahn J., Höhne M., Günther M. & Stitt M. (2004) Adjustment of diurnal starch turnover to short days: depletion of sugar during the night leads to a temporary inhibition of carbohydrate utilization, accumulation of sugars and post-translational activation of ADP-glucose pyrophosphorylase in the following light period. The Plant Journal, **39**, 847-862.

Gilbert M.E., Pou A., Zwieniecki M.A. & Holbrook N.M. (2012) On measuring the response of mesophyll conductance to carbon dioxide with the variable J method. Journal of Experimental Botany, **63**, 413-425.

Goetz M., Hooper L.C., Johnson S.D., Rodrigues J.C.M., Vivian-Smith A. & Koltunow A.M. (2007) Expression of aberrant forms of AUXIN RESPONSE FACTOR8 stimulates parthenocarpy in Arabidopsis and tomato. Plant Physiology, **145**, 351-366.

Grassi G. & Magnani F. (2005) Stomatal, mesophyll conductance and biochemical limitations to photosynthesis as affected by drought and leaf ontogeny in ash and oak trees. Plant, cell & environment, **28**, 834-849.

Harley P.C., Loreto F., Di Marco G. & Sharkey T.D. (1992) Theoretical considerations when estimating the mesophyll conductance to CO2 flux by analysis of the response of photosynthesis to CO2. Plant Physiology, **98**, 1429-1436.

Hedden P. & Thomas S.G. (2008) Annual Plant Reviews, Plant Hormone Signaling (vol. 24). John Wiley & Sons.

Hendelman A., Buxdorf K., Stav R., Kravchik M. & Arazi T. (2012) Inhibition of lamina outgrowth following Solanum lycopersicum AUXIN RESPONSE FACTOR 10 (SlARF10) derepression. Plant molecular biology, **78**, 561-576.

Hermida-Carrera C., Kapralov M.V. & Galmés J. (2016) Rubisco Catalytic Properties and Temperature Response in Crops. Plant Physiology, **171**, 2549-2561.

Hildebrandt Tatjana M., Nunes Nesi A., Araújo Wagner L. & Braun H.-P. (2015) Amino Acid Catabolism in Plants. Molecular Plant, **8**, 1563-1579.

Hunt R., Causton D., Shipley B. & Askew A. (2002) A modern tool for classical plant growth analysis. Annals of Botany, **90**, 485-488.

Ivanova A., Law S.R., Narsai R., Duncan O., Lee J.-H., Zhang B., Van Aken O., Radomiljac J.D., van der Merwe M. & Yi K. (2014) A functional antagonistic relationship between auxin and mitochondrial retrograde signaling regulates alternative oxidase1a expression in Arabidopsis. Plant physiology, **165**, 1233-1254.

Jing H., Yang X., Zhang J., Liu X., Zheng H., Dong G., Nian J., Feng J., Xia B. & Qian Q. (2015) Peptidyl-prolyl isomerization targets rice Aux/IAAs for proteasomal degradation during auxin signalling. Nature communications, **6**.

Kelly M.O. & Bradford K.J. (1986) Insensitivity of the diageotropica tomato mutant to auxin. Plant Physiology, **82**, 713-717.

Kepinski S. & Leyser O. (2002) Ubiquitination and auxin signaling: a degrading story. The Plant Cell, **14**, S81-S95.
Kopka J., Schauer N., Krueger S., Birkemeyer C., Usadel B., Bergmüller E., Dörmann P., Weckwerth W., Gibon Y. & Stitt M. (2004) GMD@ CSB. DB: the Golm metabolome database. Bioinformatics, **21**, 1635-1638.
Laskowski M., Grieneisen V.A., Hofhuis H., Colette A., Hogeweg P., Marée A.F. & Scheres B. (2008) Root system architecture from coupling cell shape to auxin transport. PLoS biology, **6**, e307.
Le J., Liu X.-G., Yang K.-Z., Chen X.-L., Zou J.-J., Wang H.-Z., Wang M., Vanneste S., Morita M., Tasaka M., Ding Z.-J., Friml J., Beeckman T. & Sack F. (2014a) Auxin transport and activity regulate stomatal patterning and development. Nat Commun, **5**.
Le J., Zou J., Yang K. & Wang M. (2014b) Signaling to stomatal initiation and cell division. Regulation of Cell Fate Determination in Plants, 56.
Leonova L., Gamburg K., Vojnikov V. & Varakina N. (1985) Promotion of respiration by auxin in the induction of cell division in suspension culture. Journal of plant growth regulation, **4**, 169-176.
Leyser O. (2017) Auxin Signaling. Plant Physiology.
Lisec J., Schauer N., Kopka J., Willmitzer L. & Fernie A.R. (2006) Gas chromatography mass spectrometry–based metabolite profiling in plants. Nature protocols, **1**, 387-396.
Logan B.A., Adams W.W. & Demmig-Adams B. (2007) Viewpoint: Avoiding common pitfalls of chlorophyll fluorescence analysis under field conditions. Functional Plant Biology, **34**, 853-859.
Long S. & Bernacchi C. (2003) Gas exchange measurements, what can they tell us about the underlying limitations to photosynthesis? Procedures and sources of error. Journal of Experimental Botany, **54**, 2393-2401.
Luedemann A., von Malotky L., Erban A. & Kopka J. (2011) TagFinder: preprocessing software for the fingerprinting and the profiling of gas chromatography–mass spectrometry based metabolome analyses. In: Plant Metabolomics, pp. 255-286. Springer.
Lytovchenko A., Sweetlove L., Pauly M. & Fernie A.R. (2002) The influence of cytosolic phosphoglucomutase on photosynthetic carbohydrate metabolism. Planta, **215**, 1013-1021.
McAdam S.A., Eléouët M.P., Best M., Brodribb T.J., Murphy M.C., Cook S.D., Dalmais M., Dimitriou T., Gélinas-Marion A. & Gill W.M. (2017) Linking Auxin with Photosynthetic Rate via Leaf Venation. Plant physiology, **175**, 351-360.
Medeiros D.B., Martins S.C., Cavalcanti J.H.F., Daloso D.M., Martinoia E., Nunes-Nesi A., DaMatta F.M., Fernie A.R. & Araújo W.L. (2016) Enhanced photosynthesis and growth in atquac1 knockout mutants are due to altered organic acid accumulation and an increase in both stomatal and mesophyll conductance. Plant physiology, **170**, 86-101.
Murashige T. & Skoog F. (1962) A revised medium for rapid growth and bio assays with tobacco tissue cultures. Physiologia plantarum, **15**, 473-497.
Nebenführ A., White T. & Lomax T.L. (2000) The diageotropica mutation alters auxin induction of a subset of the Aux/IAA gene family in tomato. Plant molecular biology, **44**, 73-84.
Niinemets Ü., Cescatti A., Rodeghiero M. & Tosens T. (2005) Leaf internal diffusion conductance limits photosynthesis more strongly in older leaves of

Mediterranean evergreen broad-leaved species. Plant, Cell & Environment, **28**, 1552-1566.
Niinemets Ü., Díaz-Espejo A., Flexas J., Galmés J. & Warren C.R. (2009) Role of mesophyll diffusion conductance in constraining potential photosynthetic productivity in the field. Journal of Experimental Botany, **60**, 2249-2270.
Nunes-Nesi A., Araújo W.L. & Fernie A.R. (2011) Targeting mitochondrial metabolism and machinery as a means to enhance photosynthesis. Plant Physiology, **155**, 101-107.
Nunes-Nesi A., Carrari F., Lytovchenko A., Smith A.M., Loureiro M.E., Ratcliffe R.G., Sweetlove L.J. & Fernie A.R. (2005) Enhanced photosynthetic performance and growth as a consequence of decreasing mitochondrial malate dehydrogenase activity in transgenic tomato plants. Plant physiology, **137**, 611-622.
Nunes-Nesi A., Sulpice R., Gibon Y. & Fernie A.R. (2008) The enigmatic contribution of mitochondrial function in photosynthesis. Journal of experimental botany, **59**, 1675-1684.
Nunes-Nesi A., Carrari F., Gibon Y., Sulpice R., Lytovchenko A., Fisahn J., Graham J., Ratcliffe R.G., Sweetlove L.J. & Fernie A.R. (2007) Deficiency of mitochondrial fumarase activity in tomato plants impairs photosynthesis via an effect on stomatal function. The Plant Journal, **50**, 1093-1106.
Paponov I.A., Paponov M., Teale W., Menges M., Chakrabortee S., Murray J.A. & Palme K. (2008) Comprehensive transcriptome analysis of auxin responses in Arabidopsis. Molecular Plant, **1**, 321-337.
Park J.Y., Kim H.J. & Kim J. (2002) Mutation in domain II of IAA1 confers diverse auxin-related phenotypes and represses auxin-activated expression of Aux/IAA genes in steroid regulator-inducible system. The Plant Journal, **32**, 669-683.
Pons T.L., Flexas J., Von Caemmerer S., Evans J.R., Genty B., Ribas-Carbo M. & Brugnoli E. (2009) Estimating mesophyll conductance to CO2: methodology, potential errors, and recommendations. Journal of Experimental Botany, erp081.
Porra R., Thompson W. & Kriedemann P. (1989) Determination of accurate extinction coefficients and simultaneous equations for assaying chlorophylls a and b extracted with four different solvents: verification of the concentration of chlorophyll standards by atomic absorption spectroscopy. Biochimica et Biophysica Acta (BBA)-Bioenergetics, **975**, 384-394.
Quint M. & Gray W.M. (2006) Auxin signaling. Current opinion in plant biology, **9**, 448-453.
Rodeghiero M., Niinemets Ü. & Cescatti A. (2007) Major diffusion leaks of clamp-on leaf cuvettes still unaccounted: how erroneous are the estimates of Farquhar et al. model parameters? Plant, cell & environment, **30**, 1006-1022.
Roessner U., Luedemann A., Brust D., Fiehn O., Linke T., Willmitzer L. & Fernie A.R. (2001) Metabolic profiling allows comprehensive phenotyping of genetically or environmentally modified plant systems. The Plant Cell, **13**, 11-29.
Schertl P., Cabassa C., Saadallah K., Bordenave M., Savouré A. & Braun H.P. (2014) Biochemical characterization of proline dehydrogenase in Arabidopsis mitochondria. FEBS Journal, **281**, 2794-2804.
Schneider C.A., Rasband W.S. & Eliceiri K.W. (2012) NIH Image to ImageJ: 25 years of image analysis. Nature methods, **9**, 671.
Sharkey T.D., Bernacchi C.J., Farquhar G.D. & Singsaas E.L. (2007) Fitting photosynthetic carbon dioxide response curves for C3 leaves. Plant, Cell & Environment, **30**, 1035-1040.

Smith A.M. & Stitt M. (2007) Coordination of carbon supply and plant growth. Plant, cell & environment, **30**, 1126-1149.

Stitt M. & Zeeman S.C. (2012) Starch turnover: pathways, regulation and role in growth. Current opinion in plant biology, **15**, 282-292.

von Groll U., Berger D. & Altmann T. (2002) The subtilisin-like serine protease SDD1 mediates cell-to-cell signaling during Arabidopsis stomatal development. The Plant Cell, **14**, 1527-1539.

Wang H., Jones B., Li Z., Frasse P., Delalande C., Regad F., Chaabouni S., Latche A., Pech J.-C. & Bouzayen M. (2005) The tomato Aux/IAA transcription factor IAA9 is involved in fruit development and leaf morphogenesis. The Plant Cell Online, **17**, 2676-2692.

Wang H., Schauer N., Usadel B., Frasse P., Zouine M., Hernould M., Latché A., Pech J.-C., Fernie A.R. & Bouzayen M. (2009) Regulatory features underlying pollination-dependent and-independent tomato fruit set revealed by transcript and primary metabolite profiling. The Plant Cell, **21**, 1428-1452.

Wong S.-L., Chen C.-W., Huang H.-W. & Weng J.-H. (2012) Using combined measurements of gas exchange and chlorophyll fluorescence to investigate the photosynthetic light responses of plant species adapted to different light regimes. Photosynthetica, **50**, 206-214.

Xu Z. & Zhou G. (2008) Responses of leaf stomatal density to water status and its relationship with photosynthesis in a grass. Journal of Experimental Botany, **59**, 3317-3325.

Yin X., Struik P.C., Romero P., Harbinson J., Evers J.B., Van Der Putten P.E. & Vos J. (2009) Using combined measurements of gas exchange and chlorophyll fluorescence to estimate parameters of a biochemical C3 photosynthesis model: a critical appraisal and a new integrated approach applied to leaves in a wheat (Triticum aestivum) canopy. Plant, cell & environment, **32**, 448-464.

Zanor M.I., Osorio S., Nunes-Nesi A., Carrari F., Lohse M., Usadel B., Kühn C., Bleiss W., Giavalisco P. & Willmitzer L. (2009) RNA interference of LIN5 in tomato confirms its role in controlling Brix content, uncovers the influence of sugars on the levels of fruit hormones, and demonstrates the importance of sucrose cleavage for normal fruit development and fertility. Plant physiology, **150**, 1204-1218.

Zhao Y. (2010) Auxin biosynthesis and its role in plant development. Annual review of plant biology, **61**, 49-64.

Zouine M., Fu Y., Chateigner-Boutin A.-L., Mila I., Frasse P., Wang H., Audran C., Roustan J.-P. & Bouzayen M. (2014) Characterization of the tomato ARF gene family uncovers a multi-levels post-transcriptional regulation including alternative splicing. PloS one, **9**, e84203.

SUPPLEMENTAL FIGURES

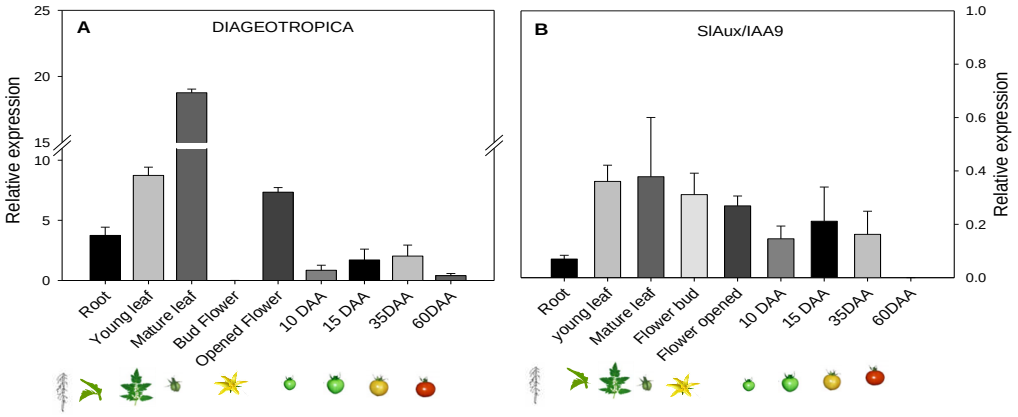

Supplemental Fig. S1. Relative expression pattern in different tissues of wild-type (WT) plants cv. Micro-Tom of the genes Diageotropica (DGT) and SlAux/IAA9 (IAA9). **A,** Relative expression of the DGT (Solyc01g111170.2.1), **B,** Relative expression of the Aux/IAA9 (Solyc04g076850.2.1). Relative transcript expression of DGT and Aux/IAA9 (ENTIRE) was determined in total RNA isolated from roots, young and mature leaves, bud and opened flowers, and in fruits of 10, 15, 35 and 60 days after anthesis (DAA). The y axis values represent the relative expression levels calculated using the $2^{-\Delta\Delta CT}$ method. To normalize gene expression was used the constitutively expressed genes actin and ubiquitin3 were used for all samples. Values are presented as means ± SE (n=4) of independent biological replicates.

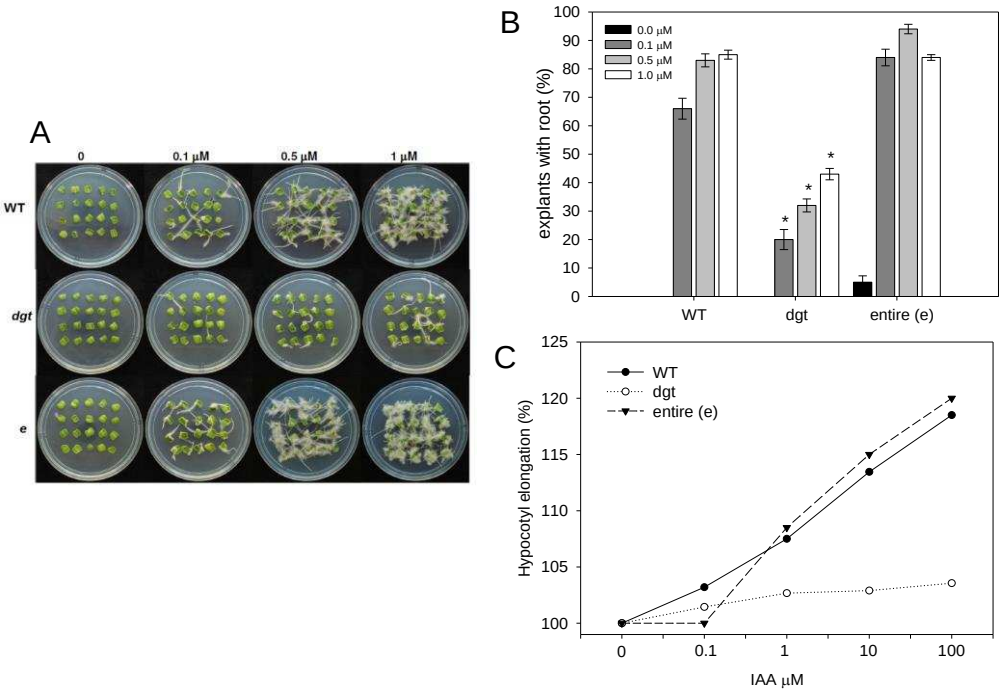

Supplemental Fig. S2. Sensibility of exogenous auxin is altered in auxin signaling mutants. **A,** Representative image of the formation of cotyledon roots following incubation at different concentration of Naphthalene Acetic Acid (NAA). **B**, percentage (%) of explants that developed root systems under increasing doses of NAA; and **C**, Dose-response test of auxin in 10-days-old hypocotyl segments. The hypocotyl elongation is given as percentage of the final length after 24 hours of incubation in the solution containing the indicated concentration of indole acetic acid (IAA) in relation to the length of the respective WT. Values are presented as means ± SE (n=5). Asterisks (*) indicate that the values from auxin signaling mutants were determined by the Student's t-test to be significantly different ($P<0.05$) from the WT.

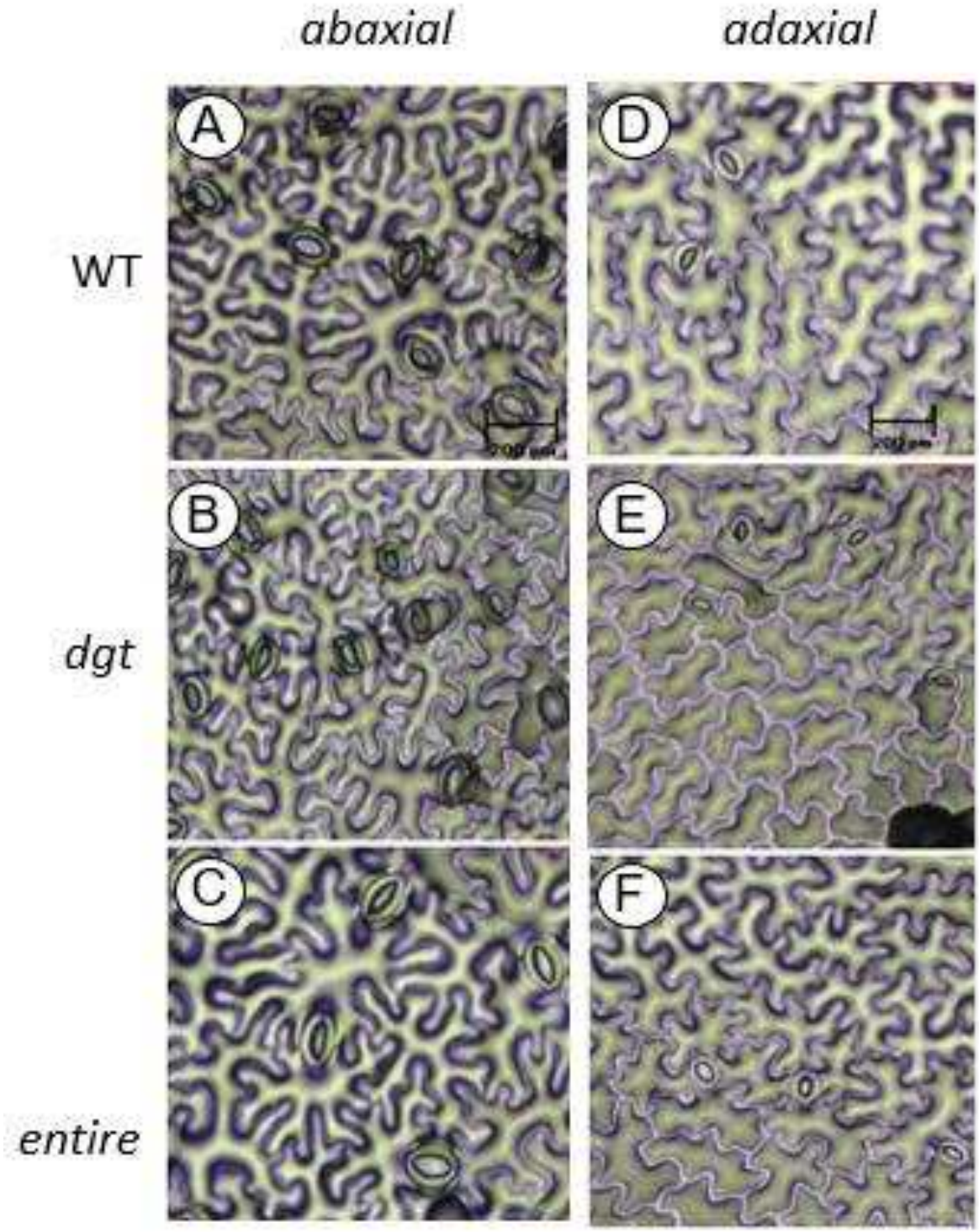

Supplemental Fig. S3. Stomatal parameters are altered in auxin signaling mutants. Light micrographs are representative of the anatomy of the adaxial and abaxial surfaces of tomato plants with either increased (entire) or reduced (diageotropica, dgt) auxin signaling in comparison to wild-type (WT). The dgt mutant plants were characterized by high stomatal density in both abaxial adaxial surfaces but with reduced stomatal pore size. A, B, and C are representative images of abaxial leaf surfaces of wild-type, dgt and entire plants, respectively; D, E, and F are representative images of adaxial leaf surfaces of wild-type, dgt and entire plants, respectively. The bar scale is: 200µm.

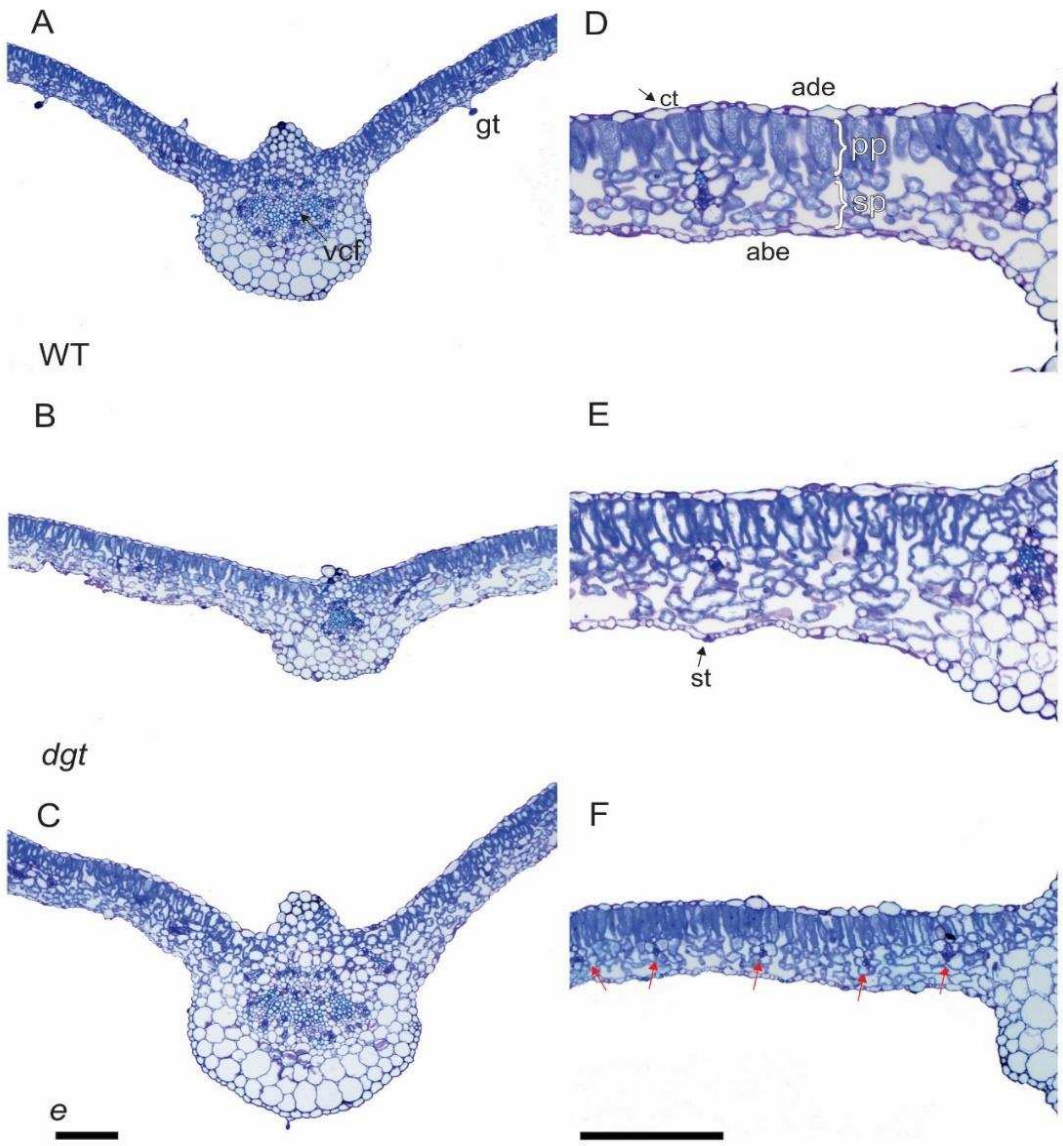

Supplemental Fig. S4. Leaf morphoanatomical parameters are altered in auxin signaling mutants. Light microscopy of cross sections are representative of the leaf anatomy of tomato plants with either increased (entire) or reduced (diageotropica, dgt) auxin signaling in comparison to wild-type (WT). A, B, and C are representative images of leaf blade cross sections of WT, dgt and entire plants, respectively; D, E, and F are representative images of leaf cross section of WT, dgt and entire plants, respectively. Abbreviations: gt: gladule thricome, vcf: vascular central bundle, ct: cuticle, ade: adaxial epidermis, abe: abaxial epidermis, pp: palisade parenchyma, sp: spongy parenchyma, red arrow indicate blade bundle. The bar scale is: 100µm.

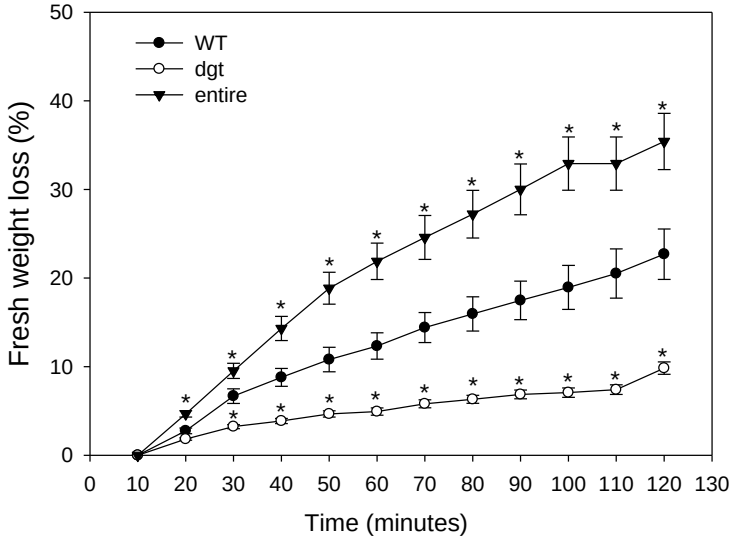

Supplemental Fig. S5. Fresh weight loss from detached leaves is affected in auxin signaling mutants. Changes in fresh weight were accompanied in detached leaves of tomato plants with either increased (entire) or reduced (diageotropica, dgt) auxin signaling and were compared to wild-type (WT) plants. Analysis were performed in 4-week-old plants and show that changes auxin signaling leads to alterations in water loss in tomato plants. Data show percentage of initial fresh weight loss from detached leaves incubated under the same plant growth conditions from up to 2 hours. Values are presented as means ± SE (n=7) obtained in two independent assays. Asterisks (*) indicate that the values from auxin signaling mutants were determined by the Student's t-test to be significantly different (P<0.05) from the WT. WT, black circle; dgt, open circle and entire, black triangles.

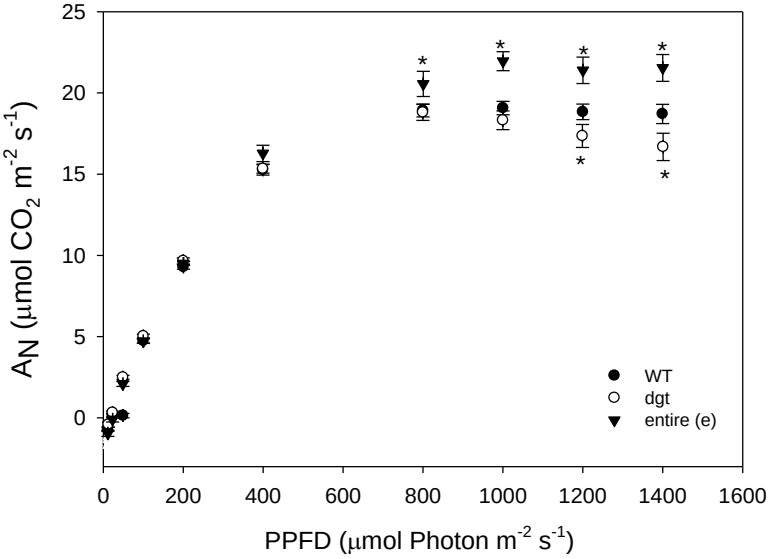

Supplemental Fig. S6. Net photosynthesis (A_N) curves in response to changes in photosynthetically active photon flux density (PPFD) in auxin signaling mutants (dgt and entire). Plants with either increased (entire) or reduced (diageotropica, dgt) auxin signaling were compared to wild-type (WT) plants growing under optimal conditions. WT, black circles; dgt, open circles; entire, black triangles. Data presented are mean ± SE (n=8) obtained using the 3th fully expanded leaf from the apex of 4-week-old plants (vegetative stage). Asterisks (*) indicate that the values from auxin signaling mutants were determined by the Student's t-test to be significantly different (P<0.05) from the WT. WT, black circle; dgt, open circle and entire, black triangles.

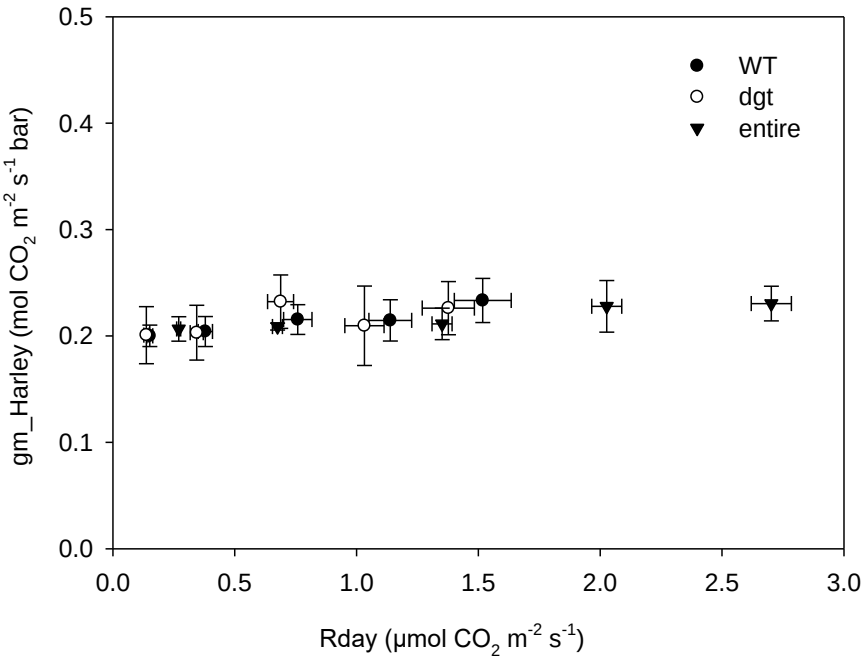

Supplemental Fig. S7. Sensibility analysis of gm under leaf respiration rate in the light in auxin signaling mutants (dgt and entire). Plants with either increased (entire) or reduced (diageotropica, dgt) auxin signaling were compared to wild-type (WT) plants growing under optimal conditions. WT, black circles; dgt, open circles; entire, black triangles. Data presented are mean ± SE (n=8) obtained using the 3th fully expanded leaf from the apex of 4-week-old plants (vegetative stage). WT, black circle; dgt, open circle and entire, black triangles. Rday, day respiration.

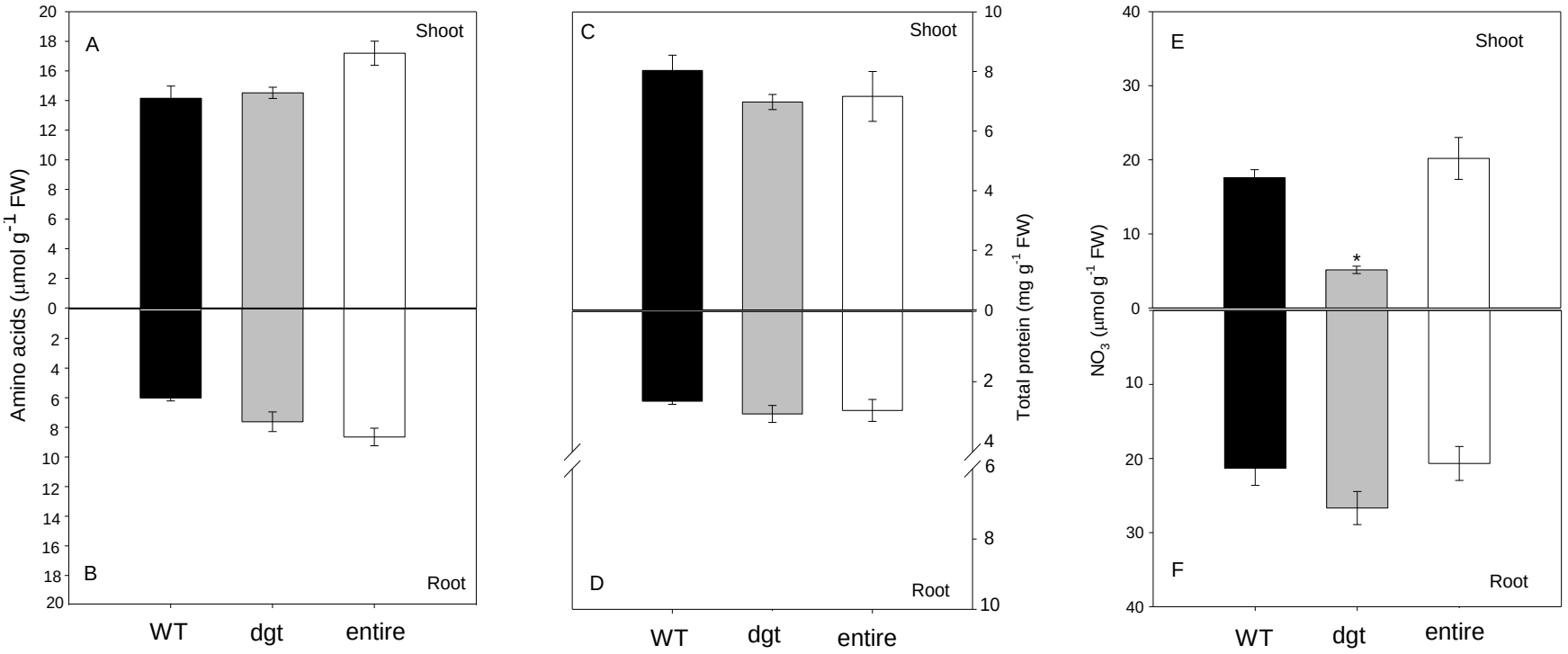

Supplemental Fig. S8. Metabolite levels are differentially altered in root and shoots of auxin signaling mutants. Key metabolite content in shoots and roots of tomato plants with either increased (entire) or reduced (diageotropica, dgt) auxin signaling were compared to wild-type (WT) plants growing under optimal conditions. (A) and (B) Amino acids content in shoot and root, respectively; (C) and (D) Total protein content in shoot and root, respectively; and (E) and (F) Nitrate content in shoot and root respectively. Samples were taken from the 3th fully expanded leaf from the apex of 4-week-old plants (vegetative stage) harvested in the middle of the light photoperiod. WT, black bars; dgt, grey bars, entire, white bars. Data presented are average ± SE (n=7). Asterisks (*) indicate that the values from auxin signaling mutants were determined by the Student's t-test to be significantly different (P<0.05) from the WT. FW: Fresh weight.

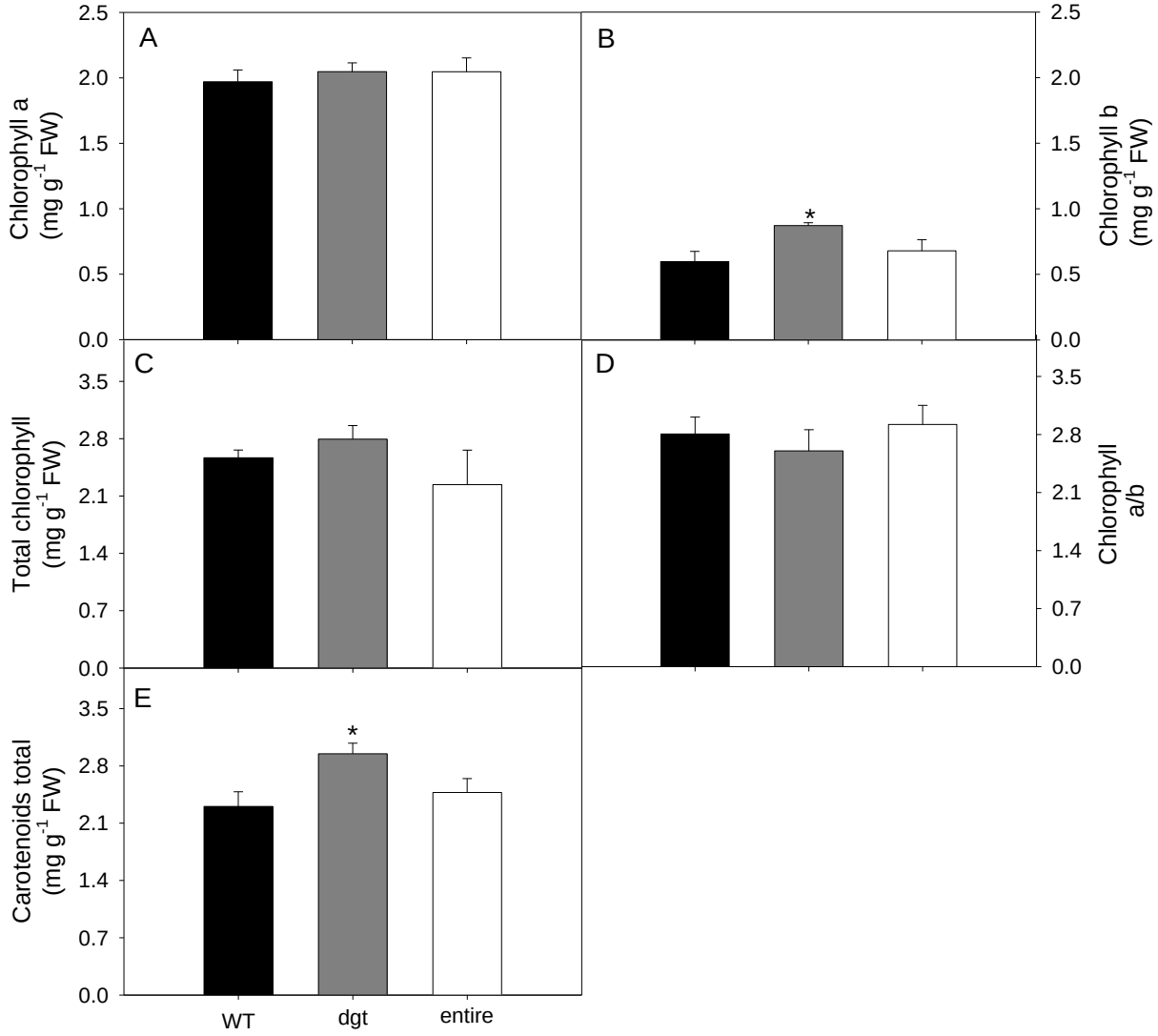

Supplemental Fig. S9 Auxin signaling impact leaf pigment content. Changes in leaf pigment of tomato plants with either increased (entire) or reduced (diageotropica, dgt) auxin signaling were compared to wild-type (WT) plants growing under optimal conditions. **A**, Chlorophyll a content; **B**, Chlorophyll b content; **C**, Total chlorophyll content; **D**, ratio between a and b chlorophyll and **E**, Total carotenoid content. Samples were taken from the 3th fully expanded leaf from the apex of 4-week-old plants (vegetative stage) harvested in the middle of the light photoperiod. WT, black bars; dgt, grey bars, entire, white bars. Data presented are average ± SE (n=7). Asterisks (*) indicate that the values from auxin signaling mutants were determined by the Student's t-test to be significantly different (P<0.05) from the WT. FW: Fresh weight.

SUPPLEMENTAL TABLES

Supplemental Table S1: Photosynthetic parameters from light-response curves are affected in auxin signaling mutants. Light response parameters obtained in WT (cv. Micro-Tom) are compared to tomato mutant plants with either increased (entire) or reduced (diageotropica, dgt) auxin signaling. Data presented are average ± SE (n=8) obtained using the 3th fully expanded leaf from the apex of 4-week-old plants (vegetative stage). Asterisks (*) indicate that the values from auxin signaling mutants were determined by the Student's t-test to be significantly different (P<0.05) from the WT.

Parameters*	WT	dgt	entire
A_{PPFD} (µmol CO_2 m^{-2} s^{-1})	20.784 ± 0.527	19.686 ± 0.646	**24.485 ± 0.875**
Ic (µmol m^{-2} s^{-1})	16.594 ± 1.313	16.212 ± 0.656	**25.066 ± 2.084**
Is (µmol m^{-2} s^{-1})	508.596 ± 41.949	**382.088 ± 26.976**	**705.650 ± 40.553**
1/Φ (µmol Photons mol^{-1} CO_2)	16.574 ± 0.354	17.643 ± 0.365	**15.217 ± 0.235**

*A_{PPFD}: Net CO_2 assimilation rate saturated by light; Ic: light compensation point; Is: light saturation point; 1/Φ: Light use efficiency.

Supplemental Table S2. Pyridine nucleotide levels and ratios are affected in response to changes in auxin signaling. Nucleotides were determined in leaves of tomato plants with either increased (entire) or reduced (diageotropica, dgt) auxin signaling and were compared to wild-type (WT) plants growing under optimal conditions. Samples were taken from the 3th fully expanded leaf from the apex of 4-week-old plants (vegetative stage) harvested in the middle of the light photoperiod. Data presented are average ± SE (n=7). Asterisks (*) indicate that the values from auxin signaling mutants were determined by the Student's t-test to be significantly different (P<0.05) from the WT. FW: Fresh weight.

Parameters* (µmol g^{-1} FW)	WT	dgt	entire
NAD^+	48.60 ± 1.33	53.26 ± 1.10	47.92 ± 0.78
NADH	63.08 ± 2.29	94.55 ±3.34	68.62 ± 3.36
$NADP^+$	39.87 ± 1.60	40.02 ± 1.60	35.57 ± 1.92
NADPH	16.32 ± 0.40	16.89 ± 0.34	16.56 ± 0.43
NADH/NAD^+	1.30 ± 0.05	1.78 ± 0.06	1.43 ± 0.07
NADPH/$NADP^+$	0.41 ± 0.15	0.42 ± 0.01	0.47 ± 0.03

Supplemental Table S3: Relative metabolite content in auxin signaling mutants. Changes in the relative metabolite content of tomato plants with either increased (entire) or reduced (diageotropica, dgt) auxin signaling were compared to wild-type (WT) plants growing under optimal conditions. Data were normalized with respect to the mean response calculated for WT. Values set in bold in dgt and e plants were determined by the student's t test to be significantly different (P≤0.05) from its corresponding WT.

	Compounds	WT	dgt	entire
Amino acids	Alanine	1 ± 0.144	0.93 ± 0.076	1.00 ± 0.124
	B-Alanine	1 ± 0.265	1.58 ± 0.206	**2.45 ± 0.201**
	Arginine	1 ± 0.178	**1.72 ± 0.124**	**6.40 ± 0.512**
	Asparagine	1 ± 0.187	**7.57 ± 2.486**	**27.82 ± 0.280**
	Aspartic acid	1 ± 0.131	**1.80 ± 0.111**	1.22 ± 0.098
	Glutamic acid	1 ± 0.074	**1.23 ± 0.027**	0.83 ± 0.088
	Glutamine	1 ± 0.150	**5.76 ± 1.768**	**34.60 ± 0.351**
	Glycine	1 ± 0.177	**1.48 ± 0.082**	1.18 ± 0.231
	Glycyl-proline	1 ± 0.199	**1.80 ± 0.135**	**0.34 ± 0.012**
	Histidine	1 ± 0.213	**1.79 ± 0.225**	**0.40 ± 0.298**
	Homoglutamine	1 ± 0.231	**1.85 ± 0.235**	1.04 ± 0.090
	Homoserine	1 ± 0.294	1.03 ± 0.124	1.48 ± 0.230
	Isoleucine	1 ± 0.031	0.93 ± 0.045	1.18 ± 0.134
	Leucine	1 ± 0.090	**0.85 ± 0.041**	1.15 ± 0.143
	Lysine	1± 0.124	**1.41 ± 0.117**	**4.41 ± 0.344**
	Methionine	1 ± 0.060	1.16 ± 0.121	**2.69 ± 0.280**
	Ornithine	1 ± 0.133	1.10 ± 0.110	**5.44 ± 0.475**
	Phenylalanine	1 ± 0.069	**1.36 ± 0.070**	1.11 ± 0.101
	Proline	1 ± 0.175	**1.36 ± 0.146**	0.81 ± 0.171
	Prolyl-glycine	1 ± 0.190	1.60 ± 0.179	1.10 ± 0.242
	Serine	1 ± 0.225	1.06 ± 0.055	2.91 ± 0.052
	Tryptophan	1 ± 0.048	**1.37 ± 0.099**	1.154 ± 0.052
	Tyrosine	1 ± 0.099	0.84 ± 0.099	0.647 ± 0.130
	Valine	1 ± 0.056	0.85 ± 0.037	**1.338 ± 0.145**
	GABA	1 ± 0.045	**18.22 ± 0.098**	0.957 ± 0.234

Organic acids	Succinate	**1 ± 0.090**	**1.46 ± 0.166**	**0.28 ± 0.602**
	Maleic Acid	1 ± 0.204	0.99 ± 0.064	0.20 ± 0.202
	Pivuvate	1 ± 0.111	**1.33 ± 0.099**	0.88 ± 0.110
	Ascorbate	1 ± 0.135	**1.42 ± 0.121**	0.75 ± 0.159
	Oxoglutarate	1 ± 0.134	**1.44 ± 0.109**	**0.33 ± 0.234**
	Oxaloacetate	1 ± 0.235	1.27 ± 0.077	1.10 ± 0.120
	Citrate	1 ± 0.283	**1.79 ± 0.122**	**0.19 ± 0.981**
	Malate	1 ± 0.075	**1.26 ± 0.077**	**0.78 ± 0.098**
	Fumarate	1 ± 0.071	**1.61 ± 0.128**	**0.48 ± 0.453**
Sugars	Maltose	1 ± 0.120	0.90 ± 0.069	**0.69 ± 0.030**
	Ribose	1 ± 0.037	0.95 ± 0.016	**0.88 ± 0.025**
	Trehalose	1 ± 0.218	0.92 ± 0.152	0.79 ± 0.184
	Ribulose	1 ± 0.230	**1.61 ± 0.156**	**0.44 ± 0.399**
	Fructose-1-phosphate	1 ± 0.090	1.21 ± 0.113	1.06 ± 0.047
	Rhamnose	1 ± 0.131	**1.60 ± 0.182**	0.80 ± 0.168
	Glucose	1 ± 0.031	**1.14 ± 0.038**	0.99 ± 0.064
	Fructose	1 ± 0.062	**1.43 ± 0.041**	1.23 ± 0.090
	Sucrose	1 ± 0.062	**1.53 ± 0.045**	1.13 ± 0.090
Others	Spermidine	1 ± 0.083	1.22 ± 0.312	**4.15 ± 0.290**
	Putrescine	1 ± 0.114	1.49 ± 0.185	**2.81 ± 0.208**
	Adenine	1 ± 0.083	**1.63 ± 0.071**	1.39 ± 0.093
	Purine	1 ± 0.087	**1.31 ± 0.054**	1.21 ± 0.098

1232

1233

Supplemental Table S4. Primers utilized for the qRT-PC.

gene	Locus	Sequence	Efficiency (%)
Actin	Solyc03g078400.2.1	Fwd 5'-GGTCCCTCTATTGTCCACAG-3'	0.88
		Rev 5'-TGCATCTCTGGTCCAGTAGGA-3'	
IAA1	Solyc06g053840.2.1	Fwd 5'-GAAAATGTTCAAGCTGAGTATC-3'	0.79
		Rev 5'-CTGATCCTTTCATTATCCTTAG-3'	
IAA2	Solyc06g084070	Fwd 5'-TGATGAACCACCACAAAAAGCAC-3'	0.84
		Rev 5'-GATCGAACCGGTGGCCATC-3'	
IAA3	Solyc09g065850	Fwd 5'- TGGCCACCAGTTCGATCATAC-3'	0.83
		Rev5'-GGTGCTCCATCCATGCTAACT-3'	
IAA9	Solyc04g076850	Fwd 5'-GTTGTCAAGTGTGTGACAGCC-3'	0.90
		Rev 5'-TGTCACTTACACATAGGGCCA-3'	
IAA19	Solyc03g120380.2	Fwd 5'-GCCTCCTGTGTGTGCTTACC-3'	0.86
		Rev 5'-AAACGGTGCTCCATCCATGC-3'	
IAA29	Solyc08g021820.2.1	Fwd 5'-GTGAAGATGGAAGGGGTGCC-3'	0.85
		Rev 5'-CCAGCAAGCATCCAGTCTCC-3'	
ARF8	Solyc02g037530.2.1	Fwd 5'- CTGCTCAAACCCAAATGCTGTC-3'	0.86
		Rev 5'- GGTAAGTGTGTTGGTGAGCCTG-3'	
ARF10	Solyc11g069500.1.1	Fwd 5'- CAGGTCCAGCAGTCCTTTCT-3'	0.84
		Rev 5' CGCTGGAAACTTGGTGGTAA-3'	
GH3.8	Solyc02g092820.2.1	Fwd 5'-TTGGACTCCAGGGTGATTTC-3'	0.77
		Rev 5'-TGTTCAACGTCGTCGTTCTG-3'	
DGT	Solyc01g111170	Fwd 5'-GAGTCGCCGTTTTAGGCTTT-3'	0.82
		Rev 5'-GCAACACAACAACCAATTACG-3'	

CHAPTER 4

The auxin-resistant diageotropica is an essential gene during tomato ripening

Chapter 4: Manuscript in preparation

The auxin-resistant diageotropica is an essential gene during tomato ripening

Willian Batista Silva[1,2], Acácio Rodrigues-Salvador[1], Alice Carvalho de Oliveira[1,2], David Barbosa Medeiros[1,2,3], Diego Sevastian Reartes[4], Lázaro Eustáquio Pereira Peres[4], Dimas Mendes Ribeiro[1], Adriano Nunes-Nesi[1], Alisdair R. Fernie[3], Agustín Zsögön[1], Wagner L. Araújo[1,2]*

1Departamento de Biologia Vegetal, Universidade Federal de Viçosa, 36570-900, Viçosa, Minas Gerais, Brazil
2Max-Planck Partner Group at the Departamento de Biologia Vegetal, Universidade Federal de Viçosa, 36570-900, Viçosa, Minas Gerais, Brazil
3Central Metabolism Group, Max Planck Institute of Molecular Plant Physiology, 14476 Potsdam-Golm, Germany
4Departmento de Ciências Biológicas, Escola Superior de Agricultura Luiz de Queiroz, Universidade de São Paulo, Piracicaba 13418-900, Brazil
Type of authorship: First author

Type of article:	Research article
Share of the work:	80%
Contribution to the publication:	planned and performed all experiments, analyzed data, prepared all figures and wrote parts of the paper
Journal:	The Plant Journal
5-year impact factor:	5.901
Situation:	In preparation

***Corresponding author:**
Wagner L. Araújo
Departamento de Biologia Vegetal,
Universidade Federal de Viçosa,
36570-900 Viçosa, Minas Gerais, Brazil
E-mail: wlaraujo@ufv.br
Tel: +55 31 3899.2169; Fax**:** +55 31 3899.2580

Highlight

- Auxin signaling is directly connected with fruit growth and ripening
- The auxin-resistant dgt alter fruit ripening modulating respiratory process by ethylene production
- Increases in auxin signaling do not affect the fruit ripening but have important role in fumarate metabolism

Footnotes:

This work was supported by funding from the Max Planck Society (to W.L.A.), the Conselho Nacional de Desenvolvimento Científico e Tecnológico (CNPq-Brazil to W.L.A.), and the Fundação de Amparo à Pesquisa do Estado de Minas Gerais (FAPEMIG-Brazil, Grant APQ- 01078-15, APQ-01357-14, and RED-00053-16). We also thank the scholarships granted by the Brazilian Federal Agency for Support and Evaluation of Graduate Education (CAPES-Brazil) to WBS. DBM was supported by a CAPES post-doctoral grant. Research fellowships granted by CNPq-Brazil to ANN and WLA are also gratefully acknowledged.

ABSTRACT

Although auxin is an important plant hormone that plays crucial roles during both fruit growth and ripening, the metabolic impacts of changes in auxin signaling during tomato (Solanum lycopersicum L.) ripening remains rather unclear. Here, we investigated the significance of the changes in auxin signaling during different stages of fruit development by analyzing changes on tomato fruit quality and primary metabolism using mutants with either reduced (diageotropica - dgt) or increased (entire) auxin signaling. Our results show that these mutations alter primary metabolism, modulating fruit growth through changes in fruit respiration. We show that dgt mutants are characterized by reduced fruit-set, total dry weight, fruit size, number of seeds per fruit and fresh weight loss during post-harvest. Increase sugars content associated with delay in ripening in dgt fruits are likely connected with reduced ethylene and respiration and starch degradation. Despite their parthenocarpy character, fruits with increased auxin perception (entire) did not displayed significant changes in ripening process with few changes in primary metabolism. Altogether, our data demonstrate that reductions in auxin signaling impact fruit set and ripening, most likely due to impacts on sugar content and starch metabolism, providing a functional link between auxin signaling and respiratory pathway.

Key words: Auxin, auxin signaling, fruit quality, primary metabolism

INTRODUCTION

Fruit development and ripening are temporally and spatially tightly regulated by a complex process involving the interplay between multiple phytohormones that influence the overall fruit quality (Nitsch, 1970, Pech et al., 2008). Five classic hormones (auxins, gibberellins, cytokinins, abscisic acid and ethylene) are known to coordinate various stages of the fruit development ranging from fruit set to ripening and senescence (McAtee et al., 2013, Kumar et al., 2014). However ethylene has been considered for many years to be the main ripening hormone, studies have shown that auxin and cytokinin are directly associated with maturation and undergoing the ripening process (Kumar et al., 2014).

The auxin is an important phytohormone that allows the initiation of fleshy fruit development triggering fruit set upon flower fertilization (Wang et al., 2005a). In addition, it has been shown that auxin also is able to modulate the fruit ripening process by interacting with ethylene and regulating many physiological processes (Muday et al., 2012, Li et al., 2016). Besides that, evidence have revealed that auxin also is able to regulate the ripening process in its own (Trainotti et al., 2007, McAtee et al., 2013). In fact, the hormone has shown the ability to regulate the expression of a number of different genes, in particular, the signaling (receptors, Auxin Response Factors and Aux/IAA) of auxin had increased expression in the mesocarp during ripening (Trainotti et al., 2007). According, fruit ripening is largely affected by endogenous auxin content (Li et al. (2017). In addition, high auxin levels has been observed in the fruits of the ripening inhibitor (rin) tomato (Solanum lycopersicum L.) mutant suggesting that decreased auxin levels might be necessary for triggering fruit ripening (Liu et al., 2005).

Studies that have analyzed how genetic manipulation of several auxin response genes, such as SlARF4, SlARF2a, SlIAA17, and SlIAA27 can impact fruit development revealed changes not only in fruit pigment and sugar content, but also increase fruit quality with postharvest shelf life (Bassa et al., 2013, Sagar et al., 2013a, Sagar et al., 2013b, Hao et al., 2015, Su et al., 2015a). It has been recently demonstrated that exogenous auxin plays an important role during ripening by controlling pigment levels and primary metabolism in postharvest tomato fruits (Li et al., 2016, Li et al., 2017). Notably, it has been demonstrated that down regulation of SIIAA9 affect the set fruit (Wang et al., 2005a) whereas both fruit size and internal anatomy are affected in the auxin-resistant diageotropica (dgt) tomato mutant (Balbi and Lomax, 2003).

Furthermore, sugar accumulation in tomato fruit is the consequence of various linked physiological processes that are genetically programmed and are under multihormonal control (Bouzayen et al. (2010). This fact apart, how and to which extent changes in auxin signaling impact metabolism during fruit ripening and fruit final quality remains to be investigated.

Thus, to study the role of auxin signaling in metabolic adjustments and final quality of fruits here we used tomato mutants either with reduced (dgt) or increased (entire) auxin perception. We show that auxin signaling regulate not only the accumulation and conversion of pigment but also impact carbohydrate and secondary metabolism during tomato fruit ripening. We further demonstrate that these effects are likely due to an effect of heterochrony coupled with an unnoticed role of auxin the regulation of key enzymes in the route of synthesis and degradation of carbohydrates. Our results also unravel the role of auxin in the mitochondria-chloroplast energetic crosstalk that are of pivotal significance during tomato fruit ripening and provide evidence that auxin signaling have a profound influence on metabolism during fruit ripening.

MATERIAL AND METHODS

Plant material and growth conditions

Seeds of the tomato (Solanum lycopersicum cv Micro-Tom) wild-type (WT) and near isogenic lines (NILs) dgt and entire in the same genetic background (cv. Micro-Tom) were obtained as described previously (Carvalho et al., 2011) were surface sterilized with 5% sodium hypochlorite for 10 min, then washed with running distilled water and subsequently sowed in a tray with commercial substrate (Tropstrato HT©).

Seven days after germination (or following the appearance of the first true leaf), seedlings were transferred to 3.5 L pots containing the same commercial substrate but supplemented with 5 g L^{-1} 4:14:8 NPK. Plants were grown in a greenhouse located in Viçosa (20°45′S, 42°15′W, 650 m above sea level), southeastern Brazil, with a minimum of 400 µmol photons m^{-2} s^{-1}. Plants were watered regularly and throughout the entire growth period the plants were maintained under naturally fluctuating conditions of light intensity, temperature and relative air humidity. WT and mutants plants were grown side by side under greenhouse in the conditions described above and their development was closely observed until the production of fruits. Each single day, new flowers were tagged and the flowering and fruiting dates recorded on the tag. For accurate determination of the fruit physiological age, flowers were tagged at anthesis as previously described (Osorio et al., 2012) and samples of fruit pericarp were collected at 10, 15, 20, 25, 30, 35, 40, 50 and 60 days after anthesis (DAA) always at the middle of the light/dark cycle. Samples were immediately frozen in liquid nitrogen and stored at -80℃ until further analysis. Six fruits per each genotype and development stages were collected from different plants and used for further metabolic analyses.

To confirm the mutants genotypes, were measure the abundance of transcripts was confirmed by quantitative real time PCR (qRT-PCR), using specific primers pair for DGT and IAA9 gene: Forward 5’-GAGTCGCCGTTTTAGGCTTT -3’, Reverse 5’-GCAACACAACAACCAATTACG-3’ and Forward 5’-TGTCAAGTGTGTGACAGCC-3’, Reverse 5’- TGTCACTTACACATAGGGCCA-3’ respectively.

Ethylene and CO_2 production

Erlenmeyer flasks (125 mL) containing fruits of different ages were stoppered with a rubber serum cap, and kept under laboratory conditions for period of 2h. The quantification o ethylene was performed in an air sample (1 mL) taken from the flask

158 headspace and injected in gas chromatograph (Hewlett Packard 5890, Series II),
159 equipped with a stainless-steel column (1.0 m x 6.0 mm) packed with Porapak-N 80–
160 100 mesh. Analyses were conducted under the following conditions: nitrogen carrier
161 gas and hydrogen fluxes 30 mL min^{-1} and air flux 320 mL min^{-1}. Column, injector, and
162 detector temperatures were 60, 110, and 150 ◦C, respectively. Ethylene peaks were
163 registered by a peak simple software (Peak Simple, Version 3.92) coupled to the
164 chromatograph, and quantified by comparison with authentic ethylene standards.
165 Quantification of carbon dioxide (CO_2) was performed in fruit samples
166 maintained in the same conditions described above. An air sample (1 mL) was taken
167 from the flask headspace and injected in a gas chromatograph (Young Lin YL6100
168 GC) equipped with a thermal conductivity detector (TCD), capillary column Rt-QPLOT.
169 Analyses were conducted under the following conditions: nitrogen carrier gas and
170 hydrogen fluxes 30 mL min^{-1}, and air flux 320 mL min^{-1}. Column, injector, and detector
171 temperatures were 50, 150, and 180◦C, respectively. Carbon dioxide peaks were
172 registered by a peak simple software (Peak Simple, Version 3.92) coupled to the
173 chromatograph, and quantified by comparison with authentic carbon dioxide
174 standards.
175
176 Color measurement and Fruit Firmness
177 For surface color assessment, fruits were marked along their equatorial axes
178 and three readings were taken using a colorimeter portable Chroma Meter, model CR
179 200 colorimeter (Minolta camera Co, Ltd., 22 Osaka, Japan). Color attributes were
180 used according to the CIELab recommendations in terms of lightness (L) and angle
181 Hue (H^o), as described previously (Choi et al., 2008). Fruit firmness of each individual
182 tomato was measured at three points of their equatorial region by using the FT327 fruit
183 pressure tester (Breuzzi Company, Milano, Italy). The probe descended toward the
184 sample with a uniform force and stopped at 1 mm depth. Three measurements were
185 averaged for each fruit and expressed in kg cm^{-2}.
186 Fruit fresh weight loss and fruit density
187 Transpiration water loss from transgenic and WT fruits was assessed by
188 measuring weight reduction over a 8-d period in seven detached fruits (50 DAA) from
189 each genotype kept at room temperature for over 8-d period. Fruit density was
190 measured also in 50 DAA fruits by obtaining their individual weight after being placed
191 in a beaker filled with water.

192

193 Determination of metabolite levels

194 Pericarp samples were collected at different fruit developmental stages and
195 were immediately frozen in liquid nitrogen, and stored at -80ºC until further analysis.
196 The levels of starch, sucrose, fructose, and glucose were determined exactly as
197 described previously (Fernie et al., 2001). Malate and fumarate were determined
198 exactly as detailed (Nunes-Nesi et al., 2007). Proteins and amino acids were
199 determined as described previously (Gibon et al., 2004). Metabolite extraction,
200 derivatization, standard addition, and sample injection for GC-MS were performed
201 according to Osorio et al. (2012).The mass spectra were cross-referenced with those
202 in the Golm Metabolome Database (Kopka et al. 2005).

203

204 Secondary metabolites determination

205 Total soluble phenols were quantified spectrophotometrically using the Folin-
206 Ciocalteu method (Sun et al., 2007). Data were expressed in $mg.g^{-1}$ using tannic acid
207 as standard. The quantification of individual secondary metabolites was performed on
208 HPLC as described in (Keinänen et al., 2001) with modifications. Briefly, 50 mg of fresh
209 weight were extracted by ethanolic extraction (Cross et al., 2006). The supernatant
210 was filtered through a Millipore filter of 0.22 µM, and aliquots of 50 µL were injected
211 into a HPLC equipped with a UV detector. Absorbance were determined at 210, 254,
212 320 and 365 nm for the determination of secondary metabolites. The elution gradient
213 was as following: Phase A- 0.25% of H_3PO_4 in ultrapure H_2O (pH 2.2), phase B- 100%
214 acetonitrile, and the program running: 0- 6 min (0-12% B), 6-10 min (12-18% B) and
215 10-30 min (18-58% B) with a flow rate of 1 mL min^{-1} on a Agilent ZORBAX Eclipse Plus
216 C18 column (150 mm, particle size 3 micron diameter). The identification and
217 concentration of metabolites were estimated by comparison with the retention time and
218 the calibration curve containing the mixture of authentic standards for each of the
219 analyzed compound.

220 Pyridine nucleotides

221 The NAD(H) and NADP(H) were determined as described previously (Gibon
222 and Larher, 1997). Briefly, pyridine nucleotides were assayed using the phenazine
223 methosulfate-catalyzed reduction of dichlorophenolindophenol in the presence of
224 ethanol and alcohol dehydrogenase (for NAD^+ and NADH) or glucose 6-phosphate
225 (G6P) and G6P dehydrogenase (for $NADP^+$ and NADPH). The equation used to

226 determine the concentration of nucleotides was obtained by linear regression from a
227 standard curve and subsequent normalization for the dry mass.
228
229 Statistical Analysis
230 The data was obtained from experiments using a completely randomized design
231 with three genotypes (wild-type cv. Micro-Tom, diageotropica and entire). The term
232 significant is used here only when the change in question has been confirmed to be
233 significant ($P < 0.05$) with Student's t test. All statistical analyses were performed using
234 the algorithm embedded into Microsoft Excel® (Microsoft, Seattle). Pearson correlation
235 coefficient was used at 5% significance level by the t-test for examining the
236 relationships among variables. In addition, we applied false discovery rate (FDR)-
237 controlling method proposed by Benjamini and Hochberg (1995).
238

RESULTS

Auxin signaling is essential for fruit development and ripening

In order to characterize how growth pattern and ripening related process are affected by auxin signaling, we dedicate our initial efforts to identify contrasting phenotypes among previously characterized tomato mutants with either increased (entire) or reduced (diageotropica, dgt) auxin signaling in respect the formation of the fruit and changes in the skin color. We have first shown that auxin can indeed affect both fruit formation and ripening speed (Fig 1-2 and Supplemental table 1). First, fruits of dgt mutant were characterized by a reduced fruit development, as depicted from their reduced size and biomass (fresh and dry weight) coupled with a slower ripening and a lower evolution of the color of the fruit skin according to brightness and hue angle parameters (Fig.1 and Supplemental table 1). Although dgt mutant plants showed an increased number of inflorescences per plant, a lower number of fruit per plant, affected by the lower fruit establishment rate expressed as fruit set (%), was observed (Supplemental table S1).

The functional lack of the DGT gene in tomato plants has been showed to affect the fecundation and fertilization by pollination, affecting the total productivity in comparison with WT plants (Mignolli et al., 2012). However, no changes in the number of seeds and seed weight was noted in dgt mutants (Supplemental Table S1). It is important to mention that the ripening in dgt mutant plants is affected not only by delaying fruit development but also associated with ethylene production as observed by the reduced climacteric peak, significantly lower at 40DAA (Fig. 2A). By contrast, plants with increased auxin signaling (entire) were characterized by drastic alterations in early fruit development with higher fruit diameter than WT fruits from 10DAA. Remarkably, this difference was preserved to the end of cell division (~20 DAA; Fig. 1B) and was associated with increased total fresh weight (Fig.1C) and respiratory rate accompanied by CO_2

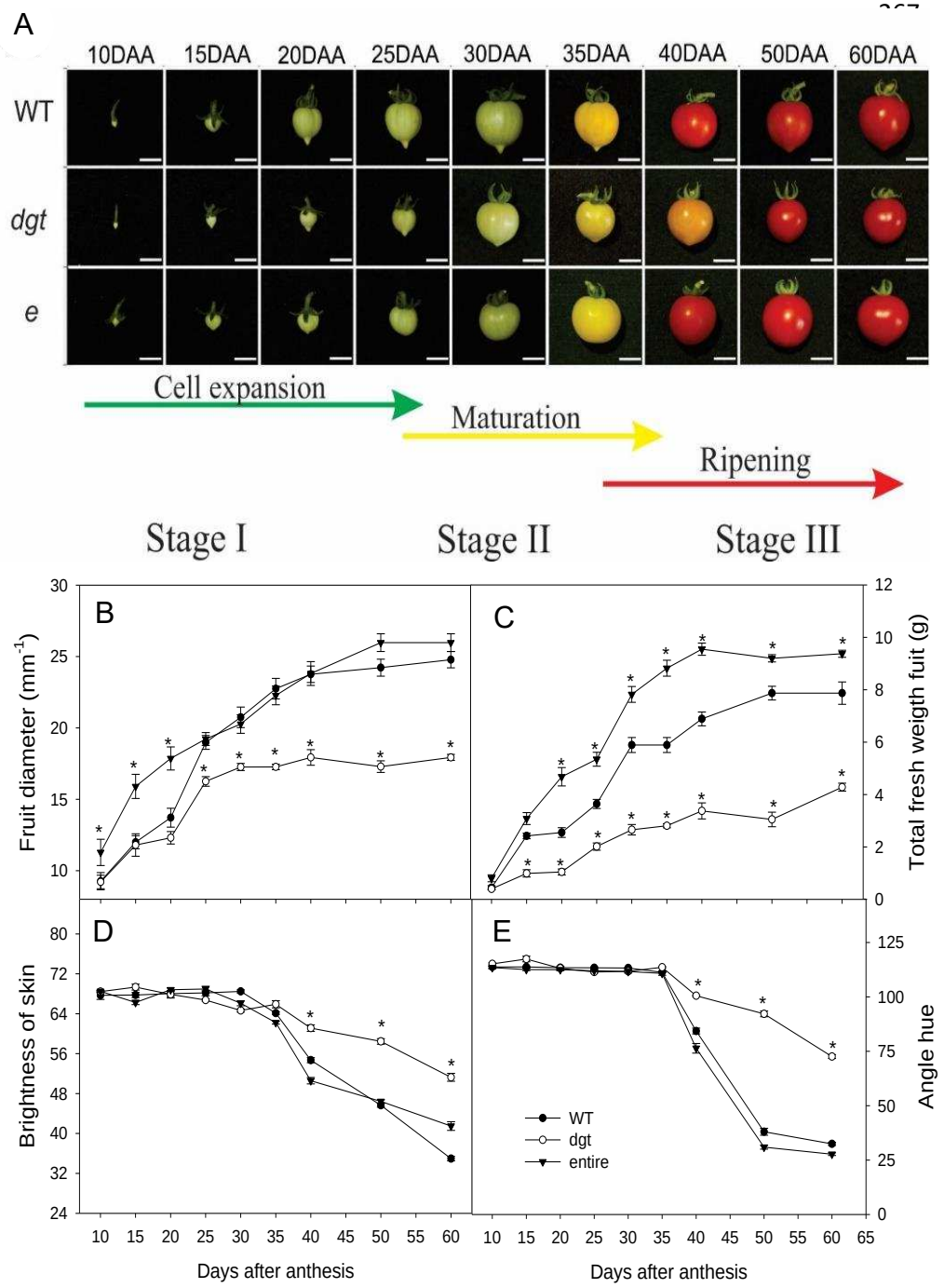

Fig. 1 – Diageotropica gene control ripening process in tomato fruit cv. Micro-Tom. Pattern of formation and ripening (A), fruit diameter (B), total fresh weight (C), brightness of skin (D) and Angle hue (D) in tomato fruits cv. Micro-Tom (wild-type) and mutants in auxin signaling diageotropica and entire, during different days after anthesis. Values are presented as means ± SE (n=7). Asterisks indicate differences between the mutants relative to wild type according to the Student's test t to be significantly different (P<0.05) from WT. Scale bar: 1 cm

release (Fig. 2B). Despite their parthenocarpic character and set fruit, entire plants were similar in appearance to WT plants in terms of flowers per fruit, fruits per plant, total dry weight size, skin color, 1000 seeds weight, total soluble solids and ethylene production (Fig.1D-C, Fig.2A and supplemental table S1).

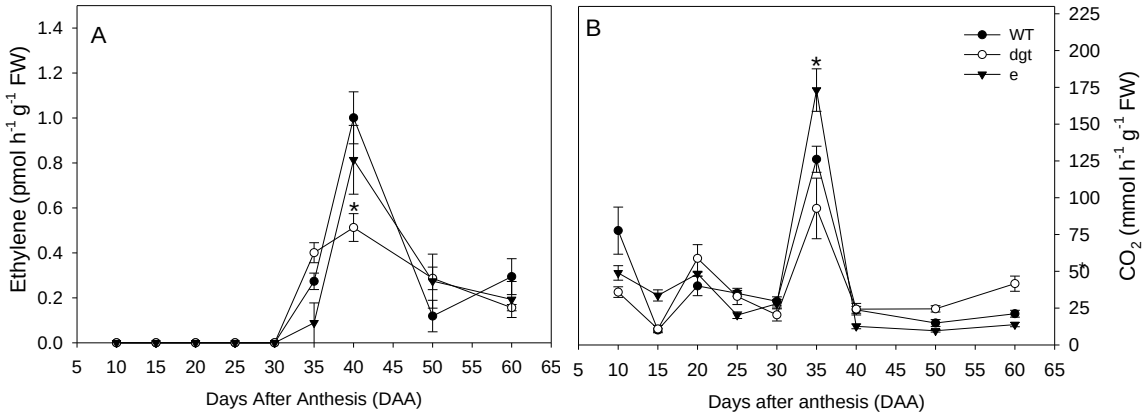

Fig. 2 - Diageotropica gene flattens climacteric peak in tomato cv. Micro-Tom fruits. Changes in the respiration and ethylene emission during ripening in wild-type (WT) and auxin signaling mutants lines (dgt and e). Ethylene production (A) and total respiration (B). Values are presented as means ± SE (n=7). Asterisks indicate values that were determined by Student's t test to be significantly different ($P < 0.05$) from their corresponding WT.

In order to confirm the reduced expression of the respective genes DIAGEOTROPICA (DGT) and Aux/IAA9 in dgt and entire mutant plants, respectively, expression analysis were performed to identify the relative expression of both genes in the mutants. Initially, we confirmed that the expression of each was significantly reduced in dgt and entire mutant plants respectively (Fig. 3A). Furthermore, the expression of DGT gene in the entire mutant and of Aux/IAA9 in the dgt mutant did not differ significantly compared to WT in leaves of plants growing under optimal conditions (Fig. 3A). We next turned our attention to the expression levels of the DIAGEOTROPICA (DGT) and SIIAA9 genes in different tissues of WT plants. Our results showed that the expression of both genes is highly variable across fruit development (Fig. 3B). qRT-PCR analysis showed that DGT is highly expressed in opened flower and its expression is reduced in fruits at 10DAA; however, in fruits at 15 and 35DAA it increases again whereas reduces in red ripped fruits (60DAA), suggesting its importance during fruit formation and beginning of ripening, which seems to be partially lost in mature fruits (Fig. 3B). On the other hand, IAA9 was highly expressed only in opened flowers, decreasing its relative expression throughout fruit development and keeping quite constantly, but no more expressed in in ripe fruits (Fig. 3B). In addition, our results are in good agreement with both previous published results

(Wang et al., 2005) and public RNA-Seq data in tomato cv. Micro-Tom plants where both genes have showed to be highly expressed in seeds, root, stems, leaves and in vitro-cultured callus (http://tomexpress.toulouse.inra.fr/select-data). This results can also be viewed in the Solanaceae Genome Network tomato expression database http://www.sgn.cornell.ed. Accordingly, the DGT seems to be highly required for fertilization processes, while IAA9 seems to be more required during initial stages of cell division and expansion, losing their function in mature fruits (Fig 3B).

Fig. 3 – Auxin signaling is genes (DGT and IAA9) is highly expressed during the formation and development of fruits**.** Relative transcript abundance of the DGT (Solyc01g111170) and AuxIAA9 (Solyc04g076850.2.1) in leaves of WT, dgt and entire mutants plants of tomato under normal growth conditions (A).

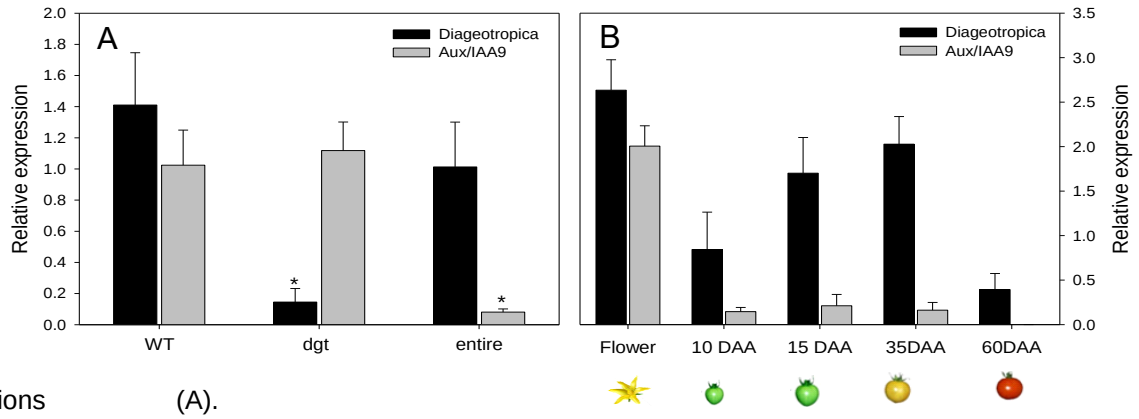

Expression pattern in different tissues in wild-type (WT) plants cv. Micro-Tom of the genes Diageotropica (DGT) and Aux/IAA9 (IAA9) (B). The RNA was isolated from mature leaves and subsequently accompanied the accumulation of transcripts by qRT-PCR using the cDNA . Data were normalized by endogenous actin gene using the equation $2^{-\Delta\Delta CT}$. DAA (days after anthesis) Values are presented as means ± SE (n=4). Asterisks indicate values that were determined by Student's t test to be significantly different ($P < 0.05$) from their corresponding WT.

DGT down-regulation delays fruit ripening and improves postharvest behavior of tomato fruits

We next characterize the effect of different auxin signaling levels caused by the down-regulation of DGT and Aux/IAA9 on tomato fruit biology and quality. First, we show that reductions in auxin signaling by DGT down-regulation modulates softening by increasing fruit firmness and starch content (Fig. 4A-B and Supplemental Fig. S1). Although fruit firmness is reduced during fruit developed in all genotypes dgt fruits were characterized by smaller reductions whilst WT and entire fruits decreased similarly fruit firmness during the time course of development (Fig. 4A). Interestingly, fruits of dgt

mutant plants display increased levels of starch in green fruit (20DAA) in comparison to WT fruits; moreover, during maturation starch levels of fruits from dgt are decreasing slower (Fig. 4B). Thus, at 40DAA both fruit firmness and starch levels are significantly higher in dgt fruits than in WT fruits which is in good agreement with the lower respiratory peak and ethylene production (Fig. 2), once the respiratory burst will convert starch to sugars used to energy production also increasing the total soluble solids content in dgt (Fig.2, Fig.4B and Supplemental Table S1). In addition, an iodine-staining experiment was performed to uncover whether starch accumulation localizes and the degradation during ripening. This analysis indicates that the presence of starch, as revealed by the blue-purple color, was manly found in the pericarp tissue with more intensive staining found in dgt fruits at 35DAA (Supplemental Fig. S1). On the other hand, although fruits of entire mutant plants seems to have higher starch content than WT fruits at early fruit development (10DAA), they also quickly decrease their starch content, showing no more significant difference between WT fruits from 25DAA onwards and starch was completely degraded in fruits at 60DAA (Fig. 4B), presenting no more iodine-staining in the pericarp tissue (Supplemental Fig. S1). Despite the functional lack of the Aux/IAA9 gene culminate with a parthenocarpy character coupled with increased set fruit as well ovary expansion in the early stages of fruit development, this mutations does seems to affect the ripening process, given that there is not so many alterations in starch and sugar content as well as in total protein in comparison with WT fruits (Fig. 4 and Supplemental Table S1). Although no changes in total protein content were noticed between WT and entire fruits, it was observed that entire increase significantly the total free amino acids levels at 25, 30 and 35DAA in comparison with WT. Remarkably, the mainly changes observed in entire fruits (Fig 4D) were observed at the beginning of climacteric peak (Fig. 1). It seems reasonable to suggest that Aux/IAA9 in tomato fruit can increase total amino acids levels by modulating the synthesis rather than directly by protein degradation.

Having established that the DGT gene seems to modulate tomato fruit development, we next decided to better characterize this effect by investigating the role of auxin signaling in the maintenance of the fruit quality and shelf life. We thus further examined the fruit postharvest desiccation also called fresh fruit loss (Fig. 4E), an aspect of great significance in fruit physiology that is typical of over ripening and that have commercial importance. Additionally, we investigate fruit density and total soluble phenols content (Fig. 4F and Supplemental Fig. S2). Our results show an

increased percentage of weight loss during storage for all genotypes, although the highest weight loss was obtained in entire and the lowest in dgt fruits after 8 days at 25ºC (Fig. 4E) in agreement with the firmness results (Fig. 4A). The fruits of dgt have reduced fresh weight loss (5.24 ± 1.11%) in the last day (8-d after harvest) in comparison with WT (9.35 ± 1.34%). Fruit density measured at 50DAA demonstrated that dgt fruits display the lower density whereas entire fruits have the highest density (Fig. 4F). During ripening, tomato fruits are characterized by enhanced levels of a large variety of phenolic derivatives and these compounds are essential for several plant functions. Total phenolic compounds for all genotypes increase during fruit ripening, coinciding with the respiratory peak (35DAA), but the highest content was observed in dgt fruits at 50 and 60DAA in comparison with WT fruits (Supplemental Fig. S2). The dgt fruit increased total phenols (≈20%) at 60DAA more than WT fruits, but fruits from entire mutant have not shown any differences in comparison with WT fruits in all times analyzed.

The metabolic impact of auxin signaling during tomato fruit development

Given the above mentioned results and the visual aspects presented by the fruits during different stages of development (Fig. 1A), we further assessed the metabolic profiles reflecting primary metabolism and explore the consequences of changes in auxin signaling on primary metabolism. To this end, we selected nine stages of development and ripening as described in “Materials and Methods”. In complement, we also analyzed the secondary metabolism by means of HPLC. Our analysis revealed that among over 35 successfully annotated compounds related to primary metabolism, considerable changes occurred in the levels of a wide range of amino acids, organic acids, and sugars (Fig. 5 and Supplemental Table S3).

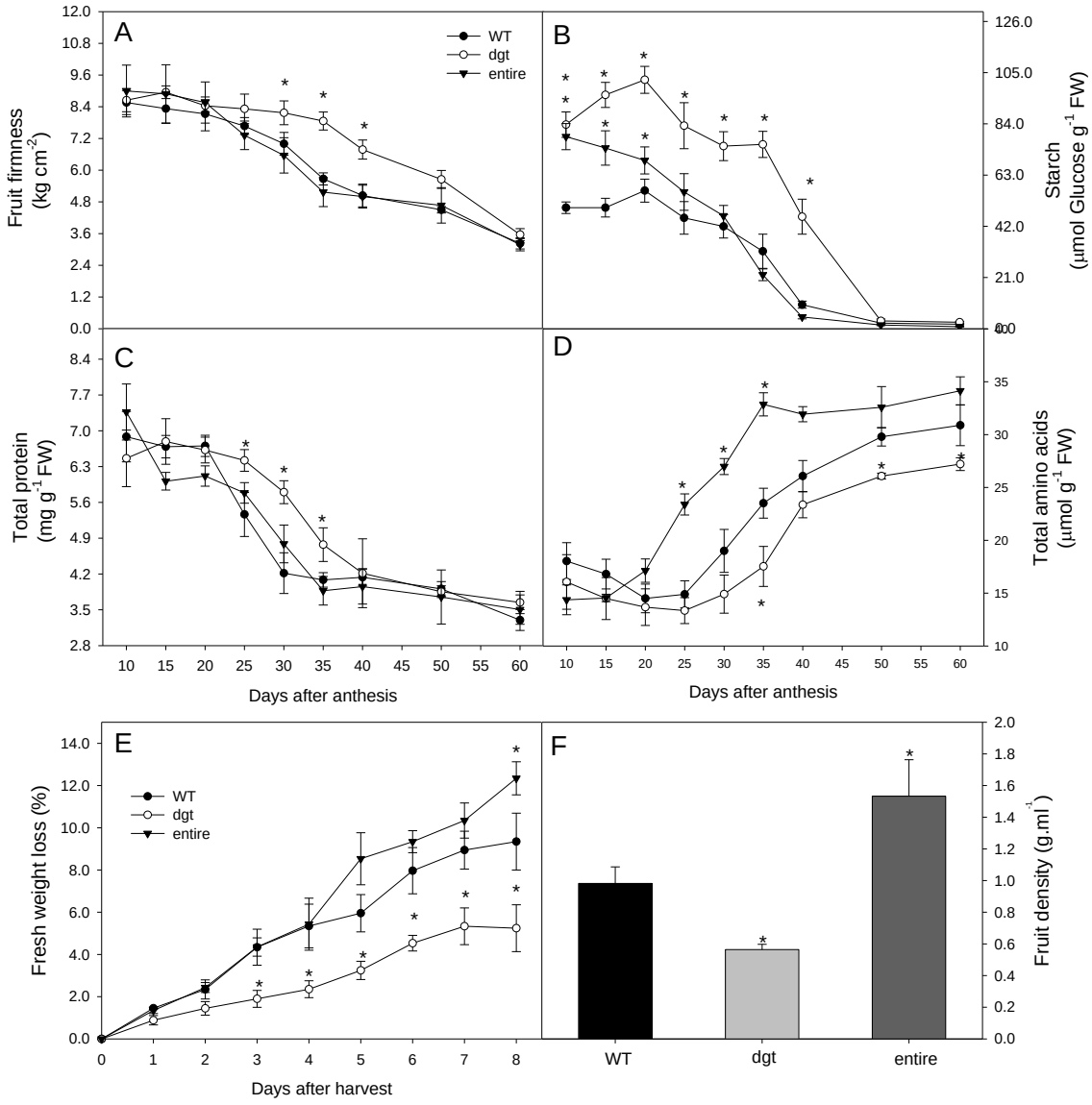

Fig. 4 - Physicochemical analyzes of tomato fruits. Firmness of fruit (A), Starch content (B), Total protein (C), Total amino acids (D), fresh weight loss (E) and fruit density (F). The fresh weight (%) and fruit density (g.ml^{-1}) was measured on fruit harvested at 50 DAA. Values are presented as means ± SE (n=7). Asterisks indicate differences between the mutants relative to wild type according to the Student's test t to be significantly different (P<0.05) from WT.

The amino acids identified during tomato fruit development in both dgt and entire revealed a total of 15 amino acids across all characterized stages plus 2 intermediates (ß-alanine and homoserine), totalizing 17 amino acids (Fig. 5). Both mutants (dgt and entire) and their respective WT all revealed marked alterations during development and ripening (Fig.5). In general, higher variations in amino acid levels between genotypes or throughout fruit development within each genotype were verified at

climacteric peak (30 and 35DAA) with dramatically reductions for both dgt and entire at 50 DAA. It was also possible to identify two major patterns of amino acids accumulation during fruit development: (i) those that increased through development, including alanine, ß-alanine, valine, glycine, phenylalanine, serine, glutamate, □-aminobutyrate (GABA), proline and tyrosine; and (ii) those that remained relatively constant, including asparagine, aspartate, glutamine, homoserine, lysine, and threonine (Fig. 5). Our results revealed that in both mutants major changes are found at 30 and 35DAA, which is in close agreement with the climacteric peak. Moreover, significant reductions in dgt fruits were observed at 50DAA, especially for ß-alanine, asparagine, GABA, glycine, isoleucine, serine, threonine and valine, which is significantly different in comparison with WT fruits (Fig. 5 and Supplemental able S3). Fruits from entire mutant plants were also characterized by such reductions but for few number of amino acids, including ß-alanine, glycine and valine (Fig. 5 and Supplemental Table S3).

The major sugars including fructose, glucose, and sucrose displayed a continuous increase during the development of tomato fruit until 60 DAA (Fig. 5 and Supplemental Table S3). Our study revealed that the contents of these sugars increased at the onset of ripening (30-35DAA- Fig.5). However, after fruits are completely ripe, the content of all three major sugars did not showed decline, except for sucrose that has few variation across fruit development. For fruits from both dgt and entire mutants glucose and fructose were higher than in WT fruits during the division and expansion phase (from 10 to 35DAA) showing even higher concentration at 60DAA (Fig.5 and Supplemental Table S3). Our analyses demonstrated that auxin signaling seems to be of pivotal significance in the modulation of sugar content across fruit development particularly considering that dgt fruits displayed reduced starch degradation during fruit development and ripening (Fig. 4B).

It was also observed an intensive variation in the levels of several organic acids measured during tomato fruit development and ripening (Fig.5). Thus, the levels of ascorbate, citrate, fumarate and malate increased during the fruit development with higher levels being found during early developmental stages (30DAA) in WT fruits, followed by reductions during ripening (Supplemental Table S3). Notably, fruits from both mutants (dgt and entire) presented a different pattern of acid accumulation and degradation during fruit development (Fig.5). In fruits of dgt mutant plants, few changes were observed in organic acids content during fruit development including an increase

in the early stages of development but without differences during climacteric time (30 to 35DAA). Fruits of dgt showed decreased organic acid content at 60DAA, significantly different for fumarate and succinate in comparison with WT fruits. Interestingly, although malate levels decreased it was maintained higher in dgt (42%) in relation to WT fruits. On the other hand, fruits from entire mutant plants were characterized as great fumarate accumulator with highest levels found at 60DAA (approximately 5-fold higher). In addition, malate levels observed in fruits from entire plants increased during pre-ripening development, until 35-40DAA but decreased during later developmental stages (at 60DAA). However, in comparison with WT fruits, the accumulation of both organic acids was significantly lower at10, 15, 20 and 25DAA and increased during the pre-ripening and ripe phase (Fig.5 and Supplemental table S3). For sake of simplicity, the metabolites highlighted in Figure 5 are either directly derived or feed the glycolytic pathway and the tricarboxylic acid (TCA) cycle. We next decided to assay the levels of pyridine dinucleotide during fruit ripening in WT, dgt and entire fruits (Table 1). Remarkably, reduced levels of NADPH and NADP(H) as well as of NADPH/$NADP^+$ ratio across fruit development, especially during early developmental stages (from 10DAA to 40DAA) were observed in fruits of dgt mutant plants (Table 1). Green fruits of dgt displayed a decrease in NADPH but with no changes in in NAD+. In the same way, it was observed a slightly reduction in NAD^+ and NADH/NAD^+ ration in both pre and ripe stages. Notably, the pattern in red fruits of dgt is slightly different with reductions in both $NADP^+$ and NAD^+. In red fruits of entire (40, 50 and 60DAA), the NADPH was slightly increased in comparison with WT the same stage. During the pre-ripening (30 and 35DAA), fruits of entire mutants plants presented slightly decreased levels of NADH. Collectively, it seems reasonable to assume that the changes observed are likely consequence of the alterations observed in respiratory activity (Fig. 2B).

Table 1 - Variations in pyridine nucleotides levels in tomato fruits in response to endogenous reduction in auxin signaling in different times of fruit development. Data presented are mean ± SE (n=7) obtained in at least two independent assays; values set in bold in dgt and entire plants were determined by the Student's t test to be significantly different (P≤0.05) from its corresponding WT (wild type).

Perimidines	Days after anthesis (DAA)								
Nucleotidesxx	10	15	20	25	30	35	40	50	60
Wild-type									
NADPH	23.34 ± 0.78	24.25 ± 0.64	24.55 ± 1.23	25.22 ± 0.54	24.45 ± 1.22	24.12 ± 1.45	23.24 ± 0.81	22.81 ± 1.22	22.77 ± 1.33
$NADP^+$	3.45 ± 0.12	3.64 ± 0.23	3.55 ± 0.12	4.23 ± 0.45	4.22 ± 0.21	4.12 ± 0.13	4.09 ± 0.32	3.66 ± 0.34	4.09 ± 0.43
NADP(H)	26.79 ± 0.88	27.89 ± 1.12	28.13 ± 0.45	29.45 ± 0.32	28.67 ± 0.55	28.24 ± 0.98	27.33 ± 0.46	26.47 ± 0.22	26.86 ± 0.56
$NADPH/NADP^+$	6.76 ± 0.54	6.66 ± 0.66	6.92 ± 0.48	5.96 ± 0.77	5.79 ± 0.32	5.85 ± 0.13	5.68 ± 0.44	6.23 ± 0.56	5.57 ± 0.42
NADH	35.56 ± 0.12	36.23 ± 0.88	36.45 ± 0.34	37.45 ± 0.78	38.76 ± 0.24	39.45 ± 1.01	37.56 ± 1.32	36.57 ± 0.76	35.45 ± 1.02
NAD^+	19.44 ± 0.33	18.54 ± 0.75	17.86 ± 0.54	17.88 ± 0.45	17.65 ± 0.78	18.67 ± 0.21	18.52 ± 0.16	19.34 ± 0.13	19.56 ± 0.55
NAD(H)	55 ± 0.55	54.77 ± 0.33	54.11 ± 0.21	55.33 ± 0.54	56.41 ± 0.99	58.12 ± 0.92	56.08 ± 0.42	55.91 ± 0.33	55.01 ± 0.64
NADH/NAD+	1.83 ± 0.11	1.95 ± 0.12	2.07 ± 0.22	2.09 ± 0.09	2.19 ± 0.08	2.11 ± 0.12	2.03 ± 0.09	1.89 ± 0.12	1.81 ± 0.11
dgt									
NADPH	**14.45 ± 0.34**	**15.43 ± 0.23**	**13.65 ± 0.28**	**14.72 ± 0.54**	**14.64 ± 0.46**	**17.09 ± 0.71**	**19.22 ± 0.45**	21.22 ± 0.56	22.53 ± 0.34
$NADP^+$	4.34 ± 0.55	**5.44 ± 0.43**	**4.34 ± 0.87**	4.33 ± 0.79	4.56 ± 0.54	4.23 ± 0.98	4.53 ± 0.64	3.23 ± 0.54	3.75 ± 0.22
NADP(H)	**21.79 ± 0.89**	**20.87 ± 0.45**	**17.99 ± 0.56**	**19.05 ± 0.43**	**19.21 ± 0.23**	**21.32 ± 0.14**	**23.75 ± 0.44**	**24.45 ± 0.87**	26.28 ± 0.36
$NADPH/NADP^+$	**4.02 ± 0.67**	**2.83 ± 0.32**	**3.14 ± 0.75**	**3.39 ± 0.34**	**3.21 ± 0.76**	**4.04 ± 0.32**	4.24 ± 0.12	6.57 ± 0.32	6.01 ± 0.13
NADH	35.66 ± 0.23	35.56 ± 0.14	35.66 ± 0.33	36.11 ± 0.11	**36.67 ± 0.56**	37.55 ± 0.13	37.77 ± 0.11	36.82 ± 0.34	35.67 ± 0.12
NAD^+	19.55 ± 0.14	18.45 ± 0.23	17.74 ± 0.11	17.32 ± 0.09	17.04 ± 0.11	**16.88 ± 0.08**	**16.33 ± 0.15**	**17.43 ± 0.12**	**16.41 ± 0.11**
NAD(H)	55.21 ± 0.22	54.01 ± 0.45	53.45 ± 0.09	53.43 ± 0.17	**53.71 ± 1.01**	**54.43 ± 0.55**	**54.15 ± 0.11**	54.25 ± 0.45	**52.08 ± 0.23**
NADH/NAD+	1.82 ± 0.15	1.93 ± 0.34	2.01 ± 0.45	2.09 ± 0.11	**2.15 ± 0.07**	**2.22 ± 0.14**	**2.31 ± 0.07**	**2.11 ± 0.08**	**2.18 ± 0.12**
entire									
NADPH	24.35 ± 1.23	23.12 ± 1.87	24.54 ± 2.10	23.55 ± 1.09	25.45 ± 0.34	25.43 ± 1.45	**25.33 ± 0.30**	**24.53 ± 1.02**	**25.32 ± 0.33**
$NADP^+$	4.55 ± 0.33	4.56 ± 0.23	3.65 ± 0.12	4.12 ± 0.23	**6.43 ± 0.56**	4.54 ± 0.43	4.52 ± 0.52	4.55 ± 0.51	4.55 ± 0.37
NADP(H)	28.90 ± 1.13	27.68 ± 0.98	28.19 ± 1.23	27.67 ± 2.33	31.88 ± 0.43	29.97 ± 0.67	29.85 ± 0.23	29.08 ± 1.23	29.87 ± 0.43
$NADPH/NADP^+$	5.35 ± 0.42	5.07 ± 0.33	6.72 ± 0.38	5.72 ± 0.16	**3.96 ± 0.33**	5.60 ± 0.56	5.60 ± 0.23	5.39 ± 0.87	5.56 ± 0.45
NADH	36.56 ± 0.44	35.44 ± 0.22	36.11 ± 0.11	36.75 ± 0.32	**36.22 ± 0.12**	**37.44 ± 0.32**	36.76 ± 0.19	35.99 ± 0.29	35.55 ± 0.21
NAD^+	19.11 ± 0.11	20.43 ± 0.15	19.22 ± 0.23	18.34 ± 0.12	17.66 ± 0.08	17.31 ± 0.11	17.83 ± 0.14	18.12 ± 0.33	18.43 ± 0.12
NAD(H)	55.67 ± 0.6	55.87 ± 0.46	55.33 ± 0.45	55.09 ± 0.3	**53.88 ± 0.45**	**54.75 ± 0.16**	**54.56 ± 0.33**	54.11 ± 0.20	53.98 ± 0.02
NADH/NAD+	**1.91 ± 0.22**	**1.73 ± 0.17**	1.88 ± 0.22	2.08 ± 0.09	2.05 ± 0.11	**2.16 ± 0.08**	2.06 ± 0.11	1.98 ± 0.06	1.93 ± 0.16

NADPH, reduced nicotinamide adenine dinucleotide phosphate; $NADP^+$; nicotinamide adenine dinucleotide phosphate, NADH; reduced nicotinamide adenine dinucleotide and NAD+; Nicotinamide adenine dinucleotide.

467 Impacts of changes in auxin signaling on secondary metabolism during tomato fruit
468 development
469
470 Given that an increased levels of total phenols in ripe fruits of dgt was observed
471 (Supplemental Fig. S2), we next turned our attention to shifts in the content of
472 secondary metabolites during fruit development. We successfully identified groups of
473 phenolic, xanthine and shikimate and thus a complete data set is presented as a
474 heatmap (Fig.5) and full data set is additionally provided (Supplementary Table S3). It
475 was possible to identify two main patterns of secondary metabolites accumulation: (i)
476 those that increased through development including cinnamic acid, shikimate,
477 theobromine and xanthosine, (2) those that remained relatively constant including
478 chlorogenic and syringic acid. Taken together, auxin signaling appears to alter the
479 accumulation of certain secondary compounds. Our results demonstrate that fruits of
480 both dgt and entire significantly increased the content of cinnamic acid at 20 and
481 25DAA, gradually reducing during ripening, similarly as observed in WT fruits. Among
482 the hydroxycinnamates, chlorogenic acid, the major nonflavonoid polyphenolic in
483 tomatoes, appears not to be modified in large proportions by the variation in auxin
484 signaling. However, the major changes were observed in preripening of dgt fruits,
485 affecting also the content of this metabolite in mature fruits (60DAA) (approximately 6-
486 fold higher) in comparison to WT fruits.
487 Shikimate has great significance in tomato fruit composition, once it produces
488 intermediate precursors of aromatic metabolites that are important with respect to fruit
489 quality (Carrari and Fernie, 2006, Tohge et al., 2014) In this work, we have shown that
490 increased auxin signaling (entire) significantly enhance the content of this acid in
491 comparison to WT fruits especially from 20to 60DAA. On the other hand, reduced auxin
492 signaling (dgt) significantly prevents the decay of shikimate content, maintaining higher
493 levels in ripe fruits (approximately 6-fold) in comparison to WT fruits at the same time.
494

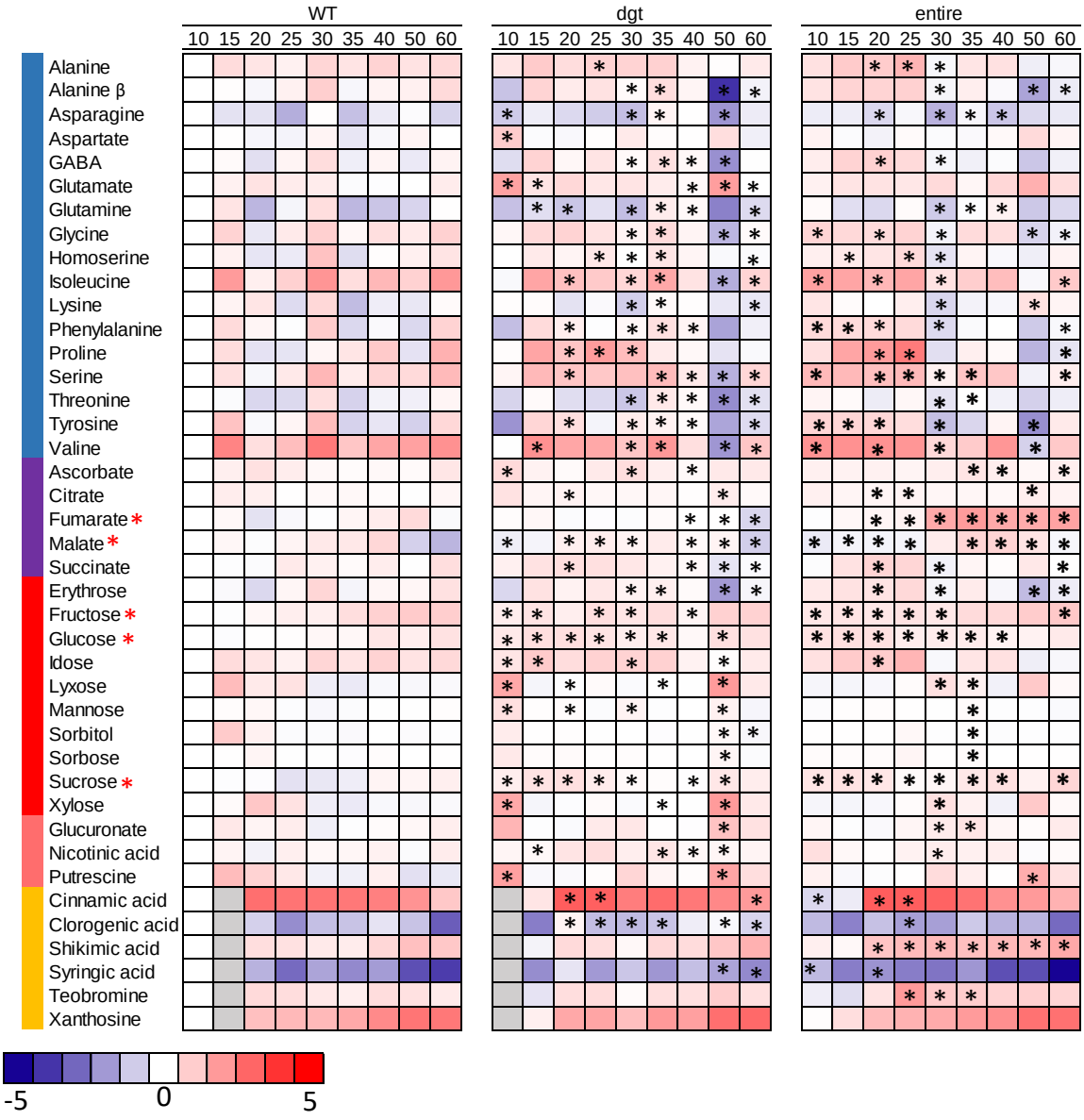

Fig. 5 - Heatmap of primary and secondary metabolism in pericarp of tomato fruits from wild-type (WT), diageotropica and entire mutants. The full data sets from these metabolic profiling studies are additionally available in Supplemental Table 3. The color code of the heat map is given at the log2 following the scale above the diagram. Data were normalized are normalized with respect to the mean response calculated for the wild type 10DAA (to allow statistical assessment, individual plants from this set were normalized in each time of development in comparison with respective time in WT). Values are presented as means ± se (n = 5). Asterisks indicate that the values from mutant lines were determined by Student's t test to be significantly different ($P < 0.05$) from the wild type. The metabolites were separated in groups by colors. Amino acids (blue), Organic acids (purple), Sugars (red), other (pink) and secondary metabolism yellow). In gray color indicate not analyzed samples. The secondary metabolites were preformatted by HPLC. GABA, γ Aminobutyrate. In red asterisks indicate the metabolites that were analyzed by photometric assay as described in material and methods.). In red asterisks indicate metabolites measured by spectrophotometer assays.

512 Multivariate analysis

513

514 To explore in more details the contribution of changes in auxin signaling in the
515 metabolite composition as well as in physical parameters across fruit developmental
516 stages, this full dataset was further analyzed using Principal Component Analysis
517 (PCA) (Supplemental Fig.S3A-B). This fingerprint analyzes revealed that indeed the
518 dominant source of variation in the combined dataset is the differential contribution of
519 the metabolite composition across fruit ripening in both genotypes. The results
520 obtained by our PCA analysis showed a clear separation between green and ripe fruits
521 using the first two components, which explain most of the variance of the dataset
522 (Supplemental Fig.S3A-B; PC1 explained 25.9% of the total variance and PC2 20.9%).
523 Surprisingly, during fruit development few variations were observed between WT, dgt
524 and entire fruits which clearly reflected in the absence of well-defined groups between
525 genotypes but rather following fruit age.

526 It was clearly observed that green fruits at 10,15,20,25 and 30 were similar to
527 each other as well as observed in fruits of dgt mutant plants at 35 and 40DAA, probably
528 due to the delay in maturation. However, a number of metabolites, such as GABA,
529 phenylalanine, ß-alanine, valine and asparagine, accounted for the main changes
530 observed in green fruits (Supplemental Fig. S3B). On the other hand, metabolic
531 changes occurring in fruit of dgt at 10DAA are best explained by the contribution of
532 glutamate and ascorbate as well as two abundant sugar, mannose and idose. Although
533 we did not observed large separations in PC2, red ripe fruits (at 50 and 60DAA) a large
534 participation of sugars, fructose and fumarate accounted for the main changes
535 observed.

536 We next decided to visualize the metabolic separation for each genotype
537 individually by using a fractional analysis of PCA in an attempt to determine which
538 changes are most closely associated with changes in auxin signaling (Supplemental
539 Fig.S4). First, when comparing the genotypes, a clear separation of green and red ripe
540 tomato fruits with changes in the contribution of the components was obtained for WT,
541 dgt and entire (35.4%, 38.9% and 47.4% for PC1 and 20.0%, 29.3% and 16.4% for
542 PC2, respectively).

543 The changes were also visualized in loading plots for each genotype.
544 Remarkable, in WT fruits the variables with greater contribution to the separation of
545 green fruit from mature ones were amino acids, nucleotides and skin color parameters.

By contrast, physical characteristics such as fruit diameter, DW fruit, sugars such as sucrose, glucose, and fructose, and total phenols were more abundant in WT fruits at 40, 50 and 60DAA (Supplemental Fig. S4A and D). Additionally, there was a clear separation between green and red ripe fruits of both WT and dgt, although fruits at 35 and 40DAA remained in the same group as green fruits. Accordingly, amino acids and organic acids such as malate, succinate, and fumarate were the main contributors to this separation. In red ripe fruits (50 and 60DAA), sugars (sucrose, glucose, and fructose) as well as NADH/NAD^+ and NADPH/$NADP^+$ had greater contribution in the changes observed in primary metabolism. (Supplemental Fig.S4B and E). Finally, increased auxin signaling (entire) led to a clear separation in three distinct groups namely green fruits(at 10, 15, 20 and 25DAA), breaker (at 30, 35 and 40) and red ripe fruits (at 50 and 60DAA). As observed in fruits of both WT and dgt, amino acids are important contributors to the separation of green fruits. Interestingly, glucose e erythrose (sugars) accounted more to the changes observed in green fruits of entire. At the breaker stage (30, 35 and 40DAA) ascorbate, malate, NADPH, NADP, NADP(H) and the NADH/NAD ration were more responsible for the separation. The contribution of aspartate and glutamate coupled with the influence of fructose, putrescine and total phenolic in ripe fruits (at 50 and 60DAA) are seemingly important in entire (Supplemental Fig.S4C and F).

The results described above allowed a quantitative description of the patterns of metabolite changes during tomato fruit development and how auxin signaling might affect the participation of this metabolites during tomato ripening. A broad combinatorial analysis of metabolites was performed by using all data points through pairwise correlation analysis (Supplemental Fig. S5). For a better visualization of correlations and to simplify the interpretation, metabolites were grouped into five classes: amino acids, organic acids, sugars, secondary compounds and others. When evaluating the strengths of these correlations and their significance several trends became apparent. Highest significant positive correlations were found for amino acids, mainly within their own class, indicating an important role of these metabolites along fruit development in tomato fruit. Additionally, total soluble solids (TSS) correlated positively with physical parameters such as fruit diameter, FW and DW per fruit (approximately 0.88, 94 and 92 respectively). On the other hand, significant negative correlations were more prominent in parameters related to skin color including brighthless, chrome and angle hue that were mainly associated with physical

parameters as fruit diameter, FW and DW per fruit (approximately, -0.70), as well as secondary metabolites, total phenols, shikimic acid and xanthosine (approximately -0.75).

DISCUSSION

Although the involvement of auxin in fruit development has been first demonstrated by the impact of its application impacting normal fruit ripening in many crop species (Cohen, 1996), surprisingly, no attempt has been made to elucidate the morphological and biochemical mechanisms underlying the responses of plants to auxin signaling during fruit development. In this study, we performed an extensive physiological and metabolic characterization of tomato fruit development by using mutants with either increased (entire) or reduced (diageotropica - dgt) auxin signaling. This approach revealed novel insights into the links between the auxin mediated regulations of fruit development in tomato together with the associated metabolic changes.

The single gene of the auxin-resistant diageotropica (dgt) mutant of tomato, that encodes a cyclophilin, displays pleiotropic auxin-related phenotypes including gravitropism, absence of lateral root branching, reduced apical dominance, altered vascular development, reduced fruit size, and reduced number of seeds (Balbi and Lomax, 2003, Oh et al., 2006, Ivanchenko et al., 2015). The second mutant used, entire, encoding Sl-IAA9, a member of the tomato Aux/IAA gene family) is also associated with pleiotropic phenotype including increased parthenocarpy rate and changes in leaf morphogenesis that include the ability to convert compound leaves to simple leaves (Wang et al., 2005b, Zhang et al., 2007).

In an attempt to first identify the expression pattern of these genes, the expression profile were monitored by qRT-PCR revealing a preferential accumulation of transcripts in early fruit development, with maximum expression in opened flower for both (Fig.3B). Interestingly, in tomato DGT seems to have great importance in the early development of fruits (until 35DAA). On the other hand, despite the highest expression in opened flowers Sl-IAA9 seems to play no function even in the early stages of development being completely dispensary in ripe fruit where it is no longer expressed (Fig.3B). Interestingly, mining microarray data available for tomato development in the

614 Heinz cultivar also revealed a strong up-regulation of Sl-IAA9 during pollination within
615 the developing fruits. In Sl-DGT, there is no available information currently
616 (http://tomexpress.toulouse.inra.fr/; Supplemental Fig.S6). Interestingly, a putative role
617 of Sl-IAA9 in early fruit has been demonstrated (Wang et al., 2005b). Additionally, Sl-
618 DGT is equally an important gene in the early stages of fruit development in tomato
619 (Balbi and Lomax (2003), in part by auxin- and ethylene-mediated gene expression.
620 We observed a delay in fruit ripening in plants with reduced auxin perception
621 (dgt), mainly associated with the fruit skin color evolution estimated by the angle hue
622 and luminosity (Fig.1). Alterations in the pigmentation is a natural process occurring
623 during tomato ripening and is associated with an increase in ABA and/or ethylene,
624 since the carotenoid accumulations is modulated by auxin-ethylene balance (Su et al.,
625 2015b). Nevertheless, auxin might also modulate pigment metabolism via regulation
626 of the expression of ripening-related transcription factor genes such as SlRIN, SlCNR
627 and SlGLK2 (Li et al. (2017). Additionally, the production of secondary color
628 metabolites seems to be strongly regulated by ethylene in tomato, although some
629 intermediates can be also produced in the absence of ethylene. Changes in the skin
630 color of dgt can be explained, at least partially, by the reduction in ethylene release
631 during the climacteric phase, associated with a lower respiratory rate (Fig.2). In
632 agreement, it is already known that despite their apparent insensitivity of auxin, dgt
633 mutant plants can also alter the regulation of ethylene synthesis (Kelly and Bradford,
634 1986). Balbi and Lomax (2003) also reported that fruit-set and fruit development in
635 tomato were dramatically altered in the dgt mutants. They argued that the lower fruit-
636 set may be a result of an effect of the dgt mutation on pollen release or on fruit-set
637 directly. In addition, it has been suggested the auxin-insensitive diageotropica (dgt)
638 mutant produces fruit upon pollination, whereas auxin treatment does not induce
639 parthenocarpy(Mignolli et al., 2012). Taken together, it is likely that pollination and
640 auxin-induced fruit set act in partially distinct cascades (Ariizumi et al., 2013). Given
641 that dgt fruits were characterized by enhanced total solids soluble (Supplemental table
642 S1) it seems reasonable to assume that the smaller fruit size was triggered by
643 differences in source-sink strength. On the other hand, despite their parthenocarpic
644 coupled with increased fruit set and size increased auxin signaling by the
645 downregulation of IAA9 (entire) in tomato did not impacted the number of flowers per
646 fruit, fruits per plant, total dry weight size, skin color, 1000 seeds weight and total
647 soluble solids and ethylene production (Supplemental table I), suggesting an important

role of this gene during early fruit development. Accordingly, increased fruit size seems to be associated with a thicker pericarp, resulting from an enhanced cell expansion and not from a higher number of cells as observed in RNAi lines of Sl-IAA17 (Su et al., 2015a). Moreover, the parthenocarpy character observed in fruits of entire have been associated with an alteration of the normal fruit set program, once the ovules of IAA9 plants were also fertile (Wang et al. (2005b). Accordingly, both the parthenocarpy and fruit-set increased with the application of either auxin or auxin transport inhibitors that cause an increase in auxin in the ovary stimulate (Gustafson, 1937).

Auxin has long been associated with fruit development, and exogenous application of auxin was shown to disturb normal fruit ripening in many crop species (Cohen (1996). Furthermore, the link between auxin signaling and sugar accumulation in fruit tissues has been demonstrated (Pandolfini et al., 2002, Wang et al., 2009b, Sagar et al., 2013a). That being said, the precise mechanisms by which this hormone impacts sugar metabolism and therefore fruit quality remain poorly understood. Fruits of dgt mutant plants were characterized by less reduction in firmness loss over fruit development, mainly at 30, 35 and 40DAA, significantly different in comparison with WT (Fig. 4A) that can be partially explained by the accumulation of starch (Fig. 4B) as well as the reduced number of pericarp cell layers (Mignolli et al., 2012). Taken together, our findings suggest the ability of auxin to regulate sugar accumulation during fruit development via DGT, while the down regulation of IAA9 (entire) seems to have a greater effect during fruit establishment. Remarkable, our work provided new evidence for the role of the DGT in the control of both fruit softening and water (weight) loss in tomatoes. It seems therefore reasonable to suggest that Sl-DGT plays a role determining fruit cell wall architecture presenting itself as a potential genetic marker for improving post-harvest handling and shelf life of tomato fruits.

During pre-ripening an increased content of total amino acid was observed (Fig.4D) coupled with significant changes in the abundance of free amino acids (Fig. 5), suggesting a high protein turnover (Sorrequieta et al. (2010). By using mutants with increased auxin signaling (entire) it seems however that the amino acids biosynthesis is increased given the absence of changes in total protein levels (Fig. 4E). To identify regulatory features underlying pollination-dependent and -independent tomato fruit set consistent changes in the levels of some amino acids during early developing fruit were also observed associated with synthesis and not with protein degradation (Wang et al. (2009b). In an attempt to better understand the changes in this metabolites and to

682 associate the participation of auxin signaling during fruit development, we decided to
683 follow the repertoire of metabolic changes that occur during fruit development by using
684 an established GC-MS approach. Several compounds were successfully identified
685 and, among them, large changes in the levels of amino acids between genotypes and
686 throughout fruit development, especially at 35 and 50 DAA were observed including
687 the differences in both organic acid and sugars during pre-ripening (Figure 5 and
688 Supplemental table S3).

689 The free amino acid content of tomato fruit pericarp increases markedly during
690 ripening transition of tomato fruit most likely by high protein turnover (Sorrequieta et
691 al., 2010). In general, pool sizes of the 20 amino acids differ strongly and change
692 dynamically depending on the developmental and physiological state of the plant cell
693 (Hildebrandt et al., 2015). The amino acids profiles during development and ripening
694 of reduced and increased auxin signaling (dgt and entire, respectively) indicate that
695 fruits of both genotypes follow similar metabolic programs (Fig.6). Thus, marked
696 changes were observed during climacteric peak and during ripe stage, mainly at
697 50DAA, suggesting that auxin signaling can seemingly modulate amino acids levels in
698 different stage across fruit development. In good agreement, Li et al. (2017) shown
699 that auxin can actively participates in the regulation of amino acid metabolism. It is
700 already known that the main amino acid involved in auxin biosynthesis is tryptophan
701 (Zhao et al., 2002), however others free amino acids might also play important roles
702 in the maintenance of auxin homeostasis via directly conjugation with auxin (Ljung,
703 2013). Further experimentation focusing at both amino acid synthesis and auxin
704 conjugation will be required to fully define the precise mechanism by which amino acid
705 metabolism and hormone-mediated control of fruit development are associated.

706 Interestingly, aromatic amino acids (phenylalanine and tyrosine) in dgt mutant
707 increased, mainly during preripening, followed by drastically reducing at 50DAA and
708 60DAA in comparison with WT. On the other hand, increased auxin perception (entire)
709 led to higher levels of the abovementioned amino acids in early stages of fruit
710 development followed by drastically reduced levels in breaker and ripe fruit,
711 characterized by intensive respiratory process. Interestingly, aromatic amino acids can
712 act as alternative respiratory substrates when carbohydrates are not abundant
713 (Ishizaki et al., 2005, Hildebrandt et al., 2015). These amino acids also serve as
714 precursors for various branches of the phenylpropanoids pathway and the biosynthetic
715 plant phenolic 2-phenylethanol and 2-phenylacetaldehyde, contributing to the several

716 secondary metabolites (Tieman et al., 2006). Our results also shown that auxin
717 influenced the secondary metabolism by changing the levels of certain compounds
718 during ripening (Fig.5). Briefly, the functional lack of DGT increased the amount of
719 xanthosine whereas entire has significantly increased levels of shikimic acid which is
720 an important precursor of aromatic amino acids (Phe, Tyr and Try). In agreement, the
721 shikimate pathway was also upregulated in antisense lines of SlIAA9, as evidenced by
722 the higher levels of both Tyr and the large increase in shikimate itself (Wang et al.
723 (2009a). In this context, the branched chain amino acid (BCAA – Leucine, Isoleucine
724 and Valine) slightly increased across fruit development, but higher levels of BCAA were
725 maintained until 40DAA followed by reduction in ripe fruits of dgt when compared with
726 WT. This results can be explained, at least partially, by a reduced respiratory demand
727 during this stages in dgt in which the usage of alternative substrates for respirations is
728 seemingly reduce. The decline in 50 and 60DAA may reflect a partial reliance of the
729 mitochondrial electron transport chain during later stages of fruit development, when
730 carbon demand is provided entirely by source leaves of the plants, as opposed to a
731 partially autonomous supply of photoassimilate during early fruit development (Osorio
732 et al., 2011). On the other hand, in fruits of entire the BCAA levels are increased mainly
733 during early developing fruit until the end of cell expansion (at 25 to 30DAA - Fig.5).
734 Wang et al. (2009b) observed that the down-regulation of SlIAA9 gene increase amino
735 acids derived from pyruvate (Leucine, Isoleucine, and Alanine) between the floral bud
736 and anthesis and this indicated a higher metabolic rate associated with fertilization-
737 independent fruit set. It is worth to mention that amino acids are not only involved in
738 the desirable taste of fruit or as intermediator of respiratory process, but they also
739 contribute to aroma. Indeed, both alanine and glutamate levels are found in high levels
740 in tomato fruits and in particular glutamate can contribute to produce many aromatic
741 compounds (Ardö, 2006, Sorrequieta et al., 2010). Interestingly, when comparing the
742 metabolic shifts displayed by both mutants used here, we observed that aspartate,
743 glutamate and alanine, which were characterized by large increases during ripening of
744 WT fruits, were only slightly increased or unaltered during earlier development and
745 ripening of auxin signaling mutants (Fig.5 and Supplemental table S3). In addition,
746 accumulation of aspartate and alanine was not evident in auxin-applied fruits at final
747 ripening stage suggesting a long-term effect of auxin on the metabolism of these two
748 amino acids (Li et al., 2017). These authors have also suggested that changes of free
749 amino acids contents induced by auxin implies that auxin may influence the volatiles

of fruit (Li et al., 2017) .Nevertheless, further work is still required to establish how auxin signaling is able to impact both amino acid metabolism and volatile production in tomato fruits respiration.

Organic acids are of pivotal significance to many aspects of tomato fruit biology and maturation. Accordingly, strong correlation between such metabolites with genes associated with ethylene and cell wall metabolism-related pathways as well as important attribute of fruit organoleptic quality has been demonstrated (Centeno et al., 2011, Osorio et al., 2011, Etienne et al., 2013). Both malate and citrate are also highly correlated to many important regulators of ripening as demonstrated in an independent study focused on early fruit development (Mounet et al., 2009). Accordingly, under normal conditions, the levels of citrate increased and reached to maximal at final ripe stage of tomatoes, while malate can reduce during ripening burst as a main substrate during tomato fruit ripening (Centeno et al., 2011) and for more details in Fig.6). These changes are partially explained by a continued activity of malate dehydrogenase (mMDH) and citrate synthase (CS), resulting in a decline in malate levels and the preferential accumulation of citrate coupled with significant changes in the redox power (Nunes-Nesi et al., 2005, Sweetlove et al., 2010, Oms-Oliu et al., 2011, Nunes-Nesi et al., 2013). In our study, fruits of dgt mutant were characterized by reduced changes in malate levels with slightly changes in citrate. On the other hand, increased auxin signaling by down-regulation of SlIAA9 (entire), was characterized by increased malate levels at end stage od ripening in comparison with WT, indicating that increased auxin perception might also enhance fruit acidity. This results are in agreement with previous results, where exogenous auxin has increase both malate and citrate levels but reduced succinate (Li et al., 2017). Another change of note is the strong increased of fumarate across fruit development, reached to maximum at final ripe stage in fruits of entire (Fig. 5 and Supplemental Table S3). Under normal condition, fumarate decrease across fruit development as described in (Carrari and Fernie, 2006). Collectively, these results demonstrate one previously unrecognized role of IAA9 and additionally auxin signalling by showing its importance in governing fruit development and primary metabolism with direct impacts on TCA cycle intermediates.

Tomato organoleptic quality is strongly influenced by the increase in total sugar and acidity in mature fruits and thus the ratio sugar/organic acid is an important indicator of flavor and fruit quality. Sucrose metabolism has a pivotal role in tomato fruit development, once sucrose is the major photoassimilate translocated to the fruit,

where it is conversed in hexoses-P and further, during early stages can be converted in starch which represents the major carbon reserve in the fruit (Zamski and Schaffer, 1996). Tomatoes contain significantly high amount of reducing sugars glucose and fructose with trace amounts sucrose (Malundo et al., 1995). Interestingly, WT fruits had their glucose and fructose content increased during fruit development, and few variations in sucrose as observed in our work (Carrari et al., 2006). Reduced auxin signaling (dgt) seems to severely affect the glucose content maintaining high levels in red ripe fruit. Notably, the enhanced starch content (Fig.4B and Fig.6) observed in fruits of dgt mutant is likely an important factor that has contributed to the increased sugar content across the fruit development. Accordingly, the transcription factors Auxin Response Factor SlARF4, ARF7 and APETALA2/ERF gene, SlAP2a, is a negative regulator of fruit ripening have been found to participate in regulation of carbohydrate metabolism in tomato fruit (Chung et al., 2010, Sagar et al., 2013a, Hao et al., 2015).

In summary, our data are highly suggestive of an unrecognized function of auxin signaling in the regulation of the accumulation and conversion of pigment as well as secondary metabolism. Collectively, our data also demonstrate that reductions in auxin signaling impact fruit set and ripening, most likely due to impacts on sugar content and starch metabolism, providing a functional link between auxin signaling and respiratory pathway. Whilst these data provide a clear connection between mitochondrial metabolism and auxin signaling, future investigation is still required including a deeper focus on growth connections to fully elucidate the precise factors underlying this metabolic phenotype impacting organic acids metabolism, mainly fumarate.

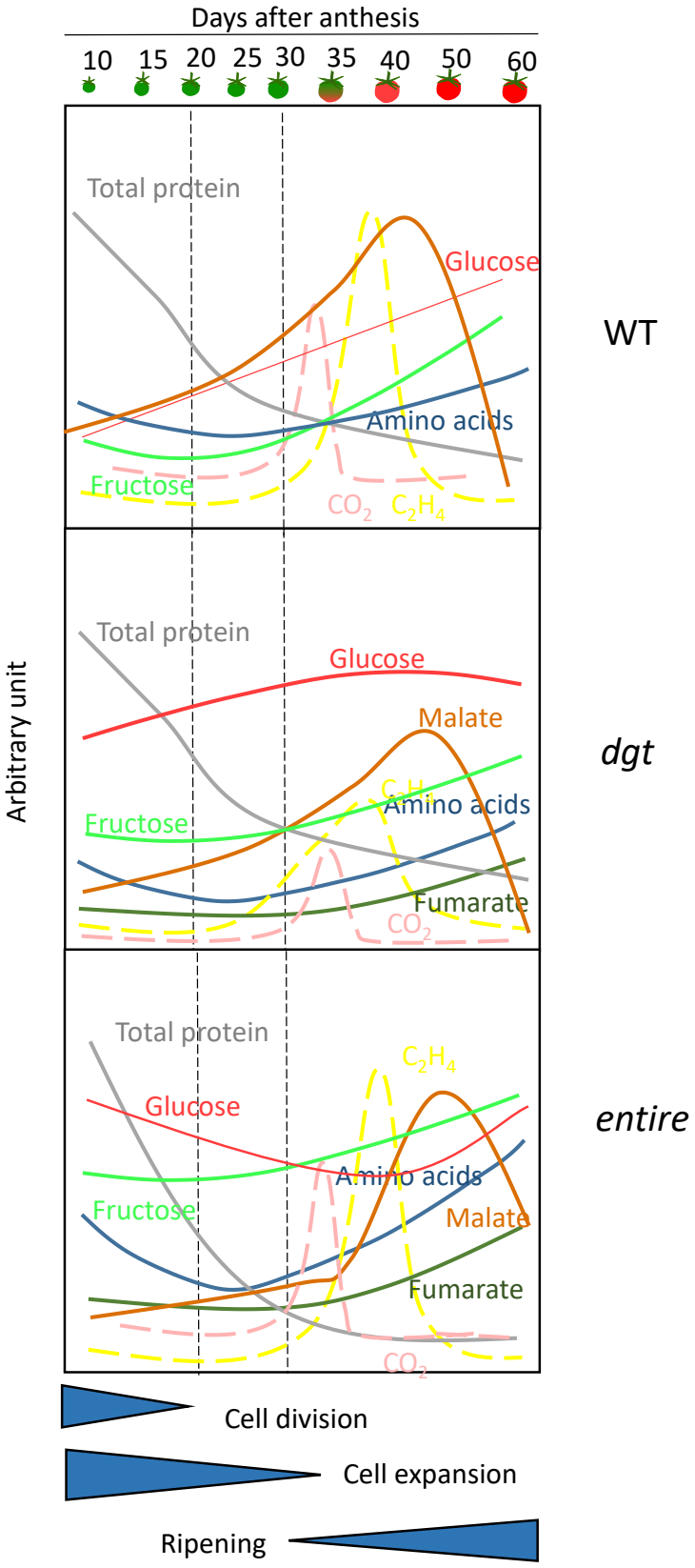

807

808 **Fig. 6 - Metabolic changes occurring in tomato fruit pericarp in different auxin signaling pattern**
809 **during development and ripening.** The data are expressed in arbitrary units for both mutants (dgt
810 and entire), but according to the data found in photometric assay (glucose, fructose, malate, fumarate,
811 total protein and total amino acids). The data of C_2H_4 and CO_2 were performed in GC (gas
812 chromatography). Adapted from Beauvoit, et al.,(2018).

Acknowledgments

Discussions with Prof. Dimas M. Ribeiro, Prof. Fábio M. DaMatta, and Prof. Samuel V.C. Martins (all from Universidade Federal de Viçosa, Brazil) were highly valuable in the development of this work.

SUPPLEMENTAL DATA

The following supplemental materials are available

Supplemental Fig. S1. Representative cross section of tomatoes fruit.

Supplemental Fig. S2. Changes in total soluble phenols content in auxin signaling mutants during different stages of development.

Supplemental Fig. S3 Principal Component analysis (PCA).

Supplemental Fig. S4 Principal Component analysis (PCA) for each genotype individually separated during different stages of fruit development.

Supplemental Fig. S5. Heat map of metabolite-metabolite correlations (pericarp) of WT and auxin signaling mutant dgt and entire during fruit development.

Supplemental Fig. S6. Microarray data analysis during development of tomato in the Heinz tomato.

Supplemental Fig. S7. Metabolic pathway scheme summarizing the metabolic changes tomato fruits during different development stage of dgt and entire mutants

Supplemental Table 1. Phenotype growth over fruit development dgt and entire mutants.

Supplemental Table 2. Metabolite correlations of tomato fruits during tomato fruit development.

Supplemental table 3 - Relative metabolite content of the different stages of development of auxin signaling tomato fruit.

Supplemental table S4. Primers utilized to qRT-PCR

REFERENCES

Ardö, Y. (2006) Flavour formation by amino acid catabolism. Biotechnology advances, **24**, 238-242.

Ariizumi, T., Shinozaki, Y. and Ezura, H. (2013) Genes that influence yield in tomato. Breeding Science, **63**, 3-13.

Balbi, V. and Lomax, T.L. (2003) Regulation of Early Tomato Fruit Development by theDiageotropica Gene. Plant Physiology, **131**, 186-197.

Bassa, C., Etemadi, M., Combier, J.-P., Bouzayen, M. and Audran-Delalande, C. (2013) Sl-IAA27 gene expression is induced during arbuscular mycorrhizal symbiosis in tomato and in Medicago truncatula. Plant Signaling & Behavior, **8**, e25637.

Benjamini, Y. and Hochberg, Y. (1995) Controlling the false discovery rate: a practical and powerful approach to multiple testing. Journal of the royal statistical society. Series B (Methodological), 289-300.

Bouzayen, M., Latché, A., Nath, P. and Pech, J.-C. (2010) Mechanism of fruit ripening. In Plant developmental biology-Biotechnological perspectives: Springer, pp. 319-339.

Carrari, F., Baxter, C., Usadel, B., Urbanczyk-Wochniak, E., Zanor, M.-I., Nunes-Nesi, A., Nikiforova, V., Centero, D., Ratzka, A. and Pauly, M. (2006) Integrated analysis of metabolite and transcript levels reveals the metabolic shifts that underlie tomato fruit development and highlight regulatory aspects of metabolic network behavior. Plant Physiology, **142**, 1380-1396.

Carrari, F. and Fernie, A.R. (2006) Metabolic regulation underlying tomato fruit development. Journal of Experimental Botany, **57**, 1883-1897.

Carvalho, R.F., Campos, M.L., Pino, L.E., Crestana, S.L., Zsögön, A., Lima, J.E., Benedito, V.A. and Peres, L.E. (2011) Convergence of developmental mutants into a single tomato model system:'Micro-Tom'as an effective toolkit for plant development research. Plant Methods, **7**, 18.

Centeno, D.C., Osorio, S., Nunes-Nesi, A., Bertolo, A.L., Carneiro, R.T., Araújo, W.L., Steinhauser, M.-C., Michalska, J., Rohrmann, J. and Geigenberger, P. (2011) Malate plays a crucial role in starch metabolism, ripening, and soluble solid content of tomato fruit and affects postharvest softening. The Plant Cell, **23**, 162-184.

Choi, S.T., Tsouvaltzis, P., Lim, C.I. and Huber, D.J. (2008) Suppression of ripening and induction of asynchronous ripening in tomato and avocado fruits subjected to complete or partial exposure to aqueous solutions of 1-methylcyclopropene. Postharvest Biology and Technology, **48**, 206-214.

Chung, M.Y., Vrebalov, J., Alba, R., Lee, J., McQuinn, R., Chung, J.D., Klein, P. and Giovannoni, J. (2010) A tomato (Solanum lycopersicum) APETALA2/ERF gene, SlAP2a, is a negative regulator of fruit ripening. The Plant Journal, **64**, 936-947.

Cohen, J.D. (1996) In vitro tomato fruit cultures demonstrate a role for indole-3-acetic acid in regulating fruit ripening. Journal of the American Society for Horticultural Science, **121**, 520-524.

Etienne, A., Génard, M., Lobit, P., Mbeguié-A-Mbéguié, D. and Bugaud, C. (2013) What controls fleshy fruit acidity? A review of malate and citrate accumulation in fruit cells. Journal of experimental botany, **64**, 1451-1469.

Fernie, A.R., Roscher, A., Ratcliffe, R.G. and Kruger, N.J. (2001) Fructose 2, 6-bisphosphate activates pyrophosphate: fructose-6-phosphate 1-phosphotransferase and increases triose phosphate to hexose phosphate cycling in heterotrophic cells. Planta, **212**, 250-263.

Gibon, Y., Bläsing, O.E., Palacios-Rojas, N., Pankovic, D., Hendriks, J.H., Fisahn, J., Höhne, M., Günther, M. and Stitt, M. (2004) Adjustment of diurnal starch turnover to short days: depletion of sugar during the night leads to a temporary inhibition of carbohydrate utilization, accumulation of sugars and post-translational activation of ADP-glucose pyrophosphorylase in the following light period. The Plant Journal, **39**, 847-862.

Gibon, Y. and Larher, F. (1997) Cycling assay for nicotinamide adenine dinucleotides: NaCl precipitation and ethanol solubilization of the reduced tetrazolium. Analytical biochemistry, **251**, 153-157.

Gustafson, F.G. (1937) Parthenocarpy induced by pollen extracts. American Journal of Botany, 102-107.

Hao, Y., Hu, G., Breitel, D., Liu, M., Mila, I., Frasse, P., Fu, Y., Aharoni, A., Bouzayen, M. and Zouine, M. (2015) Auxin response factor SlARF2 is an essential component of the regulatory mechanism controlling fruit ripening in tomato. PLoS genetics, **11**, e1005649.

Hildebrandt, T.M., Nesi, A.N., Araújo, W.L. and Braun, H.-P. (2015) Amino acid catabolism in plants. Molecular plant, **8**, 1563-1579.

Ishizaki, K., Larson, T.R., Schauer, N., Fernie, A.R., Graham, I.A. and Leaver, C.J. (2005) The critical role of Arabidopsis electron-transfer flavoprotein: ubiquinone oxidoreductase during dark-induced starvation. The Plant Cell, **17**, 2587-2600.

Ivanchenko, M.G., Zhu, J., Wang, B., Medvecká, E., Du, Y., Azzarello, E., Mancuso, S., Megraw, M., Filichkin, S. and Dubrovsky, J.G. (2015) The cyclophilin A DIAGEOTROPICA gene affects auxin transport in both root and shoot to control lateral root formation. Development, **142**, 712-721.

Keinänen, M., Oldham, N.J. and Baldwin, I.T. (2001) Rapid HPLC screening of jasmonate-induced increases in tobacco alkaloids, phenolics, and diterpene glycosides in Nicotiana attenuata. Journal of agricultural and food chemistry, **49**, 3553-3558.

Kelly, M.O. and Bradford, K.J. (1986) Insensitivity of the diageotropica tomato mutant to auxin. Plant Physiology, **82**, 713-717.

Kumar, R., Khurana, A. and Sharma, A.K. (2014) Role of plant hormones and their interplay in development and ripening of fleshy fruits. Journal of experimental botany, **65**, 4561-4575.

Li, J., Khan, Z.U., Tao, X., Mao, L., Luo, Z. and Ying, T. (2017) Effects of exogenous auxin on pigments and primary metabolite profile of postharvest tomato fruit during ripening. Scientia Horticulturae, **219**, 90-97.

Li, J., Tao, X., Li, L., Mao, L., Luo, Z., Khan, Z.U. and Ying, T. (2016) Comprehensive RNA-Seq analysis on the regulation of tomato ripening by exogenous auxin. PloS one, **11**, e0156453.

Liu, K., Kang, B.-C., Jiang, H., Moore, S.L., Li, H., Watkins, C.B., Setter, T.L. and Jahn, M.M. (2005) A GH3-like gene, CcGH3, isolated from Capsicum chinense L. fruit is regulated by auxin and ethylene. Plant molecular biology, **58**, 447-464.

Ljung, K. (2013) Auxin metabolism and homeostasis during plant development. Development, **140**, 943-950.

Malundo, T., Shewfelt, R. and Scott, J. (1995) Flavor quality of fresh tomato (Lycopersicon esculentum Mill.) as affected by sugar and acid levels. Postharvest biology and technology, **6**, 103-110.

McAtee, P., Karim, S., Schaffer, R.J. and David, K. (2013) A dynamic interplay between phytohormones is required for fruit development, maturation, and ripening. Frontiers in plant science, **4**, 79.

Mignolli, F., Mariotti, L., Lombardi, L., Vidoz, M.L., Ceccarelli, N. and Picciarelli, P. (2012) Tomato fruit development in the auxin-resistant dgt mutant is induced by pollination but not by auxin treatment. Journal of plant physiology, **169**, 1165-1172.

Mounet, F., Moing, A., Garcia, V., Petit, J., Maucourt, M., Deborde, C., Bernillon, S., Le Gall, G., Colquhoun, I. and Defernez, M. (2009) Gene and metabolite regulatory network analysis of early developing fruit tissues highlights new candidate genes for the control of tomato fruit composition and development. Plant Physiology, **149**, 1505-1528.

Muday, G.K., Rahman, A. and Binder, B.M. (2012) Auxin and ethylene: collaborators or competitors? Trends in plant science, **17**, 181-195.

Nitsch, J. (1970) Hormonal factors in growth and development. Biochemistry of fruits and their products, v. 1, 1970.

Nunes-Nesi, A., Araújo, W.L., Obata, T. and Fernie, A.R. (2013) Regulation of the mitochondrial tricarboxylic acid cycle. Current Opinion in Plant Biology, **16**, 335-343.

Nunes-Nesi, A., Carrari, F., Lytovchenko, A., Smith, A.M.O., Ehlers Loureiro, M., Ratcliffe, R.G., Sweetlove, L.J. and Fernie, A.R. (2005) Enhanced Photosynthetic Performance and Growth as a Consequence of Decreasing Mitochondrial Malate Dehydrogenase Activity in Transgenic Tomato Plants. Plant Physiology, **137**, 611-622.

Nunes-Nesi, A., Carrari, F., Gibon, Y., Sulpice, R., Lytovchenko, A., Fisahn, J., Graham, J., Ratcliffe, R.G., Sweetlove, L.J. and Fernie, A.R. (2007) Deficiency of mitochondrial fumarase activity in tomato plants impairs photosynthesis via an effect on stomatal function. The Plant Journal, **50**, 1093-1106.

Oh, K., Ivanchenko, M.G., White, T. and Lomax, T.L. (2006) The diageotropica gene of tomato encodes a cyclophilin: a novel player in auxin signaling. Planta, **224**, 133-144.

Oms-Oliu, G., Hertog, M., Van de Poel, B., Ampofo-Asiama, J., Geeraerd, A. and Nicolaï, B. (2011) Metabolic characterization of tomato fruit during preharvest development, ripening, and postharvest shelf-life. Postharvest Biology and Technology, **62**, 7-16.

Osorio, S., Alba, R., Damasceno, C.M., Lopez-Casado, G., Lohse, M., Zanor, M.I., Tohge, T., Usadel, B., Rose, J.K. and Fei, Z. (2011) Systems biology of tomato fruit development: combined transcript, protein, and metabolite analysis of tomato transcription factor (nor, rin) and ethylene receptor (Nr) mutants reveals novel regulatory interactions. Plant Physiology, **157**, 405-425.

Osorio, S., Alba, R., Nikoloski, Z., Kochevenko, A., Fernie, A.R. and Giovannoni, J.J. (2012) Integrative comparative analyses of transcript and metabolite profiles from pepper and tomato ripening and development stages uncovers species-specific patterns of network regulatory behavior. Plant physiology, **159**, 1713-1729.

Pandolfini, T., Rotino, G.L., Camerini, S., Defez, R. and Spena, A. (2002) Optimisation of transgene action at the post-transcriptional level: high quality parthenocarpic fruits in industrial tomatoes. BMC biotechnology, **2**, 1.

Pech, J.-C., Bouzayen, M. and Latché, A. (2008) Climacteric fruit ripening: ethylene-dependent and independent regulation of ripening pathways in melon fruit. Plant Science, **175**, 114-120.

Sagar, M., Chervin, C., Mila, I., Hao, Y., Roustan, J.-P., Benichou, M., Gibon, Y., Biais, B., Maury, P., Latche, A., Pech, J.-C., Bouzayen, M. and Zouine, M. (2013a) Sl-ARF4,an Auxin Response Factor involved in the control of sugar metabolism during tomato fruit development. Plant Physiology.

Sagar, M., Chervin, C., Roustan, J.-P., Bouzayen, M. and Zouine, M. (2013b) Under-expression of the Auxin Response Factor Sl-ARF4 improves post-harvest behavior of tomato fruits. Plant signaling & behavior, **8**, e25647.

Sorrequieta, A., Ferraro, G., Boggio, S.B. and Valle, E.M. (2010) Free amino acid production during tomato fruit ripening: a focus on L-glutamate. Amino acids, **38**, 1523-1532.

Su, L., Audran, C., Bouzayen, M., Roustan, J. and Chervin, C. (2015a) The Aux/IAA, Sl-IAA17 regulates quality parameters over tomato fruit development. Plant signaling & behavior, **10**, e1071001.

Su, L., Diretto, G., Purgatto, E., Danoun, S., Zouine, M., Li, Z., Roustan, J.-P., Bouzayen, M., Giuliano, G. and Chervin, C. (2015b) Carotenoid accumulation during tomato fruit ripening is modulated by the auxin-ethylene balance. BMC Plant Biology, **15**, 114.

Sun, T., Xu, Z., Wu, C.T., Janes, M., Prinyawiwatkul, W. and No, H.K. (2007) Antioxidant Activities of Different Colored Sweet Bell Peppers (Capsicum annuum L.). Journal of Food Science, **72**, S98-S102.

Sweetlove, L.J., Beard, K.F., Nunes-Nesi, A., Fernie, A.R. and Ratcliffe, R.G. (2010) Not just a circle: flux modes in the plant TCA cycle. Trends in plant science, **15**, 462-470.

Tieman, D., Taylor, M., Schauer, N., Fernie, A.R., Hanson, A.D. and Klee, H.J. (2006) Tomato aromatic amino acid decarboxylases participate in synthesis of the flavor volatiles 2-phenylethanol and 2-phenylacetaldehyde. Proceedings of the National Academy of Sciences, **103**, 8287-8292.

Tohge, T., Alseekh, S. and Fernie, A.R. (2014) On the regulation and function of secondary metabolism during fruit development and ripening. Journal of experimental botany, **65**, 4599-4611.

Trainotti, L., Tadiello, A. and Casadoro, G. (2007) The involvement of auxin in the ripening of climacteric fruits comes of age: the hormone plays a role of its own and has an intense interplay with ethylene in ripening peaches. Journal of Experimental Botany, **58**, 3299-3308.

Wang, H., Jones, B., Li, Z., Frasse, P., Delalande, C., Regad, F., Chaabouni, S., Latche, A., Pech, J.-C. and Bouzayen, M. (2005a) The tomato Aux/IAA transcription factor IAA9 is involved in fruit development and leaf morphogenesis. The Plant Cell, **17**, 2676-2692.

Wang, H., Jones, B., Li, Z., Frasse, P., Delalande, C., Regad, F., Chaabouni, S., Latche, A., Pech, J.-C. and Bouzayen, M. (2005b) The tomato Aux/IAA transcription factor IAA9 is involved in fruit development and leaf morphogenesis. The Plant Cell Online, **17**, 2676-2692.

Wang, H., Schauer, N., Usadel, B., Frasse, P., Zouine, M., Hernould, M., Latché, A., Pech, J.-C., Fernie, A.R. and Bouzayen, M. (2009a) Regulatory features

underlying pollination-dependent and-independent tomato fruit set revealed by transcript and primary metabolite profiling. The Plant Cell, **21**, 1428-1452.

Wang, H., Schauer, N., Usadel, B., Frasse, P., Zouine, M., Hernould, M., Latché, A., Pech, J.-C., Fernie, A.R. and Bouzayen, M. (2009b) Regulatory Features Underlying Pollination-Dependent and -Independent Tomato Fruit Set Revealed by Transcript and Primary Metabolite Profiling. The Plant Cell, **21**, 1428-1452.

Zamski, E. and Schaffer, A.A. (1996) Photoassimilate distribution in plants and crops: source--sink relationships. Books in soils.

Zhang, J., Chen, R., Xiao, J., Qian, C., Wang, T., Li, H., Ouyang, B. and Ye, Z. (2007) A single-base deletion mutation in SlIAA9 gene causes tomato (Solanum lycopersicum) entire mutant. Journal of plant research, **120**, 671-678.

Zhao, Y., Hull, A.K., Gupta, N.R., Goss, K.A., Alonso, J., Ecker, J.R., Normanly, J., Chory, J. and Celenza, J.L. (2002) Trp-dependent auxin biosynthesis in Arabidopsis: involvement of cytochrome P450s CYP79B2 and CYP79B3. Genes & development, **16**, 3100-3112.

Supplemental Figures

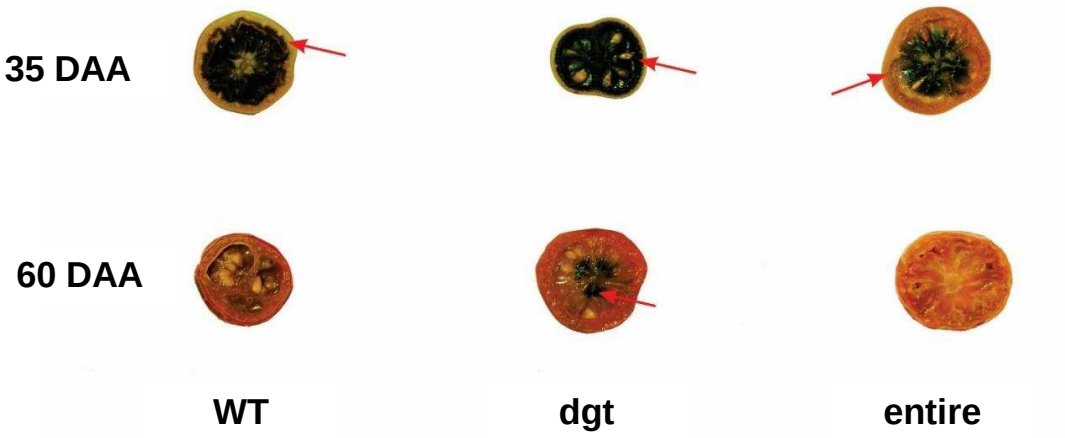

Supplemental Fig. S1. Representative cross section of tomatoes fruit. Starch content evaluated by Lugol staining in wild type and auxin signaling mutant dgt and entire (e) in 35DAA and 60DAA. Red arrows show the starch accumulation in the pericarp and placental of the fruit revealed by blue-purple color, indicative of starch reaction with iodine.

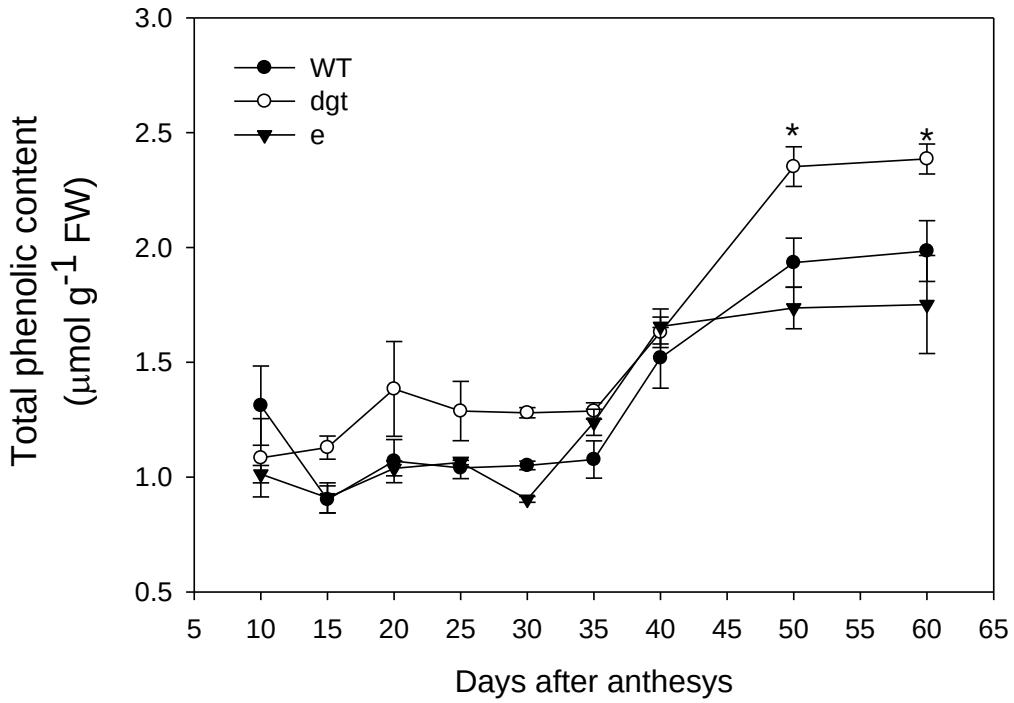

Supplemental Fig. S2. Changes in total soluble phenols content in auxin signaling mutants during different stages of development**.** Values are presented as means ± SE (n=7). Asterisks indicate differences between the mutants relative to wild type according to the Student's test t to be significantly different (P<0.05) from WT.

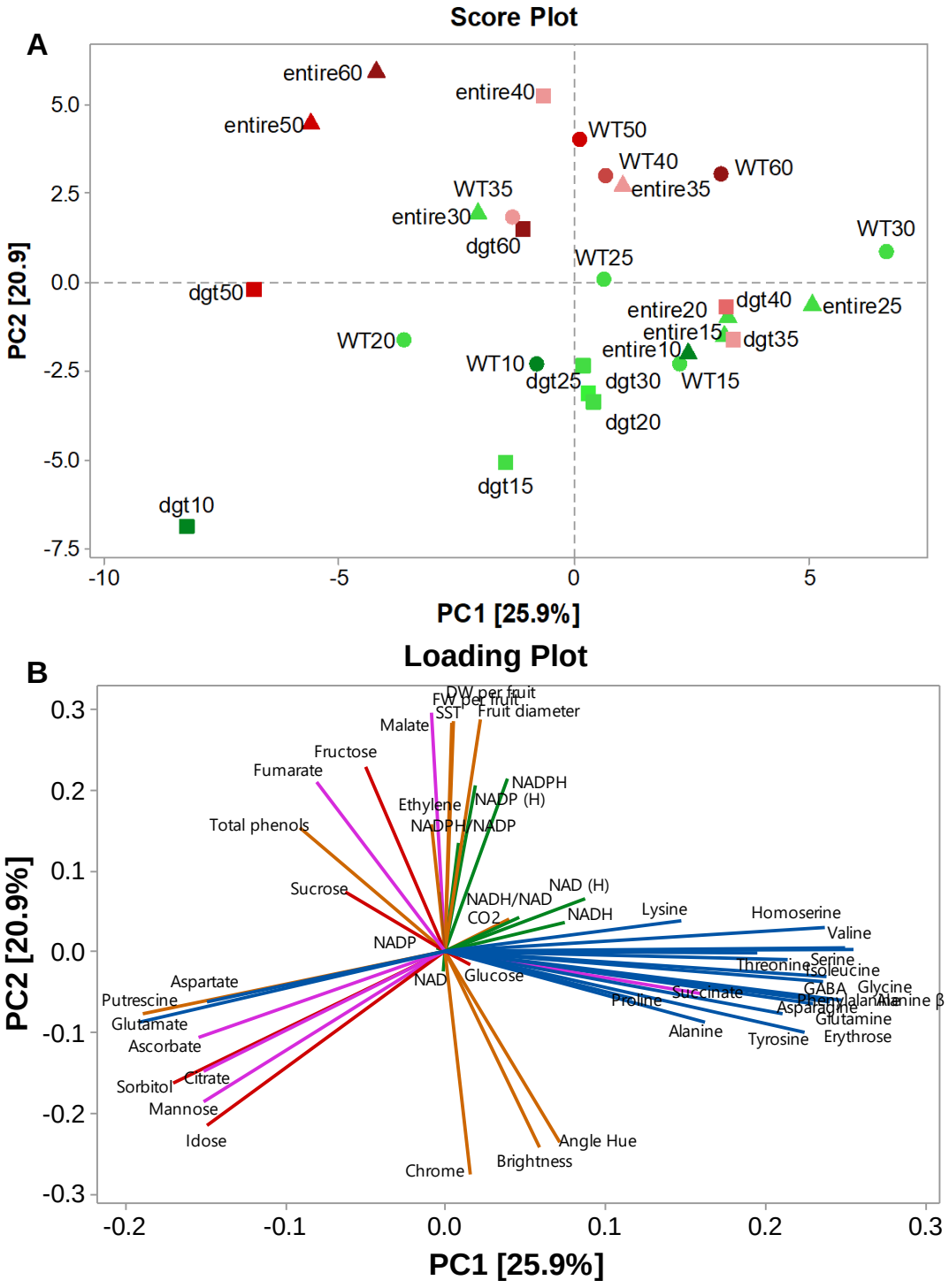

Supplemental Fig. S3 Principal component analysis (PCA). Score plot of tomato fruits in different development (10, 15, 20, 25 and 30DAA in green gradient and 35, 40, 50 and 60DAA in red gradient) stage in WT (circle) auxin signaling dgt (square) and entire (triangle) mutants. In loading plot (B), the direction and the length of the lines are directly proportional with the variables importance in separated groups. Nucleotides (dark green), Amino acids (blue), sugars (red), acids (purple), others (orange)

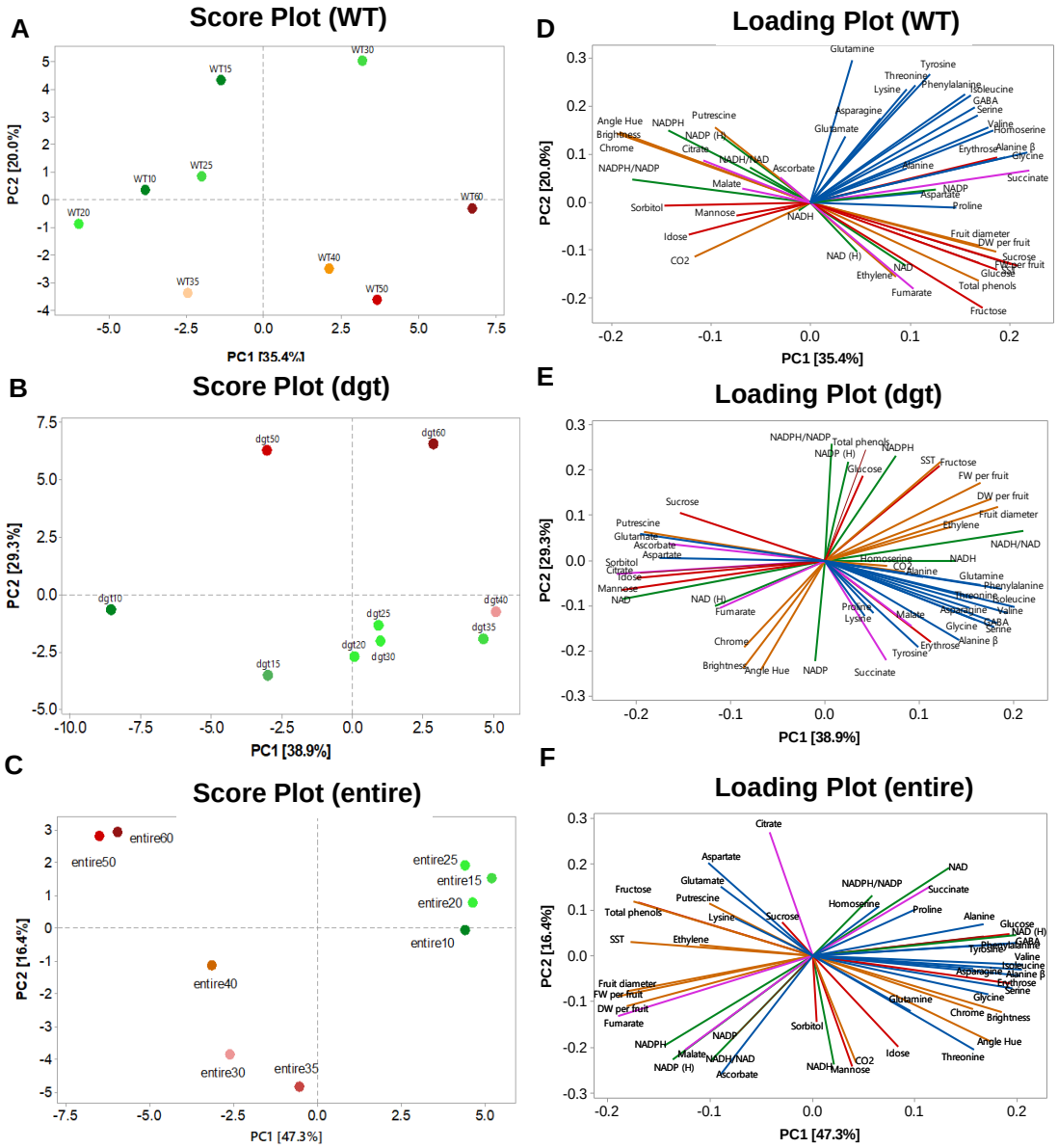

Supplemental Fig. S4 Principal component analysis (PCA) for each genotype individually separated during different stages of fruit development. Score plot to wild-type (A), Score plot to dgt (B), Score plot to entire (C), Loading plot to wild-type (D), Loading plot to dgt (E) and Loafing plot to entire (F). The colors gradient in Score plot indicate the different stages of fruit development, which greens means unripe and from pink to dark red indicate ripe fruits. However, to the Loading plot, were separated in groups according fisico-chemical analysis where, Nucleotides (dark green), Amino acids (blue), sugars (red), acids (purple), others (orange).

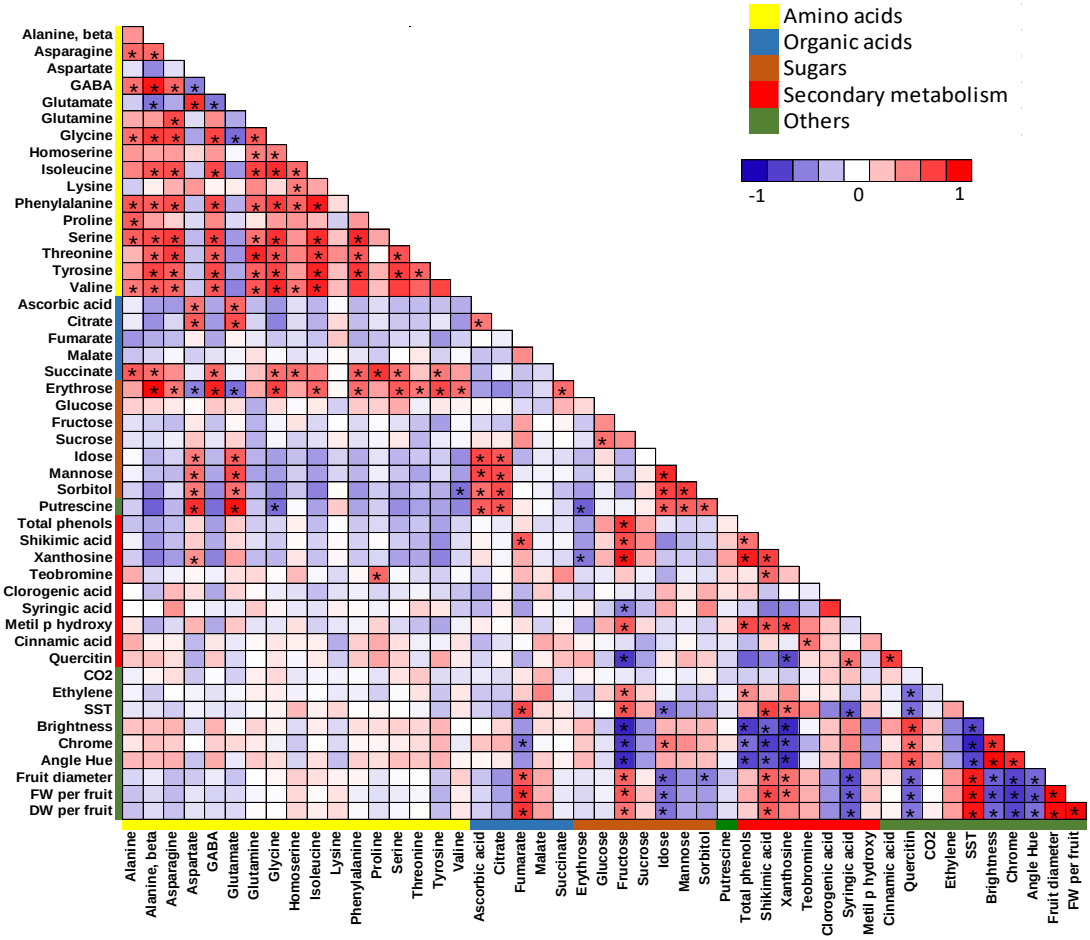

Supplemental Fig. S5. Heat map of metabolite-metabolite correlations (pericarp) of WT and auxin signaling mutant dgt and entire during fruit development. Metabolites were grouped by compound classes when known, and each square represents the correlation between the metabolite heading the column with the metabolite heading the row. Correlation coefficients and significances were calculated by Pearson correlations ($p \leq 0.05$) and presented in colors

Solyc04g076850
Sl-IAA9

Solyc01g111170
DGT

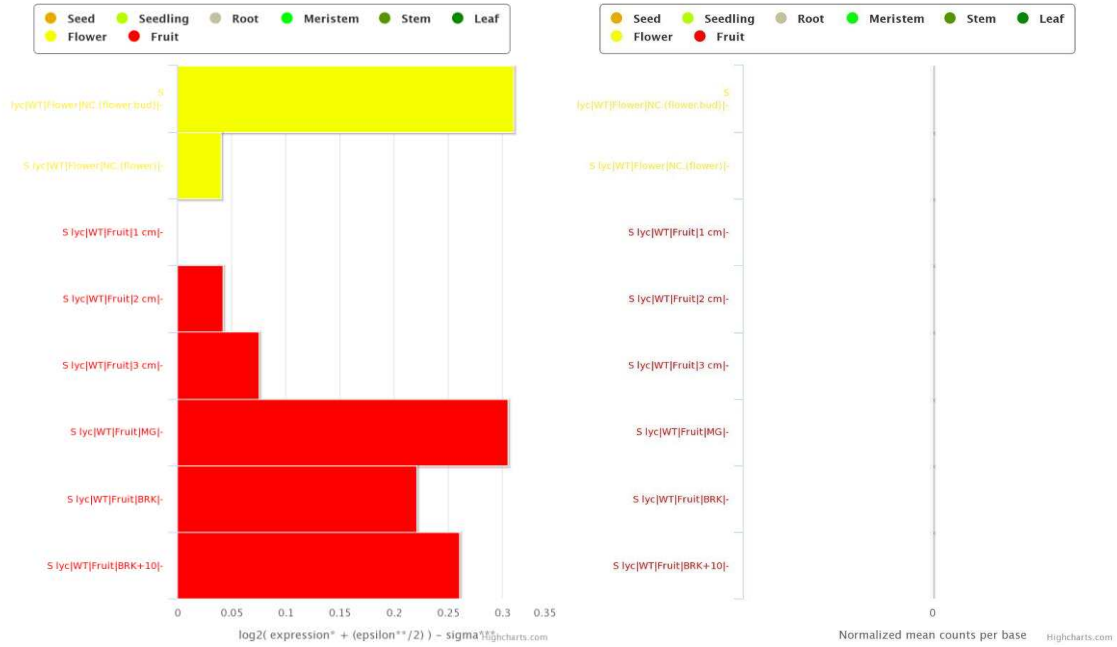

Supplemental Fig. S6. Microarray data analysis during development of tomato in the Heinz tomato. The gene expression profile is shown in log2. http://tomexpress.toulouse.inra.fr/select-data#advanced_search

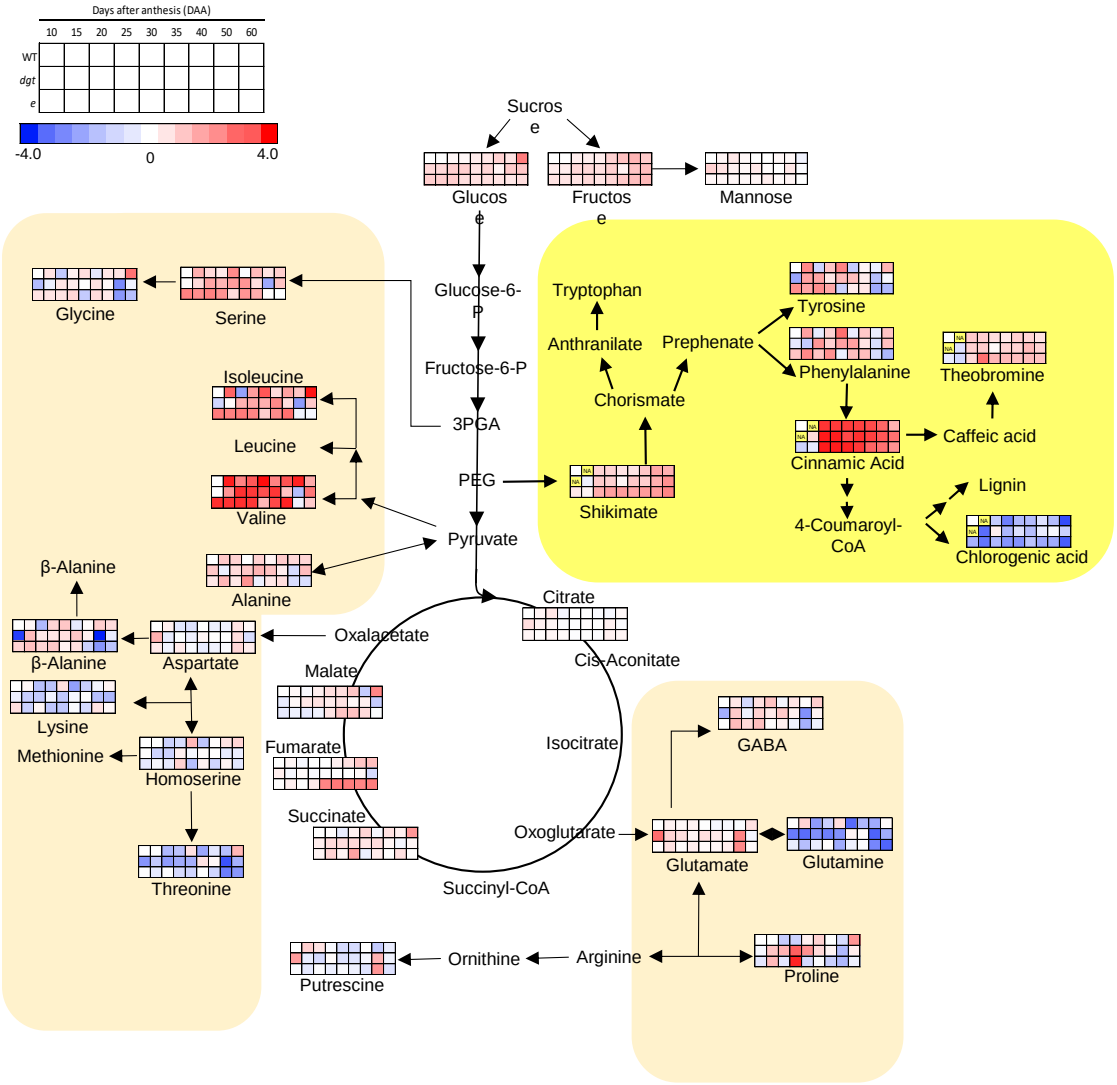

Supplemental Fig. S7 Metabolic pathway scheme summarizing the metabolic changes tomato fruits during different development stage of dgt and entire mutants. Metabolites whose levels significantly increased or decreased in the mutants fruits (mesocarp), compared to the WT. The full data sets from these metabolic profiling studies are additionally available in Supplemental Table 2. The color code of the heat map is given at the log2 following the scale above the diagram. Data are normalized with respect to the mean response calculated for the wild type 10DAA (to allow statistical assessment, individual plants from this set were normalized in the same way). Values are presented as means ± se (n = 6). In light beige color indicate amino acids pathways and in light yellow indicate secondary metabolites. NA indicate not analyzed samples. The secondary metabolites were preformatted by HPLC.

Supplemental Table 1. Phenotype growth over fruit development dgt and entire (e) mutants. Data presented are mean ± SE (n=7) obtained in one dependent assays; values set in bold in dgt and e plants were determined by the student's t test to be significantly different (p≤0.05) from its corresponding wild type.

Parameters*	WT	dgt	entire
Flowers per plant	43.37 ± 2.54	47.37 ± 3.35	45.62 ± 4.08
Fruits per plant	19.50 ± 0.59	**16.87 ± 0.78**	19.37 ± 1.99
Inflorescence per plant	5.75 ± 0.36	**7.50 ± 0.68**	8.40 ± 0.88
Set fruit (%)	45.57 ± 1.45	**38.12 ±1.34**	**58.63 ± 2.34**
Fruits per inflorescence	6.50 ± 0.65	4.78 ± 1.56	3.55 ± 0.67
Total dry weight $fruit^{-1}$ (g)	4.14 ± 0.29	**2.56 ± 0.05**	4.90 ± 0.23
1000 seeds weight (g)	2.60 ± 0.01	2.77 ± 0.008	3.07 ± 0.016
Number seeds per fruit	50.42 ± 1.17	**45.38 ± 1.77**	**28.85 ± 4.94**
Total soluble solids ºbrix	5.47 ± 0.14	**8.42 ± 0.03**	5.7 ± 0.15

The number of flowers per plant were taken based on the first flower completely open until the end of the experiment, making at the end the total sum of the flowers annotated and counting the number of fruits generated and established. The number of inflorescence per plant was analyzed at the end of the experiment, counting fruits by inflorescence. The dry mass of the fruits was carried out after the end of the cellular expansion and beginning of maturation 35DAA. Soluble solids contents were taken at 60DAA when all were already ripe

Supplemental table 2 - Metabolite correlations of tomato fruits during fruit ripening. Metabolites were grouped by compound classes when known. Pearson correlation coefficients (r) were calculated. Each cell indicates a given r value in a false color scale for a significance of p< 0.05.

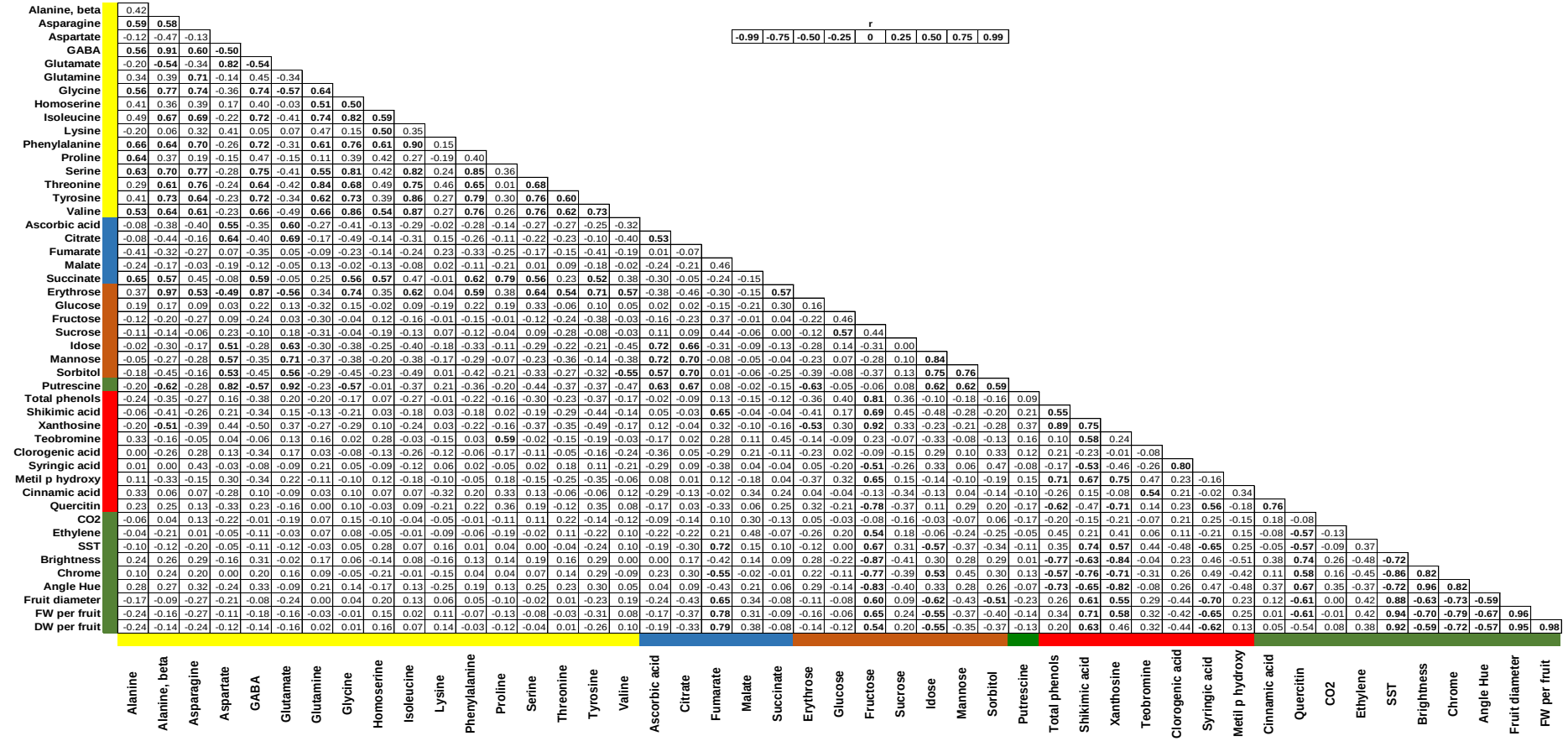

Supplemental table 3 - Relative metabolite content of the different stages of development of auxin signaling tomato fruit mutants. The metabolites were measured in WT, dgt and entire mutants in 10, 15, 20, 25, 30, 35, 40, 50 and 60 days after anthesis by GC-MS and HPLC (secondary metabolism). Data were normalized in respect to the mean response calculated for the wild type 10DAA. The statistical analysis made by Stundent's t test ($p<0.05$) for each stage of development in respective with WT as is showing in bold numbers. Values are presented as means ± se (n = 5).

	Days after anthesis (DAA)								
	10	15	20	25	30	35	40	50	60
	Wild Type (cv. Micro-Tom)								
Alanine	1.00 ± 0.219	1.73 ± 0.257	1.50 ± 0.138	1.25 ± 0.196	1.89 ± 0.271	1.52 ± 0.25	1.97 ± 0.090	1.54 0.197	1.82 ± 0.294
Alanine β	1.00 ± 0.323	6.65 ± 0.307	1.65 ± 0.457	2.71 ± 0.623	7.75 ± 0.520	0.89 ± 0.141	1.21 ± 0.088	1.26 ± 0.214	1.78 ± 0.063
Asparagine	1.00 ± 0.164	1.96 ± 0.133	0.72 ± 0.1615	1.39 ± 0.247	2.07 ± 0.131	0.42 ± 0.121	0.75 ± 0.118	0.96 ± 0.161	0.56 ± 0.086
Aspartate	1.00 ± 0.098	1.09 ± 0.344	0.65 ± 0.194	1.19 ± 0.252	1.70 ± 0.112	0.71 ± 0.149	0.90 ± 0.037	1.19 ± 0.166	1.01 ± 0.068
GABA	1.00 ± 0.237	0.93 ± 0.265	0.59 ± 0.169	1.15 ± 0.244	1.88 ± 0.099	0.79 ± 0.165	1.19 ± 0.051	0.75 ± 0.122	1.21 ± 0.126
Glutamate	1.00 ± 0.201	1.52 ± 0.364	0.37 ± 0.087	0.87 ± 0.189	1.65 ± 0.179	0.95 ± 0.176	0.97 ± 0.044	1.01 ± 0.110	1.35 ± 0.050
Glutamine	1.00 ± 0.136	2.84 ± 1.249	1.38 ± 0.675	1.58 ± 0.435	0.79 ± 0.118	0.37 ± 0.092	0.45 ± 0.049	0.56 ± 0.213	1.02 ± 0.120
Glycine	1.00 ± 0.246	2.83 ± 1.249	2.39 ± 0.675	1.57 ± 0.435	0.79 ± 0.118	1.14 ± 0.137	1.65 ± 0.104	1.38 ± 0.198	2.03 ± 0.193
Homoserine	1.00 ± 0.297	1.09 ± 0.212	1.73 ± 0.066	1.21 ± 0.067	1.39 ± 0.009	0.63 ± 0.098	1.04 ± 0.145	1.27 ± 0.225	1.53 ± 0.109
Isoleucine	1.00 ± 0.176	2.25 ± 0.761	1.96 ± 0.494	1.43 ± 0.404	0.83 ± 0.071	1.66 ± 0.289	3.03± 0.486	2.02 ± 0.640	4.86 ± 0.127
Lysine	1.00 ± 0.294	1.76 ± 0.233	1.16 ± 0.079	0.98 ± 0.244	2.18 ± 0.230	0.40 ± 0.081	0.79 ± 0.163	0.72 ± 0.183	1.08 ± 0.070
Phenylalanine	1.00 ± 0.362	1.07 ± 0.028	1.16 ± 0.037	0.99 ± 0.036	0.99 ± 0.030	0.59 ± 0.147	0.93 ± 0.054	0.59 ± 0.161	1.98 ± 0.471
Proline	1.00 ± 0.141	1.32 ± 0.066	1.29 ± 0.070	1.02 ± 0.026	1.10 ± 0.018	1.49 ± 0.287	2.27 ± 0.890	0.68 ± 0.139	3.32 ± 0.054
Serine	1.00 ± 0.241	1.21 ± 0.349	0.90 ± 0.092	0.62 ± 0.111	1.81 ± 0.042	1.35 ± 0.268	1.92 ± 0.089	1.77 ± 0.562	2.91 ± 0.023
Threonine	1.00 ± 0.170	1.13 ± 0.046	0.96 ± 0.032	1.18 ± 0.017	1.40 ± 0.026	0.55 ± 0.120	0.84 ± 0.072	0.81 ± 0.250	1.17 ± 0.074
Tyrosine	1.00 ± 0.387	0.97 ± 0.026	1.02 ± 0.0143	1.04 ± 0.014	1.14 ± 0.013	0.54 ± 0.134	0.71 ± 0.052	0.53 ± 0.057	1.84 ± 0.131
Valine	1.00 ± 0.294	0.98 ± 0.061	1.14 ± 0.061	1.31 ± 0.042	1.28 ± 0.048	2.43 ± 0.439	3.92 ± 0.527	4.26 ± 0.933	5.41 ± 0.623
Ascorbate	1.00 ± 0.202	0.67 ± 0.0595	1.29 ± 0.203	2.04 ± 0.438	5.14 ± 0.550	1.07 ± 0.135	1.13 ± 0.052	1.09 ± 0.068	1.48 ± 0.039
Citrate	1.00 ± 0.247	1.62 ± 0.440	0.90 ± 0.319	1.40 ± 0.273	3.04 ± 0.259	1.12 ± 0.028	1.07 ± 0.015	0.99 ± 0.056	1.16 ± 0.051
Fumarate	1.00 ± 0.058	1.03 ± 0.361	0.88 ± 0.234	1.24 ± 0.304	2.09 ± 0.097	1.17 ± 0.024	1.35 ± 0.043	1.77 ± 0.044	0.94 ± 0.083
Malate	1.00 ± 0.031	1.28 ± 0.031	1.00 ± 0.048	1.22 ± 0.053	1.18 ± 0.025	1.44 ±0.078	1.86 ± 0.010	0.53 ± 0.022	0.36 ± 0.028
Succinate	1.00 ± 0.083	2.53 ± 0.140	0.92 ± 0.085	1.18 ± 0.050	2.77 ± 0.250	1.09 ± 0.111	1.33 ± 0.105	0.99 ± 0.073	1.67 ± 0.110
Erythrose	1.00 ± 0.281	0.98 ± 0.076	0.95 ± 0.026	1.39 ± 0.161	1.25± 0.100	0.87 ± 0.120	1.15 ± 0.082	1.16 ± 0.182	1.61 ± 0.059
Fructose	1.00 ± 0.072	1.20 ± 0.067	0.84 ± 0.085	1.28 ± 0.060	1.12 ± 0.048	1.67 ± 0.069	2.04 ± 0.043	2.25 ± 0.067	2.14 ± 0.021
Glucose	1.00 ± 0.032	1.03 ± 0.210	0.88 ± 0.151	0.86 ± 0.112	1.20 ± 0.073	1.14 ± 0.057	1.47 ± 0.048	1.31 ± 0.031	1.57 ± 0.067
Idose	1.00 ± 0.219	1.25 ± 0.051	1.54 ± 0.627	1.34 ± 0.185	1.34 ± 0.153	1.51 ± 0.247	1.97 ± 0.090	1.54 ± 0.197	1.81 ± 0.294
Lyxose	1.00 ± 0.358	1.01 ± 0.328	0.49 ± 0.102	0.53 ± 0.150	1.36 ± 0.078	0.75 ± 0.025	0.91 ± 0.088	0.91 ± 0.113	0.93 ± 0.011
Mannose	1.00 ± 0.091	1.02 ± 0.027	1.26 ± 0.035	0.94 ± 0.035	0.94 ± 0.029	0.95 ± 0.018	0.99 ± 0.037	0.98 ± 0.040	1.03 ± 0.148
Sorbitol	1.00 ± 0.085	1.42 ± 0.364	1.20 ± 0.172	1.33 ± 0.087	0.80 ± 0.058	0.93 ± 0.029	1.01 ± 0.046	0.96 ± 0.028	0.97 ± 0.023
Sorbose	1.00 ± 0.084	1.29 ± 0.130	1.59 ± 0.113	1.32 ± 0.029	1.11 ± 0.049	0.97 ± 0.031	1.06 ± 0.048	1.01 ± 0.029	1.02 ± 0.024
Sucrose	1.00 ± 0.036	1.12 ± 0.092	0.67 ± 0.035	0.91 ± 0.027	0.97 ± 0.009	0.79 ± 0.031	1.20 ± 0.025	1.17 ± 0.075	1.29 ± 0.061
Xylose	1.00 ± 0.358	1.08 ± 0.058	0.97 ± 0.018	0.67 ± 0.022	0.72 ± 0.012	0.75 ± 0.078	0.91 ± 0.088	0.91 ± 0.113	0.93 ± 0.070
Nicotinic acid	1.00 ± 0.191	1.06 ± 0.067	1.14 ± 0.024	0.97 ± 0.045	0.90 ± 0.013	1.15 ± 0.045	1.25 ± 0.069	0.95 ± 0.035	1.34 ± 0.064
Putrescine	1.00 ± 0.120	1.11 ± 0.074	1.30 ± 0.050	0.95 ± 0.016	0.91 ± 0.020	0.81 ± 0.171	1.29 ± 0.108	0.66 ± 0.114	0.73 ± 0.064
Cinnamic acid	1.00 ± 0.205	Na	9.16 ± 0.599	8.49 ± 0.417	8.37 ± 0.908	8.02 ± 0.394	7.10 ± 0.441	5.28 ± 0.658	2.34 ±0.080
Clorogenic acid	1.00 ± 0.252	Na	0.53 ± 0.095	0.21 ± 0.021	0.42 ± 0.121	0.44 ± 0.015	0.69 ± 0.021	0.44 ± 0.086	0.11 ± 0.016
Shikimic acid	1.00 ± 0.105	Na	1.66 ± 0.132	1.60 ± 0.099	1.38 ± 0.052	1.35 ± 0.095	1.86 ± 0.076	2.63 ± 0.122	2.35 ± 0.123
Syringic acid	1.00 ± 0.185	Na	0.35 ± 0.052	0.13 ± 0.015	0.29 ± 0.076	0.20 ± 0.013	0.26 ± 0.017	0.09 ± 0.022	0.07 ± 0.007
Teobromine	1.00 ± 0.121	Na	1.77 ± 0.573	1.69 ± 0.489	1.44 ± 0.217	1.30 ± 0.093	1.70 ± 0.135	1.59 ± 0.151	1.38 ± 0.185
Xanthosine	1.00 ± 0.101	Na	2.63 ± 0.192	2.94 ± 0.213	2.95 ± 0.168	3.79 ± 0.316	6.03 ± 0.248	8.30 ± 0.224	8.01 ± 0.504

	Days after anthesis (DAA)								
	10	15	20	25	30	35	40	50	60
	dgt								
Alanine	1.51 ± 0.261	2.24 ± 0.123	1.69 ± 0.268	**2.01 ± 0.207**	1.98 ± 0.298	2.04 ± 0.048	2.00 ± 0.032	1.04 ± 0.162	1.39 ± 0.358
Alanine β	0.44 ± 0.265	1.95 ± 0.108	1.37 ± 0.325	1.57 ± 0.185	**1.08 ± 0.239**	**1.67 ± 0.167**	1.72 ± 0.180	**0.06 ± 0.008**	**0.85 ± 0.203**
Asparagine	**0.49 ± 0.094**	0.78 ± 0.185	0.60 ± 0.168	0.50 ± 0.053	**0.42 ± 0.147**	**1.20 ± 0.103**	1.09 ± 0.130	**0.24 ± 0.074**	0.77 ± 0.199
Aspartate	**2.21 ± 0.146**	0.95 ± 0.069	0.92 ± 0.085	1.03 ± 0.187	1.38 ± 0.132	1.05 ± 0.040	1.07 ± 0.053	1.67 ± 0.198	0.81 ± 0.070
GABA	0.63 ± 0.212	1.98 ± 0.101	1.13 ± 0.260	1.53 ± 0.193	**1.11 ± 0.187**	**1.61 ± 0.142**	**1.57 ± 0.138**	**0.22 ± 0.033**	0.99 ± 0.067
Glutamate	**4.20 ± 1.057**	**1.53 ± 0.082**	1.83 ± 0.269	1.47 ± 0.216	1.52 ± 0.234	1.35 ± 0.068	**1.37 ± 0.071**	**4.44 ± 0.273**	**1.01 ± 0.027**
Glutamine	0.43 ± 0.195	**0.64 ± 0.132**	0.46 ± 0.139	0.66 ± 0.184	**0.41 ± 0.131**	**1.36 ± 0.135**	**1.44 ± 0.158**	0.18 ± 0.025	**0.61 ± 0.080**
Glycine	1.14 ± 0.396	1.81 ± 0.122	**1.98 ± 0.198**	1.57 ± 0.109	**1.20 ± 0.247**	**1.79 ± 0.068**	1.80 ± 0.069	**0.37 ± 0.041**	**1.00 ± 0.150**
Homoserine	1.01 ± 0.196	1.39 ± 0.374	1.19 ± 0.333	**1.44 ± 0.073**	**1.03 ± 0.244**	**1.49 ± 0.199**	1.68 ± 0.338	0.92 ± 0.103	**0.95 ± 0.047**
Isoleucine	0.92 ± 0.255	3.99 ± 0.799	**2.65 ± 0.744**	2.26 ± 0.178	**1.89 ± 0.654**	**3.85 ± 0.469**	4.21 ± 0.566	**0.33 ± 0.059**	**1.96 ± 0.270**
Lysine	1.04 ± 0.150	1.06 ± 0.271	0.68 ± 0.105	0.93 ± 0.162	**0.52 ± 0.106**	**1.11 ± 0.108**	1.16 ± 0.116	0.73 ± 0.136	**0.73 ± 0.102**
Phenylalanine	0.41 ± 0.016	1.75 ± 0.397	**1.30 ± 0.306**	0.97 ± 0.073	**1.14 ± 0.215**	**1.62 ± 0.233**	**1.79 ± 0.282**	0.28 ± 0.040	0.81 ± 0.132
Proline	1.05 ± 0.429	3.98 ± 1.634	**2.46 ± 0.250**	**4.60 ± 0.747**	**2.82 ± 0.445**	1.38 ± 0.050	1.45 ± 0.018	0.69 ± 0.290	0.92 ± 0.227
Serine	1.17 ± 0.314	2.94 ± 0.303	**2.44 ± 0.153**	2.35 ± 0.302	2.65 ± 0.145	**2.86 ± 0.270**	**3.02 ± 0.373**	**0.35 ± 0.039**	**1.88 ± 0.136**
Threonine	0.56 ± 0.151	1.09 ±0.218	0.63 ± 0.175	0.60 ± 0.095	**0.46 ± 0.092**	**1.41 ± 0.158**	**1.37 ±0.1381**	0.21 ± 0.045	**0.66 ± 0.088**
Tyrosine	0.23 ± 0.028	1.89 ± 0.432	**1.65 ± 0.127**	0.86 ± 0.115	**1.36 ± 0.028**	**1.22 ± 0.149**	**1.32 ± 0.174**	0.29 ± 0.014	**0.62 ± 0.148**
Valine	0.99 ± 0.462	**5.48 ± 0.791**	3.92 ± 1.134	3.80 ± 0.426	**2.44 ± 0.752**	**4.92 ± 0.528**	5.31 ± 0.631	**0.24 ± 0.031**	**2.40 ± 0.278**
Ascorbate	**1.78 ± 0.182**	**1.23 ± 0.024**	1.09 ± 0.124	1.39 ± 0.058	**1.68 ± 0.105**	1.31 ± 0.079	**1.41 ± 0.092**	1.41 ± 0.105	1.41 ± 0.072
Citrate	1.58 ± 0.054	1.17 ± 0.016	**1.23 ± 0.023**	1.14 ± 0.062	1.14 ± 0.037	1.15 ± 0.032	1.16 ± 0.031	**1.35 ± 0.032**	1.11 ± 0.019
Fumarate	1.06 ± 0.057	1.13 ± 0.016	0.95 ± 0.085	0.97 ± 0.034	0.96 ± 0.011	1.09 ± 0.061	**1.05 ± 0.070**	**1.02 ± 0.011**	**0.57 ± 0.036**
Malate	**0.79 ± 0.025**	0.86 ± 0.016	**1.29 ± 0.003**	**1.33 ± 0.025**	**1.21 ± 0.010**	1.36 ± 0.021	**1.39 ± 0.018**	**1.19 ± 0.003**	**0.51 ± 0.016**
Succinate	1.27 ± 0.175	1.56 ± 0.243	**1.64 ± 0.186**	1.63 ± 0.287	1.44 ± 0.199	1.25 ± 0.090	1.39 ± 0.034	**0.71 ± 0.041**	**0.94 ± 0.026**
Erythrose	0.58 ± 0.219	1.57 ± 0.080	1.22 ± 0.213	1.45 ± 0.178	**1.22 ± 0.108**	**1.29 ± 0.096**	1.33 ± 0.122	**0.25 ± 0.030**	**0.87 ± 0.174**
Fructose	**1.33 ± 0.052**	**1.53 ± 0.072**	1.32 ± 0.284	**1.68 ± 0.039**	**1.48 ± 0.073**	1.71 ± 0.064	**1.71 ± 0.062**	2.05 ± 0.045	2.01 ± 0.090
Glucose	**1.42 ± 0.051**	**1.66 ± 0.022**	**1.64 ± 0.047**	**1.52 ± 0.044**	**1.31 ± 0.043**	**1.45 ± 0.053**	1.45 ± 0.053	**1.64 ± 0.061**	1.61 ± 0.093
Idose	**1.51 ± 0.261**	**2.24 ± 0.122**	1.68 ± 0.268	2.01 ± 0.207	**1.98 ± 0.298**	2.04 ± 0.048	2.00 ± 0.032	**1.04 ± 0.162**	1.39 ± 0.358
Lyxose	**3.78 ± 0.726**	0.87 ± 0.079	**0.97 ± 0.088**	1.09 ± 0.103	0.94 ± 0.206	**1.00 ± 0.025**	0.99 ± 0.027	**4.66 ± 0.572**	1.41 ± 0.180
Mannose	**1.62 ± 0.103**	**1.04 ± 0.019**	**1.08 ± 0.034**	0.95 ± 0.059	**1.22 ± 0.037**	0.98 ± 0.021	1.03 ± 0.037	**1.25 ± 0.028**	**0.88 ± 0.045**
Sorbitol	1.35 ± 0.149	**1.03 ± 0.015**	1.04 ± 0.033	0.99 ± 0.027	1.01 ± 0.031	0.97 ± 0.017	1.00 ± 0.019	**1.12 ± 0.026**	0.91 ± 0.026
Sorbose	1.41 ± 0.156	**1.07 ± 0.016**	1.09 ± 0.034	1.04 ± 0.028	1.06 ± 0.032	1.02 ± 0.018	1.04 ± 0.020	**1.17 ± 0.027**	0.95 ± 0.027
Sucrose	**1.30 ± 0.026**	**1.55 ± 0.071**	**1.61 ± 0.180**	**1.34 ± 0.072**	**1.10 ± 0.077**	1.05 ± 0.106	**0.95 ± 0.063**	**1.46 ± 0.043**	1.32 ± 0.081
Xylose	**3.78 ± 0.726**	0.87 ± 0.079	0.97 ± 0.088	1.09 ± 0.103	0.94 ± 0.206	**1.01 ± 0.025**	0.99 ± 0.027	**4.66 ± 0.572**	1.41 ± 0.181
Nicotinic acid	1.18 ± 0.044	**1.12 ± 0.085**	**1.52 ± 0.084**	1.68 ± 0.159	1.31 ± 0.166	**1.49 ± 0.055**	**1.55 ± 0.057**	**1.15 ± 0.032**	1.20 ± 0.061
Putrescine	**4.32 ± 0.541**	0.92 ± 0.024	**0.93 ± 0.117**	1.06 ± 0.156	1.88 ± 0.519	1.17 ± 0.238	1.19 ± 0.239	**3.98 ± 0.647**	1.66 ± 0.325
Cinnamic acid	Na	1.51 ± 0.333	**12.12 ± 1.234**	**11.60 ± 1.213**	7.37 ± 2.051	9.57 ± 0.682	7.99 ±1.070	6.26 ± 0.885	**4.72 ±0.811**
Clorogenic acid	Na	0.17 ± 0.053	**1.19 ± 0.138**	**0.41 ± 0.052**	**0.39 ±0.044**	**0.45 ± 0.076**	0.79 ± 0.163	**0.92 ± 0.070**	**0.56 ± 0.057**
Shikimic acid	Na	0.85 ± 0.071	1.79 ± 0.081	1.68 ± 0.100	1.13 ± 0.250	1.32 ± 0.183	1.73 ± 0.086	2.38 ± 0.127	2.34 ± 0.244
Syringic acid	Na	0.21 ± 0.061	0.30 ± 0.114	0.15 ± 0.034	0.46 ± 0.128	0.24 ± 0.035	0.42 ± 0.078	**0.29 ± 0.016**	**0.20 ± 0.041**
Teobromine	Na	0.69 ± 0.076	1.66 ± 0.194	1.73 ± 0.141	1.08 ± 0.242	1.64 ± 0.131	1.63 ± 0.247	2.14 ± 0.234	1.62 ± 0.334
Xanthosine	Na	1.29 ± 0.173	**3.80 ± 0.077**	**3.99 ± 0.289**	2.70 ± 0.891	**4.84 ± 0.254**	**4.33 ± 0.297**	**9.21 ± 0.331**	**10.09 ± 0.287**

	Days after anthesis (DAA)								
	10	15	20	25	30	35	40	50	60
	entire								
Alanine	1.59 ± 0.155	2.24 ± 0.123	**2.22 ± 0.121**	**3.14 ± 0.133**	**0.91 ± 0.175**	1.49 ± 0.324	1.59 ± 0.202	**0.79 ± 0.147**	0.91 ± 0.233
Alanine β	1.54 ± 0.175	1.95 ± 0.108	**1.95 ± 0.112**	2.03 ± 0.146	**0.88 ± 0.185**	1.31 ± 0.260	0.93 ± 0.266	**0.29 ± 0.059**	**0.76 ± 0.270**
Asparagine	0.77 ± 0.076	0.78 ± 0.185	**0.58 ± 0.061**	0.90 ± 0.207	**0.35 ± 0.076**	**0.89 ± 0.129**	**0.46 ± 0.078**	0.59 ± 0.147	0.74 ± 0.224
Aspartate	1.23 ± 0.104	0.95 ± 0.07	0.85 ± 0.020	1.08 ± 0.097	0.95 ± 0.216	0.93 ± 0.187	1.10 ± 0.150	1.79 ± 0.248	1.20 ± 0.201
GABA	1.33 ± 0.232	1.98 ± 0.101	**2.03 ± 0.084**	1.79 ± 0.066	**0.88 ± 0.138**	0.82 ± 0.161	0.95 ± 0.225	0.46 ± 0.078	0.82 ± 0.185
Glutamate	1.24 ± 0.071	1.53 ± 0.082	1.54 ± 0.083	1.46 ± 0.059	1.77 ± 0.551	1.16 ± 0.136	1.85 ± 0.575	**3.37 ± 0.553**	1.70 ± 0.355
Glutamine	1.09 ± 0.254	0.64 ± 0.132	0.59 ± 0.141	1.06 ± 0.105	**0.49 ± 0.094**	**0.97 ± 0.170**	**1.22 ± 0.102**	0.47 ± 0.135	0.59 ± 0.166
Glycine	**1.92 ± 0.167**	1.81 ± 0.122	**1.75 ± 0.088**	1.98 ± 0.218	**0.86 ± 0.182**	1.75 ± 0.252	1.66 ± 0.129	**0.55 ± 0.135**	**0.83 ± 0.206**
Homoserine	1.29 ± 0.189	1.39 ± 0.374	1.50 ± 0.388	**1.77 ± 0.143**	**0.69 ± 0.230**	1.19 ± 0.247	0.92 ± 0.109	0.79 ± 0.147	1.21 ± 0.285
Isoleucine	**4.24 ± 0.554**	3.99 ± 0.799	**3.06 ± 0.284**	4.03 ± 0.677	**1.57 ± 0.412**	2.15 ± 0.521	2.76 ± 0.681	0.90 ± 0.161	**2.29 ± 0.991**
Lysine	1.50 ± 0.234	1.07 ± 0.271	1.01 ± 0.277	1.31 ± 0.268	**0.57 ± 0.104**	0.84 ± 0.199	0.89 ± 0.041	**1.60 ± 0.228**	1.19 ± 0.287
Phenylalanine	**1.77 ± 0.142**	**1.75 ± 0.039**	**1.77 ± 0.397**	1.78 ± 0.280	**0.60 ± 0.124**	0.94 ± 0.155	1.01 ± 0.229	0.48 ± 0.112	**0.91 ± 0.395**
Proline	1.61 ± 0.410	3.98 ± 1.634	**4.68 ± 1.512**	**7.65 ± 1.443**	0.65 ± 0.144	1.28 ± 0.387	1.11 ± 0.395	0.36 ± 0.040	**0.69 ± 0.194**
Serine	**2.95 ± 0.387**	2.94 ± 0.30	**2.71 ± 0.177**	**2.92 ± 0.179**	**1.25 ± 0.271**	**2.45 ± 0.376**	2.37 ± 0.1984	0.83 ± 0.135	**1.31 ± 0.412**
Threonine	1.18 ± 0.183	1.09 ± 0.218	0.77 ± 0.093	1.14 ± 0.174	**0.69 ± 0.096**	**1.03 ± 0.165**	0.83 ± 0.172	0.53 ± 0.134	0.78 ± 0.249
Tyrosine	**1.94 ± 0.177**	**1.88 ± 0.0432**	**1.85 ± 0.433**	1.69 ± 0.373	**0.43 ± 0.078**	0.57 ± 0.1016	1.19 ± 0.274	**0.21 ± 0.007**	1.38 ± 0.464
Valine	**5.29 ± 0.599**	5.48 ± 0.791	**5.33 ± 0.803**	5.04 ± 0.783	**1.82 ± 0.599**	2.25 ± 0.641	5.01 ± 0.649	**0.54 ± 0.127**	2.30 ± 1.071
Ascorbate	1.27 ± 0.094	**1.23 ± 0.025**	1.24 ± 0.026	1.19 ± 0.071	1.32 ± 0.093	**1.50 ± 0.036**	**1.34 ± 0.018**	1.13 ± 0.135	**1.28 ± 0.064**
Citrate	1.28 ± 0.022	1.17 ± 0.017	**1.17 ± 0.016**	**1.18 ± 0.020**	1.16 ± 0.071	1.16 ± 0.032	1.12 ± 0.019	**1.31 ± 0.017**	1.22 ± 0.041
Fumarate	0.98 ± 0.025	1.14 ± 0.017	**1.17 ± 0.014**	**1.22 ± 0.028**	**3.75 ± 0.161**	**4.64 ± 0.235**	**3.77 ± 0.092**	**3.66 ± 0.095**	**4.11 ± 0.188**
Malate	**0.75 ± 0.025**	**0.86 ± 0.016**	**0.86 ± 0.016**	**0.87 ± 0.011**	1.35 ± 0.024	**1.92 ± 0.021**	**1.94 ± 0.010**	**1.53 ± 0.015**	**0.08 ± 0.098**
Succinate	0.96 ± 0.261	1.56 ± 0.243	**1.95 ± 0.258**	1.90 ± 0.280	**0.84 ± 0.117**	1.18 ± 0.165	1.06 ± 0.113	1.44 ± 0.181	**1.03 ± 0.086**
Erythrose	1.41 ± 0.135	1.56 ± 0.080	**1.56 ± 0.075**	1.81 ± 0.144	**0.87 ± 0.156**	1.37 ± 0.237	0.89 ± 0.215	**0.40 ± 0.044**	**0.78 ± 0.212**
Fructose	**1.45 ± 0.057**	**1.53 ± 0.072**	**1.46 ± 0.064**	**1.57 ± 0.032**	**1.43 ± 0.029**	1.74 ± 0.066	1.79 ± 0.087	2.21 ± 0.059	**2.32 ± 0.060**
Glucose	**1.55 ± 0.061**	**1.66 ± 0.024**	**1.58 ± 0.067**	**1.34 ± 0.022**	**1.35 ± 0.013**	**1.36 ± 0.012**	**1.21 ± 0.067**	1.22 ± 0.055	1.38 ± 0.075
Idose	1.59 ± 0.155	2.24 ± 0.123	**2.22 ± 0.121**	3.14 ± 0.133	0.91 ± 0.174	1.49 ± 0.324	1.59 ± 0.202	0.79 ± 0.147	0.90 ± 0.233
Lyxose	0.88 ± 0.066	0.87 ± 0.079	**0.91 ± 0.073**	1.07 ± 0.104	**1.60 ± 0.088**	**1.26 ± 0.170**	0.83 ± 0.090	2.30 ± 0.907	1.09 ± 0.145
Mannose	0.96 ± 0.048	1.04 ± 0.020	**1.05 ± 0.023**	1.02 ± 0.055	0.99 ± 0.053	**1.09 ± 0.036**	0.98 ± 0.013	0.98 ± 0.053	0.94 ± 0.031
Sorbitol	1.02 ± 0.017	1.02 ± 0.015	1.03 ± 0.017	1.12 ± 0.151	0.97 ± 0.040	**1.04 ± 0.038**	0.96 ± 0.014	0.98 ± 0.007	0.98 ± 0.038
Sorbose	1.07 ± 0.018	1.07 ± 0.016	1.08 ± 0.018	1.17 ± 0.153	1.02 ± 0.042	**1.09 ± 0.040**	1.01 ± 0.015	1.03 ± 0.008	1.03 ± 0.040
Sucrose	**1.48 ± 0.074**	**1.55 ± 0.071**	**1.46 ± 0.063**	**1.09 ± 0.037**	**1.15 ± 0.089**	**1.43 ± 0.045**	**1.59 ± 0.123**	1.25 ± 0.112	**1.89 ± 0.099**
Xylose	0.88 ± 0.066	0.87 ± 0.079	0.91 ± 0.073	1.07 ± 0.103	**1.60 ± 0.088**	**1.26 ± 0.170**	0.83 ±0.090	2.31 ± 0.906	1.10 ± 0.145
Nicotinic acid	**1.64 ± 0.091**	1.12 ± 0.085	1.03 ± 0.095	1.22 ± 0.032	**1.33 ± 0.050**	1.27 ± 0.054	1.31 ± 0.038	0.96 ± 0.071	1.09 ± 0.046
Putrescine	1.25 ± 0.105	0.92 ± 0.024	0.96 ± 0.045	1.02 ± 0.071	1.73 ± 0.627	1.30 ± 0.304	1.03 ± 0.161	**3.54 ± 0.567**	1.59 ± 0.493
Cinnamic acid	**0.59 ± 0.143**	0.77 ±0.308	**12.06 ± 1.170**	**11.85 ± 1.493**	**10.94 ± 0.447**	8.61 ± 0.540	5.45 ± 0.566	4.76 ± 0.627	3.29 ± 0.281
Clorogenic acid	0.39 ± 0.109	0.18 ± 0.030	0.43 ± 0.134	**0.27 ± 0.009**	0.27 ±0.038	0.48 ± 0.029	**0.35 ± 0.034**	0.36 ± 0.034	0.13 ± 0.029
Shikimic acid	1.29 ± 0.149	1.13 ± 0.113	**2.44 ± 0.169**	**2.86 ± 0.228**	**2.95 ± 0.053**	**2.67 ± 0.093**	**2.97 ± 0.104**	**2.96 ± 0.149**	**3.79 ± 0.220**
Syringic acid	**0.39 ± 0.095**	0.17 ± 0.044	**0.23 ± 0.067**	0.17 ± 0.011	0.15 ± 0.014	0.24 ± 0.024	0.09 ± 0.013	0.09 ± 0.015	0.03 ± 0.007
Teobromine	0.79 ± 0.160	0.63 ± 0.138	1.54 ± 0.107	**4.77 ± 0.602**	**2.23 ± 0.158**	**2.18 ± 0.189**	1.99 ± 0.136	2.08 ± 0.226	1.93 ± 0.193
Xanthosine	1.04 ± 0.141	1.66 ± 0.244	2.82 ± 0.335	3.27 ± 0.232	3.67 ± 0.374	4.64 ± 0.286	5.65 ± 0.263	**8.70 ± 0.322**	**8.88 ± 0.328**

Amino acids

Acids

Sugars

Others

Secondary metabolism

Supplemental table S4. Primers utilized to qRT-PCR

gene	Locus	Sequence	Efficiency (%)
Actin	Solyc03g078400.2.1	Fwd 5'-GGTCCCTCTATTGTCCACAG-3' Rev 5'-TGCATCTCTGGTCCAGTAGGA-3'	0.88
IAA9	Solyc04g076850	Fwd 5'-GTTGTCAAGTGTGTGACAGCC-3' Rev 5'-TGTCACTTACACATAGGGCCA-3'	0.9
DGT	Solyc01g111170	Fwd 5'-GAGTCGCCGTTTTAGGCTTT-3' Rev 5'-GCAACACAACAACCAATTACG-3'	0.82

CHAPTER 5

Concluding Remarks

Chapter 5 - Concluding Remarks

This thesis was largely focused on obtaining a comprehensive picture of the functional contribution of auxin signaling in different tissues and during fruit development in tomatoes. Briefly, the mains goals of the work presented here were: (i) to discuss the conceptual basis of different approaches used in metabolomics studies, namely those techniques that use stable and radiolabelled compounds (^{13}C and ^{14}C, respectively), presenting some examples of how metabolic fluxes are estimated as well as their historical application and limitations, providing an update on recent technical developments; (ii) to obtain novel insights into how and to which extent alterations in auxin signaling levels might differently affect plant growth in general and finally, (iii) to demonstrate the significance of auxin signaling describing novel connections between auxin signaling and fruit ripening from a metabolic perspective. In attempt to reach these aims several different but complementary experimental approaches were taken, and the results obtained were presented in one review and two independent research articles that are organized as a compilation of three independent but standalone chapter. Although each chapter presented here has an independent discussion focusing on the results described within it, this final chapter discusses this thesis in its integrity in an attempt to detail the main findings in a broader context. Finally, an outlook detailing possible avenues for future research is provided using the work presented here as its foundation describing the challenges and perspectives in understanding auxin signaling function during plant development.

The importance of metabolic analysis coupled with analysis of flux is increasingly becoming an essential component of current efforts to increase our understanding of the control and regulation of metabolic networks. Additionally, the combination of both approaches (using stable and radiolabeled isotopes) allow the inclusion of the knowledge inferred from each other, and it seems reasonable to suggest that it will likely be highly informative in elucidating function of metabolic pathways in a network context. In chapter 2, we examined the relative advantages and disadvantages of radioisotope and stable isotope labelling approaches. We also posit that the coupling of modeling approaches and the feeding experiments can be highly pertinent to elucidate the underlying mechanisms of complex metabolic networks and pathways of intricate biological systems. Of course, it seems also challenging the usage of both approaches for broader community given the lack of accessible tools for

certain experiments coupled with difficulties in both data analysis and interpretation. Nevertheless, we posit that stable labeling does not replace but rather function as a true complement of radiolabeled approaches which retain considerable utility particularly in the analysis of macromolecules. It seems clear that further development is still required to make stable isotope enabled metabolomics approaches more accessible to biologists and to the metabolomics community.

Given the importance of metabolic studies (some of which we described in Chapter 2), we have sought to improve our understanding of the role played by auxin signaling during plant growth and development, as well as the associated metabolic mechanisms by which auxin play their role. Thus, within the Chapter 3 we decide to investigate the significance of auxin signaling via the repression of two different genes that affect the auxin perception namely DGT and SlIAA9 in tomato plants cv. Micro-Tom. We show that both mutations compromise photosynthetic capacity and alter primary metabolism, modulating growth though significant alterations in the mitochondrial respiratory process. The loss of function of DIAGEOTROPICA protein reduces the perception of auxin which causes growth reduction by changes in the photosynthetic rate through diffusional limitation by reductions in g_s, affecting the photosynthetic and transpiration rate. Consequently, dgt mutant plants were characterized by increase WUEi, which allows us to postulate that dgt mutant could have an interesting performance under conditions of water limitation. In addition, the reduction of the perception of auxin directly affects the capacity of use of the reserves since transitory starch catabolism seems to be compromised. Conversely, dgt increases the protein half-life of the other SlAux/IAAs following public gene expression data. This effect can be explained, at least partially, by the ability of interaction with motif dragon P-P by peptidyl-prolyl cis/trans isomerase activity of cyclophilins (Jing et al., 2015). In contrast, the increased perception of auxin observed in entire mutant plants not only culminates with leaf anatomical alterations, but also increases the growth through reduced stomatal and biochemical limitations, increasing the capacity of use of $CO_2$by enhancing both photosynthesis and the usage of reserves during both dark and day respiration. Interestingly, those plants also display pronounced changes in the levels of TCA cycle intermediates suggesting that increased auxin perception may promote the consumption of ADP by inducing higher ATP synthesis to sustain cell expansion. Thus, the relationship here observed between higher respiratory rate and rapid growth can be explained, at least partially, by the TCA cycle mediated regulation

of photosynthesis in illuminated leaves (Nunes-Nesi et al., 2008; Nunes-Nesi et al., 2011; Nunes-Nesi et al., 2013). When considered together, these results obtained here suggest a significant impact of auxin signaling on cellular carbon and energetic metabolism, particularly in leaves. It is important to mention that nitrogen metabolism was also strongly influenced by the drastic increasing in auxin perception (entire), with large variations for certain amino acids. However, the metabolic and molecular cues underlying such connections remains contentious and therefore, further work is still required to establish precisely how auxin is able to impact both photosynthesis and respiration.

We next went forward to better understand the link between auxin signaling and fruit ripening process. Auxin is an important plant hormone playing crucial roles during fruit growth regulation (Zhao, 2010). Auxin can also modulate fruit ripening on its own manner and by interacting with other hormones regulating many physiological processes. Accordingly, it is well established that interactions between auxin and ethylene are of pivotal importance to control ripening in grape fruits, mainly by a mechanism where ethylene control auxin biosynthesis via TAR and YUCCA genes (Böttcher et al., 2013). It has been recently demonstrated by a global transcriptome profiling analysis that there is substantial ethylene-auxin interaction during ripening of tomato fruits (Li, Tao, et al., 2017). Moreover, exogenous applications of auxin to fruit usually leads to ripening delay and therefore auxin is commonly regarded as a negative regulator of fruit ripening (Ziliotto et al., 2012; Chen et al., 2016; Li, Khan, et al., 2017). However, compelling evidence has demonstrated that auxin may play more intricate roles in regulating the ripening process through interaction with ethylene and other plant hormones (Böttcher et al., 2013; Tadiello et al., 2016). These facts apart, the metabolic impacts of changes in auxin signaling during tomato ripening remains rather unsolved. Thus, in Chapter 4, we performed a broad analyses of the changes in auxin signaling during different stages of fruit development metabolism using the same mutants used before with either increased (entire) or reduced (diageotropica - dgt) auxin signaling . Our results shown that auxin signaling appears to be a master regulator of tomato fruit ripening, given that dgt mutant plants, which has reduced auxin sensitivity, were characterized by delay of fruit ripening impacting the climacteric peak and respiratory process by an ethylene dependent mechanism. DGT seems to also modulate both sugar levels and starch content. Our results suggest that reduced auxin signaling can impact tomato flavor by alterations in sugar and organic acids ratio.

It is important to mention that such parameters are commonly used in postharvest studies. Although fruits of entire mutant plants displayed minor changes in fruit ripening with few alterations in sugar and organic acids in comparison with WT fruits, it is important to mention, however, that the SIIAA9 directly impacts fumarate content, considerably increasing during fruit development, suggesting an important role of this gene in regulation of the TCA cycle. We show that auxin signaling regulate not only the accumulation and conversion of pigment but also impact carbohydrate and secondary metabolism during tomato fruit ripening. We further demonstrate that these effects are likely due to an effect of heterochrony coupled with an unnoticed role of auxin the regulation of key enzymes in the route of synthesis and degradation of carbohydrates. .Additionally, entire has shown increasing in total amino acids without changes in total protein. Our results show that these mutations alter primary metabolism, modulating fruit growth through changes in fruit respiration. Altogether, the uncovered data demonstrate the involvement of auxin signaling in the control of fruit set and ripening, unravelling the role of auxin in the mitochondria-chloroplast energetic crosstalk that are of pivotal significance during tomato fruit ripening , and providing novel insights into the link between auxin signaling and respiratory pathway. Further work is clearly required to establish how auxin signaling is able to impact both amino acid metabolism and volatile production in tomato fruits respiration.

When considered together the results of this work clearly demonstrate that fluctuations in auxin perception are rather more complex than initially thought. With the inclusion and knowledge inferred from differential tissue responses to auxin perception, the work presented here clearly suggest that in order to better understand the function of auxin signaling one need to evaluate not only in different tissues but also the metabolic interconnections that are associated with the pathways of biosynthesis and degradation of this highly intriguing hormone. Furthermore, it is likely that many aspects of the regulation of auxin signaling, biosynthesis, transport and degradation remain contentious. In addition, the results discussed here provided novel insights into the functions of auxin in different tissues and highlights the complexity and specificity of plant metabolism in response to changes in auxin signaling. Whilst our data provide a clear connection between mitochondrial metabolism and auxin signaling, future investigation is still required including a deeper focus on growth connections to fully elucidate the precise factors underlying this metabolic phenotype organic acids metabolism, mainly in fumarate. Considering the absence of coupled

works associating fluctuations in auxin perception and its impacts on metabolism, our work has demonstrated a broad physiological and metabolic impact of two auxin-related genes (DGT and IAA9) in tomato plants. It can be anticipated that manipulation of auxin signaling coupled with extensive metabolic studies will, therefore, likely prove highly insightful in identifying further non-textbook aspects of this important phytohormone that should be tested to provide more comprehensive description of whole plant metabolism. Therefore, the synthesis of knowledge emanating from our studies coupled with increasing sophistication in metabolic studies and mathematical modelling is likely to enable us to pursue new avenues of research to increase our understanding of the complex metabolic changes associated with auxin function and how adjustment in response to fluctuation in auxin perception can control plant growth phase and fruit ripening in valuable crop plants.

REFERENCES

BÖTTCHER, C. et al. Interactions between ethylene and auxin are crucial to the control of grape (Vitis vinifera L.) berry ripening. **BMC Plant Biology,** v. 13, n. 1, p. 222, 2013/12/23 2013. ISSN 1471-2229. Disponível em: < https://doi.org/10.1186/1471-2229-13-222 >.

CHEN, J. et al. Transcriptome profiling of postharvest strawberry fruit in response to exogenous auxin and abscisic acid. **Planta,** v. 243, n. 1, p. 183-197, 2016. ISSN 0032-0935.

JING, H. et al. Peptidyl-prolyl isomerization targets rice Aux/IAAs for proteasomal degradation during auxin signalling. **Nature communications,** v. 6, 2015.

LI, J. et al. Effects of exogenous auxin on pigments and primary metabolite profile of postharvest tomato fruit during ripening. **Scientia Horticulturae,** v. 219, p. 90-97, 2017. ISSN 0304-4238.

LI, J. et al. Global transcriptome profiling analysis of ethylene-auxin interaction during tomato fruit ripening. **Postharvest Biology and Technology,** v. 130, p. 28-38, 2017/08/01/ 2017. ISSN 0925-5214. Disponível em: < http://www.sciencedirect.com/science/article/pii/S0925521416306263 >.

NUNES-NESI, A.; ARAÚJO, W. L.; FERNIE, A. R. Targeting mitochondrial metabolism and machinery as a means to enhance photosynthesis. **Plant Physiology,** v. 155, n. 1, p. 101-107, 2011. ISSN 1532-2548.

NUNES-NESI, A. et al. Regulation of the mitochondrial tricarboxylic acid cycle. **Current Opinion in Plant Biology,** v. 16, n. 3, p. 335-343, 2013/06/01/ 2013. ISSN 1369-5266. Disponível em: < http://www.sciencedirect.com/science/article/pii/S1369526613000162 >.

NUNES-NESI, A. et al. The enigmatic contribution of mitochondrial function in photosynthesis. **Journal of experimental botany,** v. 59, n. 7, p. 1675-1684, 2008. ISSN 1460-2431.

TADIELLO, A. et al. On the role of ethylene, auxin and a GOLVEN-like peptide hormone in the regulation of peach ripening. **BMC plant biology,** v. 16, n. 1, p. 44, 2016. ISSN 1471-2229.

ZHAO, Y. Auxin biosynthesis and its role in plant development. **Annual review of plant biology,** v. 61, p. 49-64, 2010. ISSN 1543-5008.

ZILIOTTO, F. et al. Grape berry ripening delay induced by a pre-véraison NAA treatment is paralleled by a shift in the expression pattern of auxin-and ethylene-related genes. **BMC Plant Biology,** v. 12, n. 1, p. 185, 2012. ISSN 1471-2229.